

DOT/FAA/AR-04/11

Office of Aviation Research
Washington, D.C. 20591

Fire-Safe Polymers and Polymer Composites

September 2004

Final Report

This document is available to the U.S. public through the National Technical Information Service (NTIS), Springfield, Virginia 22161.



U.S. Department of Transportation
Federal Aviation Administration

NOTICE

This document is disseminated under the sponsorship of the U.S. Department of Transportation in the interest of information exchange. The United States Government assumes no liability for the contents or use thereof. The United States Government does not endorse products or manufacturers. Trade or manufacturer's names appear herein solely because they are considered essential to the objective of this report. This document does not constitute FAA certification policy. Consult your local FAA aircraft certification office as to its use.

This report is available at the Federal Aviation Administration William J. Hughes Technical Center's Full-Text Technical Reports page: actlibrary.act.faa.gov in Adobe Acrobat portable document format (PDF).

1. Report No. DOT/FAA/AR-04/11		2. Government Accession No.		3. Recipient's Catalog No.	
4. Title and Subtitle FIRE-SAFE POLYMERS AND POLYMER COMPOSITES				5. Report Date September 2004	
				6. Performing Organization Code	
7. Author(s) Huiqing Zhang				8. Performing Organization Report No.	
9. Performing Organization Name and Address Polymer Science and Engineering University of Massachusetts Amhurst, MA 01003				10. Work Unit No. (TRAIS)	
				11. Contract or Grant No.	
12. Sponsoring Agency Name and Address U.S. Department of Transportation Federal Aviation Administration Office of Aviation Research Washington, DC 20591				13. Type of Report and Period Covered	
				14. Sponsoring Agency Code ANM-110	
15. Supplementary Notes The FAA William J. Hughes Technical Center COTR was Dr. Richard Lyon. ©Copyright by Huiqing Zhang 2003 All Rights Reserved					
16. Abstract The intrinsic relationships between polymer structure, composition, and fire behavior have been explored to develop new fire-safe polymeric materials. Three milligram-scale methods (pyrolysis-combustion flow calorimetry (PCFC), simultaneous thermal analysis, and pyrolysis gas chromatography/mass spectrometry (GC/MS)) have been combined to fully characterize the thermal decomposition and flammability of polymers and polymer composites. Thermal stability, mass loss rate, char yield, and properties of decomposition volatiles were found to be the most important parameters in determining polymer flammability. Most polymers decompose by either an unzipping or a random chain scission mechanism with an endothermic decomposition of 100-900 J/g. Aromatic or heteroaromatic rings, conjugated double or triple bonds, and heteroatoms such as halogens, N, O, S, P, and Si, are the basic structural units for fire-resistant polymers. The flammability of polymers can also be successfully estimated by combining the pyrolysis GC/MS results or chemical structures with the thermogravimetric analysis. The thermal decomposition and flammability of two groups of inherently fire-resistant polymers—poly(hydroxyamide) (PHA) and its derivatives and bisphenol C (BPC II) polyarylates—have been systematically studied. PHA and most of its derivatives have extremely low heat release rates and very high char yields upon combustion. PHA and its halogen derivatives can completely cyclize into quasi-polybenzoxazole structures at low temperatures. However, the methoxy and phosphate derivatives show a very different behavior during decomposition and combustion. Molecular modeling shows that the formation of an enol intermediate is the rate-determining step in the thermal cyclization of PHA. BPC II-polyarylate is another extremely flame-resistant polymer. It can be used as an efficient flame-retardant agent in copolymers and blends. From the PCFC results, the total heat of combustion of these copolymers or blends changes linearly with composition, but the change of maximum heat release rates also depends on the chemical structure of the components. The flammability of various polymers and polymer composites measured by PCFC; cone calorimeter, ASTM E1354; and the Ohio State University (OSU) calorimeter, ASTM E906, were also compared. For pure polymers, there was a relatively good correlation between different methods. However, for polymer composites with inert fillers or flame-retardant additives, the OSU and cone calorimetries are more suitable evaluation methods.					
17. Key Words Polymer, Fire, Flammability, Thermal analysis, Combustion			18. Distribution Statement This document is available to the public through the National Technical Information Service (NTIS), Springfield, Virginia 22161.		
19. Security Classif. (of this report) Unclassified		20. Security Classif. (of this page) Unclassified		21. No. of Pages 209	22. Price

TABLE OF CONTENTS

	Page
EXECUTIVE SUMMARY	xix
1. FIRE AND POLYMERS	1-1
1.1 Introduction	1-1
1.2 Polymer Combustion Process	1-2
1.3 Standard Assessments and Tests	1-3
1.4 Flame-Retardant Chemistry	1-4
1.5 Inhibition of Polymer Combustion	1-5
1.5.1 Intrinsically Fire-Resistant Polymers	1-5
1.5.2 Flame-Retardant Additives	1-6
1.6 Thermal Decomposition Mechanisms of Polymers	1-11
1.7 Experimental Techniques for Thermal Decomposition of Polymers	1-12
2. QUANTATIVE MEASUREMENTS ON THE THERMAL DECOMPOSITION AND FLAMMABILITY OF POLYMERS	2-1
2.1 Introduction	2-1
2.2 Methodology of Flammability Calculations	2-2
2.2.1 Calculation of the Composition of the Volatiles	2-3
2.2.2 Calculation of Total Heat of Combustion and Heat Release Capacity of Polymers	2-4
2.3 Experimental	2-5
2.3.1 Pyrolysis GC/MS	2-5
2.3.2 Simultaneous Thermal Analysis	2-5
2.3.3 Pyrolysis-Combustion Flow Calorimeter	2-6
2.3.4 Materials	2-7
2.4 Results	2-8
2.4.1 Thermal Stability and Decomposition Process of Polymers	2-8
2.4.2 Thermal Decomposition Products of Polymers	2-13
2.4.3 Flammability	2-16
2.4.4 Bond Dissociation Energies of the Polymers	2-18

2.4.5	Flammability Calculated by Pyrolysis GC/MS and STA Results	2-21
2.4.6	Flammability Estimated by Using Chemical Structure and TGA Results	2-22
2.5	Discussion	2-28
3.	LOW FLAMMABILITY AND THERMAL DECOMPOSITION OF POLY (HYDROXYAMIDE) AND ITS DERIVATIVES	3-1
3.1	Introduction	3-1
3.2	Experimental	3-2
3.2.1	Materials	3-2
3.2.2	Film Preparation	3-3
3.2.3	Characterization	3-3
3.3	Results	3-3
3.3.1	Thermal Stability and Decomposition Process of PHAs	3-3
3.3.2	Flammability	3-10
3.3.3	Characterization of Chars by IR and Elemental Analysis	3-13
3.3.4	Identification of Volatiles by GC/MS	3-15
3.3.5	Thermal Decomposition Mechanisms	3-19
3.4	Discussion	3-23
4.	FIRE-RESISTANT, UV/VISIBLE-SENSITIVE POLYARYLATES, COPOLYMERS, AND BLENDS	4-1
4.1	Introduction	4-1
4.2	Experimental	4-2
4.2.1	Materials	4-2
4.2.2	Characterization	4-2
4.3	Results	4-2
4.3.1	Flammability and Thermal Decomposition of BPA-Polyarylates	4-2
4.3.2	Thermal Decomposition and Flammability of Homopolyarylates	4-3
4.3.3	UV/Visible-Sensitive Chalcon II-Polyarylate	4-6
4.3.4	Thermal Decomposition and Flammability of Copolymers and Terpolymers	4-8

4.3.5	Thermal Decomposition and Flammability of Blends	4-12
4.4	Discussion	4-15
5.	EFFECTS OF FLAME-RETARDANT ADDITIVES AND CORRELATIONS AMONG PCFC, OSU, AND CONE CALORIMETERS	5-1
5.1	Introduction	5-1
5.2	Experimental	5-2
5.2.1	Test Samples	5-2
5.2.2	Sample Preparation	5-2
5.2.3	Characterization	5-2
5.3	Results	5-5
5.3.1	Poly(Methyl Methacrylate)/Clay Nanocomposites	5-5
5.3.2	Poly(Ether Ether Ketone) and Composites	5-7
5.3.3	Xydar [®] and Its Composites	5-12
5.3.4	Polyphthalamides and Composites	5-17
5.3.5	Epoxy Resins With Phosphate Flame Retardants	5-28
5.3.6	Ignitability	5-32
5.3.7	Heat Release Rate	5-33
5.3.8	Correlation Between Different Flammability Tests	5-35
5.4	Discussion	5-39
6.	STRUCTURE-COMPOSITION-FLAMMABILITY RELATIONSHIPS OF POLYMERS	6-1
6.1	Introduction	6-1
6.2	Experimental	6-1
6.2.1	Materials	6-1
6.2.2	Characterization	6-1
6.3	Chemical Structure	6-1
6.3.1	Main Chain—Polysulfones	6-1
6.3.2	Semiorganic Network Structure—Polycarbynes and Polysilynes	6-11
6.3.3	Substituents	6-14
6.3.4	Flame-Retardant Comonomers	6-20
6.4	Composition—Copolymers and Blends	6-26
6.4.1	Poly(Methyl Methacrylate)/Polystyrene Random Copolymers	6-26
6.4.2	Poly(Methyl Methacrylate)/Polystyrene Blends	6-26

6.5	Molecular Weight	6-28
6.5.1	Poly(Methyl Methacrylate)	6-28
6.5.2	Polystyrene	6-30
6.5.3	Poly(Ethylene Oxide)	6-32
6.5.4	Mechanisms of the Effects of the Molecular Weight	6-32
6.6	Free-Radical Scavenger—TEMPO	6-33
6.6.1	Polystyrene or PMMA/TEMPO Blends	6-34
6.6.2	The PMMA/PS Random Copolymers Initiated by TEMPO	6-34
6.7	Discussion	6-38
7.	MOLECULAR MODELING OF THERMAL CYCLIZATION OF POLY(HYDROXYAMIDE)	7-1
7.1	Introduction	7-1
7.2	Previous Experimental Results	7-1
7.3	Results	7-3
7.4	Discussion	7-7
8.	CONCLUSIONS AND RECOMMENDATIONS	8-1
8.1	Conclusions	8-1
8.1.1	Characterization of Thermal Decomposition and Flammability of Polymers	8-1
8.1.2	Inherently Fire-Resistant Polymers	8-2
8.1.3	Effects of Flame-Retardant Additives and Correlations Among Different Flammability Tests	8-4
8.1.4	Structure, Composition, and Flammability Relationships	8-5
8.1.5	Thermal Cyclization Mechanism of PHA	8-6
8.2	Recommendations	8-6
9	REFERENCES	9-1
10.	BIBLIOGRAPHY	10-1
	APPENDIX A—SUPPLEMENTARY DATA	

LIST OF FIGURES

Figure	Page
1-1 Schematic Diagram of Polymer Burning	1-2
1-2 Intrinsically Fire-Resistant Polymers	1-6
1-3 Intumescent Compounds	1-9
1-4 Some Preceramic Polymers	1-10
2-1 Schematic Picture of PCFC	2-6
2-2 Chemical Structures of Some Polymers	2-7
2-3 The STA and DTG Curves of Aliphatic Polymers (10°C/min in N ₂) (a) HDPE, (b) PS, (c) PMMA, and (d) PVC	2-10
2-4 The STA and DTG Curves of Aromatic Polymers (10°C/min in N ₂) (a) PC and (b) PPhS	2-11
2-5 The STA and DTG Curves of Polymers With Exothermic Decomposition (10°C/min in N ₂) (a) PAN and (b) BPC II-Polyarylate	2-11
2-6 Activation Energies of Thermal Decomposition Calculated by TGA Data (a) HDPE, (b) Nylon 66, and (c) PPhS	2-12
2-7 Pyrolysis GC/MS Traces of Additional Polymers (4.3°C/s to 930°C) (a) PMMA, (b) PE, and (c) PS	2-14
2-8 Pyrolysis GC/MS Traces of Aromatic Polymers (4.3°C/s to 930°C) (a) PC and (b) PPhS	2-15
2-9 Pyrolysis GC/MS Traces of Polymers at a Fast Heating Rate (10°C/ms to 930°C) (a) HDPE and (b) PC	2-16
2-10 The TGA Curves of Kevlar [®] and Nylon 66	2-21
2-11 Calculation of Gross Heat of Combustion of Small Organic Compounds (a) Oxygen Consumption and (b) Atom Additivity	2-24
2-12 Comparison of Calculated Net Heat of Combustion of Polymers With PCFC Results (a) Oxygen Consumption and (b) Element Additivity	2-25
2-13 Comparison of Calculated Heat Release Capacity of Polymers With PCFC Results (a) Oxygen Consumption and (b) Element Additivity	2-27

2-14	Correlation Between Char Yield and Molar Fraction of Effective Char-Forming Atoms in Polymers	2-28
3-1	Structures of PHA and Its Derivatives	3-2
3-2	The TGA Curves of PHA-1 and 2 in N ₂	3-5
3-3	X-Ray Diffraction of PHA-1 and 2	3-5
3-4	The TGA Curves of PHA-1 and Its Derivatives in N ₂ (a) PHA-1 and Halogenated PHAs, (b) PHAs With Methoxy Groups, and (c) PHAs With Phosphinate or Phosphate Groups	3-6
3-5	Effects of Oxygen on the Decomposition of PHA-1 and Its Derivatives (a) PHA-1 and Its Methoxy Derivative, (b) Halogenated PHAs, and (c) Phosphate PHAs, (1) in N ₂ and (2) in Air	3-8
3-6	High-Temperature DSC Curves of PHA-1 and Its Derivatives (a) PHA-1 and Halogenated PHAs, (b) PHAs With Methoxy groups, and (c) PHAs With Phosphinate or Phosphate Groups	3-9
3-7	Derivative TGA Curves of PHA-1 and Its Derivatives (a) PHA-1 and Halogenated PHAs, (b) PHAs With Methoxy Groups, and (c) PHAs With Phosphinate or Phosphate Groups	3-12
3-8	Infrared Spectra of PHA-1 at Different Temperatures	3-14
3-9	Pyrolysis GC/MS Traces of PHA-1 and Its Derivatives (Heating to 930°C at 4.3°C/s) (a) PHA-1, (b) PHA-3, (c) PHA-5, (d) PHA-7, (e) PHA-10, and (f) PHA-12	3-16
3-10	Pyrolysis GC/MS Traces of PHA-1 at Different Temperature Ranges (Heating Rate, 4.3°C/s) (a) 250° ~ 383°C and (b) 383° ~ 930°C	3-17
3-11	Pyrolysis GC/MS Traces of PHA-7 at Different Temperature Ranges (Heating Rate, 4.3°C/s) (a) 350° ~ 469°C and (b) 469° ~ 930°C	3-18
3-12	Pyrolysis GC/MS Traces of PHA-10 at Different Temperature Ranges (Heating Rate, 4.3°C/s) (a) 250° ~ 500°C and (b) 500° ~ 930°C	3-19
3-13	Presumed Cyclization of PHA and Its Derivatives	3-20
3-14	Water Generated by Intermolecular Reaction	3-20
3-15	Proposed Thermal Decomposition Mechanisms of PHAs	3-21
4-1	Structures of BPA-, Chalcon II-, and BPC II-Polyarylates	4-2

4-2	The TGA and DTG Curves of BPA-, Chalcon II-, and BPC II-Polyarylates	4-3
4-3	High-Temperature DSC Curves of BPA-, Chalcon II-, and BPC II-Polyarylates	4-4
4-4	Pyrolysis GC/MS Traces of BPA-, Chalcon II-, and BPC II-Polyarylates (Temperature Range: 250° ~ 930°C, Heating Rate: 4.3°C/s) (a) BPA-Polyarylate, (b) Chalcon II-Polyarylate, and (c) BPC II-Polyarylate	4-5
4-5	Ultraviolet Spectra of Polyarylates Containing Chalcon II-Monomer (a) Homopolymers and (b) BPA-Chalcon II Copolymers	4-6
4-6	Photo-Cross-Linking of Chalcon II-Polyarylate	4-7
4-7	Thermal Decomposition of Chalcon II-Polyarylate After UV/Visible-Exposure (a) Full TGA Curves and (b) Initial Decomposition	4-7
4-8	Thermal Decomposition of Chalcon II-BPC II Copolymers (The Numbers Are Molar Ratios) (a) TGA and (b) DSC	4-8
4-9	Thermal Decomposition of BPA-Chalcon II-BPC II Terpolymers (The Numbers Are Molar Ratios) (a) TGA and (b) DSC	4-9
4-10	Ternary Plot of Flammability of Copolymers and Terpolymers	4-10
4-11	Composition and Flammability Relationship of Copolymers (a) Heat Release Capacity, (b) Total Heat Released, (1) BPA-Chalcon II, (2) BPA-BPC II, and (3) Chalcon II-BPC II	4-11
4-12	The TGA Curves of PSF (BPA-)/BPC II-Polyarylate Blends (a) PSF/BPC II- Polyarylate and (b) BPA-/BPC II-Polyarylate	4-12
4-13	The TGA Curves of PS (PEO)/BPC II-Polyarylate Blends (a) PS/BPC II- Polyarylate and (b) PEO/BPC II-Polyarylate	4-13
4-14	Structure-Composition-Flammability of Blends Containing BPC II-Polyarylate (a) Heat Release Capacity, (b) Total Heat Released, and (c) Char Yield, (1) PS, (2) PEO, (3) BPA-polyarylate, and (4) PSF	4-14
5-1	Thermal Decomposition of PMMA/Clay Nanocomposites	5-6
5-2	Thermal Decomposition of PEEK and Its Composites in N ₂	5-7
5-3	Thermal Decomposition of PEEK and Its Composites in Air	5-8
5-4	High-Temperature DSC Curves of PEEKs	5-8
5-5	Pyrolysis GC/MS Traces of PEEK (a) 300°-930°C, 4.3°C/s; (b) 300°-930°C, 10°C/ms; and (c) 585°-590°C, 10°C/min	5-10

5-6	Cone HRR Curves of PEEK and Its Composites	5-11
5-7	Thermal Decomposition of Xydar [®] and Its Composites in N ₂	5-12
5-8	High-Temperature DSC Curves of Xydar [®] and Its Composites	5-13
5-9	Thermal Decomposition of Xydar [®] Materials in Air	5-14
5-10	Pyrolysis GC/MS Traces of Xydar [®] (4.3°C/s to 930°C)	5-15
5-11	Ohio State University HRR Curves of Xydar [®] Composites by Thermopile	5-15
5-12	Cone HRR Curves of Xydar [®] Composites	5-17
5-13	Thermal Decomposition of PPA Materials (a) A-1000 Series and (b) A-6000 Series	5-18
5-14	High-Temperature DSC Curves of PPA Materials	5-19
5-15	Pyrolysis GC/MS Traces of PPA Materials (Pyrolysis Condition: 300°~930°C at a Heating Rate of 4.3°C/s for (a) A-1000; (b) A-6000; (c) AF-1133 V-0; (d) AFA-6133 V-0, 10°C/min for (e) AF-1133 V-0, 400°~405°C; and (f) AFA-6133 V-0, 405°~410°C)	5-20
5-16	Ohio State University HRR Curves of A-1000 Series	5-23
5-17	Ohio State University HRR Curves of A-6000 Series	5-25
5-18	Cone HRR Curves of A-1000 Series	5-25
5-19	Cone HRR Curves of A-6000 Series	5-26
5-20	Composition of Phosphate-Retarded Epoxy Resin	5-28
5-21	Thermal Decomposition of Epoxy/Phosphate Composites (a) DMMP, 20°C/min; (b) TMP, 40°C/min; and (c) TPP, 40°C/min	5-29
5-22	Pyrolysis GC/MS Traces of Epoxy/DMMP Composites (Heat Rate, 4.3°C/s) (a) 150°~300°C and (b) 300°~930°C	5-30
5-23	Cone HRR Curves of Epoxy/TMP Composites	5-32
5-24	Ignition Time of Polymers Under Different External Heat Fluxes	5-33
5-25	Peak Heat Release Rate of Polymers Under Different External Heat Fluxes	5-34
5-26	Correlations of PHRR Between Different Flammability Tests	5-37

5-27	Correlations of Total Heat Released Between Different Flammability Tests	5-38
6-1	Chemical Structures of Polysulfones	6-2
6-2	Thermogravimetric Analysis and DTG Curves of Polysulfones in N ₂	6-2
6-3	The TGA and DTG Curves of Polysulfones in Air	6-3
6-4	High-Temperature DSC Curves of Polysulfones	6-3
6-5	The TGA and DTG Curves of Polysulfones at Different Heating Rates (a) PSU, (b) PES, and (c) PPhS	6-5
6-6	Kissinger Plot of Polysulfones Decomposed in N ₂	6-6
6-7	Pyrolysis GC/MS Traces of Polysulfones (a) PSU, (b) PES, and (c) PPhS	6-7
6-8	The OSU HRR Curves of Polysulfones Measured by Thermopile	6-9
6-9	Cone HRR Curves of Polysulfones	6-11
6-10	Schematic Structures of Polycarbynes and Polysilynes	6-12
6-11	The TGA and DTG Curves of Polycarbynes	6-12
6-12	The TGA and DTG Curves of Polysilynes	6-13
6-13	Chemical Structures of Polymethacrylates	6-14
6-14	The TGA and DTG Curves of Polymethacrylates	6-15
6-15	Thermal Decomposition Products of Polymethacrylates (a) Ethyl Methacrylate, (b) Isobutyl Methacrylate, and (c) Benzyl Methacrylate	6-16
6-16	Chemical Structures of Cyano-Substituted Polymers	6-17
6-17	The TGA and DTG Curves of Cyano-Substituted Polyamides	6-17
6-18	The TGA and DTG Curves of PA-CN(X) and Poly(Azomethine) Compared With Technora [®] and Kevlar [®]	6-18
6-19	High-Temperature DSC Curves of CN-Substituted Polymers	6-18
6-20	Pyrolysis GC/MS Traces of PA-CN (X) and Poly(Azomethine) (a) Technora [®] , (b) PA-CN (25), (c) PA-CN (50), and (d) Poly(Azomethine)	6-19
6-21	Copolymerization of Polyethylene With POSS-Norbornene	6-21
6-22	The TGA and DTG Curves of the PE/POSS Copolymer	6-21

6-23	Flammability-Composition Relationship of PE/POSS Copolymers	6-22
6-24	Synthesis of Cross-Linked Epoxy Vinyl Ester Resins Based on BPC I and II	6-23
6-25	The TGA and DSC Curves of BPC II-Based Epoxy Vinyl Ester Resins (B Series) (a) TGA and (b) DSC	6-24
6-26	Pyrolysis GC/MS Traces of BPC I-Based Epoxy Vinyl Ester Resin A1 (a) 170°~330°C and (b) 170°~930°C	6-25
6-27	The TGA Curves of PMMA/PS Copolymers by Radical Polymerization	6-26
6-28	Flammability-Composition Relationship of PMMA/PS Random Copolymers	6-27
6-29	Thermal Decomposition Processes of PMMA/PS Blends	6-27
6-30	Flammability-Composition Relationship of PMMA/PS Blends	6-28
6-31	The TGA and DTG Curves of PMMAs With Different Molecular Weights (a) TGA and (b) DTG	6-29
6-32	The PCFC Curves of PMMAs With Different Molecular Weights	6-30
6-33	Thermal Decomposition of PS With Different Molecular Weights	6-31
6-34	Thermal Decomposition of PEO With Different Molecular Weight	6-32
6-35	Thermal Decomposition of PMMAs With Low Molecular Weight	6-33
6-36	The TGA and DTG Curves of PS/TEMPO Blends	6-34
6-37	The TGA and DTG Curves of PMMA/TEMPO Blends	6-35
6-38	TEMPO-Initiated PMMA/PS Copolymers	6-35
6-39	The TGA and DTG Curves of TEMPO-Initiated PMMA/PS Copolymers	6-36
6-40	Flammability-Composition Relationship of PMMA/PS Copolymers Initiated by TEMPO	6-36
6-41	Pyrolysis GC/MS Traces of PMMA/PS Copolymers (a) Random Copolymer and (b) TEMPO Initiated	6-37
6-42	Effects of TEMPO on Polymer Decomposition	6-37
7-1	Thermal Decomposition Processes of PHA and Its Derivatives	7-2
7-2	Possible Thermal Cyclization Mechanism of PHA and Its Derivatives	7-2

7-3	Bond Dissociation Energies of PHA, Its Methoxy and Phosphate Derivatives (unit in kJ/mol)	7-3
7-4	Molecular Structures of the Model Compound	7-4
7-5	Proposed Cyclization Mechanism of PHA	7-4
7-6	Keto-Enol Rearrangement by a Direct Hydrogen Shift	7-4
7-7	Keto-Enol Rearrangement by a Six-Member Ring Transition State	7-5
7-8	Enol-Structure Transformations by Rotation and Bending	7-6
7-9	Cyclization Into PBO Through ENL2 Intermediate	7-6
7-10	Cyclization Into PBO Through ENL4 Intermediate	7-7

LIST OF TABLES

Tables	Page
2-1 Cross-Section Regression Coefficients	2-3
2-2 Thermal Decomposition Properties of Polymers	2-9
2-3 Flammability of Different Polymers (930°C at 4.3°C/s)	2-17
2-4 Bond Dissociation Energies of Polymers	2-19
2-5 Bond Dissociation Energies in Aliphatic-Aromatic Polymers	2-20
2-6 Correlation Between Different Methods	2-22
3-1 Thermal Decomposition of PHA and Its Derivatives in N ₂	3-4
3-2 Flammability of PHA and Its Derivatives	3-11
3-3 Elemental Analyses of PHA-1 and Its Chars at Different Temperatures	3-13
3-4 Infrared Band Assignments of PHA and PBO	3-14
4-1 Flammability and Thermal Decomposition of BPA-Polyarylates	4-3
4-2 Flammability and Thermal Decomposition of Homopolyarylates	4-4
4-3 Flammability and Thermal Decomposition of Co- and Terpolymers	4-10
5-1 Sample Compositions	5-3
5-2 Flammability and Thermal Decomposition of PMMA/Clay Nanocomposites	5-6
5-3 Gel Permeation Chromatography GPC Results of PMMAs	5-7
5-4 Thermal Decomposition Properties of PEEKs	5-9
5-5 Flammability of PEEKs Measured by PCFC	5-11
5-6 Flammability of PEEKs Measured by the Cone Calorimeter	5-11
5-7 Thermal Decomposition Properties of Xydar [®] Materials in N ₂	5-13
5-8 Thermal Decomposition Properties of Xydar [®] Materials in Air	5-14
5-9 Flammability of Xydar [®] and Its Composites by PCFC	5-14
5-10 Ohio State University Results of Xydar [®] Composites	5-16

5-11	Cone Calorimeter Results of Xydar [®] Composites	5-17
5-12	Thermal Decomposition and Flammability of PPA Materials	5-22
5-13	Flammability of A-1000 Series Measured by the OSU Calorimeter	5-23
5-14	Flammability of A-6000 Series Measured by the OSU Calorimeter	5-24
5-15	Cone Calorimeter Results of PPA Materials	5-27
5-16	Thermal Decomposition and Flammability of Epoxy/Phosphate Composites	5-31
5-17	Cone Calorimeter Results of Epoxy/TMP Composites	5-31
5-18	Critical Heat Flux and Thermal Property Calculated From the Cone Calorimeter	5-33
5-19	Material Flammability Obtained by Cone Calorimeter Data	5-35
5-20	Flammability Measured by PCFC, OSU, and Cone Calorimeters	5-36
6-1	Thermal Decomposition Properties of Polysulfones	6-4
6-2	Bond Dissociation Energies and Activation Energies of Polysulfones	6-6
6-3	Flammability of Polysulfones Measured by PCFC	6-8
6-4	Flammability of Polysulfones Measured by the OSU Calorimeter	6-8
6-5	Flammability of Polysulfones Measured by the Cone Calorimeter	6-10
6-6	Flammability and Thermal Decomposition of Polycarbines and Polysilynes	6-14
6-7	Flammability and Thermal Decomposition of Polymethacrylates	6-15
6-8	Flammability and Thermal Decomposition of PA-CN(X) Polyamides	6-20
6-9	Thermal Decomposition Products of PE/POSS Copolymers	6-21
6-10	Flammability and Thermal Decomposition of PE/POSS Copolymers	6-22
6-11	Composition of BPC-Based Epoxy Vinyl Ester Resins (wt%)	6-23
6-12	Thermal Decomposition and Flammability of BPC-Based Epoxy Vinyl Ester Resins	6-25
6-13	Flammability and Thermal Decomposition of PMMA/PS Copolymers	6-27
6-14	Flammability and Thermal Decomposition of PMMA/PS Blends	6-28
6-15	Flammability and Thermal Decomposition of PMMAs	6-30

6-16	Flammability and Thermal Decomposition of PS	6-31
6-17	Flammability and Thermal Decomposition of PEOs	6-32
6-18	Flammability of PS/TEMPO Blends	6-34
6-19	Flammability of PMMA/TEMPO Blends	6-35
6-20	Flammability and Thermal Decomposition of PMMA/PS Copolymers Initiated by TEMPO	6-36

LIST OF ACRONYMS

BPA	Bisphenol A
BPC II	Bisphenol C
CO	Carbon monoxide
Cov	Coefficient of variation
CTMA Br	Cetyltrimethylammonium
CUMIRP	Center for University of Massachusetts/Industry Research on Polymers
DMAc	N,N-dimethylacetamide
DMMP	Dimethoxy methyl phosphate
DMSO	Dimethyl sulfoxide
DSC	Differential scanning calorimetry
DTG	Derivative of thermogravimetric
EHC	Effective heat of combustion
FAA	Federal Aviation Administration
FH	Fluorohectorite
FTIR	Fourier Transform Infrared Spectroscopy
GC	Gas chromatography
H/C	Hydrogen to carbon ratio
HCl	Hydrogen chloride
HDPE	High-density polyethylene
HF	Hartree-Fock
HRR	Heat release rate
HRR _{av}	Mean value from t _{ig} to 180 sec. after
IR	Infrared spectroscopy
LOI	Limiting oxygen index
MMT	Montmorillonite
M _p	Molecular weights
MS	Mass spectrometry
N ₂	Nitrogen
NBS	National Bureau of Standards
NIST	National Institute of Standards and Technology
NMP	N-methylpyrrolidinone
OSU	Ohio State University
P(α-M-S)	Poly(α-methyl styrene)
PAN	Poly(acrylonitrile)
PBI	Polybenzimidazole
PBO	Polybenzoxazole
PBT	Poly(butylene terephthalate)
PBZT	Polybenzthiazoles
PC	Polycarbonate
PCFC	Pyrolysis-combustion flow calorimeter
PDMS	Polydimethylsiloxane
PE	Polyethylene
PEEK	Poly(ether ether ketone)
PEO	Poly(ethylene oxide)
PES	Poly(ether sulfone)

PET	Poly(ethylene terephthalate)
PHA	Poly(hydroxyamide)
PHRR	Peak heat release rate
PI	Polyimide
PMMA	Poly(methyl methacrylate)
POB	Polybenzoxazole
POM	Poly(oxymethylene)
POSS	Polyhedral Oligomeric Sisesquioxanes
PP	Polypropylene
PPA	Polyphthamide (Amodel®)
PPhS	Poly(phenyl sulfone)
PPO	Poly(phenylene oxide)
PS	Polystyrene
PSF	Polysulfone
PSU	BPA-polysulfone
PTFE	Poly(tetrafluoroethylene)
PVC	Poly(vinyl chloride)
S	Styrene
SEA	Smoke extinction area
STA	Simultaneous thermal analysis
TGA	Thermogravimetric analysis
THF	Tetrahydrofuran
THR	Total heat released
TIC	Total ionization current
TMP	Trimethyl phosphate
TPP	Triphenyl phosphide
UV	Ultraviolet

EXECUTIVE SUMMARY

The intrinsic relationships between polymer structure, composition, and fire behavior have been explored to develop new fire-safe polymeric materials.

Different experimental techniques, i.e., three milligram-scale methods (pyrolysis-combustion flow calorimetry (PCFC), simultaneous thermal analysis, and pyrolysis gas chromatography/mass spectrometry (GC/MS)), have been combined to fully characterize the thermal decomposition and flammability of polymers and polymer composites. Thermal stability, mass loss rate, char yield, and properties of decomposition volatiles were found to be the most important parameters in determining polymer flammability. Most polymers decompose by either an unzipping or a random chain scission mechanism with an endothermic decomposition of 100-900 J/g. Aromatic or heteroaromatic rings, conjugated double or triple bonds, and heteroatoms such as halogens, N, O, S, P, and Si, are the basic structural units for fire-resistant polymers. The flammability of polymers can also be successfully estimated by combining the pyrolysis GC/MS results or chemical structures with the thermogravimetric analysis.

The thermal decomposition and flammability of two groups of inherently fire-resistant polymers—poly(hydroxyamide) (PHA) and its derivatives and bisphenol C (BPC II) polyarylates—have been systematically studied. PHA and most of its derivatives have extremely low heat release rates and very high char yields upon combustion. PHA and its halogen derivatives can completely cyclize into quasi-polybenzoxazole structures at low temperatures. However, the methoxy and phosphate derivatives show a very different behavior during decomposition and combustion. Molecular modeling shows that the formation of an enol intermediate is the rate-determining step in the thermal cyclization of PHA. BPC II-polyarylate is another extremely flame-resistant polymer. It can be used as an efficient flame-retardant agent in copolymers and blends. From the PCFC results, the total heat of combustion of these copolymers or blends changes linearly with composition, but the change of maximum heat release rates also depends on the chemical structure of the components.

The flammability of various polymers and polymer composites measured by PCFC; cone calorimeter, ASTM E1354; and the Ohio State University (OSU) calorimeter, ASTM E906, were also compared. For pure polymers, there was a relatively good correlation between different methods. However, for polymer composites with inert fillers or flame-retardant additives, the OSU and cone calorimetries are more suitable evaluation methods.

1. FIRE AND POLYMERS.

1.1 INTRODUCTION.

Polymers are widely used in many applications. However, most polymers, like the majority of other organic compounds, will burn readily in air or oxygen. The flammability of polymers is a serious issue and severely limits their applications [1 and 2]. Recent fire safety concerns put even more stringent requirements for the materials used in enclosed and inescapable areas, such as electronic enclosures, high-rise buildings, submarines, ships, and aircraft cabins [3]. Lightweight, high-performance polymeric materials offer many advantages in these applications over conventional metal and ceramic materials, but they greatly increase the fire risk because of their flammability and possible release of toxic by-products.

According to some studies, about 20% of those who die in airplane crashes are killed by fire, most often because several tons of polymers used in seat fabrics, overhead bins, and wall and windows will burn, leaving passengers limited time to escape [4]. In order to improve aircraft safety, the Federal Aviation Administration (FAA) initiated a long range Fire Research Program in 1995. The long-term objective is “to eliminate burning aircraft cabin materials as a cause of death,” which will require an order-of-magnitude reduction in cabin fire hazards relative to current cabin materials [5]. For this reason, sponsored by the FAA, National Institute of Standards and Technology (NIST), the U.S. Army, and industry, the Center for University of Massachusetts/Industry Research on Polymers (CUMIRP) established a new research cluster, Fire-Safe Polymers and Polymer Composites, which involved synthesis, characterization, modeling, and processing. The goal of this cluster was not only to develop new fire-safe materials to be used in future commercial aircraft, but also to understand the thermal decomposition and fire-resistance mechanisms on a molecular level to reduce unwanted fires and extend polymer applications.

The research conducted in this report was part of the CUMIRP Cluster F program and was focused on the following fundamental studies:

- Developing and using new experimental techniques to characterize the thermal decomposition and flammability of polymers;
- Establishing the correlation between polymer structure, composition, and their macroscopic flammability;
- Understanding the effects of various flame-retardant additives on the polymer flammability;
- Deducing polymer thermal decomposition and fire-resistance mechanisms.

Different experimental techniques, i.e., pyrolysis gas chromatography/mass spectrometry (GC/MS), simultaneous thermal analysis (STA), and pyrolysis-combustion flow calorimetry (PCFC), were combined to measure the flammability and thermal decomposition of different polymeric materials. All three methods required only a very small amount of sample (about a milligram or less), so they are especially suitable for research materials that are only available in

limited quantities. As a result, these methods are efficient screening tools for newly synthesized fire-safe materials. By discovering the intrinsic relationships between polymer structures, composition, and their fire behavior, the research goal is to help identify and design new fire-safe polymeric materials.

1.2 POLYMER COMBUSTION PROCESS.

Many polymers, if subjected to some suitable ignition sources, will undergo self-sustained combustion in air or oxygen [6]. In general, nonpolymeric materials (e.g., matches, cigarettes, torches, or electric arcs) are the main sources of ignition, but polymers are most frequently responsible for the propagation of a fire. A burning polymer constitutes a highly complex combustion system. Chemical reactions may take place in three interdependent regions: within the condensed phase, at the interface between the condensed phase and gas phase, and in the gas phase.

Polymer combustion occurs as a cycle of coupled events [7]: (1) heating of the polymer, (2) decomposition, (3) ignition, and (4) combustion. The polymer is first heated to a temperature at which it starts to decompose and gives out gaseous products that are usually combustible. These products then diffuse into the flame zone above the burning polymer. If there is an ignition source, they will undergo combustion in the gas phase and liberate more heat. Under steady-state burning conditions, some of the heat is transferred back to the polymer surface, producing more volatile polymer fragments to sustain the combustion cycle. This process is shown in figure 1-1.

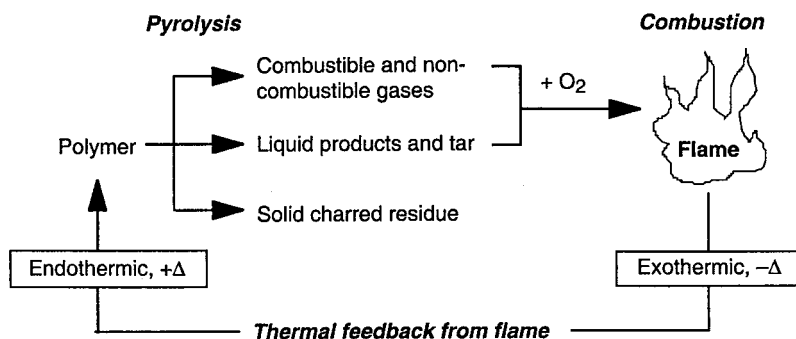


FIGURE 1-1. SCHEMATIC DIAGRAM OF POLYMER BURNING [8]

There are two types of combustion involved when polymers are burned: flaming combustion and nonflaming combustion [9].

Flames are self-propagating combustion reactions in which both the fuel and the oxidant are present in the gas phase. Since most polymers are hydrocarbon based, the flame above burning polymers is usually a hydrocarbon flame. The principal reactions in the flames are free-radical reactions. The most important radicals in hydrocarbon flames are simple species such as H·, O·, and OH·, and a small amount of HO₂·, HCO·, and CH₃·. Chain-branching reactions in the

combustion process, for example $H\cdot + O_2 \rightarrow HO\cdot + O\cdot$, can accelerate the burning of polymers by generating more radicals. Smoke formation in flames is highly dependent on the structure of the gaseous fuel and on the fuel-to-oxidant ratio. Normally, polymers containing purely aliphatic structural units produce relatively little smoke, while polymers with aromatic groups in the main chain produce intermediate amounts of smoke.

Nonflaming combustion, including smouldering and glowing combustion, propagates through the polymer by a thermal front or wave, involving the surface oxidation of the pyrolysis products [7]. Glowing combustion differs from smouldering combustion in that it is accompanied by pale flames of carbon burning to form carbon monoxide. Smouldering combustion usually occurs with polymeric materials of high-surface area that can form a residual carbonaceous char. It is generally accompanied by the generation of smoke due to pyrolysis at or near the surface. Glowing combustion occurs after the initial charring of the material.

From a practical point of view, it is also important to consider the associated fire hazards. The effects resulting from polymer combustion, which can threaten human life, include oxygen depletion, flame, heat, smoke, hot and toxic combustion gases, and structural failure. The two major causes of fire-related deaths are inhalation of toxic gases and burns [10 and 11].

1.3 STANDARD ASSESSMENTS AND TESTS.

To fully evaluate the fire behavior of different polymers, it is necessary to develop standard tests for assessing the flammability and other combustion-related properties of polymers. Most countries have standards and codes for the classification of materials with respect to their combustion behavior, but the experimental setup used in existing standard tests varies considerably, according to the nature, shape, and size of the polymeric materials to be tested. The fire tests most commonly used in the USA are the UL 94 small-flame test [12], the ASTM E 84 Steiner Tunnel [13], and the ASTM E 622 National Bureau of Standards (NBS) smoke chamber [14]. However, these tests can be used only as guides and suffer from problems with precision and reproducibility.

The majority of fire tests used now are concerned with the determination of the following fire properties of materials [10].

- Ease of ignition—how readily a material ignites
- Flame spread—how rapidly fire spreads across a surface
- Fire endurance—how rapidly fire penetrates a wall or barrier
- Rate of heat release—how much heat is released and how quickly
- Ease of extinction—how rapidly or how easily the flame chemistry leads to extinction
- Smoke evolution—amount, evolution rate, and composition of smoke released during stages of a fire

- Toxic gas evolution—amount, evolution rate, and composition of gases released during stages of a fire

Among them, the oxygen concentration test is a very important ignition test, from which the limiting oxygen index (LOI) [15] can be obtained. The LOI is defined as the minimum oxygen concentration at ambient temperature needed in an inert gaseous medium for the material to achieve sustained burning after ignition. The precision and reproducibility of the results are two reasons for the wide acceptance of this method.

According to the research done at NIST [16], the heat release rate (HRR) is the most important variable in a fire. Therefore, it is easy to assess the fire hazard of a product by measuring the HRR in a realistic large-scale test or predicting it from small-scale engineering tests. The heat release calorimeters are available in three scales: room-scale, single full-article scale, and small-scale, also known as bench-scale. The small-scale cone calorimeter is the one used by most polymer and flame retardant additive manufacturers [17]. For air transportation, the FAA has a number of flammability requirements [18]. The most important is the test for cabin wall materials using the Ohio State University (OSU) HRR apparatus. The criteria used by the FAA are very strenuous, and only advanced composites especially designed for aircraft use are normally able to pass the requirements.

1.4 FLAME-RETARDANT CHEMISTRY.

When a polymer breaks down in thermal decomposition, the following types of products may be formed [7]: (1) combustible gases, e.g., methane, ethane, and carbon monoxide; (2) noncombustible gases, e.g., carbon dioxide, hydrogen chloride, and hydrogen bromide; (3) liquids, which are often partially degraded polymers; (4) finely divided solid particles consisting of decomposing polymer fragments or soot in the combustion gases; and (5) discrete solids in the form of a carbonaceous residue or char. The evolution of large volumes of highly flammable gases will clearly tend to increase the flammability of polymers. Liquid products are not as readily combustible as gaseous products, but liquids can spread heat to adjacent parts of the polymer structure. Therefore, reducing the amount and speed of generation of combustible gases and preventing flame spreading are the most basic methodologies to achieve flame retardancy.

Generally, there are two mechanisms by which polymer combustion can be inhibited [10]. One is solid-phase inhibition, involving changes in the polymer substrates. Low-density, high-porosity chars tend to be the most desirable decomposition products from the nonflammability point of view. The chars can have the useful functions including helping to preserve structural integrity, insulating the underlying polymer from the heat of the flame, and preventing production of new fuel and further burning. However, a char sometimes undergoes smoldering combustion, leading to the formation of large amounts of smoke. This effect usually happens only at very high temperatures. Another very important factor in the polymer combustion cycle is the net heat of combustion of the gaseous products, which is the heat released by the combined combustion reactions minus the heat needed to bring the polymer from its initial state to the combustion stage. Therefore, if a system can evolve water and some other noncombustible gases or have large endothermic demands for thermal decomposition, the flammability can be reduced.

The other flame-retardant mechanism is vapor-phase inhibition, involving changes in the flame chemistry. In these systems, reactive species such as bromine and chlorine are built into the polymer and are transformed into volatile free-radical inhibitors during burning, such as hydrogen chloride (HCl). These materials diffuse into the flame and inhibit the radical reactions by changing highly reactive species $H\cdot$ and $HO\cdot$ into less reactive $Br\cdot$ and $Cl\cdot$. Two examples of the radical scavenge reactions are $H\cdot + HCl \rightarrow H_2 + Cl\cdot$ and $HO\cdot + HCl \rightarrow H_2O + Cl\cdot$. As a result, the combustion cycle is interrupted.

For many materials, both solid and vapor-phase inhibition are involved. It is difficult in practice to distinguish among the different mechanisms by which the flaming combustion of an organic polymer is being inhibited.

1.5 INHIBITION OF POLYMER COMBUSTION.

The most efficient way to prevent polymer combustion is to design inherently fire-resistant polymers that have high thermal stability, resistance to the spread of flame, and low burning rate even under high heat flux [19]. However, these materials are generally not easy to process and are very expensive. Another strategy is to use flame-retardant additives to inhibit the combustion of polymers, especially for the commodity polymers. The details about these two choices are discussed below.

1.5.1 Intrinsically Fire-Resistant Polymers.

Most polymers with high thermal stability are intrinsically fire resistant. Due to their high decomposition temperature, the initial breakdown will be effectively prevented and the combustion process will not be initiated. This high-temperature property of polymers can be improved by increasing the interactions between polymer chains or by chain stiffening [20]. Chain interactions can be enhanced by several means, such as increasing crystallinity, the introduction of polar groups, and hydrogen bonding. Chain stiffening can be accomplished by the use of aromatic or heterocyclic structures in the polymer backbone, such as in poly(p-phenylene), aromatic polyamides, and polyesters. In addition, polymers containing considerable numbers of aromatic groups in the structural units have great tendencies to condense into chars on heating. They, therefore, produce less flammable gaseous products in a flame. In all, polymers that have high thermal stability and generate less flammable volatiles on decomposition are the most desired fire-resistant polymers.

There are three general types of structures for the intrinsically fire-resistant polymers: linear single-strand polymers consisting of a sequence of cyclic aromatic or heterocyclic structures, ladder polymers, and inorganic or semiorganic polymers [20]. So far, most carbon-based, fire-resistant polymers are prepared by incorporating highly stable, rigid, aromatic, or heterocyclic ring systems directly into the polymer chain [21-23], such as polyimide (PI), polybenzoxazole (PBO), polybenzimidazole (PBI), and polybenzthiazoles (PBZT) (see figure 1-2). The synthetic routes to such polyaromatic heterocyclic polymers involve a two-step process in which soluble high-molecular-weight prepolymers are first synthesized, and then rigid stable rings are formed by thermally or chemically induced condensation of reactive groups on the polymer chains.

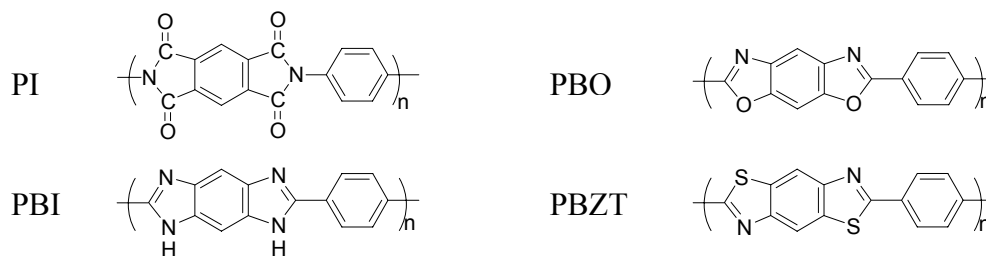


FIGURE 1-2. INTRINSICALLY FIRE-RESISTANT POLYMERS

Ladder polymers are a very special type of rigid-chain polymers [24 and 25]. These polymers are double-stranded structures consisting of two polymer chains periodically bound together by chemical bonds such as cyclized polyacrylonitrile ($\left(\text{C}_6\text{H}_2\text{N}_2 \right)_n$). In principle, these materials

should show superior thermal stability because the polymer chains cannot be severed by breaking a single bond.

The synthesis of inorganic and semiorganic polymers has been aimed at the production of stable, polymeric materials having linear chains consisting of such typical repeating units as silicon-nitrogen, boron-nitrogen, and phosphorus-nitrogen [26 and 27]. The nonburning characteristics of inorganic elements and the formation of nonflammable protective coatings are the two main reasons for the fire resistance of these polymers.

1.5.2 Flame-Retardant Additives.

From the manufacturing point of view, the introduction of flame-retardant additives undoubtedly constitutes the easiest way of making a polymer less flammable. There are two types of additives: reactive and additive flame retardants [28]. The reactive flame retardants are the compounds containing heteroatoms known to confer some degree of flame retardance, and they are built chemically into the polymer molecule. Alternatively, the additive flame retardant can be physically mixed with existing polymers. In this case, the compounds do not react chemically with the polymers. The flame retardants most abundantly used at the present time are based largely on six elements: boron, aluminum, phosphorus, antimony, chlorine, and bromine. In addition, nitrogen and silicon can also confer some degree of flame retardance. Other elements and their compounds have proved to be less effective. Combinations of flame retardants often have synergistic or antagonistic effects. Sometimes a heteroatom already present in the polymer backbone may interact with a flame retardant and, thus, exhibit synergism or antagonism.

Although additive flame retardants are widely used in polymers, there are some limitations such as poor compatibility, high volatility, deleterious effects on the properties of polymers, and increase of the production of carbon monoxide (CO) and smoke [29].

Flame-retardant additives can act by a variety of mechanisms in either the condensed phase or the gas phase [28]. They can terminate the free-radical reactions in the condensed phase, act as heat sinks due to their heat capacity, form a nonflammable protective coating or char to insulate the flammable polymer from the source of the heat and oxidant, and interrupt the flame

combustion in the gas phase. It is difficult, however, to unequivocally attribute a single mode of action to a particular additive or class of additives. Many flame retardants appear to be capable of functioning simultaneously by several different mechanisms, often depending on the nature of the organic polymers.

1.5.2.1 Inorganic Hydroxide Flame Retardants.

Inorganic hydroxides are a very important class of flame retardants due to their relatively low cost, ease of handling, and low toxicity [30]. Aluminium oxide trihydrate is used in the largest quantities by far as an inorganic flame retardant for polymers [31]. It is normally introduced into polymers in large quantities (>50% by weight) in order to attain a significant flame-retardant effect. This addition reduces the amount of combustible materials available for decomposition. During decomposition, this filler compound acts as a heat sink and, thus, delays the polymer from reaching its decomposition temperature [32]. When heated, it decomposes to form anhydrous alumina and releases water, which is an endothermic reaction. This energy consumption can remove the heat from the substrate, slow the decomposition of the substrate, and keep it below its ignition temperature. Also, water released into the vapor phase dilutes the concentration of the combustible gases. The oxide residue generated during decomposition has a relatively high heat capacity, which can reduce the heat transfer to the substrates. Another advantage of using inorganic hydroxides is that they can reduce the amount of smoke generated on combustion [33].

Due to its low thermal stability, aluminum oxide trihydrate should be used below 200°C. Other inorganic hydroxides and hydroxycarbonates [34] also have some flame-retardant action. For example, magnesium hydroxide is more thermally stable and can be used above 300°C.

1.5.2.2 Halogenated Flame Retardants.

Halogen-containing flame retardants make up one of the largest groups of additives in the plastic industry. As reactive flame retardants, halogen-containing alkenes, cycloalkanes, and styrene can be copolymerized directly with the corresponding nonhalogenated monomers [35]. As additive flame retardants, these organic-halogenated compounds are most commonly used in conjunction with phosphorus compounds or with metal oxides, especially antimony oxide. The stability of the halogen compounds goes as $F > Cl > Br > I$. Iodine compounds are not sufficiently stable to be used commercially, whereas the fluorine compounds are too stable to be generally useful. Bromine and chlorine compounds are the most generally used halogen-containing flame retardants. Bromine compounds are more effective than chlorine compounds on a weight basis, but they are considerably more expensive.

Halogen-containing flame retardants may function either in the vapor phase or in the condensed phase [29 and 35]. The action of the flame retardant depends on the structure of the additive and of the polymer. Generally, the radicals produced by thermal decomposition of a halogenated flame retardant can interact with the polymer to form hydrogen halide. Hydrogen halides inhibit the radical propagation reactions that take place in the flame by reacting with the most active radicals, H· and OH·. It also should be noted that aromatic-brominated compounds can produce large amounts of char.

Although halogen compounds are quite widely used on their own in flame retardants, their effectiveness is sometimes considerably increased by a free-radical initiator and antimony trioxide. Antimony-halogen systems can affect the combustion of polymers by their ability to act both in the gas and the condensed phases [7].

Although there is an increasing legislation against the use of halogenated compounds in disposable items that must be recycled or land filled, brominated and chlorinated flame retardants still occupy the largest share of the flame-retardant market.

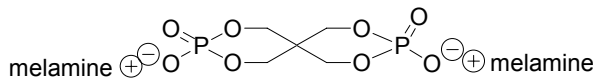
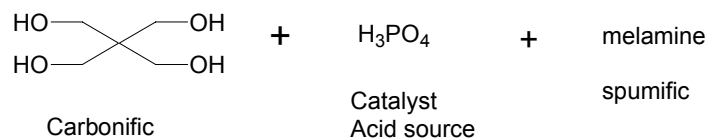
1.5.2.3 Phosphorus-Based Flame Retardants.

Both inorganic and organic phosphorus compounds are useful for imparting flame retardance to many polymers. Phosphorus flame retardants include elemental red phosphorus, water-soluble inorganic phosphates, insoluble ammonium polyphosphate, organophosphates and phosphonates, phosphine oxides, and chloroaliphatic and bromoaromatic phosphates [36].

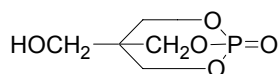
Both additive and reactive flame retardants are commercially available. Additive compounds, especially phosphates, are widely used for highly hydroxylated polymers such as cellulose. The most extensively employed reactive flame retardants are phosphorus-containing polyols used in polyurethane foams [37]. Other reactive flame retardants include vinyl and allyl phosphonates [38].

The flame-retardance mechanisms of these phosphorus compounds include the formation of a surface glass to protect the substrate from oxygen and flame, promoting of charring, and free-radical inhibition generally proposed for halogens [35]. The flame-retardant mechanism for phosphorus depends on the type of phosphorus compound and the chemical structure of the polymer. Phosphorus flame retardants containing halogens or nitrogen are often stated to exhibit synergistic behavior due to the formation of phosphorus halides or oxyhalides or P-N bonds on decomposition [39 and 40].

Recently, there is an increased interest in intumescent systems, which can develop a foamed char on the surface of the polymeric materials during burning. The combination of ammonium polyphosphate, dipentaerythritol, and melamine is the most commonly used intumescent flame-retardant system [41]. Generally, intumescence requires a carbonific (char former) such as a polyol, a catalyst or acid source such as a phosphate, and a spumific (gas generator) such as a nitrogen source. The mechanism involves decomposition of the phosphate to phosphoric acid, esterification of the polyol, and, subsequently, decomposition and regeneration of the phosphoric acid. Ammonium polyphosphate with a high ammonia content helps blow the forming char to a porous product. This surface char insulates the substrate from flame, heat, and oxygen. There are also some self-intumescent compounds that contain all three required functions in a single molecule (figure 1-3). Such intumescent coatings can satisfy environmental and toxicity issues because the coatings are halogen-free and the decomposition gases are water and ammonia.



Chargard 329 (Great Lakes Chemical)



CN-1197 (Great Lakes Chemical)

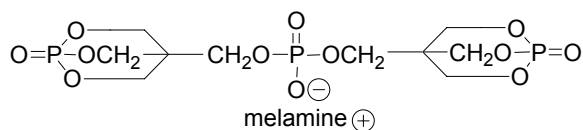


FIGURE 1-3. INTUMESCENT COMPOUNDS [41]

1.5.2.4 Nitrogen-Based Flame Retardants.

The presence of nitrogen in natural polymers appears to exert some degree of flame retardance, as shown by the relatively low flammability of wool, silk, and leather [42]. Synthetic polymers that contain nitrogen are not so resistant to combustion. A number of nitrogen-containing organic compounds are used as reactive flame retardants for certain polymers. These include triazines, isocyanates, urea, guanidine, and cyanuric acid derivatives [43]. Some of these compounds are also employed as additive flame retardants, often in conjunction with phosphorus compounds, to reduce the flammability of cellulosic textiles. In the latter cases, the nitrogen appears to act to a considerable extent by strengthening the attachment of phosphorus to the polymer, but nothing is yet certain about the mechanisms of action. One possible explanation is that the release of nitrogen or ammonia dilutes the volatile polymer decomposition products and, hence, makes them less flammable. Ammonium salts and metal-amine complexes have also been quite widely used as flame retardants for certain applications, such as ammonium phosphates for wood.

1.5.2.5 Silicon-Containing Flame Retardants.

There is a renewed interest in using silicon-based flame retardants as substitutes for the halogens or phosphorus [44]. Almost all forms of silicon have been explored: silicones, silicas, organosilanes, silsesquioxanes, and silicates. The most common flame retardant based on silicon is in the form of polyorganosiloxane, in particular, polydimethylsiloxane (PDMS). The flammabilities of the block copolymers of various types of polycarbonate (PC) and poly(ether imide) with PDMS [45] show significant decreases. Silicon can also be incorporated into the

branches of the polymer chains [46]. Under certain cases, the addition of silica can also affect the flammability properties of materials [47]. The formation of a silicon-based protective surface layer appears to be the flame-retardant mechanism for silicone and silica systems.

Polycarbosilane, polysilastyrene, and polysilsesquioxane preceramic polymers, shown in figure 1-4, are also used to blend with various thermoplastics, [48 and 49].

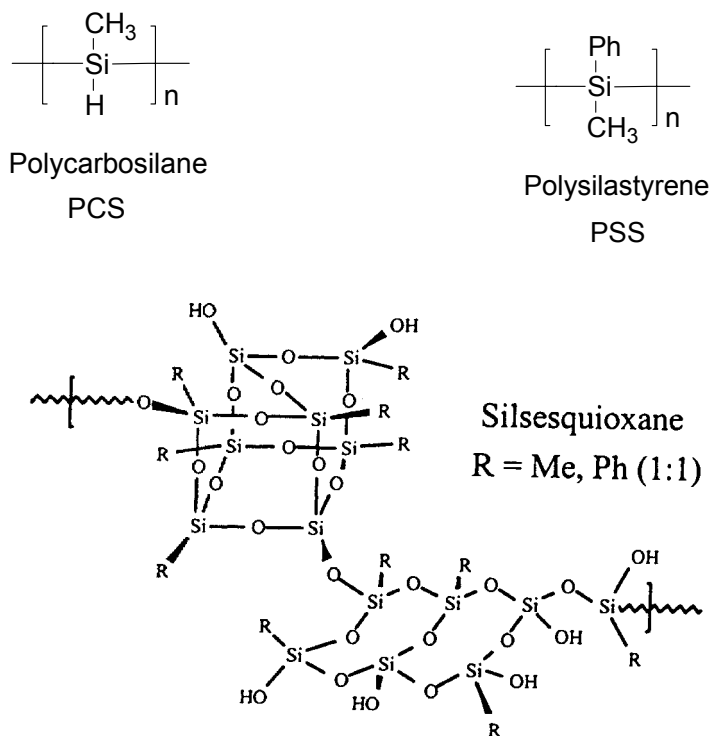


FIGURE 1-4. SOME PRECERAMIC POLYMERS

Studies [48 and 49] show that they are all effective flame retardants. They can reduce the peak HRR and average HRR, but the total heat released remains unchanged. The primary reason for the lower HRR for the blends is the reduced mass loss rate, i.e., the rate at which fuel is released into the gas phase is slowed by the presence of the ceramic char.

Recently, there is a great interest in the flammability properties of polymer-clay (layered-silicate) nanocomposites [50 and 51]. Cone calorimetry data show that both the peak and average heat release rate are reduced significantly for intercalated and delaminated nanocomposites with low silicate mass fraction (3%-5%), but there is little improvement in the char yield. Polymer-clay nanocomposites are materials that may fulfill the requirements for a high-performance, additive-type flame-retardant system.

In general, a condensed-phase mechanism, which involves a protective surface layer, is proposed for silicon-based flame retardants.

1.5.2.6 Boron-Based Flame Retardants.

Borate treatments were the first to be extensively applied to cotton and then to wool. Boric acid and borax are frequently used together [52]. On evaporation of the water of hydration, the polymers swell and an intumescent coating is formed on the surface, which insulates the bulk of the polymer from the heat source. The enhancement of the char formation, the endothermic dehydration process and the dilution of the gaseous breakdown products by the water released could be the reasons for the flame retardance of boron-containing additives. Cyclic borate esters have been used as durable additives for cellulose, and boric acid and polyols have been incorporated into rigid polyurethane foams [7].

1.5.2.7 Polymeric Flame Retardants.

Polymeric flame retardants have been much less studied than their small molecule counterparts even though they have many advantages. By the incorporation of a polymeric flame retardant, the physical and mechanical properties of the polymer are less affected. It can also avoid the outward diffusion in the system and consequent risk of environmental contamination. Polydibromostyrene and polyphosphazenes are among some of these flame retardants [53 and 54]. In a broad sense, all the fire-resistant polymers can be used as polymeric flame retardants to be blended with some other polymers to enhance fire retardancy. As a matter of fact, this is a very convenient way to adjust polymer flammability by composition.

1.6 THERMAL DECOMPOSITION MECHANISMS OF POLYMERS.

The thermal decomposition of polymers involves interacting chemical and physical processes [7 and 10]. The chemical processes are responsible for the generation of flammable volatiles and physical changes, such as melting and charring, can alter the decomposition and burning characteristics of a material. In most cases, a solid polymer, when heated to a certain temperature, will decompose to give varying amounts of volatile products and solid residues. These residues can be carbonaceous (char), inorganic (originating from heteroatoms contained in the original polymer, either within the structure or as a result of additive incorporation), or a combination of both. Many fire tests have shown that char formation is an important route to achieve flame retardancy, but little is understood about the detailed structure of char or how it forms. Van Krevelen [55] has proposed a two-step model for charring. Below 550°C, the polymers decompose to fuel gases, tars, and a primary char. On further heating above 550°C, the primary char is slowly converted to a conglomerate of loosely linked small graphitic regions, which is virtually independent of the structure of original polymers. Levchik and Wilkie [56] also proposed that the char formation of polymers includes the following steps: cross-linking, aromatization, fusion of aromatics, turbostratic char formation (an incomplete process of graphitization), and graphitization. The formation of char can be promoted through many chemical reactions, including graft copolymerization, Lewis acid catalysis, Friedel-Crafts chemistry, redox reactions, and the use of various additives. As to the structure of char, it is believed that char is composed of polynuclear aromatic compounds with heteroatoms (O, N, P, S), consisting of crystalline and amorphous regions.

The thermal decomposition processes for different polymers are varied and complex. The rate, mechanism, and product composition of these thermal decomposition processes depend on both the physical properties and chemical composition of the original material. In the thermal decomposition of organic polymers, four general mechanisms can be identified [7]: (1) random-chain scission (polyethylene), (2) end-chain scission (unzipping) (poly(methyl methacrylate)), (3) chain stripping (poly(vinyl chloride)), and (4) cross-linking (high-charring polymers). Some polymers undergo a reaction that exclusively belongs to one category. Others exhibit mixed behavior, depending on the structures of polymers. Many of the addition polymers, such as vinyl polymers, seem to decompose through a reverse polymerization (initiation, propagation, chain transfer, and termination) or random chain scission. Polymers prepared by a condensation process, such as polyesters and polyamides, decompose according to random chain scission followed by cross-linking into carbonaceous chars. However, the detailed decomposition mechanisms of different polymers are greatly dependent on their chemical structure and composition.

1.7 EXPERIMENTAL TECHNIQUES FOR THERMAL DECOMPOSITION OF POLYMERS.

To discover new fire-resistant polymers and to help understand how and why polymers burn using structure-property correlations, small-scale experimental techniques suitable for research materials need to be developed. Thermogravimetric analysis (TGA) is an important method to study the thermal reactions of polymers in the condensed phase [57]. By far, most experimental work has been carried out in an inert gas atmosphere. Few studies have been made of the influence of oxygen on the thermal decomposition of polymers. It was suggested that oxygen from the surrounding atmosphere is usually completely consumed in the flame zone so that the pyrolysis of the condensed-phase polymer takes place in the absence of oxygen [7]. However, some experimental results suggest that oxygen is also involved in the thermal decomposition of some polymers, but the extent of its involvement varies considerably with the nature of the polymer and the experimental conditions under which it burns [58].

TGA data can provide information about the thermal stability of various polymeric materials, the rate and amount of volatile products to which they give rise under a range of well-controlled conditions, and the amount of the corresponding solid residue. Experiments involve both isothermal weight-loss measurements and nonisothermal techniques. The isothermal technique requires almost instantaneous heating of the polymer sample to the desired temperature. The nonisothermal technique involves a programmed linear increase of sample temperature as a function of time. It is also very convenient for getting the mass loss rate versus time from the derivative of the thermogravimetric (DTG) data by differentiating the TGA curve. DTG is a good procedure to identify the temperature range at which the various stages of thermal decomposition take place and the order in which they occur. In addition to the rate of decomposition, the heat involved in the decomposition process is also of interest. Common differential scanning calorimetry (DSC) cannot be used for thermal decomposition process due to its low applicable temperature (below 600°C). Simultaneous STA with TGA and DSC performed at the same time to a high temperature of 1200°C is very useful in measuring the heat evolved or absorbed during decomposition.

In addition to the kinetics and thermodynamics of the thermal decomposition process, there are also concerns with the nature of the decomposition process. Pyrolysis GC/MS is a simple but rapid and extremely sensitive method to characterize the volatiles produced during polymer decomposition [59]. It is also capable of measuring the relative composition of the volatiles so that the heat of combustion of pyrolysis gases can be estimated. By identifying the decomposition products at different temperatures and different heating rates, the decomposition mechanism can be elucidated. There are also some other methods that can be used to characterize volatiles, such as infrared spectroscopy (IR) and thermal volatilization analysis [60].

Chars are complex materials that are usually insoluble. This limits their characterization to the tools used in solid-state chemistry and physics. The chemical structure of the char is usually characterized by elemental analysis. Other properties are characterized through microscopy, various spectroscopies, X-ray diffraction, and thermal conductivity [61].

In all, it is not easy to evaluate the fire behavior of polymers because the thermal decomposition processes of polymers are varied and complex, and the fire performance of polymers is also dependent on the test methods and experimental conditions used. There are still unsolved issues regarding the fire-retardant mechanisms. Therefore, a combination of techniques is essential to the understanding of the complex issue of fire-retardant polymers.

2. QUANTATIVE MEASUREMENTS ON THE THERMAL DECOMPOSITION AND FLAMMABILITY OF POLYMERS.

2.1 INTRODUCTION.

How to evaluate the fire performance of polymers accurately is a very important issue. There are already some standard tests for assessing the flammability of polymers, such as the oxygen concentration test [15], Underwriter Laboratories Test for Flammability of Plastic Materials (UL 94) [12], the ASTM E 84 Steiner Tunnel [13], the NBS smoke chamber tests [14], the cone calorimeter test [62], and the OSU calorimeter test [63].

However, all the standard tests available now require relatively large samples (at least tens of grams), and the results are highly dependent on the sample configuration and combustion conditions. Thus, it was recognized that it would be a great improvement if a new, small-scale, convenient, and quantitative test could be developed to measure flammability of materials. PCFC, which was designed by the FAA, is such a flammability test [64-66]. It is operated on the oxygen consumption principle, i.e., the net heat of complete combustion of typical organic molecules per mole of oxygen consumed is relatively constant, $C = 419 \pm 19 \text{ kJ/mol-O}_2 = 13.1 \pm 0.6 \text{ kJ/g-O}_2$, and independent of the chemical composition of the combusted materials. Using only milligram samples, it is an extremely good method to characterize materials that are only available in a small amount. The samples are pyrolyzed in an inert gas stream followed by high-temperature, nonflame combustion of the volatiles in excess oxygen. The heat release rate, total heat of combustion of the volatiles as well as the char yield can be directly obtained from PCFC. Heat release capacity (J/g-K), which is defined by dividing the heat release rate by the linear heating rate and sample weight, is a material flammability parameter that, in theory, depends only on the chemical composition of the solid. Therefore, it should be a reliable measure of the fire hazard of a material [64-66].

The correlations between PCFC and some standard tests, such as oxygen bomb calorimeter according to ASTM D 2382, cone calorimeter at 50 kW/m^2 incident heat flux according to ASTM E 1354 and UL 94, are all fairly good [67]. A transition from burning (HB) to self-extinguishing (V-0) behavior in the UL 94 test occurs over a relatively narrow range of heat release capacities, 300-400 J/g-K. In the PCFC method, pyrolysis is limited to small samples, so there is no temperature gradient and mass transfer limitation. Hence, the intrinsic material flammability can be evaluated. However, because the sample temperature is uniform during pyrolysis and combustion and the heat produced in combustion cannot be delivered back to pyrolysis process, the PCFC results do not exactly reflect the transient aspects of the fire behavior associated with sample thickness, temperature gradient, char buildup, heat feedback and some other physical processes in a real fire. In addition, complete combustion of the fuel gases in the high-temperature furnace is an equilibrium process and will not reflect the gas-phase, flame-retardant effect of some additives, which is kinetically based.

In this section, this new milligram-scale combustion calorimeter PCFC has been used to quantitatively measure polymer flammability. With the aid of two other experimental techniques, pyrolysis GC/MS (Py-GC/MS) and STA, the correlations between polymer structure, composition, and their thermal decomposition/flammability have been explored. By analyzing the decomposition products at different pyrolysis conditions using pyrolysis GC/MS and

measuring the corresponding decomposition process using STA, the heat release rates and total heats of combustion of polymers were calculated. By parametric fits of some mechanistic models to TGA data, the kinetic parameters, such as the activation energy of thermal decomposition, were determined. The bond dissociation energies of some polymers have also been calculated by using a quantum computational method, B3LYP density-functional method with a standard polarized split-valence 6-31G (d) basis set. The relationship of bond dissociation energies and activation energies of thermal decomposition was examined. Furthermore, the heat release rates, total heat released, and char yields of different polymers were estimated by using a simple calculation method based on the known chemical structure of polymers and TGA results.

2.2 METHODOLOGY OF FLAMMABILITY CALCULATIONS.

The three methods described above—pyrolysis GC/MS, STA and PCFC—are all essential in determining the fire properties of polymers. They are complementary to each other. By relating the results from one method to another, the whole decomposition and combustion process of polymers can be elucidated, and the validation of each method can also be achieved.

It was found that the heat released (Q_c) during transient heating of a material to or above its oxygen-free thermal decomposition temperature in time, t , is [64-66]

$$Q_c(t) = -\int_0^t \frac{d}{dx} [h_{c,v}^o(x)m_v(x)] dx \quad 2-1$$

where $h_{c,v}^o$ is the enthalpy of complete combustion per unit mass of volatile pyrolysis products and m_v is the amount of volatiles generated.

The peak heat release rate per unit mass is [64-66]

$$\dot{h}_c^{max} = \frac{\dot{Q}_c^{max}}{m_o} = \frac{h_{c,v}^o(T) dm(T)}{m_o dt} \Big|_{T=T_p} \quad 2-2$$

where

$h_{c,v}^o(T_p)$ is the net heat of complete combustion per unit mass of volatiles liberated at the peak mass loss rate temperature T_p

$\frac{1}{m_o} \frac{dm}{dt} \Big|_{T=T_p}$ is the maximum mass loss rate

The heat release capacity can be expressed as [64-66]:

$$\eta_c = \frac{\dot{h}_c^{max}}{\beta} = \frac{h_{c,v}^o(1-\mu)E_a}{eRT_p^2} = \frac{1}{\beta} \frac{C\Delta\dot{m}_{O_2}^{max}}{m_o} \quad 2-3$$

where β is the heating rate, μ is the char yield, and E_a is the activation energy, $C = 419 \pm 19$ kJ/mol-O₂ = 13.1 ± 0.6 kJ/g-O₂, and $\Delta \dot{m}_{O_2}^{max}$ is the instantaneous mass consumption rate of oxygen at the peak pyrolysis rate.

According to equation 2-1, the total heat of combustion of pyrolysis gases can be calculated by summing the heat of combustion of all the volatiles released during the entire decomposition process. In a similar way, the peak of heat release rate can be calculated from the maximum mass loss rate and the heat of combustion of the volatiles generated at that temperature, according to equation 2-2. These two parameters calculated from pyrolysis GC/MS and STA results should be comparable to those directly measured from PCFC experiments based on the oxygen consumption principle.

2.2.1 Calculation of the Composition of the Volatiles.

Although the qualitative analysis (or identification) of the decomposition products of most known polymers has been already performed and published, little has been done on the quantitative analysis of the pyrolysis gases by using mass spectrometry (MS) as a detector. It is because the total ionization current (TIC) signal from the MS does not directly correspond to the relative concentration of each volatile; neither does the area under each peak. There are relative response ratios (response factors) between them. Several models have been proposed to predict the response factors. One model presumes that only the total ionization cross sections of molecules are important in adjusting their total ion current differences. It has been found that equation 2-4 is valid for a large variety of molecules over a large range of pressure [68 and 69].

$$I_t = Q \cdot I_e \cdot d \cdot N \quad 2-4$$

where I_t is the total ion current, I_e is the ionizing electron current, Q is the total ionization cross section, d is the ionizing path length, and N is the concentration of the molecules.

Because few total ionization cross-section values are available in the literature, a method to predict the total ionization cross section is required. Fitch and Sauter [70] conducted a multiple linear regression analysis between the electron impact total ionization cross sections reported in the literature and the atomic composition. The regression equation is

$$Q = 0.082 + \sum a_i \cdot n_i \quad 2-5$$

where a_i and n_i are the coefficient and number of each of the eight atom types, H, C, N, O, F, Cl, Br, and I (see table 2-1).

TABLE 2-1. CROSS-SECTION REGRESSION COEFFICIENTS [70]

Atom	C	H	O	Cl	Br	I	F	N	S
a_i	1.43	0.73	1.10	3.98	5.19	6.62	0.61	1.20	3.80

The scheme is based on the additivity of atomic ionization cross sections. The coefficients for the calculation are determined by linear regression using 179 total ionization cross-section measurements taken from the literature. The largest errors are found in the group of inorganic gases. The average cross-section prediction error was found to be 4.69% by this approach.

In this section, this method is used to estimate the total ionization cross section of each volatile and then to calculate its relative concentration according to equation 2-4.

2.2.2 Calculation of Total Heat of Combustion and Heat Release Capacity of Polymers.

To calculate the total heat of combustion of polymers, the heats of combustion of all decomposition volatiles need to be known. It is not realistic to expect to find tabulated, experimental data on all organic compounds. Fortunately, the heat of combustion can be calculated from the heat of formation by using

$$\Delta_c H = \sum n_p \Delta_f H_p - \sum n_r \Delta_f H_r \quad (2-6)$$

where $\Delta_f H_p$ and $\Delta_f H_r$ are the heats of formation of products and reactants, respectively. The heats of formation of many simpler molecules have already been measured, and for more complex species, Benson's group additivity method [71] was used to estimate their heats of formation.

$$\Delta H_f = \sum n_i H_{f,i} \quad (2-7)$$

where $H_{f,i}$ is the contribution of the i th group to the heat of formation. After the heat of formation of a molecule is determined, its heat of combustion can be calculated according to equation 2-6. Then the net heat of combustion of polymer can be estimated by using equation 2-8.

$$\Delta H_c = (1 - \mu) \frac{\sum n_i \Delta H_{c,i}}{\sum n_i M_i} \quad (2-8)$$

where n_i (mol%) is the molar fraction of the i th decomposition volatile, $\Delta H_{c,i}$ (kJ/mol) is the heat of combustion of the i th component, M_i (g/mol) is the molar mass of the i th component, and μ is the char yield (g/g) at final temperature.

In addition, the maximum mass loss rate can be easily obtained from the derivative of TGA curves (DTG). Then, by analyzing the decomposition products at that temperature, the heat release capacity can be calculated according to equation 2-9

$$\eta = \left(\frac{1}{m_o} \cdot \frac{dm}{dt} \Big|_{max} \cdot \frac{\sum n_i \Delta H_{c,i}}{\sum n_i \cdot M_i} \Big|_{T=T_p} \right) \cdot \frac{1}{\beta} \quad (2-9)$$

where

$\frac{dm}{dt}|_{\max}$ (g/s) is the maximum mass loss rate

m_o (g) is initial sample mass

β (K/s) is the heating rate

2.3 EXPERIMENTAL.

2.3.1 Pyrolysis GC/MS.

The general configuration for pyrolysis GC/MS was the heated interface mounted on the top of the gas chromatography (GC) injection port. On the detection side of the GC (Hewlett-Packard 5890 Series II), a mass selective detector (Hewlett-Packard 5972 Series) was used. The pyroprobe was a commercial device (Pyroprobe 2000, CDS Analytical) connected with a heated interface to the GC/MS. The probe was 6.4 mm in diameter containing a 3-mm-diameter, 25-mm-long platinum resistance coil. The probe is capable of controlled linear heating rates ranging from 2×10^{-2} to 2×10^4 K/s, according to the manufacturer's literature. The column was a fused-silica capillary column (cross-linked 5% PH ME siloxane, 0.25 mm in diameter and 30 m long, Hewlett-Packard).

The samples were pyrolyzed in the heated interface, and the pyrolysis products were flushed directly into the column. The GC oven was then ramped at $10^\circ\text{C}/\text{min}$ from 36°C to 295°C and held at that temperature for 15 min. The masses scanned ranged from m/z 11 to 500.

Three pyrolysis conditions have been used:

1. Pyrolyzing the sample to 930°C at a heating rate of $4.3^\circ\text{C}/\text{s}$ and collecting all the decomposition volatiles (same conditions used in PCFC measurements).
2. Pyrolyzing the sample to 930°C at $10^\circ\text{C}/\text{ms}$ and collecting all the decomposition volatiles.
3. Pyrolyzing the sample at $10^\circ\text{C}/\text{min}$ to the temperature of maximum mass loss rate and only collecting the decomposition volatiles at $\pm 5^\circ\text{C}$ of that temperature.

2.3.2 Simultaneous Thermal Analysis.

The thermal decomposition process of polymers was investigated by the Rheometric Scientific Simultaneous Thermal Analyzer (STA 1500), which combines the complementary techniques of DSC and TGA in a single sample. It has a wide temperature range (ambient to 1500°C). Because it was assumed that the decomposition of polymers at a burning surface is anaerobic, all the experiments were done under a nitrogen atmosphere. To avoid mass and heat transfer effects, the sample weight was kept small, around 10 mg, and the heating rate was $10^\circ\text{C}/\text{min}$.

2.3.3 Pyrolysis-Combustion Flow Calorimeter.

The detailed information about PCFC can be found in the literatures [64-66]. The PCFC contains the following major parts: pyrolyzer, combustor, gas scrubbers, flow meters, oxygen analyzer, and data acquisition system (figure 2-1).

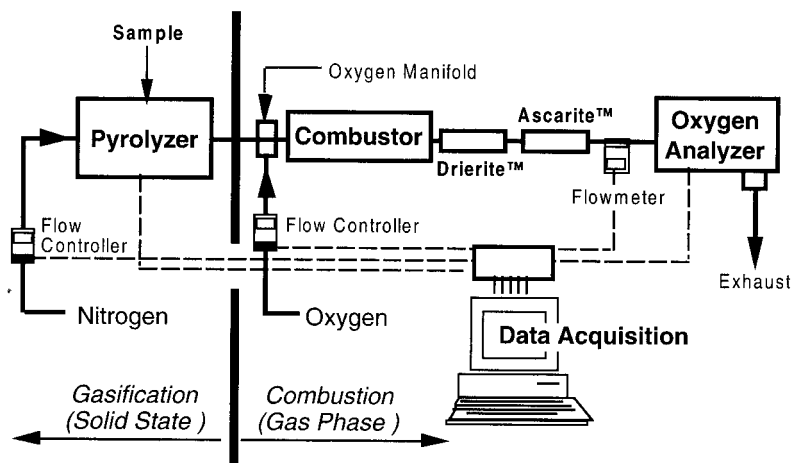


FIGURE 2-1. SCHEMATIC PICTURE OF PCFC [66]

The pyrolyzer consists of a temperature-controlled, heated stainless steel interface that can accept a pyroprobe. The combustor was a coiled Inconel tube contained in a ceramic furnace that can maintain a maximum temperature of 1200°C. The gas scrubbers were tightly packed anhydrous calcium sulfate (Drierite) and sodium hydroxide coated silica (Ascarite) to remove H₂O and CO₂ from the flow stream after combustion. The oxygen analyzer was zirconia-based (Panametrics Series 350). The mass flow rate of pure nitrogen (82 cm³/min) and oxygen (18 cm³/min) were controlled by the flow meters.

Basic operation involves anaerobic pyrolyzing the sample and measuring the heat released by complete combustion of the volatiles using the oxygen consumption principle [64-66]. In a typical test, 1-milligram samples were introduced into the pyrolyzer in a quartz capillary tube. The pyrolyzer interface temperature was slightly below the initial decomposition temperature to prevent condensation of high-molecular-weight thermal decomposition products. The sample was pyrolyzed to 930°C at 4.3°C/s in pure nitrogen (pyrolysis). Then the volatiles were swept from the pyrolyzer, mixed with excess oxygen, and fed through a combustor at a preset temperature of 900°C to achieve complete combustion. Afterwards, Drierite and Ascarite were used to remove carbon dioxide, water, and acid gases from the combustion stream. Finally, the flow rate and oxygen concentration were measured and used to calculate the heat release rate and the heat of combustion of the sample.

PCFC is a nonflaming combustion test. The heat release rate of the polymers can be calculated from the measured oxygen consumption after signal deconvolution to correct for flow dispersion. Then, the heat release capacity was obtained by dividing maximum heat release rate by the sample weight and the heating rate. The total heat of combustion of the fuel gases per unit

sample mass was obtained by direct integration of the heat release rate versus time. Char yield was determined by weighing the sample before and after the test. The coefficient of variation of the heat release capacity was used to evaluate the repeatability of the experiments.

2.3.4 Materials.

Oxygen and nitrogen gases for testing were of 99.99% purity grade, obtained from Merriam-Graves Industrial Gases and Welding Products. About 25 polymers from Aldrich Chemical Company and Scientific Polymer Products as well as some research polymers were tested. All the samples were dried overnight at 100°C under vacuum and stored in a desiccator. The samples included high-density polyethylene (HDPE), polypropylene (PP), polystyrene (PS), poly(α -methyl styrene) [P(α -M-S)] ($M_n=960$ g/mol), poly(tetrafluoroethylene) (PTFE) (Dupont Co.), poly(vinyl chloride) (PVC), polychloral (Prof. Vogl at UMass), poly(acrylonitrile) (PAN), poly(methyl methacrylate) (PMMA) ($M_n=35,000$ g/mol), poly(oxymethylene) (POM), poly(ethylene oxide) (PEO), poly(phenylene oxide) (PPO), Nylon 66, PC, poly(ethylene terephthalate) (PET), poly(butylene terephthalate)(PBT), poly(ether ether ketone) (PEEK), poly(phenyl sulfone) (PPhS), Kevlar® 29 (Dupont Co.), Nomex® (Dupont Co.), ULTEM® (GE Plastics), PI, PBZT (Dupont Co.), BPC II-polyarylate (Prof. Brzozowski in Warsaw University of Technology), and poly(hydroxyamide) (PHA) (Prof. Kantor at UMass). The chemical structures of some of the polymers are listed in figure 2-2.

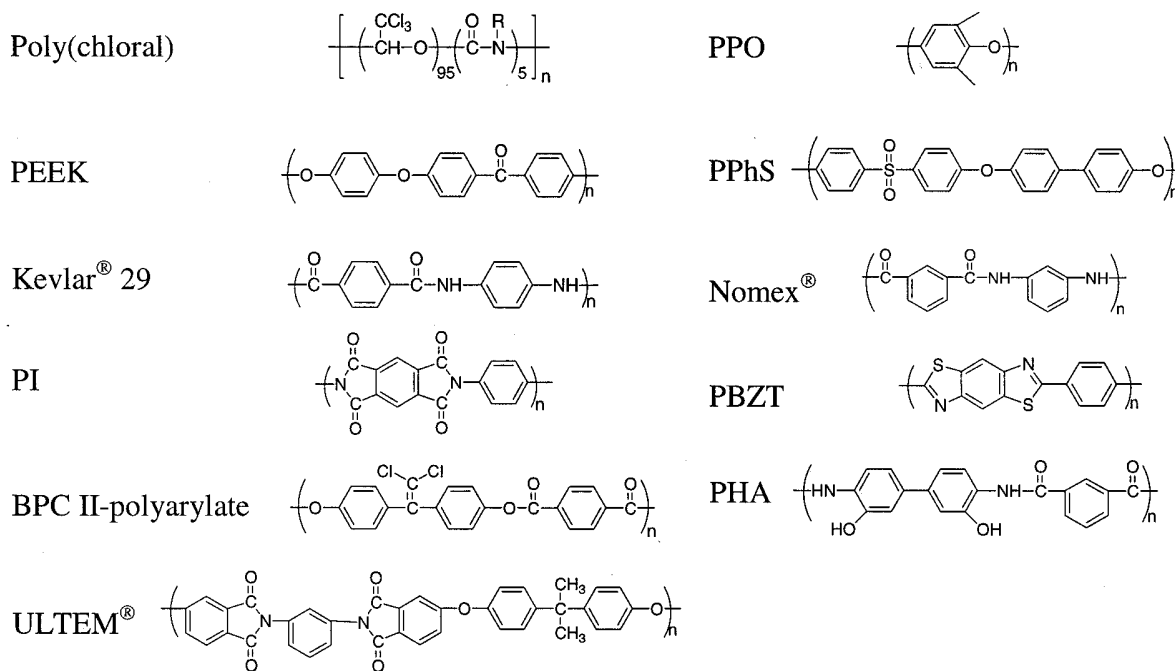


FIGURE 2-2. CHEMICAL STRUCTURES OF SOME POLYMERS

2.4 RESULTS.

2.4.1 Thermal Stability and Decomposition Process of Polymers.

It was suggested that oxygen from the surrounding atmosphere is usually completely consumed in the flame zone so that the pyrolysis of the condensed-phase polymer takes place in the absence of oxygen [72 and 7]. In addition, recent work [64] shows that char yield in a fire is equal to the anaerobic pyrolysis residue at the flaming surface temperature, which suggests that the char formation takes place in an oxygen-free environment where solid-state oxidation reactions are slow compared to polymer dissociation and gas/char formation. Therefore, in this section, all the STA analyses were performed under nitrogen (N_2). The derivative of TGA (DTG) curves, which indicate the mass loss rates of polymers, were obtained by differentiating the TGA curves.

The thermal decomposition process is usually characterized by a number of experimental parameters [73]: (1) the temperature of initial decomposition, $T_{99\%}$ or T_{onset} ; (2) the temperature of the maximum rate of decomposition, T_{max} , at which the mass loss rate is in maximum; (3) the average of activation energy, E_a , determined from the temperature dependence of the rate of weight loss, assuming that the decomposition process is a first-order reaction; (4) char yield, the solid residue left at very high temperature; and (5) heat of decomposition, ΔH , heat evolved or absorbed during decomposition. Table 2-2 summarizes several important parameters on the thermal decomposition of some polymers.

There are two temperatures that are usually used to characterize the initial decomposition of polymers. One is the temperature at 1% weight loss, $T_{99\%}$. The other is the onset decomposition temperature, T_{onset} , which is determined by the extrapolation of two tangent lines of the TGA curve. Generally, T_{onset} is about 20°~50°C higher than $T_{99\%}$, depending on the slope of the weight loss curves. At T_{onset} , the polymers usually already had a large weight loss (about 10%). Therefore, T_{onset} does not really reflect the initial decomposition of polymers. In contrast, it is more reasonable to use $T_{99\%}$ as the temperature to characterize the thermal stability of the polymers. However, $T_{99\%}$ can easily be affected by the vaporization of water and solvents absorbed or the small molecule additives. Therefore, $T_{95\%}$ is used by some people as a replacement.

According to table 2-2, most aliphatic polymers (polymers with aliphatic backbones), especially the ones with bulky side groups such as PMMA and P(α -M-S), are less stable than wholly aromatic polymers such as PI. However, there are some other important factors, such as secondary or van der Waals bonding forces, cross-linking, and multiple bonding, that can affect the thermal stability of polymers. For example, due to its high crystallinity, HDPE is much more stable than PET and PBT. It can also be seen that the char yield increases with the aromaticity of the polymers. In addition, it was found that the temperature at the maximum of heat flow (peak of the DSC curve) is very close to the temperature at the maximum mass loss rate (peak of the DTG curve), which indicates that the heat and mass loss events during decomposition are interrelated.

TABLE 2-2. THERMAL DECOMPOSITION PROPERTIES OF POLYMERS

Polymers	T _{99%} ^a (°C)	Max. Mass loss rate (10 ³ /s)	T _{max} ^b (°C)	T _{max} ^c (°C)	ΔH ^d (J/g)	Char Yield (%)	Ea ^e (kJ/mol)	ΔT ^f (°C)
PMMA ^g	167	2.06	370	371	687	0	254 46 158	147-170 199-282 312-412
Poly(chloral)	194	1.19	221	277	380	0	-	-
P(α-M-S) ^g	202	2.52	336	340	443	0	47 149	155-285 285-344
PVC ^h	246	1.74	294	285	140	6	140 206	183-300 383-458
PAN ^h	283	5.0	310	291	-444 ⁱ	39	158	240-313
POM	316	4.56	384	386	937	0	232	312-395
PS	336	5.29	417	418	683	0	289	351-420
PBT	350	4.18	404	402	281	0	298	331-411
PP	363	5.23	461	450	370	0	97 394	316-376 408-477
Nylon 66	372	3.45	452	452	140	0	238	356-474
BPC II- polyarylate	372	0.6	472	466	-302 ⁱ	51	166	290-393
PET	382	3.70	440	432	174	8	281	347-450
PPO	397	2.48	456	461	150	23	306	417-453
HDPE	413	6.4	471	471	256	0	242 476	387-452 453-495
PTFE ^h	456	2.9	573	579	447	0	247 368	416-506 537-588
PC	448	3.8	514	478	111	17	298	430-520
PI	461	0.5	602	602	62	52	106	445-594
PPhS	481	1.71	573	-	-	42	226	480-575
PHA ^h	250	0.4	633	-	-	56	43 366	227-354 567-593
Kevlar [®]	513	1.96	576	578	228	31	368	515-571
PEEK	539	2.2	586	-	-	46	512	530-576
PBZT	659	0.38	729	707	338	58	286	653-718

^a Temperature at 1% weight loss

^b Temperature at maximum mass loss rate

^c Temperature at the peak of heat flow (determined from DSC curve)

^d Heat of decomposition (determined from DSC curves)

^e Activation energy calculated according to TGA curves

^f Temperature range for Ea calculations

^g Several decomposition stages, depending on molecular weight

^h Two distinct decomposition stages

ⁱ Exothermic decomposition peak

Figures 2-3 lists the STA (TGA/DSC) and DTG curves of several aliphatic polymers. It was found that most aliphatic polymers such as PP, HDPE, and PS decompose in a single stage with zero char yield, but some polymers such as P(α -M-S), PMMA, PVC, and PTFE decompose in more than one stage. In addition, the thermal decomposition processes of PMMA and P(α -M-S) also depend on their molecular weight. The effects of molecular weight on the decomposition of polymers will be discussed in detail in section 6.

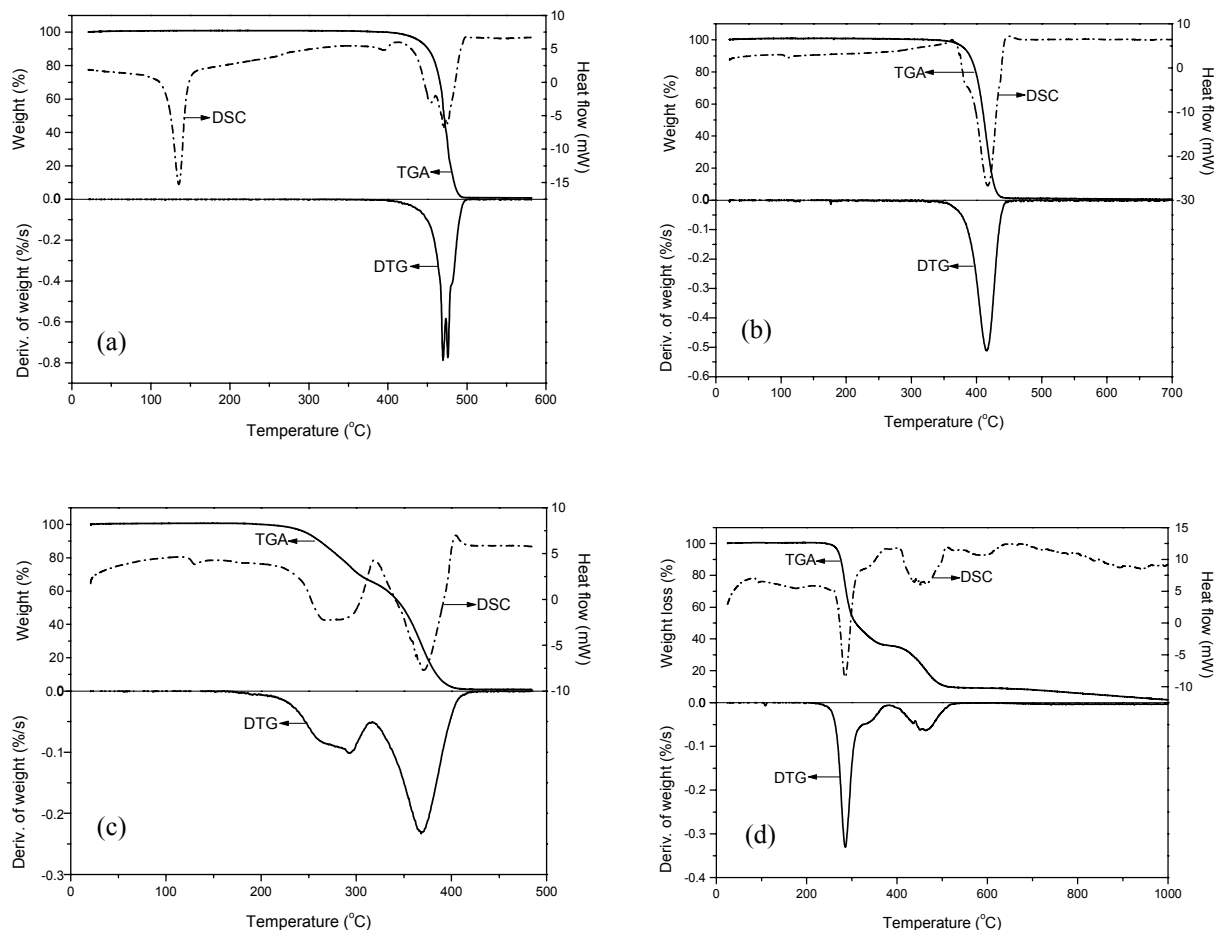


FIGURE 2-3. THE STA AND DTG CURVES OF ALIPHATIC POLYMERS (10°C/min IN N₂) (a) HDPE, (b) PS, (c) PMMA, AND (d) PVC

However, most aromatic polymers such as BPA-polycarbonate and (PPhS) usually have a major sharp weight loss with a certain amount of char left at high temperatures (figure 2-4). It is believed that there are two stages corresponding to two types of decomposition reactions [73]. One takes place at relatively low temperatures involving chain scission reactions to form low-molecular-weight fragments and gases. The other is the recombination reaction resulting from the formation of final char, which happens at high temperatures.

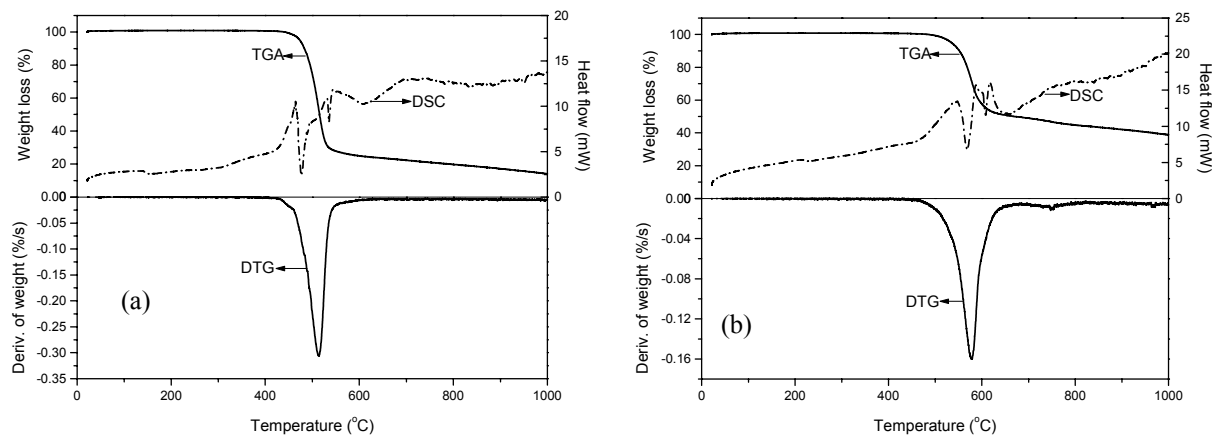


FIGURE 2-4. THE STA AND DTG CURVES OF AROMATIC POLYMERS (10°C/min IN N₂) (a) PC AND (b) PPhS

It was also found that the heat of decomposition for most polymers is endothermic, ranging from 100 J/g to 900 J/g. For some aromatic high-temperature polymers, such as PEEK and PPhS (figure 2-4(b)), the heat events during decomposition are very complex. A baseline uplift is usually observed at the beginning of the decomposition of most charring aromatic polymers. However, the mechanism is not clear yet.

A few polymers such as PAN and BPC II-polyarylate (figure 2-5) show an exothermic decomposition peak, but different mechanisms may be involved. For PAN, it is due to the cyclization reaction, while for BPC II-polyarylate, it is due to the formation of HCl and some complicated cross-linking reactions. Most polymers with exothermic decomposition contain either halogens or some unsaturated double or triple bonds, which can lead to char formation by cross-linking or cyclization reactions. In general, the heat of decomposition is the consequence of several processes, such as bond dissociation, new bond formation, and volatile evaporation.

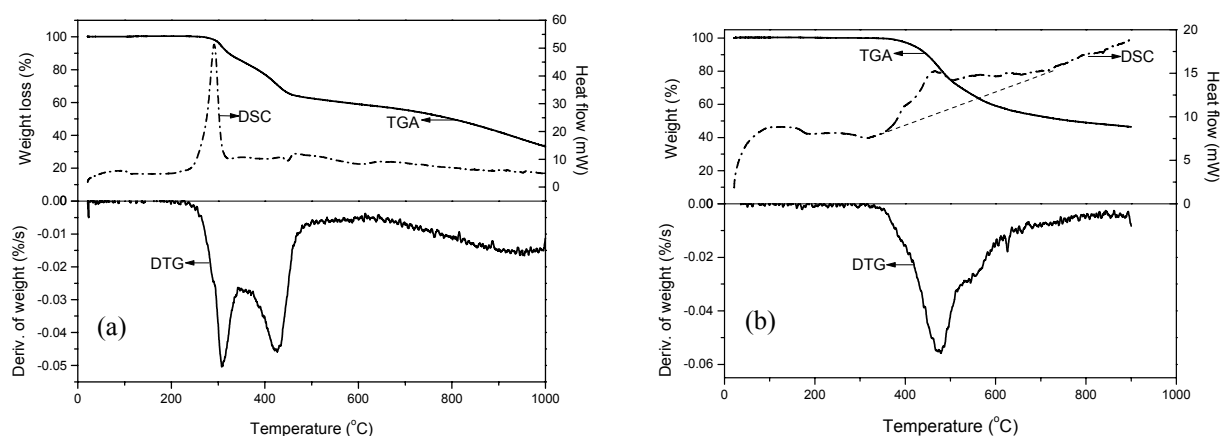


FIGURE 2-5. THE STA AND DTG CURVES OF POLYMERS WITH EXOTHERMIC DECOMPOSITION (10°C/min IN N₂) (a) PAN AND (b) BPC II-POLYARYLATE

If the thermal decomposition of polymers is assumed to be a first-order reaction, the average activation energy, E_a , can be determined from the temperature dependence of the rate of weight loss according to equation 2-11.

$$\ln\left(-\frac{1}{m} \cdot \frac{dm}{dt}\right) = \ln A - \frac{E_a}{RT} \quad (2-11)$$

where m is the sample weight, dm/dt is the weight loss rate, A is the pre-exponential factor, R is the gas constant, and T is the temperature. The calculated activation energies of some polymers are listed in table 2-2.

It was found that for the polymers with low char yields such as HDPE, PS, and nylon 66 (figure 2-6(b)), the assumption of first-order decomposition is applicable to almost the whole major decomposition temperature range (about 70°C). However, for the high-charring aromatic polymers such as PC and PPhS (figure 2-6(c)), the valid temperature range is only from the beginning to the middle of the major decomposition stage. Therefore, a first-order reaction might not be a good kinetic model for the decomposition of some aromatic polymers, such as BPC II-polyarylate and PI, due to their intensive charring process at high temperatures.

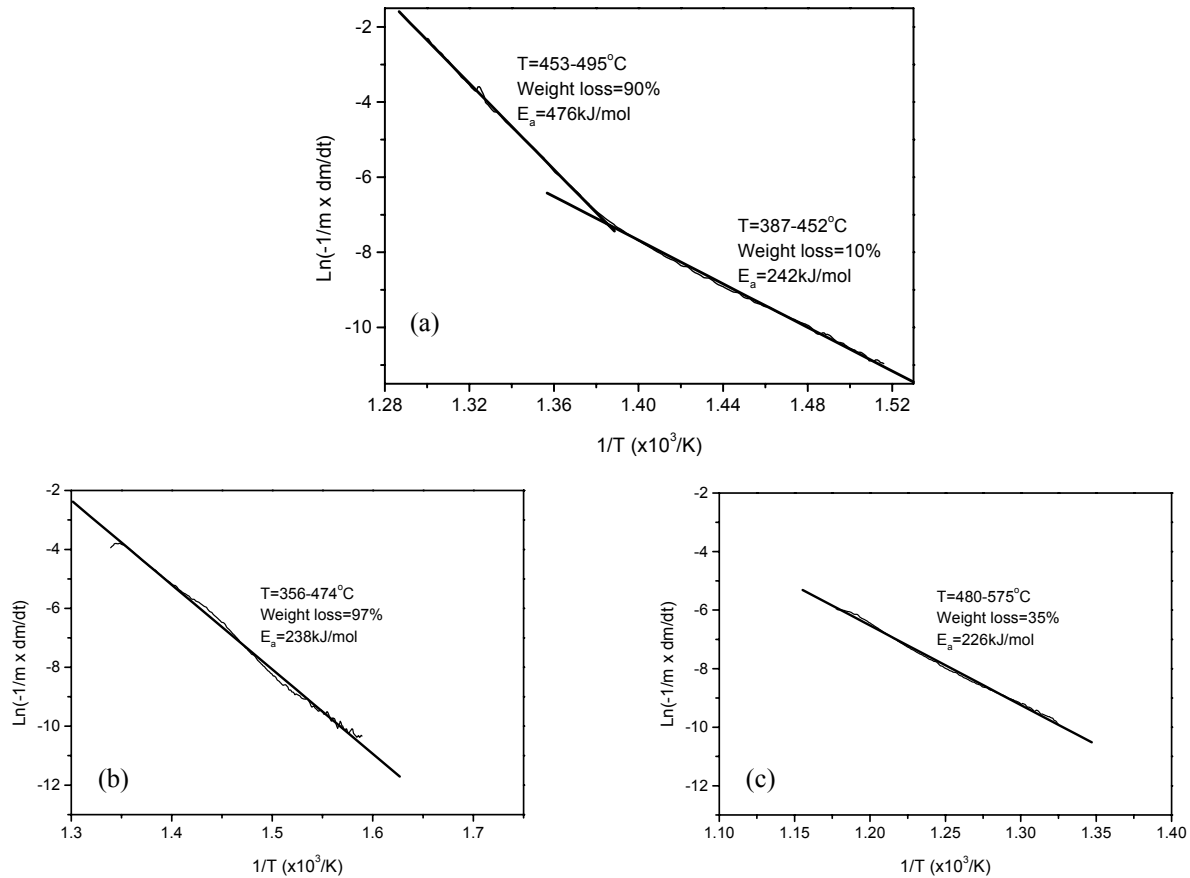


FIGURE 2-6. ACTIVATION ENERGIES OF THERMAL DECOMPOSITION CALCULATED BY TGA DATA (a) HDPE, (b) NYLON 66, AND (c) PPhS

It is easy to understand that polymers with several decomposition stages have several activation energies that correspond to different temperature ranges and weight losses. However, it is interesting that HDPE (figure 2-6(a)) and PP also have two activation energies, though they only show one distinct decomposition stage in TGA. The first E_a (97 kJ/mol for PP and 242 kJ/mol for HDPE) corresponds to a low temperature range during which the polymers only have about 2%~10% weight loss. This is probably because the initial decomposition, which starts from the defects of the polymer chain, does not require a lot of energy. The second E_a (279 kJ/mol for PP and 476 kJ/mol for HDPE) corresponds to the C-C main-chain scission of the polymers. Generally, the activation energies of different polymers are greatly dependent on their chemical structures, ranging from 100 kJ/mol to 500 kJ/mol.

2.4.2 Thermal Decomposition Products of Polymers.

The total ion current pyrograms (TIC) of several polymers are shown in figures 2-7 through 2-9. For the polymers made by additional polymerization, there are two general types of decomposition: end-chain scission (depropagation or unzipping) and random-chain scission.

The main decomposition product of P(α -M-S), POM, and PMMA (figure 2-7(a)) is the monomer. Therefore, the major decomposition mechanism is unzipping. The chain depolymerizes by successive release of monomer units from a chain end or at a weak link, which is essentially the reverse of chain polymerization.

For Polyethylene (PE) and PP (figure 2-7(b)), the decomposition products are a series of alkenes, alkanes, and dienes. Therefore, the decomposition mechanism is random scission along the polymer chain, giving a mixture of hydrocarbons that are usually large compared with the monomer unit. The decomposition products of PP are more complex because of the chain transfer reactions during pyrolysis.

The main decomposition products of PS and PPO are monomer, dimer, and trimer (figure 2-7(c)). Therefore, the decomposition mechanism is the combination of random scission and unzipping.

However, for all the aromatic condensation polymers such as polyester and polyamide, when heated to high temperatures, the polymer chains usually randomly break at the heteroatom bridges (figure 2-8). They then decompose in varying degrees to carbonaceous char residue through a set of complex reactions involving cross-linking and bond scissions. Depending on the chemical structure of the polymers, the major decomposition products usually include CO₂, CO, and a series of aromatic phenols, amines, acids, ethers as well as some complicated rearrangement compounds.

It was found that when the polymers decompose under a faster heating rate, such as 10°C/ms, they will release more low-molecule-weight fragments, but the types of the major decomposition products are essentially unchanged (figure 2-9).

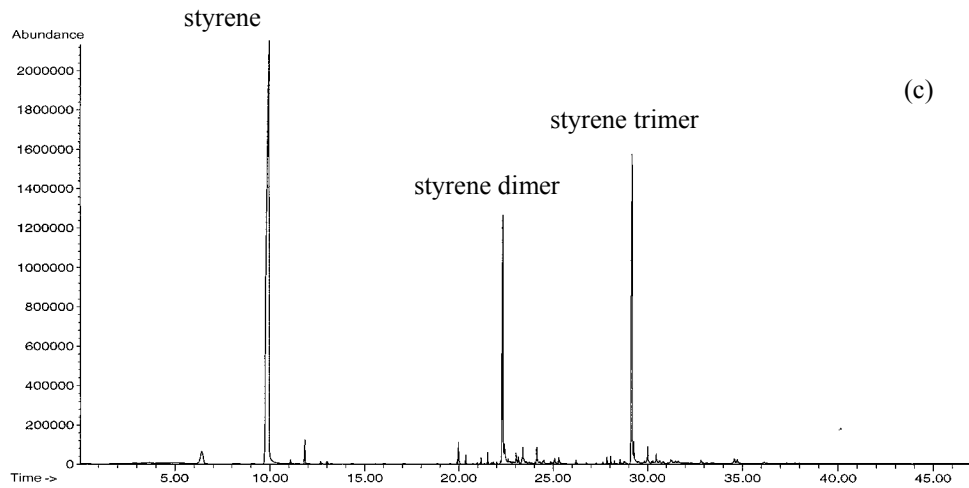
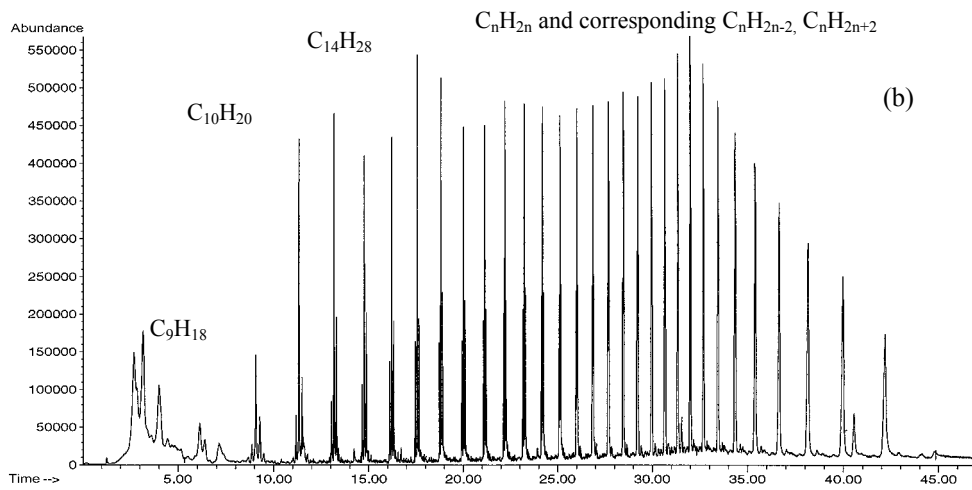
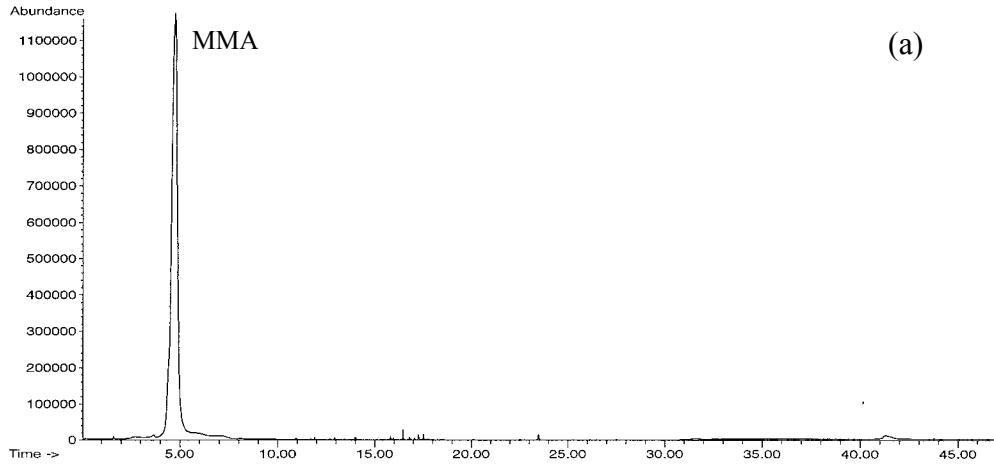


FIGURE 2-7. PYROLYSIS GC/MS TRACES OF ADDITIONAL POLYMERS (4.3°C/s TO 930°C) (a) PMMA, (b) PE, AND (c) PS

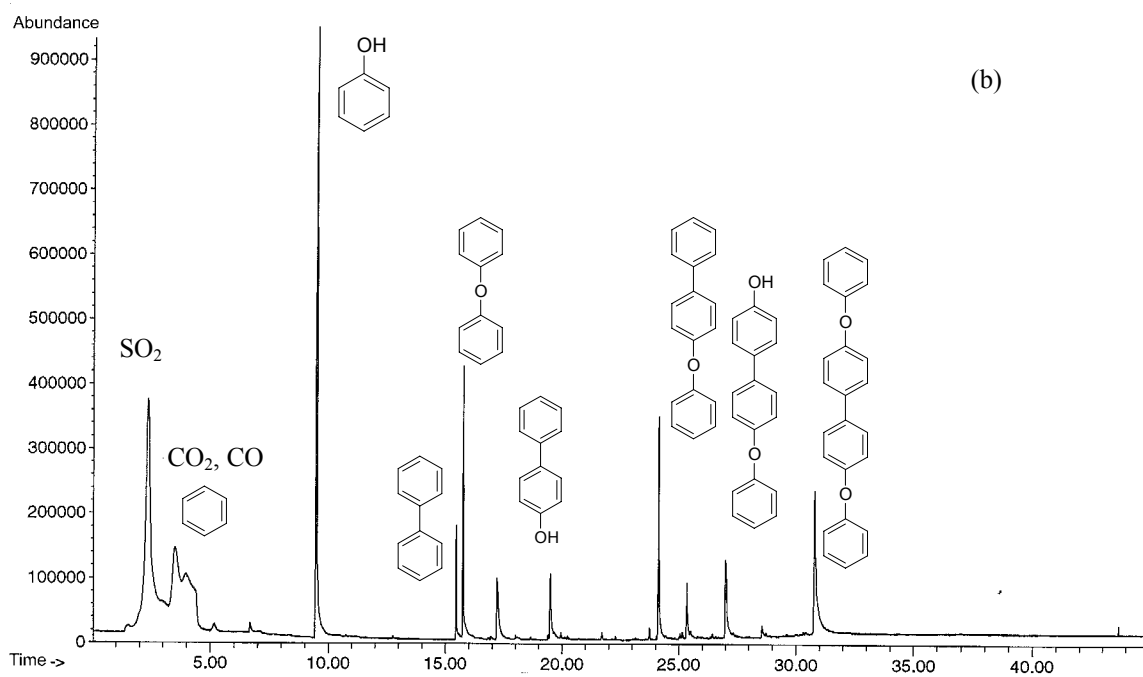
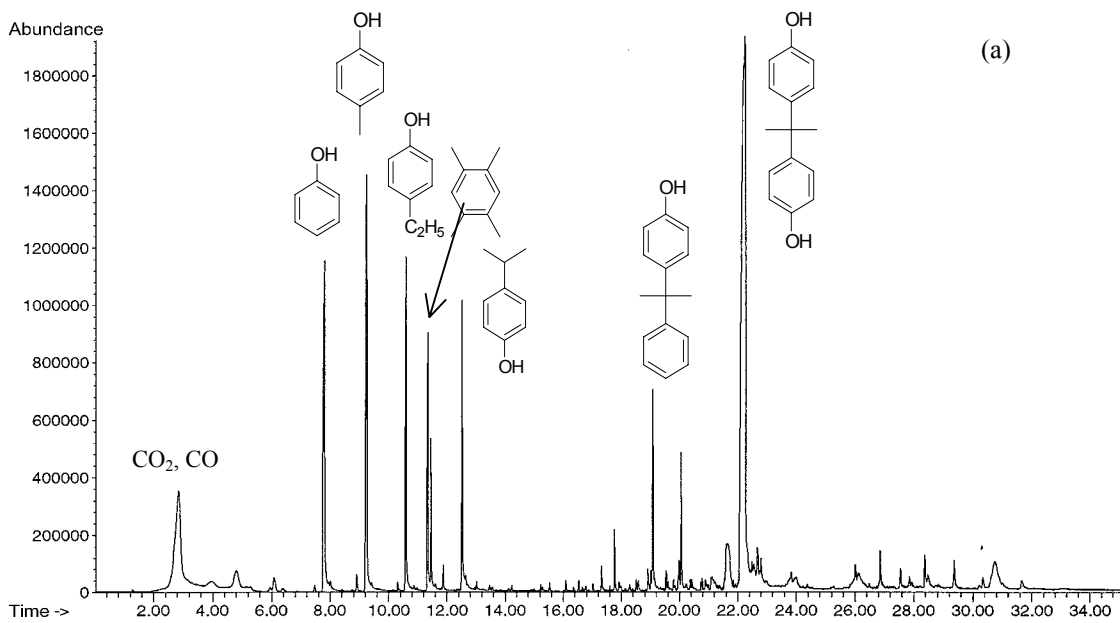


FIGURE 2-8. PYROLYSIS GC/MS TRACES OF AROMATIC POLYMERS (4.3°C/S TO 930°C) (a) PC AND (b) PPhS

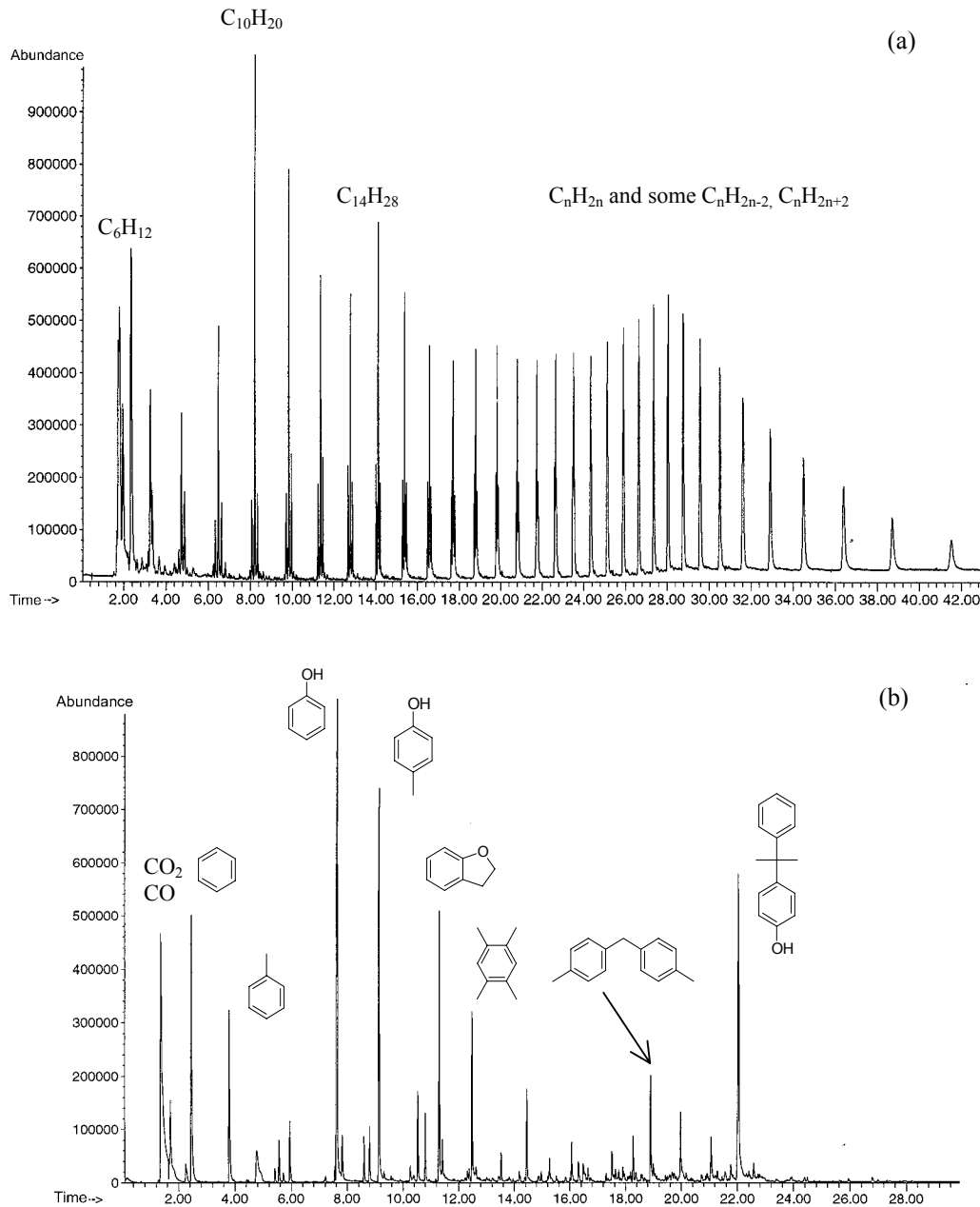


FIGURE 2-9. PYROLYSIS GC/MS TRACES OF POLYMERS AT A FAST HEATING RATE ($10^{\circ}C/ms$ TO $930^{\circ}C$) (a) HDPE AND (b) PC

2.4.3 Flammability.

The PCFC results of different polymers are listed in table 2-3. It can be seen that aliphatic hydrocarbon polymers such as PE, PP, and PS are much more flammable than the polymers that contain aromatic, heteroaromatic rings, or heteroatoms (halogens, N, S, O etc.). This is because these aliphatic polyhydrocarbons can be completely decomposed at a rapid rate with no char and generate a lot of hydrocarbon volatiles with high fuel values. Aromatic polymers usually produce relatively high char yields. The char can reduce the amount and release rate of volatile

fuels and act as a barrier for heat and mass transfer. Therefore, aromatic polymers generally have lower flammability. However, this is not always true because the flammability is a function of both solid- and gas-phase chemistry. For example, PPO has a char yield of 23%, but it is much more flammable than PMMA whose char yield is zero. The high flammability of PPO is mainly due to its highly flammable decomposition volatiles—a series of phenols. PTFE and poly(chloral) also have very low flammability but zero char yield. The introduction of halogen atoms into polymer structures can efficiently reduce the flammability of the polymers because the halogenated decomposition volatiles have relatively low flammability and can also confer some flame-retardant effect in the gas phase. The polymers (such as BPC II-polyarylate) containing both halogens and aromatic structures have extremely low flammability.

TABLE 2-3. FLAMMABILITY OF DIFFERENT POLYMERS (930°C AT 4.3°C/s)

Polymers	H. R. Capacity (J/g-K)	Total Heat (kJ/g)	Char Yield (%)	Cov.* (%)
PP	1584	41	0	4.3
PE	1558	40	0	18.5
PS	1199	38	0	5.2
P(α-M-S)	730	37	0	6.7
Nylon 66	648	28	0	14.3
PEO	580	23	4	4.0
PPO	553	22	23	8.2
PBT	420	22	0	8.5
PET	393	17	8	8.5
PC	382	19	17	9.3
PMMA	376	23	0	4.6
Kevlar [®]	292	15	36	1.9
POM	261	14	0	8.8
PEEK	163	13	46	3.6
PPhS	156	12	39	2.5
ULTEM [®]	121	12	49	8.3
PTFE	58	6	0	7.0
Nomex [®]	45	12	53	6.0
PHA	42	10	56	4.3
Poly(chloral)	33	5	0	5.0
PI	29	9	53	4.8
PBZT	24	5	58	11.0
BPC II- polyarylate	12	4	51	3.2

*Coefficient variation of heat release capacity.

Generally, if the heat release capacity of a material is below 100 J/g-K, it is fire resistant. It can be seen that PHA, PI, PBZT, and BPC II-polyarylate are all fire-resistant polymers. Their extremely low flammability is attributed to the following features: high thermal stability, high char yields, low maximum mass loss rate, and the ability to release flame-retardant molecules, such as water and HCl. In all, the high degree of aromaticity (which can promote formation of highly cross-linked carbonaceous char), combined with the inclusion of heteroatoms such as halogen, N, and S (which, on thermal decomposition, gives products with low heat of combustion), can greatly improve the fire resistance of materials.

Normally, the cov. of the heat release capacity of all the polymers measured is within 10% except for PE and nylon 66. The systematic error for the total heat released is 1 kJ/g. Under standard conditions, the PCFC method is very precise and highly reproducible. Moreover, it is applicable to a wide variety of materials (plastics, films, textiles, etc.). So far, it is probably the most valuable flammability test for research materials, though it will never totally replace the other fire tests. One special advantage of this method is that it gives numerical results that can capture some intrinsic relations between a material's chemical structure and its flammability.

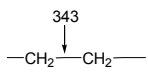
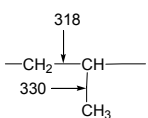
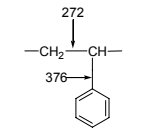
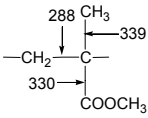
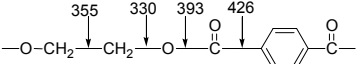
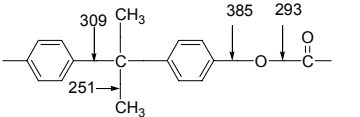
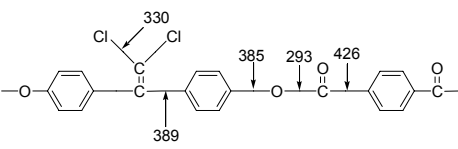
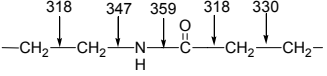
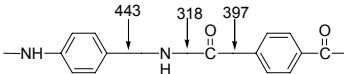
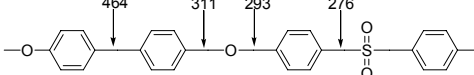
2.4.4 Bond Dissociation Energies of the Polymers.

The B3LYP density-functional method [74 and 75] with a standard polarized split-valence 6-31G(d) basis set [76] was used for the calculation of bond dissociation energies of the polymers. The method was chosen to achieve the maximum accuracy with a reasonable computational time. The restricted version of the method was used for closed-shell species, while the unrestricted version was used for radicals. The energies were obtained by calculating enthalpies of the bond dissociation reactions of some small model compounds with the same structure as the polymers. The computed energies of optimized structures of model compounds and their radical fragments were corrected for zero-point energy contribution. All the calculations were carried out using the Gaussian 98 package of programs [77]. The results of the calculations are shown in table 2-4.

It is found that the weakest bond in HDPE, PP, PS, and PMMA is the main chain C-C bond. Therefore, these polymers prefer to break along the polymer main chain rather than to strip any side groups, and their major decomposition products contain intact monomer units such as monomer and oligomers. However, the introduction of side groups will inevitably weaken the strength of the C-C backbone. As a result, the thermal stability of PP, PS, and PMMA is lower than HDPE. For condensation polymers, the weakest bond is usually located around the heteroatomic linkage such as ether, ester, amide, and sulfone groups. However, there are usually several bonds whose strength is very close to the weakest bond. As a result, the decomposition of most condensation polymers is probably initiated by the breakdown of several different bonds around the same temperature.

According to table 2-4, except for PE, PP, BPC II-polyarylate, and nylon 66, the decomposition activation energies of the other polymers measured by TGA are all relatively close to the bond dissociation energies of their weakest bonds if the computational uncertainty is considered. This result suggests that the initial breakdown of these polymers is mainly caused by the rupture of the weakest bonds in the polymer chain.

TABLE 2-4. BOND DISSOCIATION ENERGIES OF POLYMERS

Polymers	Bond Dissociation Energies ^a (kJ/mol)	E _a ^b (kJ/mol)	Weight Loss ^c (%)
PE		242 476	10 90
PP		128 394	1.5 87
PS		289	75%
PMMA		254 46 158	1 20 63
PET		281	78
PC		298	55
BPC II- Polyarylate		166	5
Nylon 66		238	97
Kevlar [®]		368	22
PPhS		226	35

^a B3LYP density-functional method with a standard polarized split-valence 6-31G(d) basis set. The mean error is 33kJ/mol

^b Calculated by TGA data

^cWeight loss corresponding to the temperature range for E_a calculated (refer to table 2-2)

However, it seems that the correlation between bond dissociation energy and activation energy is not very simple because sometimes the activation energy calculated from TGA data does not directly correspond to the dissociation of one specific bond, but it is due to the breakdown of several bonds. In addition, the assumption of first-order decomposition is not valid for all polymers, especially high-charring aromatic polymers.

It was also found that the bond dissociation energies of ester or amide linkage in condensation polymers are greatly dependent on the structures of the chemical units, which are linked to the nitrogen or oxygen atom (table 2-5). If an aliphatic unit is connected to the nitrogen or oxygen, the bond dissociation energies are 360 kJ/mol for amide linkage and 390 kJ/mol for ester linkage. If it is an aromatic unit, the bond dissociation energies are lower (318 kJ/mol for amide linkage and 293 kJ/mol for ester linkage). It seems that the ester and amide linkages in wholly aliphatic structures are much stronger than those in wholly aromatic structures. However, the bond dissociation energies of the weakest bonds in all polyamides with different aliphatic-aromatic structure combinations are about the same (318 kJ/mol), though they are related to different types of bonds.

TABLE 2-5. BOND DISSOCIATION ENERGIES IN ALIPHATIC-AROMATIC POLYMERS

Polymers	Polyamides (kJ/mol)	Polyesters (kJ/mol)
Aliphatic		
Aliphatic-aromatic		
Aromatic		

These bond dissociation energy calculations seem contradictory to the TGA results, which show that polymers with aliphatic structures usually have lower thermal stability than those with aromatic structures. For example, Kevlar[®] and nylon 66 are polyamides and have the same weakest-bond dissociation energies, but Kevlar[®] is much more thermally stable than nylon 66, according to TGA analyses (figure 2-10). It is because in TGA measurements, the thermal stability is characterized by the temperature at which the polymers start to lose weight. If a polymer chain is already broken at several points, but without obvious weight loss, the TGA curve will not change at all. Therefore, TGA results will not reflect the initial breakdown of

polymers unless there is a significant weight loss. For aliphatic polymers, after the decomposition is initiated by bond scission, low-molecule-weight volatiles that can be easily evaporated are produced. However, aromatic polymers usually form relatively large aromatic fragments that can be kept in solid state for a longer time and sometimes further recombine into more condensed structure. Thus, a significant weight loss can only be observed at high temperatures. As a result, the weight loss in aliphatic polymers is more detectable compared to aromatic polymers. In all, the lower-thermal stability of aliphatic polymers measured by TGA does not necessarily mean that the bonds in aliphatic polymers are weaker than those in aromatic polymers.

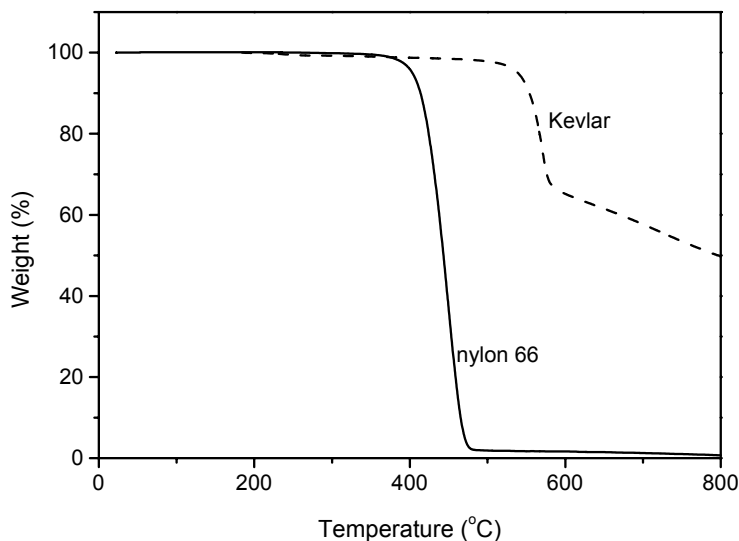


FIGURE 2-10. THE TGA CURVES OF KEVLAR[®] AND NYLON 66

2.4.5 Flammability Calculated by Pyrolysis GC/MS and STA Results.

According to the procedures described earlier, the heat release capacity and total heat of combustion of the polymers can be calculated by combining the pyrolysis GC/MS and STA results. In table 2-6, the calculated values are compared to the experimental values from PCFC.

The total heat of combustion calculated in the table is the total net heat of combustion, which is obtained by using the gross heat of combustion minus heat of vaporization of water produced during combustion. The gross heat of combustion is the standard molar enthalpy (heat) of combustion at 298.15 (K), and the products of combustion are taken to be CO₂ (gas), N₂ (gas), and H₂O (liquid) in their standard states. There are several error sources during calculations; for example, some peaks in GC/MS pyrograms are difficult to identify, some peaks are overlapped and difficult to separate, and some of the small peaks (molar concentration smaller than 5%) are neglected in the calculations. In addition, the relative electron impact total ionization cross sections for the decomposition volatiles are estimated by an empirical equation. The heat of combustion for some complicated compounds are also estimated by using Benson's law. Considering all these possible errors, one can see that the different methods correlate to each other very well, which indicates that the thermal decomposition process and decomposition

volatiles are two important factors in determining the polymer flammability. It can also be seen that the char yield obtained by STA is very close to PCFC, though different heating rates are used in these two methods.

TABLE 2-6. CORRELATION BETWEEN DIFFERENT METHODS

Polymers	Heat release Capacity (J/g-K)		Total Heat Released (kJ/g)		Char Yield at 930°C (%)	
	Calculated ^a	PCFC ^b	Calculated ^c	PCFC ^b	STA ^d	PCFC ^b
PE	-	1558	45	40	0	0
PP	-	1584	45	41	0	0
PS	1277	1199	41	37	0	0
P(α-M-S)	695	730	41	38	0	0
PPO	635	553	22	22	23	23
Nylon 66	509	648	21	28	0	0
PC	470	382	19	19	17	22
PET	407	393	16	17	8	5
PMMA	345	376	24	23	0	0
POM	233	261	17	14	0	0
PEEK	211	163	11	13	46	46
Kevlar [®]	207	292	16	15	32	36
PHA	-	42	9	10	56	57
Poly(chloral)	34	33	5	5	0	0
PI	31	29	6	9	50	53

^a Calculated by measuring the maximum mass loss rate and collecting the decomposition volatiles at maximum mass loss temperature (heating rate, 10°C/min)

^b Pyrolyze at 4.3°C/s to 930°C

^c Calculated by pyrolyzing the polymer at 4.3°C/s to 930°C and collect all the decomposition volatiles

^d Heating rate 10°C/min

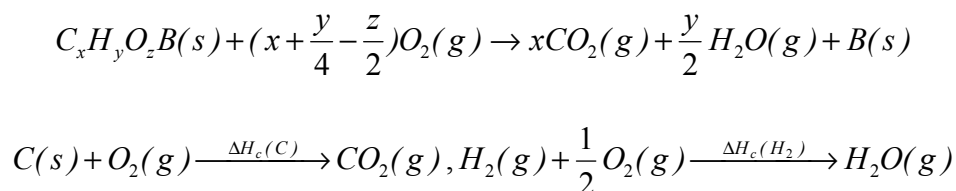
2.4.6 Flammability Estimated by Using Chemical Structure and TGA Results.

If complete combustion of all the volatiles released during polymer decomposition is achieved, the net heat of combustion of polymers can be estimated by two simple calculation methods. One is based on the oxygen consumption principle, which is also exploited in both PCFC and cone calorimeter tests. The amount of oxygen needed for complete combustion of the structural unit can be calculated according to the stoichiometry of the combustion equation. The second method is based on the additivity of contributions of the individual atoms comprising the polymers. In this calculation, only the heats of combustion of carbon and hydrogen were

considered so as to simplify the calculation. All the oxygen atoms in the polymers were excluded by combustion with hydrogen atoms to form H₂O, which will not contribute to the heat of combustion during calculations. As a result, the effective number of hydrogen atoms used in the calculations was less than that in the formula for oxygen-containing polymers. Other heteroatoms, such as N, S, P, and halogens, were assumed to have no contribution to the heat released. Therefore, they have no fuel values, but only add dead weight to polymers. In both methods, char yields were used to adjust the net heat of combustion in terms of per unit mass of solid polymers. They can be either measured by TGA or calculated by molar group additivity. All the char yields used here were measured by TGA.

The principles of the two calculation methods for estimation of net heat of combustion are summarized below.

Combustion equation:



Method 1: Oxygen consumption principle

$$\Delta H_c(C_xH_yO_zB)(kJ/g) = \frac{\left(x + \frac{y}{4} - \frac{z}{2}\right)(mol-O_2/mol) \times 419(kJ/mol-O_2)}{M(C_xH_yO_zB)(g/mol)} \times (1 - \text{char fraction})$$

Method 2: atom t additivity principle

$$\Delta H_c(C_xH_yO_zB)(kJ/g) = \frac{x\Delta H_c(C)(kJ/mol) + \frac{1}{2}(y - 2z)\Delta H_c(H_2)(kJ/mol)}{M(C_xH_yO_zB)(g/mol)} \times (1 - \text{char fraction})$$

in which M is the molecular weight of the repeating unit, $\Delta H_c(C)$ is the heat of combustion of carbon atom, and $\Delta H_c(H_2)$ is the heat of combustion of hydrogen.

2.4.6.1 Net Heat of Combustion of Polymers.

The two methods, oxygen consumption and atom additivity, have been used to calculate the gross heats of combustion of 48 small molecule organic compounds (appendix A, table A-1). The net heat of combustion obtained directly by the oxygen consumption principle has been converted to gross heat of combustion by considering the heat of vaporization of the water. It was found that the calculated values are very close to the reference values [78] (figure 2-11). The average relative deviations are $\pm 6\%$ for the oxygen consumption method and $\pm 9\%$ for the atom additivity method. Both methods are insensitive to the structure differences between compounds with the same formula because they did not consider the interactions between atoms.

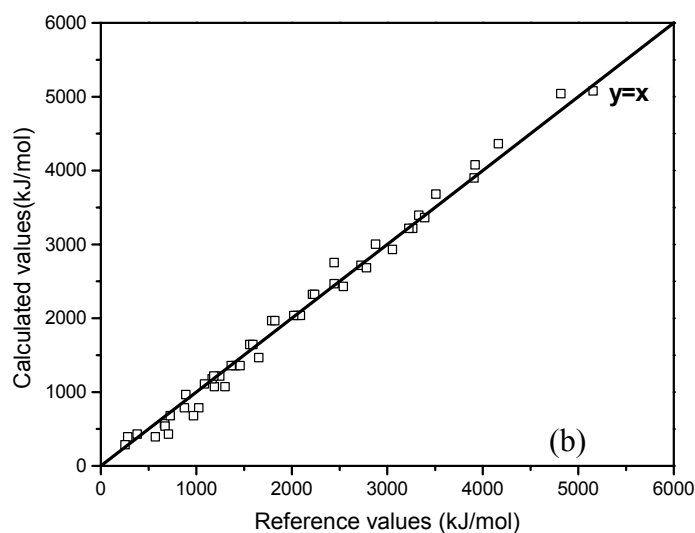
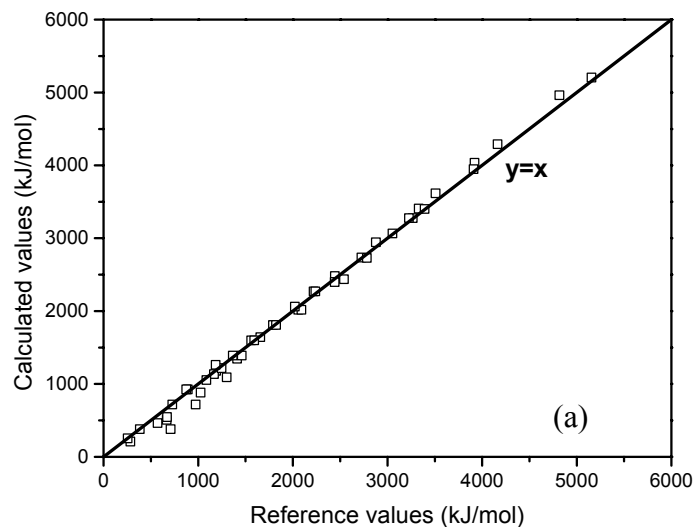


FIGURE 2-11. CALCULATION OF GROSS HEAT OF COMBUSTION OF SMALL ORGANIC COMPOUNDS (a) OXYGEN CONSUMPTION AND (b) ATOM ADDITIVITY

The net heats of combustion of 35 polymers were also calculated by both methods (appendix A, table A-2). The calculated values were compared with PCFC results (figure 2-12). It can be seen that the calculated values correlate relatively well with the experimental values. The standard deviations are ± 3 kJ/g for both methods. However, for nylon 66, Chalcon II-polyarylate, Xydar[®], PBZT, and some halogen-containing polymers such as BPC II-polycarbonate and BPC II-polyarylate, the accuracy is not as good, and deviations up to 6-7 kJ/g may occur. The reason for this discrepancy arises, in large, apart from the assumptions used in these calculations. First, the composition of the char is assumed to be the same as the original polymer, so its effect on the heat of combustion can be easily estimated by a linear weight reduction. However, the char has a more condensed structure and contains more carbons and less hydrogens than the original polymer. Therefore, to improve the accuracy, the elemental composition of the char should be identified. Second, contributions of the heteroatoms, such as S, P, and halogens, were

completely neglected in calculations because their heats of combustion are usually very low. However, for some polymers, this simplification might not be appropriate because these heteroatoms might interact with the other atoms and have further effects on the polymer flammability. Aside from these limitations, the atom additivity is found to be a fair approximation for estimating net heat of combustion of different polymers. Although the heat of combustion of polymers greatly depends on the number and heat of combustion of each type of atom present, it is also greatly dependent on their internal bonding between atoms that will significantly affect their char yield measured by TGA. However, such interactions cannot be handled by simple atom additivity.

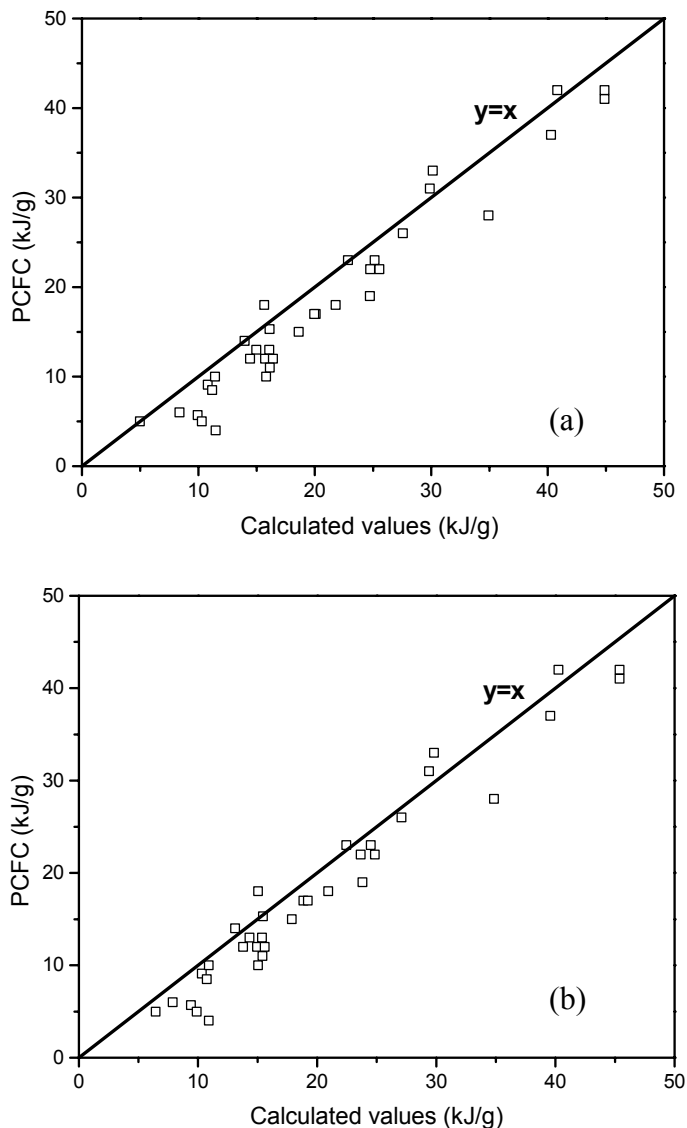


FIGURE 2-12. COMPARISON OF CALCULATED NET HEAT OF COMBUSTION OF POLYMERS WITH PCFC RESULTS (a) OXYGEN CONSUMPTION AND (b) ELEMENT ADDITIVITY

The calculations based on atom additivity also show that hydrogen atoms have the biggest contribution to the heat of combustion of polymers due to its high fuel value and low weight. Therefore, they are the major burning sources of polymers. On the contrary, the heteroatoms are usually heavier than carbon and hydrogen atoms, but they do not produce a lot of heat when burned. Therefore, any units that have low hydrogen to carbon ratio (H/C) and high content of heteroatoms are ideal structures for fire-resistant polymers. The low H/C ratio is usually achieved by introducing the aromatic or heteroaromatic ring structures, which can also increase the thermal stability and char yields of the polymers.

2.4.6.2 Heat Release Capacity.

If the instantaneous heat of combustion per unit mass of the volatiles remains constant during decomposition, the heat release capacity should be proportional to its maximum mass loss rate and can be estimated by the following equation

$$\text{Heat release capacity (J/g-K)} = \text{Total heat released (J/g)} * \text{Max. mass loss rate (/s)/Heating rate (K/s)}$$

According to table A-2 in appendix A and figure 2-13, the correlations between calculated heat release capacities with those from PCFC measurements are relatively good. The average relative deviations are about $\pm 20\%$ for both methods. The large discrepancies are mainly due to three reasons. (1) The decomposition volatiles released at different temperatures are different. Therefore, the heat released at a certain temperature might not be simply proportional to the mass loss rate at that temperature. It is also greatly determined by the heat of combustion of the volatiles released at that temperature. (2) It is difficult to measure the maximum mass loss rate very accurately by TGA. (3) The errors in the term of total heat of combustion might be transferred to the calculation of heat release capacity and sometimes magnified by the high mass loss rates. As a result, the most serious deviations occur with Chalcon II-polyarylate, Xydar[®], and especially some halogen-containing polymers such as PTFE, BPC II-polycarbonate, and BPC II-polyarylate. The deviations of PTFE, BPC II-polycarbonate, and BPC II-polyarylate are not included when calculating average relative deviation.

It can be seen that the heat release capacity, which is proportional to the maximum heat release rate, is greatly dependent on two parameters: maximum mass loss rate and heat of combustion of volatiles at that temperature. The mass loss rate, in turn, is greatly dependent on the char yield. Therefore, enhancement of char formation is very important in reducing both net heat of combustion and heat release rate.

2.4.6.3 Char Yield.

The char formation tendency is also greatly determined by the structure of polymers. It was found that char yields can be roughly estimated by molar group additivity [73]. In the research, it has been observed that there are some simple correlations between char yield and the molar fraction of the effective char-forming atoms in the polymers (table A-3 in appendix A and figure 2-14). The effective char-forming components are identified as (1) main chain aromatic carbon atoms that are not separated by long aliphatic spacers such as $-(\text{CH}_2)_n-$ ($n > 2$), (2) C, N, S in heteroaromatic rings, and (3) double or triple bonds such as C=C, C=S, C=N in main chain

that are also conjugated with aromatic rings. Due to the existence of isopropyl groups that are easily broken apart, the number of effective char-forming atoms in bisphenol A structure is reduced to 6 compared with the 12 aromatic carbons in the polymer.

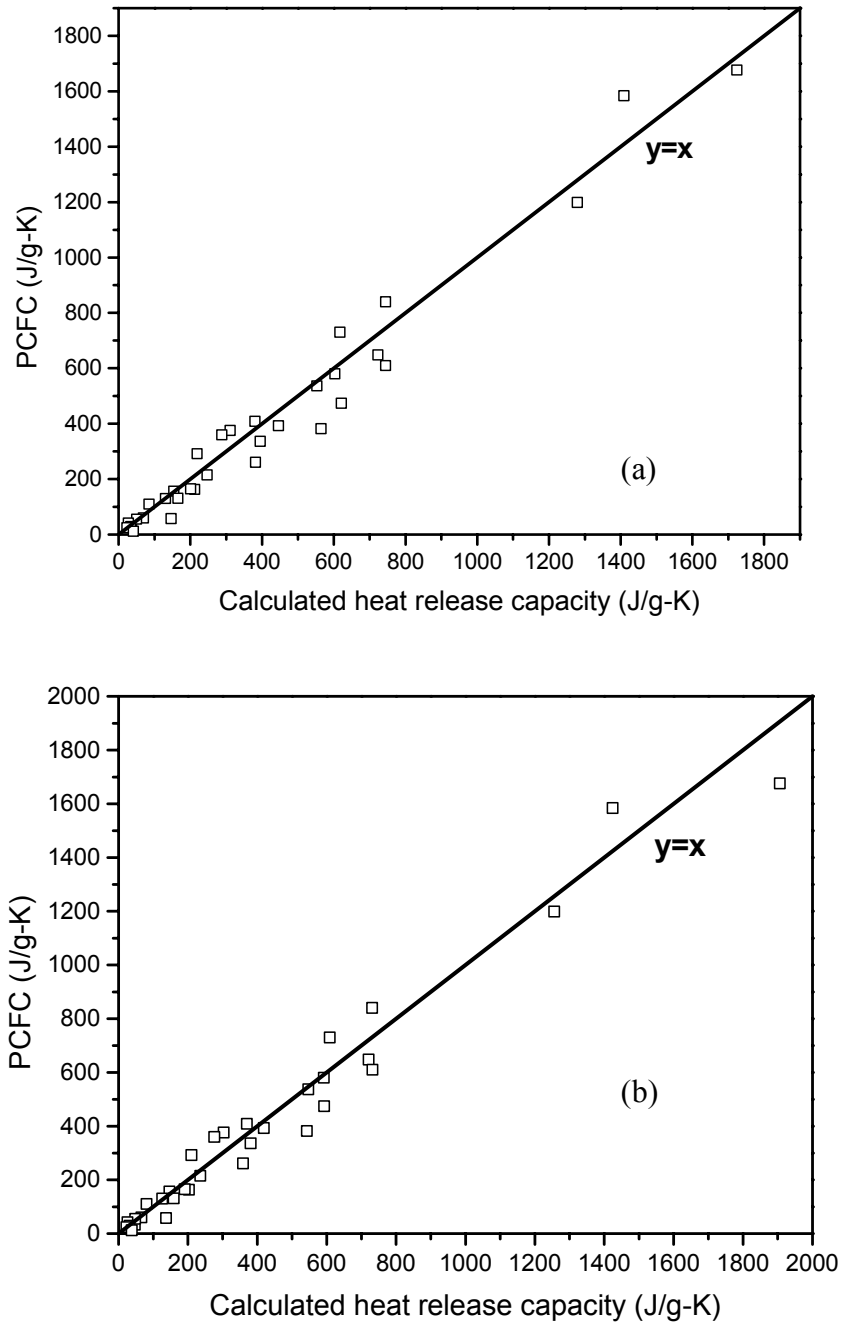


FIGURE 2-13. COMPARISON OF CALCULATED HEAT RELEASE CAPACITY OF POLYMERS WITH PCFC RESULTS (a) OXYGEN CONSUMPTION AND (b) ELEMENT ADDITIVITY

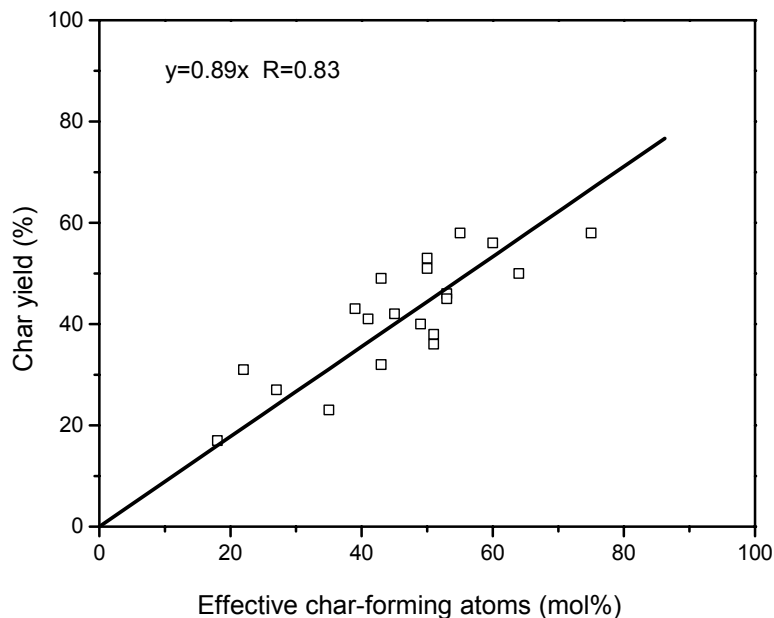


FIGURE 2-14. CORRELATION BETWEEN CHAR YIELD AND MOLAR FRACTION OF EFFECTIVE CHAR-FORMING ATOMS IN POLYMERS

It can be seen that the molar fraction of the effective char-forming atoms is a reasonable measure for estimating the char yields of the polymers, although big deviations are observed in several polymers such as PPO, PI, Kevlar, PBZT, poly(amide-imide), and PES. The discrepancies are due to the following reasons. The proposed method is only based on the independent contributions of some individual atoms, but it does not include the interactions between different atoms, which are actually very important during the char formation process. For example, the alkyl substituents and ether linkages might greatly reduce the effectiveness of the aromatic carbons on char formation. The carbonyl groups in PI might be easily released as volatile CO; therefore, they might not contribute to the char formation, though they are in a heterocyclic structure. In addition, some errors might come from TGA measurements, which is usually around 2%. Despite all these limitations, several structures, such as aromatic rings, heteroaromatic rings, and some conjugate systems, are found in the major structures that can promote char formation.

2.5 DISCUSSION.

Polymer thermal decomposition and flammability were evaluated by pyrolysis GC/MS, STA, and PCFC methods. There was good agreement between the different methods. Several important parameters can determine the ease of polymer combustion, including thermal stability, mass loss rate, the nature and properties of the decomposition products, and the char yield. Most polymers decompose in a single step by a random chain-scission mechanism. Some polymers such as PMMA, P(α -M-S), and POM decompose by an unzipping mechanism. The heats of decomposition for most polymers are endothermic, ranging from 100 to 900 J/g. A few polymers, such as BPC II-polymers and PAN, show an exothermic peak. The maximum mass

loss rate and the heat of combustion of volatiles are important factors in determining the heat release capacity. In addition, the quantum computation results show that there is no simple correlation between bond dissociation energy and activation energy calculated from TGA data. The relatively low thermal stability of aliphatic polymers is mainly due to the easy release of small molecular volatiles, which can be easily detected by TGA. The net heat of complete combustion and heat release capacity of polymers can be successfully estimated by both oxygen consumption and atom additivity principles. The calculated results from both methods correlate relatively well with the PCFC experimental results. It was found that nonburning heteroatoms such as O, N, S, P in polymer structures play an important role in reducing the total heat of combustion because these atoms only add mass without adding significant heat. Aromatic rings, heteroaromatic rings, and any units that can lead to the formation of fused-aromatic ring structures will contribute to the char formation. Generally, the ideal fire-resistant polymers should have the following characteristics: high decomposition temperature, high char yield, low amount and release rate of volatile fuels and low heat of combustion of these fuels, endothermic-phase transition or decomposition, and release of chemical flame-retardant molecules, such as halogen and water. In all, introducing condensed aromatic or heteroaromatic rings and heteroatoms (halogen, N, S, O, P, Si, etc.) is the basic way to reduce polymer flammability.

3. LOW FLAMMABILITY AND THERMAL DECOMPOSITION OF POLY (HYDROXYAMIDE) AND ITS DERIVATIVES.

3.1 INTRODUCTION.

PBOs, which consist of alternating phenylene and condensed aromatic heterocyclic rings, have not only good chemical resistance, high modulus, and high strength but also high thermal stability and low flammability [79-81]. The first PBO was synthesized by Brinker and co-workers [82]. Later, Moyer and Kubota reported the preparation of fully aromatic PBOs by polycondensation reactions to yield the precursor PHA, followed by thermal cyclodehydration to poly(benzoxazole) structures [83 and 84]. However, these PBO polymers are infusible and are soluble only in concentrated sulfuric acid and polyphosphoric acid, so they are difficult to process. Thus, high costs of the finished polymers and of specialized fabrication techniques greatly limit their applications. Later, the effects of introducing hinge atoms or groups into the polymer chain were investigated to increase their flexibility. For example, incorporation of fluorinated linking groups into the polymer backbone enhanced solubility, while good thermo-oxidative stability and high glass transition temperature were retained [85 and 86]. Hsiao and Dai [87] also synthesized a new aromatic poly(ether benzoxazoles) via the introduction of diphenoxy benzene units into the polymer backbone, which greatly improved the solubility.

However, very little research has been performed on the precursor PHAs. Pearce, et al. have reported detailed investigations on the syntheses, thermal properties, and oxygen index of a series of wholly aromatic polyamides based on substituted and unsubstituted m- or p- phenylene diamine with both isophthaloyl and terephthaloyl chlorides [88-92]. Pearce, et al. found that the ortho-, halogen-, nitro-, and cyano-substituted polyamides produce the highest char yield, which are due to cross-linking at high temperatures and the formation of thermally stable benzoxazole rings [93-98]. The amount of PBO structure formed was dependent on the nature of the substituents. The more electron-withdrawing the substituent (e.g., F or NO₂), the more benzoxazole structure is formed. Recently, Kantor, et al. [99] have synthesized a high-molecular-weight poly(3,3'-dihydroxy-biphenyl-isophthalamide) (PHA) as well as a series of halogen, methoxy, phosphinate, and phosphate derivatives. It was found that this PHA cannot only cyclize into fire-resistant PBO, but also absorb some heat and liberate noncombustible water vapor during cyclization [100 and 23]. In addition, all these polymers show a very good solubility in aprotic solvents such as N-methylpyrrolidinone (NMP), N,N-dimethylacetamide (DMAc), and N,N-dimethylformamide. Therefore, they are potential candidates as solvent-processable, fire-resistant polymers for many high-performance applications.

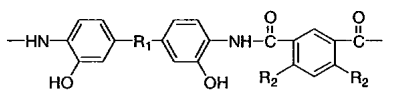
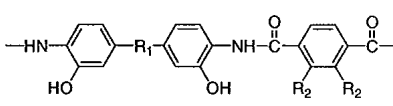
In this section, the low flammability of poly(hydroxyamide) (PHA) and its halogen, methoxy, phosphinate, and phosphate derivatives was characterized by multiple analytical techniques, emphasizing that the thermal decomposition behavior is the basis for the polymer flammability. Pyrolysis gases from these polymers were identified by GC/MS. The residual chars were characterized by Fourier Transform Infrared Spectroscopy (FTIR) and elemental analysis. STA was applied to study the thermal decomposition process, and flammability was measured by PCFC. Halogens, phosphonates, and phosphates were examined because of their expected flame-retardant effects, while methoxy derivatives were examined because of their easy syntheses. Thermal decomposition mechanisms were also proposed for these polymers.

3.2 EXPERIMENTAL.

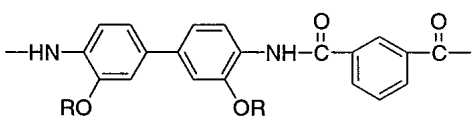
3.2.1 Materials.

The chemical structures of PHA and its derivatives (figure 3-1) are given below. All the samples were supplied by Jungsoo Kim at the University of Massachusetts, Amherst [101].

(a) PHA and halogenated PHAs

					
	R ₁	R ₂	R ₁	R ₂	
PHA-1	-	H	-	H	PHA-2
PHA-3	-	Br	-	Br	PHA-4
PHA-5	C(CF ₃) ₂	Br	C(CF ₃) ₂	Br	PHA-6

(b) PHAs with methoxy groups

Structure			
Polymers	PHA-7	PHA-8	PHA-9
R	Me	Me/H (mol/mol)=50/50	Me/PO(OMe) ₂ (mol/mol)=50/50

(c) PHAs with phosphinate or phosphate groups

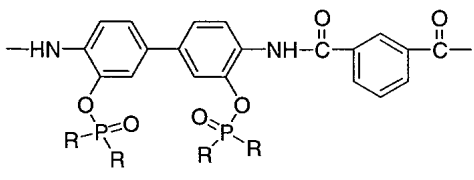
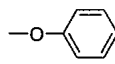
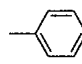
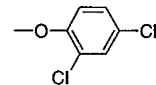
Structure					
Polymer	PHA-10	PHA-11	PHA-12	PHA-13	PHA-14
R			-OC ₂ H ₅		-OCH ₃

FIGURE 3-1. STRUCTURES OF PHA AND ITS DERIVATIVES

3.2.2 Film Preparation.

PHA-1 was dissolved in DMAc at room temperature with 1 wt% of LiCl. The polymer solution was coated onto a glass plate and dried in a vacuum oven at 100°C for one day. While still on the glass plate, the film was then cleaned in an ultrasonic cleaner three times for 30 minutes each time. Afterwards, the film was dried again in a vacuum oven at 120°C for one day. The film was then used for IR analysis.

3.2.3 Characterization.

The thermal decomposition process was examined under N₂ or air by a TA Instruments 2050 TGA. STA was also performed under N₂ with a Rheometric Scientific STA 1500 to study the mass change and the heat absorbed or evolved during the decomposition at high temperatures. Char yield of the polymers is defined here as the percentage of solid residue at 930°C under N₂. Sample weights for all the thermal analyses were approximately 10 mg, and the heating rate was 10°C/min.

Flammability of all the polymers was measured with PCFC. Samples of 1.0 ±0.1 mg were pyrolyzed in a commercial device (CDS Pyroprobe 2000) to 930°C at 4.3°C/s under N₂. The volatiles were continuously swept away by a N₂ flow, mixed with a metered flow of O₂, and completely combusted at 900°C. The consumption rate of O₂ was continuously measured. The heat release results were taken as the average of five measurements for each sample. The coefficient of variation of heat release capacity is around 10%, and the systematic error for total heat released is around 1 kJ/g.

Composition of the volatiles was analyzed by pyrolysis GC/MS. Samples of 0.2~0.3 mg were pyrolyzed under the same conditions used in the PCFC measurements (4.3°C/s to 930°C). The volatiles from pyrolysis were then separated by a Hewlett-Packard 5890 Series II gas chromatograph and analyzed by a Hewlett-Packard 5972 series mass spectrometer. A fused-silica capillary GC column (cross-linked 5% PH ME siloxane, 0.25 mm in diameter and 30 m long) was used. The GC oven was programmed from 36° to 295°C at a heating rate of 10°C/min and then held at 295°C for 15 minutes. Masses were scanned from m/z 11 to 550.

Transmission IR spectra were recorded on a Bio-rad FTS 175C FTIR instrument. The samples for IR analyses were prepared by heating the solution-cast films to desired temperatures at 10°C/min under N₂ in a TGA furnace.

Elemental analyses were obtained on a Control Equipment Model 240XA elemental analyzer.

3.3 RESULTS.

3.3.1 Thermal Stability and Decomposition Process of PHAs.

Table 3-1 summarizes the thermal decomposition properties of PHA and its derivatives. The following discussion examines the details of the different decomposition behavior.

TABLE 3-1. THERMAL DECOMPOSITION OF PHA AND ITS DERIVATIVES IN N₂

Polymers	η_{inh}^a	$T_{99\%}^b$ (°C)	T_2^c (°C)	ΔW_1^d (%)	ΔH_1^e (J/g)	ΔT^f (°C)
PHA-1	0.60	250	586	11	116	240-383
PHA-2	-	290	622	10	145	270-456
PHA-3	0.49	240	485	13	106	250-400
PHA-4	-	284	515	12	110	260-430
PHA-5	0.25	274	508	8	104	245-356
PHA-6	-	282	501	7	108	260-360
PHA-7	0.62	363	591	37	-	363-469
PHA-8	0.70	240	592	6	105	240-335
PHA-9	-	218	574	7	33	230-310
PHA-10	0.44	270	640	45	-	210-500
PHA-11	0.55	300	606	56	-	270-545
PHA-12	- ^g	182	651	16	72	180-360
PHA-13	- ^g	200	654	21	106	180-306
PHA-14	- ^g	184	652	23	121	180-370

^a 0.5g/dl in NMP at room temperature

^b Temperature at 1% weight loss

^c Onset decomposition temperature of the last stage

^d Weight loss during the first stage

^e Heat absorbed during the first stage

^f Temperature range of the first stage

^g Polymers are only partially soluble in NMP

TGA results of PHA-1 and 2 are shown in figure 3-2. It can be seen that they all decompose in two distinct and well-separated stages. The temperature at 1% weight loss ($T_{99\%}$) of PHA-1 (250°C) is lower than PHA-2 (290°C). This difference indicates that PHA-2 (para) is more thermally stable than PHA-1 (iso) due to its regular symmetric structure. X-ray diffraction results (figure 3-3) proved that PHA-2 has a higher crystallinity than PHA-1.

It was found that the thermal decomposition process, flammability, and decomposition products of corresponding iso- and para-type PHAs are similar to each other, except para-PHAs have higher thermal stability. Only the flammability and thermal decomposition properties of iso-PHAs are discussed below.

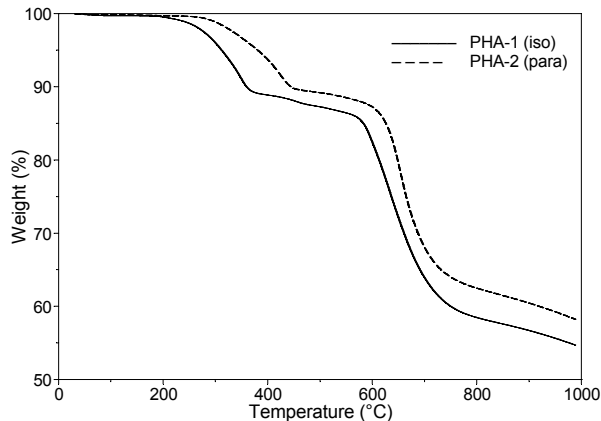


FIGURE 3-2. TGA CURVES OF PHA-1 AND 2 IN N₂

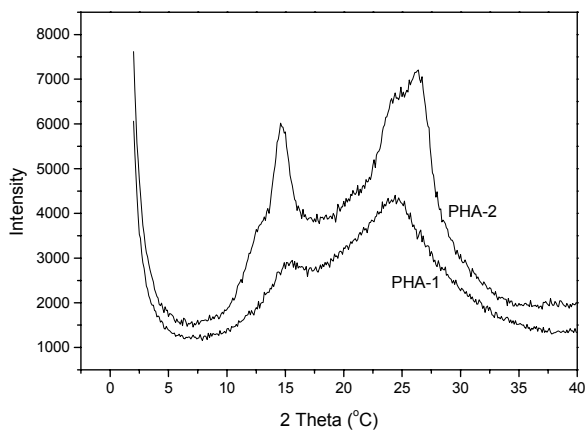


FIGURE 3-3. X-RAY DIFFRACTION OF PHA-1 AND 2

The thermal decomposition processes of PHA-1 and its derivatives under N₂ are shown in figure 3-4.

According to figure 3-4(a), PHA-1 lost about 11% weight in the first decomposition stage (250°~383°C), which agrees very well with the calculated water loss due to the cyclization reaction (11.5%). The second stage (586°~821°C) is associated with a further 30% weight loss due to the extensive breakdown of the PBO backbone. The weight loss then levels off, producing a high char yield of 56%.

Halogenated PHAs (PHA-3 and 5) also decompose in two stages, which is similar to PHA-1 (figure 3-4(a)). Introduction of bromine groups in PHA-3 slightly decreases the thermal stability of the first stage (240°C). In contrast, trifluoromethyl groups have the effect of increasing the thermal stability of PHA-5 (274°C). However, the onset decomposition temperature of the second stage is greatly reduced in both polymers [PHA-3 (484°C) and PHA-5 (508°C)] compared with PHA-1 (586°C). This is because the halogenated PBOs formed at the end of the first stage are less stable. At high temperatures, the halogen groups can be easily stripped away from the polymer main chain before any backbone scission.

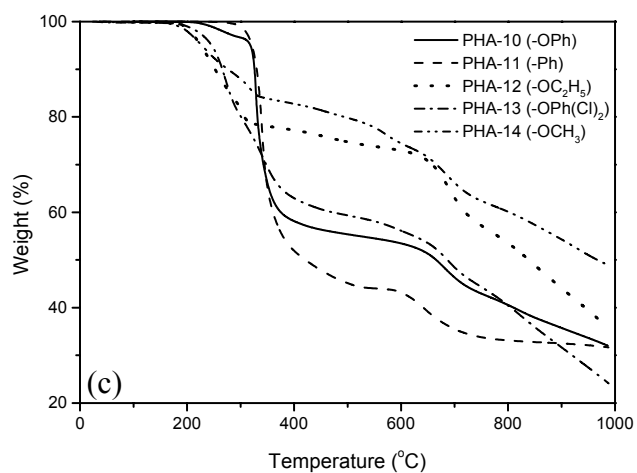
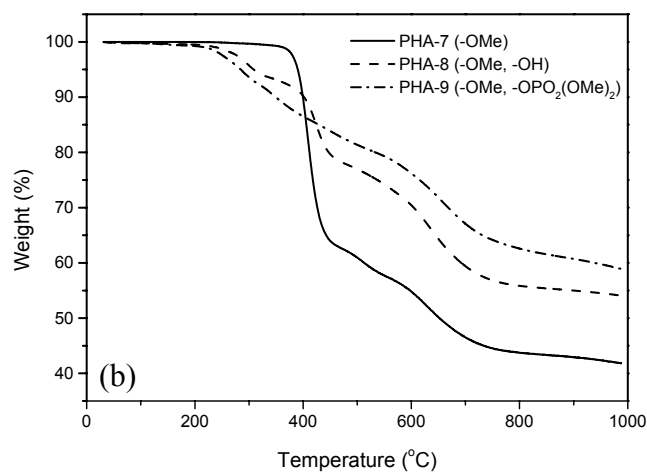
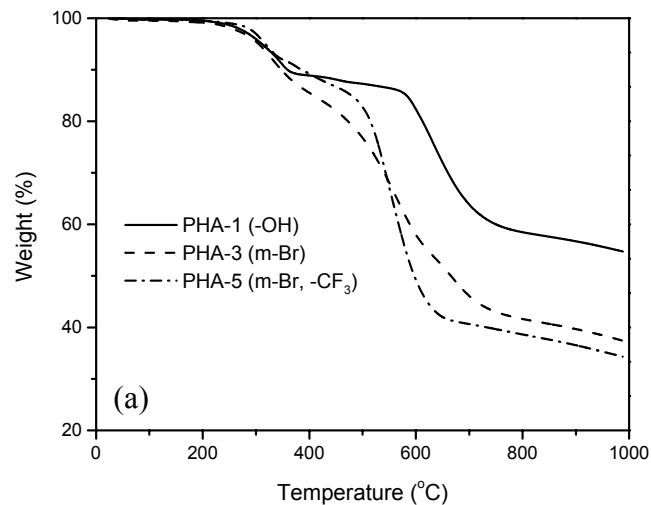


FIGURE 3-4. THE TGA CURVES OF PHA-1 AND ITS DERIVATIVES IN N₂ (a) PHA-1 AND HALOGENATED PHAs, (b) PHAs WITH METHOXY GROUPS, AND (c) PHAs WITH PHOSPHINATE OR PHOSPHATE GROUPS

In PHA-7, hydroxyl groups are totally replaced by methoxy groups. PHA-7 is quite stable up to about 363°C, but then it has a sharp weight loss between 363°~469°C. The 40% weight loss in the first stage is apparently not due to the analogous PHA-to-PBO cyclization reaction in which 17 wt% methanol would be released, but it is mainly due to the release of 1,3-dimethyl isophthalate from the polymer main chain. Copolymer PHA-8, with both methoxy and hydroxyl groups, shows three stages of decomposition. The first stage (240°~334°C) is due to the cyclization of hydroxyl groups (6 wt% water loss as expected). The second stage (397°~476°C) is related to the decomposition of the structures containing methoxy groups, and the third stage is the high-temperature decomposition of polymer backbone. The thermal stability of PHA-9 is very low due to the presence of large phosphate groups (-PO₂(OMe)₂). It begins to decompose around 218°C. Although PHA-7, 8, and 9 have different side groups, they all show a similar decomposing stage between 600°~800°C, which is due to the decomposition of one particular structure.

The thermal decomposition processes of PHA-10 to 14, which contains different phosphinate or phosphate groups, are very different from each other (figure 3-4(c)). PHA-10 and 11 have relatively high thermal stability (300°C) due to their relatively strong bonds in phosphinate or phosphate groups. However, PHA-12 to 14 start to lose weight around 180°C. It is believed that at low temperatures (180°~500°C), the main decomposition is the cleavage of phosphinate or phosphate side groups from the polymer main chain due to their relatively weak linkage and further decomposition of these phosphinates or phosphates. At high temperatures (above 500°C), the polymer breaks along the main chain. Similar to PHA-1 and PHA-7 to 9, these phosphinate or phosphate PHAs all start a new decomposition step around 600°C, which suggests that all these PHAs are converted into a similar structure that might contain some PBO rings before 600°C.

In N₂, all the PHAs can produce high char yields. Char can act as a thermal and mass transfer barrier and greatly reduce the flammability of polymers. However, when PHAs are decomposed in air, the TGA curves are somewhat different (figure 3-5). Although oxygen has no effect on the first decomposition stage, it reduces the thermal stability of the second stage except for the PHAs with halogen groups (figure 3-5(b)). Above 600°C, all the PHAs except for those with phosphinate or phosphate groups (figure 3-5(c)) completely burn without leaving any char. It was concluded that oxygen does not affect the initial thermal stability, but that it can oxidize the carbonaceous char very easily at high temperatures. The presence of the halogen groups can improve the thermo-oxidative stability, while phosphate groups can preserve more char during burning.

Besides the thermal stability and decomposition processes, another important thermal property that can be obtained only by STA measurements is the enthalpy change associated with the weight loss. The high-temperature DSC curves of PHA and its derivatives are shown in figure 3-6.

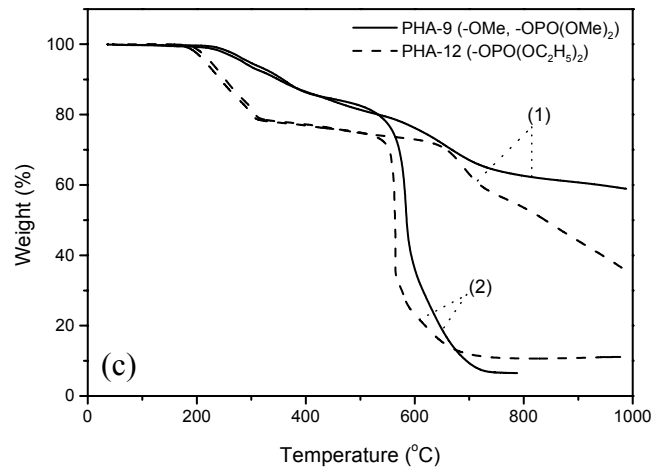
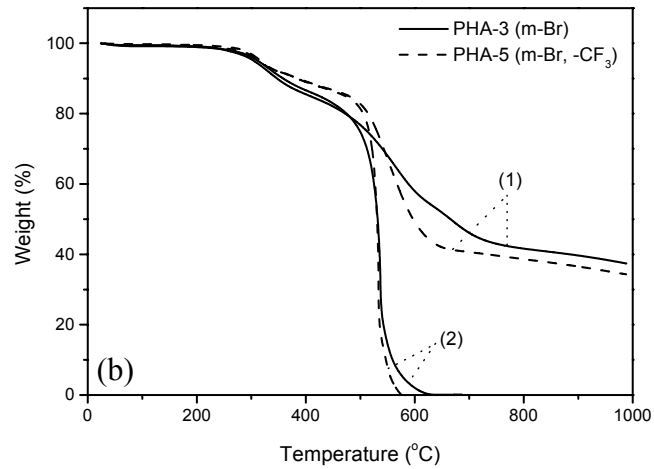
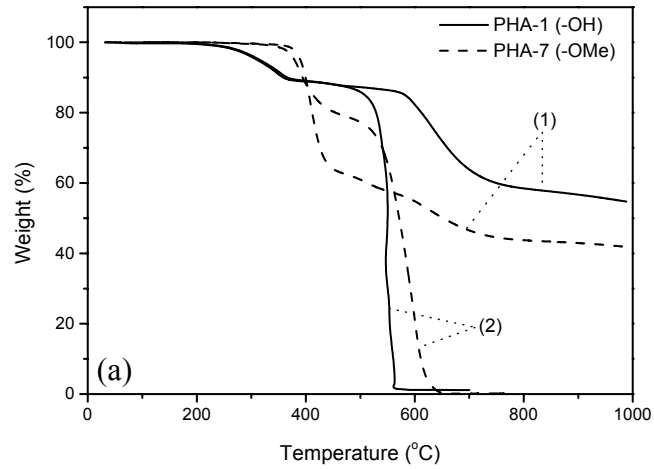


FIGURE 3-5. EFFECTS OF OXYGEN ON THE DECOMPOSITION OF PHA-1 AND ITS DERIVATIVES (a) PHA-1 AND ITS METHOXY DERIVATIVE, (b) HALOGENATED PHAs, AND (c) PHOSPHATE PHAs, (1) IN N₂ AND (2) IN AIR

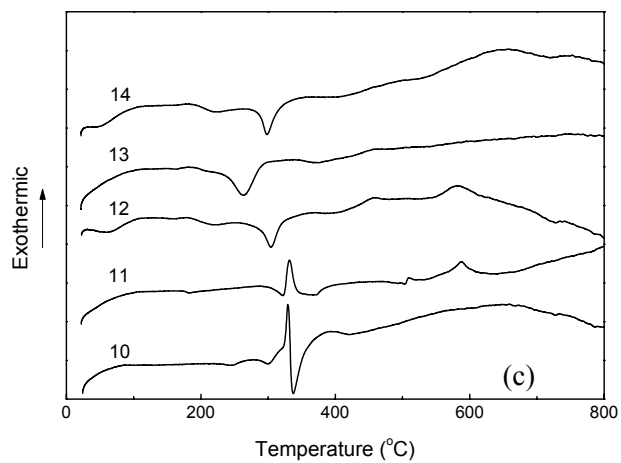
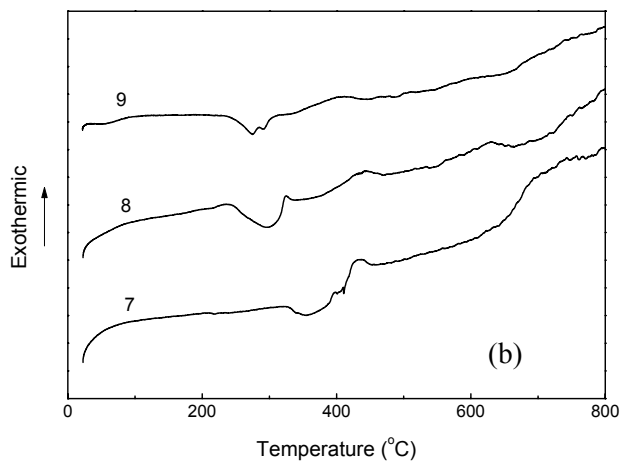
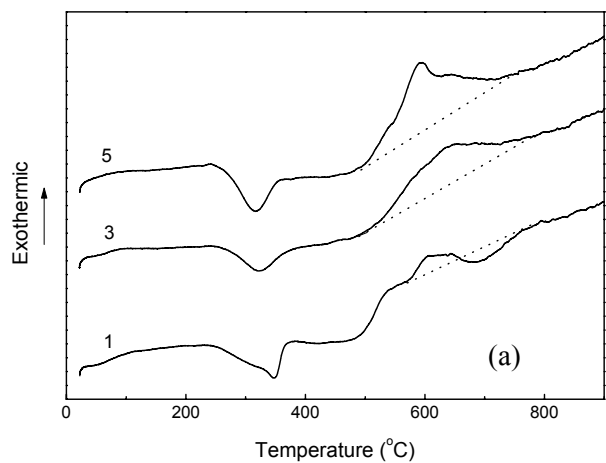


FIGURE 3-6. HIGH-TEMPERATURE DSC CURVES OF PHA-1 AND ITS DERIVATIVES (a) PHA-1 AND HALOGENATED PHAs, (b) PHAs WITH METHOXY GROUPS, AND (c) PHAs WITH PHOSPHINATE OR PHOSPHATE GROUPS

All the PHAs (except for PHA-10 and 11) show an endothermic peak in the early stage of decomposition, but they differ at high temperatures. In the cases of PHA-1, 3, and 5 (figure 3-6(a)), the heat absorbed in the first stage is around 105~120 J/g as a consequence of the cyclization reaction and vaporization of water. In the second stage, PHA-1 shows a combination of endo- and exothermic behavior, which might be due to the combined effects of decomposition and char formation processes. PHA-3 and 5 instead show a distinct exothermic peak in the second stage, which might be due to the release of HBr and some cross-linking reactions. For PHA-7 with methoxy groups (figure 3-6(b)), the endothermic peak between 320°~395°C might result from the melting of the polymer and some possible cyclization reactions. The exothermic peak that follows (396°~469°C) is probably due to a series of thermal decomposition reactions, including the breaking of the polymer main chain. The heat events in phosphinate or phosphate PHAs (figure 3-6(c)) are more complicated. PHA-12 to 14 show endothermic peaks at low temperatures (180°~360°C) due to the release and decomposition of phosphinate or phosphate side groups. However, PHA-10 and 11 have a combination of endo- and exothermic peaks in the first stage (300°~430°C). The enthalpy change of methoxy, phosphinate, or phosphate PHAs is difficult to determine at high temperatures.

3.3.2 Flammability.

The PCFC results (table 3-2) show that PHA and most of its derivatives have rather low flammability compared to commercial polymers such as PE, PS, and PC. Fire resistance of PHA-1 is close to polyimide. Moreover, bromine and trifluoromethyl groups can further reduce the flammability by releasing halogenated decomposition products with low flammability. As a result, PHA-5 is one of the few polymers that have extremely low flammability. The flammability of PHA-7 is relatively high, but it can be reduced by partially replacing methoxy groups with hydroxyl (PHA-8) or phosphate groups (PHA-9) to form a copolymer, which can extend the decomposition temperature range and slow down the decomposition rate.

However, if methoxy or hydroxyl groups are totally substituted by different phosphinate or phosphate groups (PHA-10 to 14), the flammability of polymers is greatly dependent on the types of substituents. PHA-10 and 11, which contain phenyl or phenoxy groups in the phosphinate or phosphates, have relatively higher flammability. The higher flammability is due to their relatively faster decomposition rates and release of more flammable compounds such as benzene and phenol. The flammability of PHA-12 to 14 is greatly reduced due to the significant reduction in the mass loss rates. Therefore, the introduction of bulky phosphinate or phosphate side groups to a thermally stable PHA backbone does not always improve the flame resistance of the polymer even though the phosphinate or phosphate groups are widely used in the industry as flame-retardant additives for plastics. Worse, the flammability of the polymer might be increased due to fast cleavage of these bulky fuel-forming side groups.

TABLE 3-2. FLAMMABILITY OF PHA AND ITS DERIVATIVES

Polymers	Heat Release Capacity ^a (J/g-K)	Total Heat ^a (kJ/g)	T _{max} ^b (°C)	Maximum Mass Loss Rate (x 10 ³ /s)	Char Yield (%)
PHA-7	130	17	409	1.4	43
PHA-1	42	10	633	0.4	56
PHA-8	33	11	425	0.5	55
PHA-9	18	9	658	0.2	60
PHA-3	17	5	563	0.4	39
PHA-5	8	3	553	0.7	36
PHA-10	340	15	327	3.3	36
PHA-11	210	21	341	2.9	32
PHA-12	73	9	304	0.4	41
PHA-13	59	8	271	0.6	29
PHA-14	19	8	319	0.2	52
PE	1558	40	471	7.0	0
PS	1199	37	417	5.2	0
PC	382	19	514	3.3	17
Kevlar	292	15	576	2.5	32
PEEK	163	13	586	2.2	46
PI	29	9	602	0.5	50

^a PCFC results. The rest are derivative of TGA results.

^b The temperature at maximum mass loss rate.

Generally, PHAs with low mass loss rates usually have low heat release capacity (except for halogenated PHAs). This is because there are generally two factors that can determine the heat release capacity: maximum mass loss rate and the heat of combustion of the decomposition products at that temperature. For PHAs with similar backbone structures, the major decomposition products are not very different. Therefore, the mass loss rate becomes the most important factor that can determine the heat release rate. According to figure 3-7, PHA-1 and halogenated PHAs (PHA-3 and 5) decompose faster at high temperatures (maximum mass loss rates occur around 550°~650°C) due to the massive main-chain scission, while PHA-7, 8, and phosphinate or phosphate PHAs (PHA-10 to 14) have their maximum mass loss rates at low temperatures (around 300°~500°C) due to the fast cleavage of methyl, phosphinate, or phosphate groups.

Although PHA-8 is the copolymer of PHA-1 and PHA-7, its flammability is almost the same as PHA-1 rather than an average of the two homopolymers. This nonlinearity means that copolymerization of two polymers with different thermal stability, thermal decomposition process and flammability might be a good way to reduce flammability. The copolymerization can broaden the whole decomposition range and reduce the mass loss rate, therefore reducing the heat release rate.

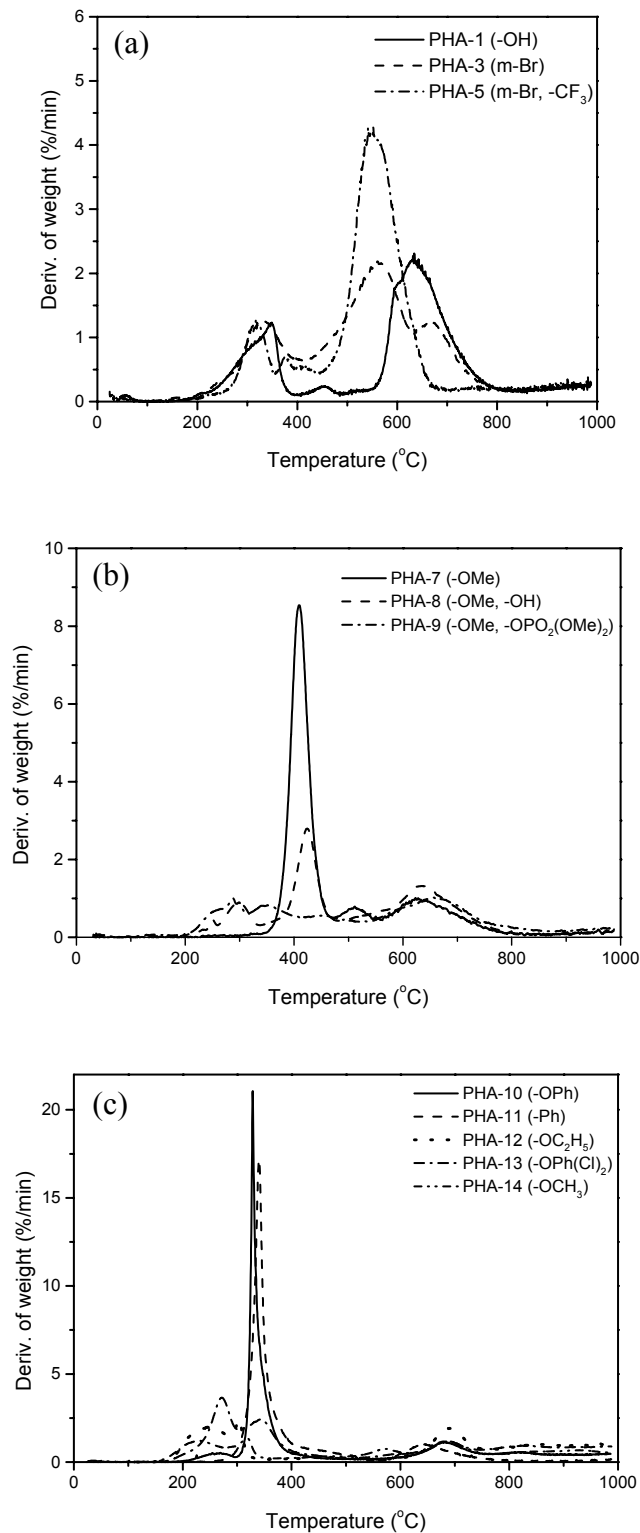


FIGURE 3-7. DERIVATIVE TGA CURVES OF PHA-1 AND ITS DERIVATIVES (a) PHA-1 AND HALOGENATED PHAs, (b) PHAs WITH METHOXY GROUPS, AND (c) PHAs WITH PHOSPHINATE OR PHOSPHATE GROUPS

In conclusion, the major reasons for the low flammability of most PHA polymers are the stable aromatic backbone structures, low mass loss rates, high char yields, and the ability to release flame-retardant molecules (such as water and halogenated compounds), which can act physically or chemically during combustion. However, the introduction of bulky, fuel-forming phosphinate or phosphate groups should be avoided in order to get good flame resistance.

3.3.3 Characterization of Chars by IR and Elemental Analysis.

Chars are complex materials that contain fused aromatic structures and may include heteroatoms (O, N, P, and S). They are usually insoluble, which limits their characterization to the tools used in solid-state chemistry and physics. The composition of the char is usually characterized by elemental analysis. Table 3-3 lists some elemental analyses of PHA-1 pyrolyzed at different temperatures.

TABLE 3-3. ELEMENTAL ANALYSES OF PHA-1 AND ITS CHARS AT DIFFERENT TEMPERATURES

Temperature (°C)	Measured (wt%)				Calculated (wt%)				Residual Weight (%)
	C	H	N	O	C	H	N	O	
25 (PHA)	67.26	3.78	7.56	21.4	69.4	4.1	8.1	18.4	100
400 (PBO)	75.96	3.26	8.62	12.16	77.4	3.2	9	10.4	90
650	79.97	2.93	7.84	9.26					75
1000	87.07	0.44	3.78	8.71					50

According to table 3-3, the char of PHA-1 at 400°C has the same elemental composition as PBO, which supports the assumption that the first stage (250°~383°C) is due to the cyclization reaction. With the temperature increasing, the contents of H, N, and O decrease dramatically, but the carbon content increases. At 1000°C, the formula of the char can be written as $C_{27}H_{1.63}NO_2$, which suggests that the structure of the char at high temperatures must be some fused aromatic and heteroaromatic rings with low hydrogen content.

The IR spectra of PHA-1 chars produced at different temperatures are shown in figure 3-8. The tentative band assignments are given in table 3-4 [101]. According to the IR results, there is no difference between the spectra of room temperature and 250°C, which indicates that PHA-1 is stable until 250°C. When the polymer is heated to 350°C, the intensity of the broad absorption at 3294 cm^{-1} (O-H stretch) is greatly decreased because some of the hydroxyl groups have been converted into benzoxazole rings. In addition, most peaks in the region 2000 to 500 cm^{-1} either shift or split into two peaks due to the ongoing cyclization reaction, which involves some coexisting structures. Some new peaks also show up, such as the peaks at 1267, 1051, and 705 cm^{-1} that are associated with the benzoxazole rings. At 400°C, the peaks at 3405 cm^{-1} (N-H stretch) and 3294 cm^{-1} (O-H stretch) completely disappear, which suggests that the N-H and O-H groups have been totally changed into benzoxazole rings. The region near 1650-1500 cm^{-1} is very characteristic of benzoxazole. The C=C/C=N stretching vibrations (1624 cm^{-1}) and the peak at 1541 cm^{-1} are characteristics of the conjugation between the benzene and the oxazole rings. A broad peak at 1280-1231 cm^{-1} is due to the oxazole-ring breathing mode, and

heterocyclic-ring vibration is found at 705 cm^{-1} . The confirmation of PBO structure at 400°C by IR further supports the proposition that the PHA undergoes cyclization reaction in the first decomposition stage.

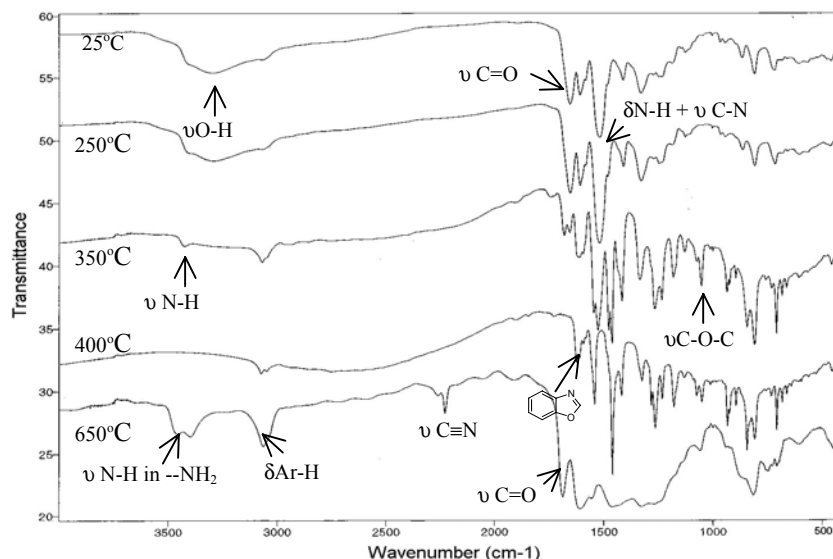


FIGURE 3-8. INFRARED SPECTRA OF PHA-1 AT DIFFERENT TEMPERATURES

TABLE 3-4. INFRARED BAND ASSIGNMENTS OF PHA AND PBO

Wavenumber (cm^{-1})	Tentative Assignment
3405 (m)	Free non-hydrogen-bonded N-H stretching
3294 (b)	Self-associate O-H stretching
3068 (sh)	Aromatic C-H stretching
1653 (s)	C=O stretching
1608(m), 1582(sh), 1409(m)	Aromatic C-C stretching
1518 (vs)	N-H vibration and C-N stretching
1230 (w)	Aromatic C-O stretching
863(m), 806(m)	C-H out-of-plane bending in 1,2,4 three substituted benzene rings
712 (m)	C-H bending in 1,3 two substituted benzene rings
1624 (m)*	C=C/C=N stretching
1541(s)*	Ring vibration characteristics of conjugation between benzene and oxazole ring
1460 (vs)*	In plane ring vibration characteristic of two-substituted benzoxazole
1282 (s), 1264 (s)*	Oxazole ring breathing
1073(m), 1049(m)*	C-O-C stretching in benzoxazole ring

*Bands in PBO. All the peak positions refer to spectra collected at ambient temperature. s: strong; m: medium; w: weak; sh: shoulder; vs: very strong; b: broad.

When PHA-1 further decomposes at 650°C, the color of the film changes from amber to black. In the IR spectrum at 650°C, several features are apparent. New peaks at 3457, 3397 cm^{-1} (apparently N-H stretch in NH_2 groups), 2228 cm^{-1} ($\text{C}\equiv\text{N}$ stretch in aromatic nitrile groups), and 1685 cm^{-1} (carbonyl groups) can be easily identified. The peaks in the region from 1600 to 1200 cm^{-1} become broader and less resolved, but most of the aromatic bands are still present. In addition, the absorptions at 3061 cm^{-1} (aromatic C-H stretching) and 900-700 cm^{-1} (substituted benzene ring vibration) become broader and stronger. All the results suggest that as the pyrolysis proceeds, the char becomes more and more aromatic in character and it contains some CN, NH_2 and CO functional groups.

3.3.4 Identification of Volatiles by GC/MS.

The volatiles from all the PHAs are characterized by pyrolysis GC/MS to aid the development of decomposition mechanisms. The TIC pyrograms (pyrolysis GC/MS traces) of some PHAs are shown in figure 3-9.

All the volatiles can be divided into four groups: (1) low boiling point products such as CO , CO_2 , H_2O , CH_3OH , and HCN , which cannot be separated effectively by normal GC operation and may come from the cyclization reaction or decomposition of the backbone; (2) aromatic hydrocarbons, amines, amides, nitriles, benzoxazoles, and isocyanates, which correspond to the partial fragments of polymer main chain; (3) Halogenated, methyl, phosphinate, and phosphate compounds, which are attributed to the cleavage of the substituents; (4) high boiling point products formed by isomerization, rearrangement, or cross-linking reactions at high temperatures, such as 3,4-diphenyl-1H-pyrazole.

About 70 wt% of volatiles ultimately released from PHAs (except for phosphinate or phosphate PHAs) are CO_2 , CO , H_2O , and HCN , of which CO_2 and CO are present in the largest quantities (around 50 wt%). In contrast, major decomposition products of PHA-10~14 consist of phosphinates, phosphates, and their ester fragments such as phenol, benzene, 2,4-dichlorophenol, methanol, and ethanol. For the halogenated PHAs, bromine was observed in the volatiles not only as HBr but also in the form of a small amount of brominated aromatic compounds (such as $\text{C}_6\text{H}_4\text{Br}_2$ and $\text{C}_6\text{H}_3\text{Br}_3$). However, fluorine was only detected as fluorinated compounds (such as CF_3Br and $\text{CF}_3\text{CH}_2\text{Br}$). All these halogenated products have low flammability on their own and are very good gas-phase flame-retardants during combustion.

An important characteristic of the decomposition of PHAs with methoxy groups is that their decomposition products contain significant amounts of methyl- or methoxy-substituted aromatic compounds. The methyl or methoxy groups might come from the cleavage of side groups.

It was also found that HCN (about 5~10 wt%) is only produced at high temperatures from these polymers, usually above 500°C. With temperature increase, the CO/CO_2 ratio increases.

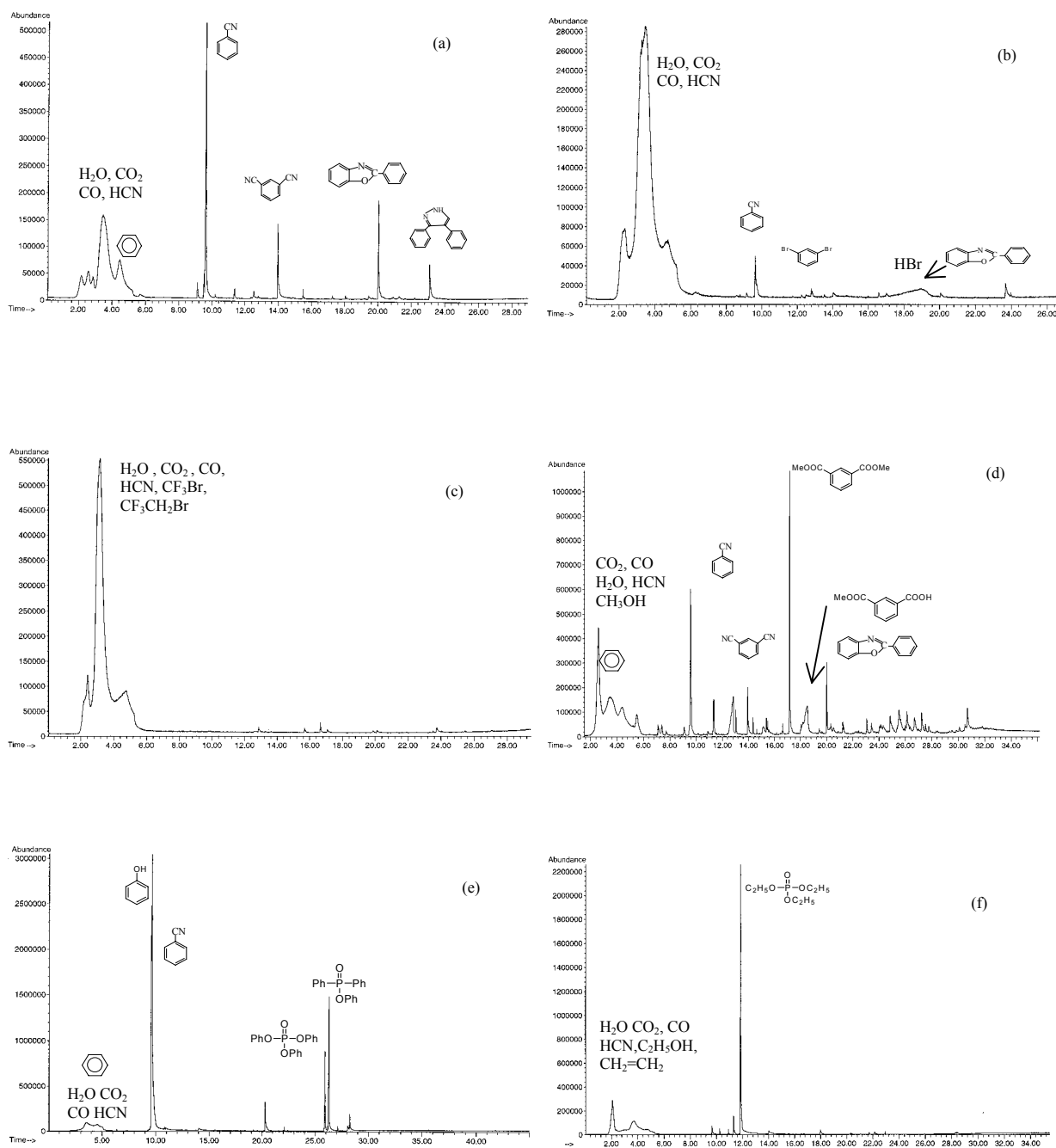


FIGURE 3-9. PYROLYSIS GC/MS TRACES OF PHA-1 AND ITS DERIVATIVES (HEATING TO 930°C AT 4.3°C/s) (a) PHA-1, (b) PHA-3, (c) PHA-5, (d) PHA-7, (e) PHA-10, AND (f) PHA-12

The thermal decomposition products at different temperature ranges are also studied. For PHAs containing only hydroxy groups (PHA-1 (figure 3-10), PHA-3 and 5), the main decomposition products during the first stage are water and a small amount of CO₂, which suggests some hydrolytic decomposition. The water generated during cyclization could be responsible for this hydrolysis. When these polymers are heated to higher temperatures, they release some aromatic compounds, such as the heterocyclic-aromatic species 2-phenyl benzoxazole, which is a typical structure within PBO. However, the major volatiles are still CO₂, CO, H₂O, and HCN, which along with high char yields are responsible for their low flammability.

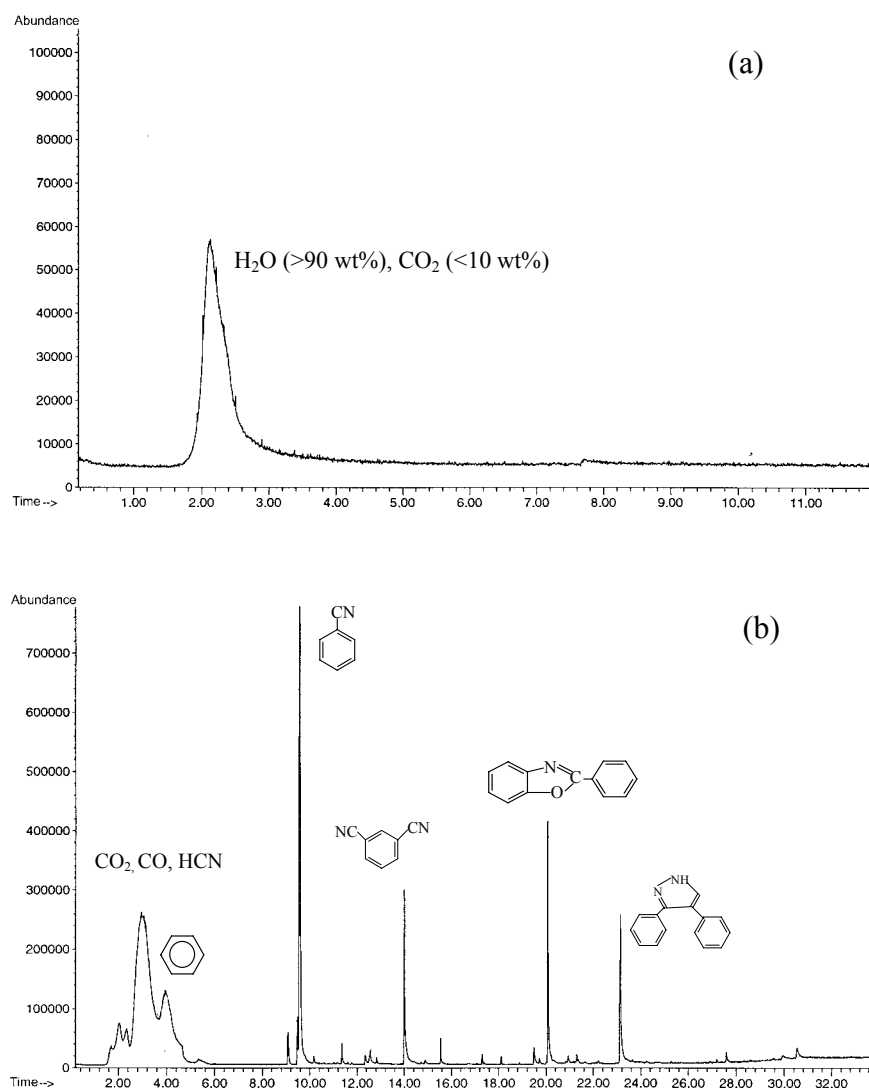


FIGURE 3-10. PYROLYSIS GC/MS TRACES OF PHA-1 AT DIFFERENT TEMPERATURE RANGES (HEATING RATE, 4.3°C/s) (a) 250° ~ 383°C AND (b) 383° ~ 930°C

In contrast, for PHAs with methoxy groups (PHA-7 (figure 3-11) to 9), the decomposition products at low temperatures not only contain CO₂, CO, H₂O, and CH₃OH but also a large amount of 1,3-dimethyl isophthalate. At higher temperatures, these polymers give out more aromatic compounds with methoxy or methyl substituents.

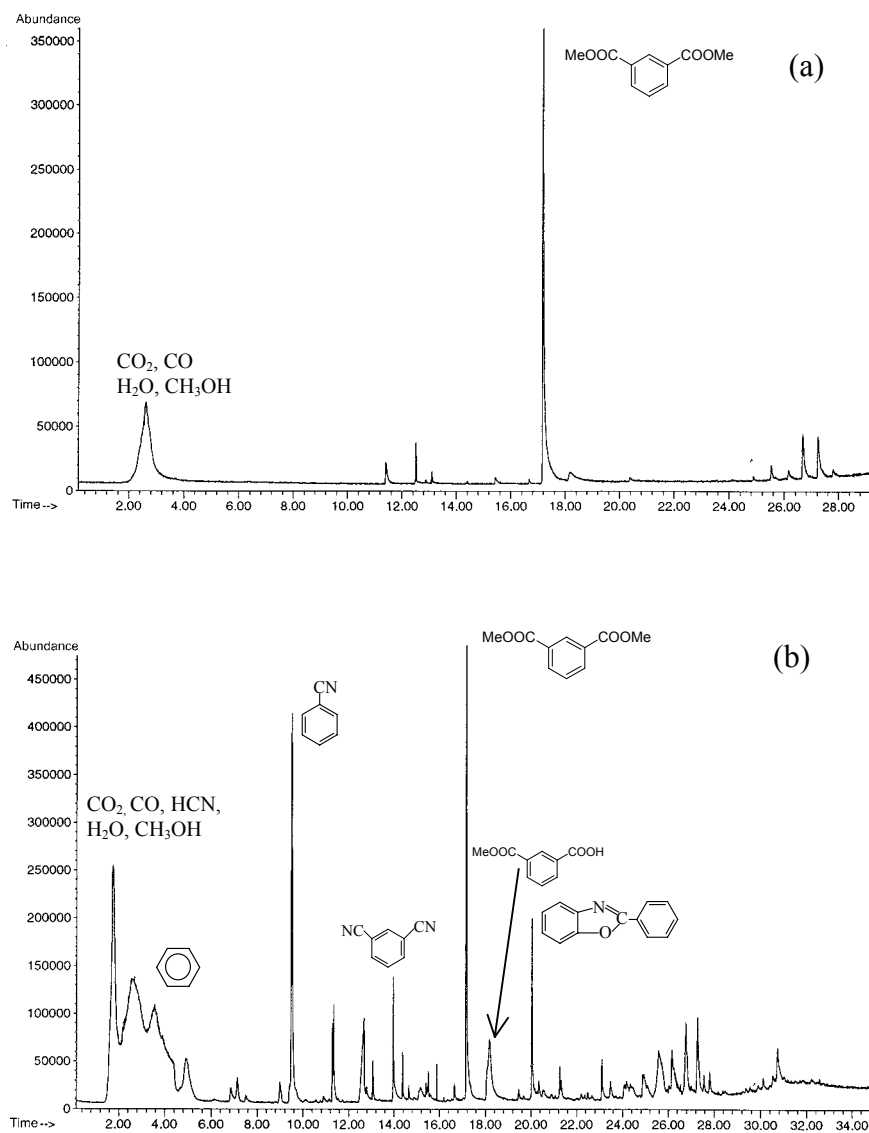


FIGURE 3-11. PYROLYSIS GC/MS TRACES OF PHA-7 AT DIFFERENT TEMPERATURE RANGES (HEATING RATE, 4.3°C/s) (a) 350° ~ 469°C AND (b) 469° ~ 930°C

The major decomposition products of phosphinate or phosphate PHAs below 500°C (figure 3-12) are flammable phosphinates and phosphates as well as their ester fragments, which lead to their high flammability. At high temperatures, some aromatic compounds from the polymer backbone are released.

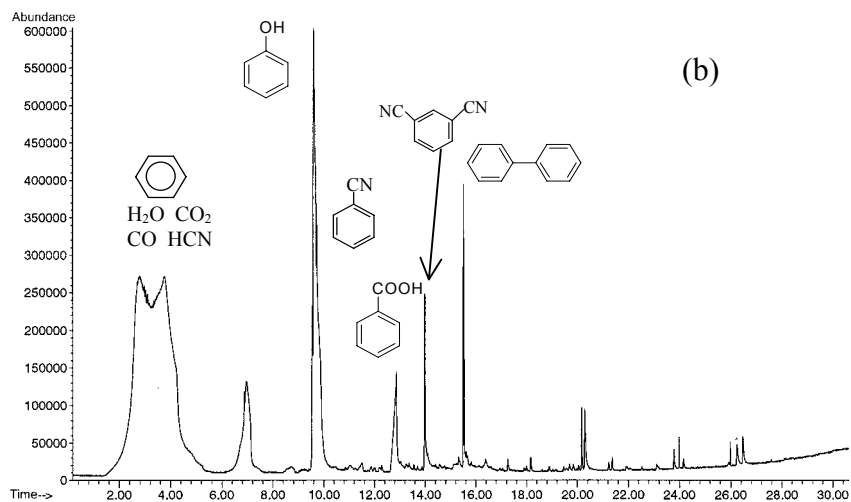
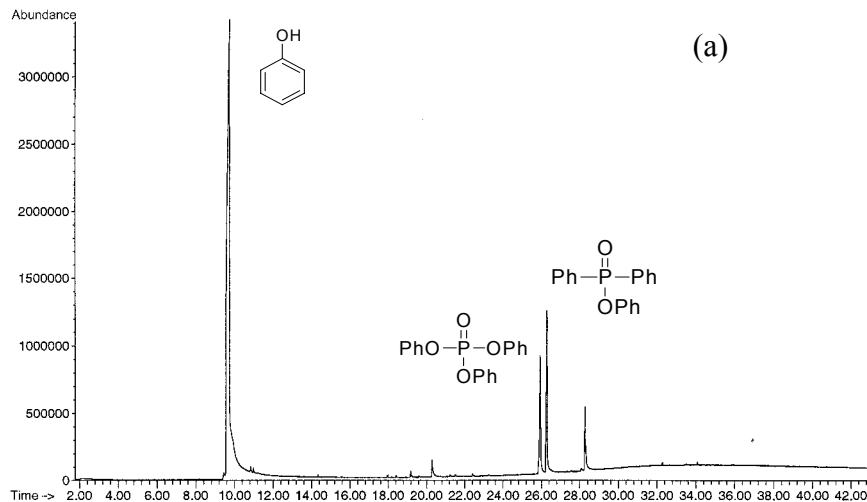


FIGURE 3-12. PYROLYSIS GC/MS TRACES OF PHA-10 AT DIFFERENT TEMPERATURE RANGES (HEATING RATE, 4.3°C/s)
(a) 250° ~ 500°C AND (b) 500° ~ 930°C

In summary, at low temperatures (below 500°C), most volatiles released are CO₂, H₂O, CH₃OH, phosphinate, phosphates, and their ester fragments, depending on the structures of the PHAs. At high temperatures (above 500°C), PHAs produce more aromatic volatiles resulted from backbone scission.

3.3.5 Thermal Decomposition Mechanisms.

Thermal decomposition mechanisms of PHA-1 and its derivatives were proposed by identification of the major volatiles. The cyclization of PHA-1 into PBO is well known [82-84]. Pearce, et al. have also studied the basic mechanisms for the formation of PBOs from ortho halogen-, nitro-, and cyano-substituted polyamides [93-98]. They found that the char yield and

flame resistance of these polyamides can all be greatly improved due to the ring-forming reaction during their pyrolysis. However, there is no detailed research on the thermal decomposition of methoxy and phosphinate or phosphate PHAs.

Possibly, PHA derivatives might decompose by the same mechanism as PHA-1, shown in figure 3-13. First, they are cyclized to PBO by releasing some small molecules (ROH). The PBO structures then break down at high temperatures. In the following discussion, it will be shown whether this mechanism is valid to all the PHA derivatives.

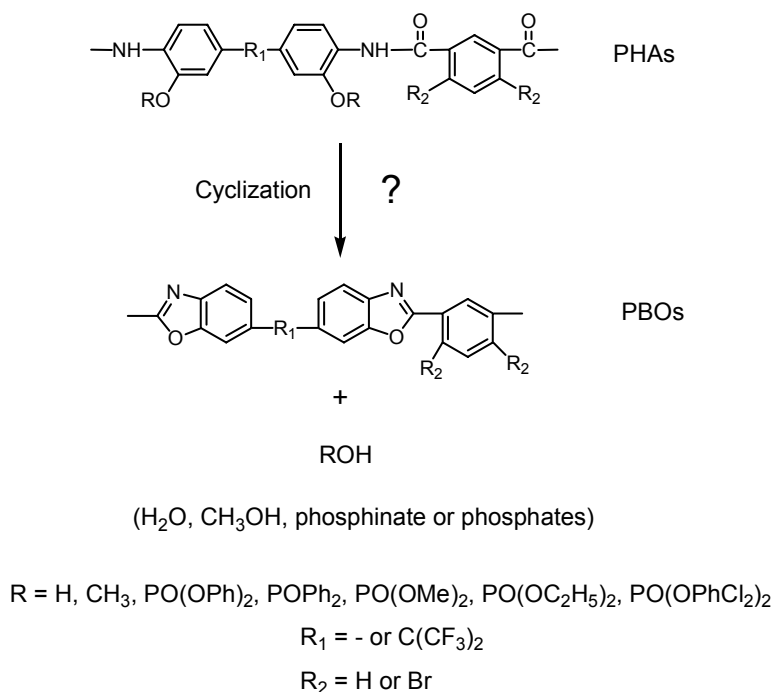


FIGURE 3-13. PRESUMED CYCLIZATION OF PHA AND ITS DERIVATIVES

Based on the GC/MS trace of PHA-1 at low temperatures, water is the major volatile, which comes from intramolecular cyclization. In addition, H₂O could also be generated by the intermolecular condensation of iminol forms [94] (figure 3-14). However, this reaction has a lower probability of occurring because the presence of 2-phenyl benzoxazole in the high-temperature decomposition volatiles strongly suggests that H₂O is formed by intramolecular cyclization (figure 3-15(a)(I)).

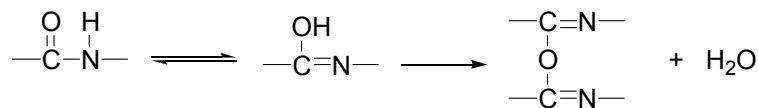
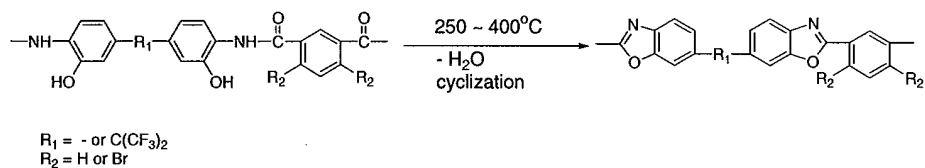


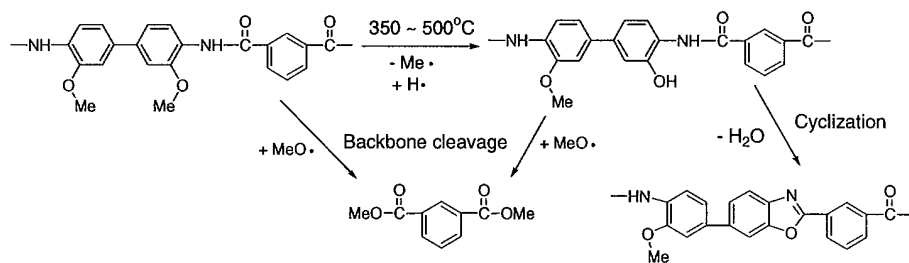
FIGURE 3-14. WATER GENERATED BY INTERMOLECULAR REACTION

(a) Low temperatures (< 500°C)

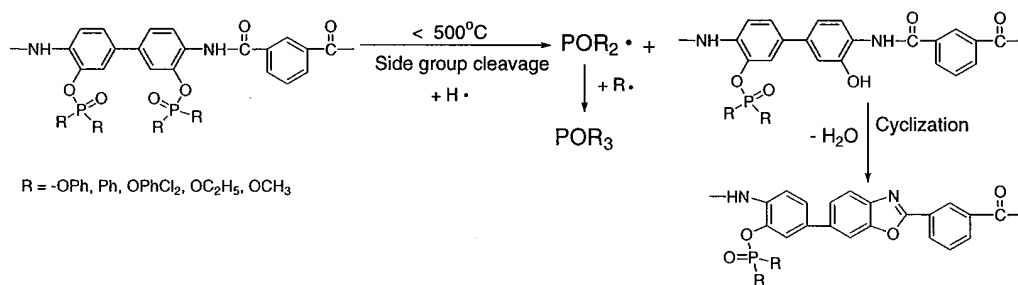
(I) PHA and halogenated PHAs (PHA-1, 3, 5)



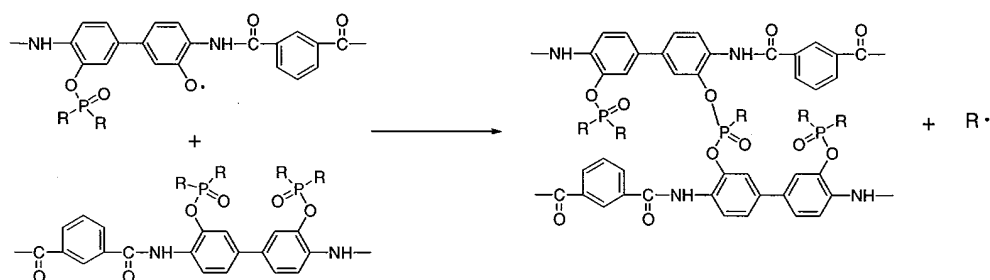
(II) PHAs with methoxy groups (PHA-7 ~ 9)



(III) Phosphinate or phosphate PHAs (PHA-10~14)



Cross-linking reaction



(b) High temperatures (> 500°C)

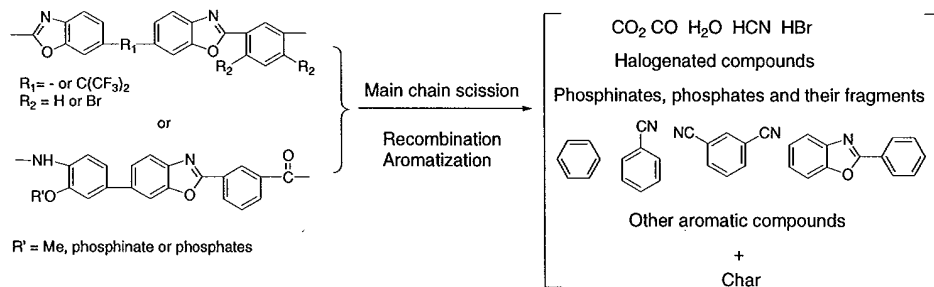


FIGURE 3-15. PROPOSED THERMAL DECOMPOSITION MECHANISMS OF PHAs

A small amount of CO₂ is detected in the first decomposition stage of PHA-1. This might be due to the hydrolytic cleavage of the amide linkage, which can lead to the formation of two fragments with NH₂ and COOH end-groups. The COOH groups would then decarboxylate to give out CO₂. This hydrolytic reaction is quite possible because a significant amount of H₂O is present in this stage.

The second stage is the decomposition of the PBO structure formed. High-temperature thermal decomposition might be initiated by random homolytic cleavage of the strong phenyl-phenyl bond in the main chain, followed by hydrogen transfer, rearrangement, cross-linking, and other secondary reactions. Decomposition products from the second stage include five major aromatic compounds: benzene, benzonitrile, benzenedicarbonitrile, 2-phenyl benzoxazole, and 3,4-diphenyl-1H-pyrazole (figure 3-10). PHA-3 and 5 decompose in almost the same way as PHA-1, but the amount of aromatic volatile is greatly reduced by the introduction of heavy bromine atom (figure 3-9(b)). HBr is formed above 400°C by homolytic cleavage of the aromatic C-Br bond, followed by hydrogen abstraction.

Although the only structural difference between PHA-7 and PHA-1 is OCH₃ versus OH side groups, their decomposition mechanisms are very different. The detection of 2-phenyl benzoxazole from PHA-7 at high temperatures indicates that some cyclization reactions also occurred in the first decomposition stage. However, if PHA-7 is cyclized according to the same mechanism proposed for PHA-1, about 17 wt% methanol should be released. However, only 1.5 wt% methanol is detected by pyrolysis GC/MS, and the 40% weight loss in the first stage is due to other compounds such as CO₂, CO, H₂O, and dimethyl isophthalate (figure 3-11). The formation of dimethyl isophthalate can only be done by breaking the polymer main chain. Therefore, it is believed that both cyclization and main-chain scission occurred in PHA-7 during the first decomposition stage (figure 3-15(a)(II)). In addition, the cyclization reaction does not proceed by releasing methanol, but more likely through another route that releases water (approximately 5 wt% detected by pyrolysis GC/MS). Then, at the end of the first stage, PHA-7 is converted into a structure with both benzoxazole rings and methoxy groups. Because both PHA-1 and 7 have the same backbone structures, the difference in decomposition mechanisms must be attributed to the side groups. The O-Me bond (50 kcal/mol), the weakest bond in PHA-7, is much weaker than O-H bonds (72 kcal/mol) in PHA-1. As a result, the methyl groups can be cleaved easily from the polymer backbone and react with the other aromatic radicals to form various methyl- or methoxy-substituted compounds. The decomposition mechanism of the copolymer PHA-8 appears to be a combination of that for PHA-7 and 1.

Similarly, the bulky phosphinate or phosphate side groups in PHA-10~14 can be easily cleaved from the polymer backbone at low temperatures (figure 3-15(a)(III)). Then following the same route as PHA-7, the polymers can be partially cyclized. Therefore, before any main-chain scission (above 500°C), the polymers are transformed into a structure with both benzoxazole rings and phosphinate or phosphate groups. According to elemental analysis, the char at 930°C still contains a certain amount of phosphorus, which might be trapped by some cross-linking reactions during decomposition (figure 3-15(a)(III)). This observation also proves that phosphorous can reduce flammability by promoting the char formation.

The methoxy and phosphate PHA-9 is a copolymer of PHA-7 and 14. At low temperatures (below 500°C), this polymer breaks at both side-chain and main-chain positions to give out trimethyl phosphate and dimethyl isophthalate.

At high temperatures (above 500°C), the decomposition of methoxy and phosphinate or phosphate PHAs is basically due to the random main-chain scission of a general structure that contains both benzoxazole rings and methoxy, phosphinate, or phosphate groups (figure 3-15(b)). For PHA and halogenated PHAs, they have been totally converted into quasi-PBO structures at the end of the first stage. Many reactions can occur at high temperatures, such as main-chain scission to give out different aromatic volatiles and recombination and aromatization to form char.

The thermal decomposition mechanisms of all the PHAs are summarized in figure 3-15.

3.4 DISCUSSION.

PHA and most of its derivatives have very low flammability, especially the ones containing halogen groups. PHA-7 with methoxy groups is more thermally stable, but it exhibits higher flammability due to the main-chain scission at low temperatures. PHA-10 and 11 are also relatively flammable due to the extensive cleavage of fuel-forming phosphinate or phosphate groups. The thermal decomposition process of the PHAs can be roughly divided into two stages. In the first stage (below 500°C), small molecules such as water, methanol, and phosphinates or phosphates, as well as their ester fragments, are released to form some quasi-PBO structures. In the second stage (above 500°C), the random scission of the polymer backbone will occur. Most PHAs show an endothermic peak at low temperatures, but due to different mechanisms such as cyclization, melting, and decomposition. Halogenated PHA-3 and 5 show a distinct exothermic peak at high temperatures due to the formation of HBr and some cross-linking reactions. IR and elemental analysis all prove that the first decomposition stage of PHA-1 corresponds to cyclization into PBO. The major decomposition products of most PHAs (except for phosphinate or phosphate PHAs) are CO, CO₂, H₂O, HCN, and a small amount of aromatic compounds. The low-flammable volatiles, low mass loss rates, and high char yields are the major reasons for their low flammability. Different from the complete cyclization of PHA and halogenated PHAs, methoxy-, phosphinate- or phosphate-substituted PHAs can only partially cyclize into PBO structures.

4. FIRE-RESISTANT, UV/VISIBLE-SENSITIVE POLYARYLATES, COPOLYMERS, AND BLENDS.

4.1 INTRODUCTION.

Polyarylates, a group of aromatic polyesters of phthalic acid and bisphenols, represent a very important family of engineering thermoplastics with enhanced long-term resistance to elevated temperature in advanced applications. They have many good properties, such as high modulus, flexural recovery, high heat deflection temperature, low notch sensitivity, and good electrical properties. Most of all, these materials show a high resistance to ignition and flame spreading without additives [6].

Varying the structures of phthalic acids and bisphenols, a series of polyarylates have been synthesized. Among them, polyarylates based on chloral and its derivatives have been found to be extremely fire resistant [102]. Especially, polyarylates based on BPC II have received considerable interest due to their good solubility, mechanical, dielectrical, optical, and excellent heat- and flame-resistant properties [103-105]. Brzozowski was one of the first to use BPC-II in the synthesis of polycarbonates and polyarylates through interfacial polycondensation [106-108]. It was found that these polymers are the least combustible and fuming of all existing thermoplastics. Recently, ultraviolet (UV)/visible-sensitive polyarylates with improved thermal and chemical stability have become Brzozowski's major research interests [109-112]. Chalcon II (4, 4'-dihydroxy-3-ethoxy-benzylidenoacetophenone)-polyarylate is of particular importance due to its high UV-sensitivity, economic (high yield), and ecological (nontoxic) advantages [111 and 113]. Its copolymers with bisphenol A (BPA) or BPC II monomer meet the main requirements for photo-resists (e.g., high UV sensitivity, high chemical resistance, high adhesion, high tenacity, and good solubility in harmless solvents). In addition, the images have a very good resolution and contrast and can be easily developed. Therefore, these polyarylates are potentially useful in the photolithography process and some other photopolymer applications [111].

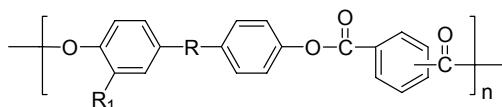
Although it is important to develop new fire-resistant polymers, the simplest way to control flammability from a commercial standpoint is to modify the structure and composition of existing polymers by either copolymerization or polymer blending. This can minimize the effects of small molecule, flame-retardant additives on the processing and performance of the host polymers and avert outward diffusion in the system and the consequent risk of environmental contamination. On the other hand, some other properties of the host polymers might also be improved by incorporation of another component. However, two important issues must be considered when blending. One is the compatibility between polymers. The other is the cost efficiency of blending a small amount of a very flame-retardant, high-charring polymer with a large amount of very flammable, low-charring polymer. Until now, little has been done in the field of flammability-composition relations except for some studies on BPA- and BPC II-polycarbonates [114 and 61].

In this section, the thermal decomposition behavior and flammability of three polyarylates based on BPA, BPC II, Chalcon II, and their copolymers and blends were fully characterized. The relationships between flammability and chemical structure/composition of these polyarylates have also been investigated.

4.2 EXPERIMENTAL.

4.2.1 Materials.

Homopolyarylates based on BPA, BPC II, and Chalcon II (figure 4-1) as well as corresponding copolymers were provided by Prof. Brzozowski, Warsaw University of Technology. Polymer blends were made by mixing different polymers with varied weight ratios in methylene chloride, then solution-casting into films.



	R	R ₁
BPA	C(CH ₃) ₂	H
BPC II	C(=CCl ₂)	H
Chalcon II	CH=CHC(O)	OC ₂ H ₅

FIGURE 4-1. STRUCTURES OF BPA-, CHALCON II-, AND BPC II-POLYARYLATES

The polymers used for blending are polysulfone (-O-Ph-C(CH₃)₂-Ph-O-Ph-SO₂-Ph-) supplied by BP Amoco Co.; polystyrene (M_p=514,000) obtained from Polymer Laboratories; and poly(ethylene oxide) (M_n = 600,000) purchased from Aldrich.

4.2.2 Characterization.

DSC measurements were carried out on a DuPont 2910 instrument. The heating rate was 10°C/min. The experimental conditions for TGA, STA, pyrolysis GC/MS, and PCFC measurements were the same as those described in section 2.3.

UV/visible spectra were recorded by using a UV/visible spectrophotometer (Hewlett-Packard 8453).

The cured samples used for TGA and PCFC analyses were prepared under an OAI 500W deep-UV lamp with intensity of 10 mW/cm².

4.3 RESULTS.

4.3.1 Flammability and Thermal Decomposition of BPA-Polyarylates.

Three kinds of phase transfer catalysts—cetyltrimethylammonium bromide (CTMA Br), crown ether (18-crown-6), and dimethyl sulfoxide (DMSO)—were used to optimize the interfacial polymerization conditions of BPA-polyarylate [115]. It has been found that the polymers obtained by using 18-crown-6 and DMSO have higher molecular weight, thus, higher glass transition temperature (T_g) and higher thermal stability. However, the increase of molecular weight has no significant effect on the flammability of BPA-polyarylate due to its random-scission decomposition mechanism (table 4-1).

TABLE 4-1. FLAMMABILITY AND THERMAL DECOMPOSITION OF BPA-POLYARYLATES

Catalysts	H.R. Capacity (J/g-K)	Total Heat Released (kJ/g)	Char Yield (%)	T _{95%} ^a (°C)	T _g ^b (°C)
CTMA Br	360	18	27	431	155
DMSO	380	19	27	463	166
18-crown-6	400	19	26	458	174

^aTemperature at 5% weight loss from TGA

^bGlass transition temperature from DSC

4.3.2 Thermal Decomposition and Flammability of Homopolyarylates.

Thermal decomposition processes of BPA-, Chalcon II-, and BPC II-homopolyarylates are shown in figure 4-2. It can be seen that all the polymers decompose in a single step. They all have a relatively high thermal stability and will not start to lose weight dramatically until 370°C. However, the bridging groups and side groups in the bisphenols do have some effects on the heat resistance of polyarylates. The introduction of 1,1-dichloroethylene groups (BPC II) leads to an obvious drop (40°C) in thermal stability when compared to BPA-polyarylate. The thermal stability of Chalcon II-polyarylate is also greatly reduced due to the presence of bulky ethoxy side groups. The order of the thermal stability of these homopolyarylates is BPA > BPC II > Chalcon II. The derivative of TGA curves (DTG curves) shows that the mass loss rate of BPC II- and Chalcon II-polyarylates are significantly lower than BPA-polyarylate, which indicates that BPC II- and Chalcon II-polyarylates decompose much slower. Moreover, these two polymers can produce more char at high temperatures (above 400°C) due to the cross-linking of double bonds.

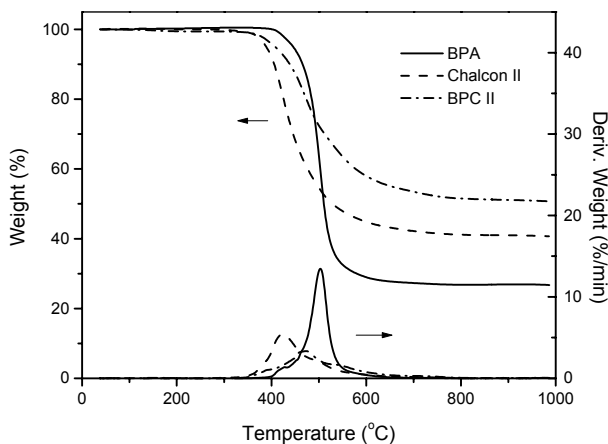


FIGURE 4-2. THE TGA AND DTG CURVES OF BPA-, CHALCON II-, AND BPC II-POLYARYLATES

The high-temperature DSC curves are shown in figure 4-3. It can be seen that all the polymers are amorphous, with T_gs around 140°~150°C and onset decomposition temperatures around

400°C (table 4-2). The large temperature window between softening and thermal decomposition allows processing by injection and extrusion molding. During decomposition, BPA- and Chalcon II-polyarylates show an endothermic peak, but BPC II-polyarylate decomposes exothermically, which may be due to the formation of HCl or some cross-linking reactions.

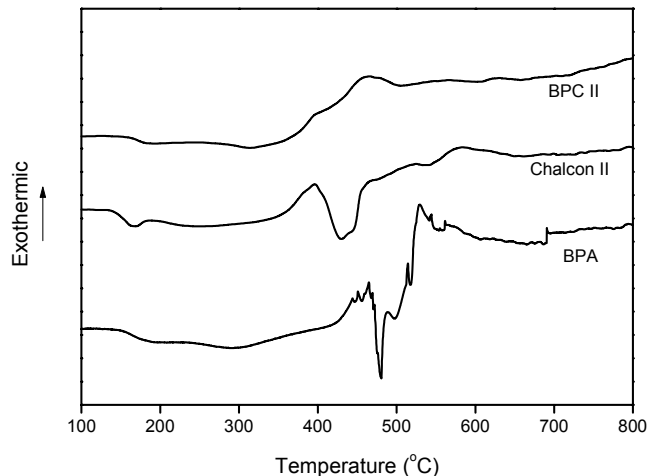


FIGURE 4-3. HIGH-TEMPERATURE DSC CURVES OF BPA-, CHALCON II-, AND BPC II-POLYARYLATES

TABLE 4-2. FLAMMABILITY AND THERMAL DECOMPOSITION OF HOMOPOLYARYLATES

Polymer	H.R. Capacity (J/g-K)	Total Heat (kJ/g)	Char Yield (%)	T _{max} ^a (°C)	Max. Mass Loss Rate (x10 ³ /s)	T _g ^b (°C)	T _{95%} ^c (°C)	ΔH ^d (J/g)
BPA	360	18	27	488	2.2	155	431	168
Chalcon II	110	10	41	425	0.9	136	389	203
BPC II	12	4	51	472	0.6	151	407	302 ^e

^a Temperature at maximum mass loss rate from DTG curves

^b Glass transition temperature from DSC

^c Temperature at 5% weight loss

^d Heat of decomposition measured from STA

^e Exothermic decomposition peak

Table 4-2 shows the PCFC results as well as some TGA results, which show that different bridging groups in bisphenols also have a big influence on the flammability of polymers. Generally, the flammability of polymers is determined by many factors, of which, rate of decomposition (mass loss rate) and the amount and flammability of volatiles produced are the most important. The introduction of cross-linking groups (double bond in Chalcon II and BPC II) can greatly enhance the formation of char and therefore reduce the amount of fuel generated. It was found that the BPC II unit (1,1'-diphenyl-ethylenedichloride) is the major structure responsible for the char-forming process [116-118]. On the other hand, according to the pyrolysis GC/MS analyses (figure 4-4), the major decomposition products of BPA- and

Chalcon II-polyarylates are a series of phenols and some other flammable aromatic compounds. BPC II-polyarylate releases a lower amount of flammable compounds but more CO₂, CO, HCl, and some chlorinated aromatic compounds that have relatively low fuel values and may also confer flame-retardant effects in the gas phase. Therefore, the reduced heat release capacity and total heat of combustion of Chalcon II-polyarylate (compared with BPA-polyarylate) is mainly due to a lower mass loss rate and less fuel generated. While in the case of BPC II-polyarylate, release of less flammable decomposition products is another important factor for its low flammability. In all, compared with some other commercial polymers, Chalcon II-, and BPC II-polyarylates are more heat and flame resistant, and BPC II-polyarylate has especially low flammability.

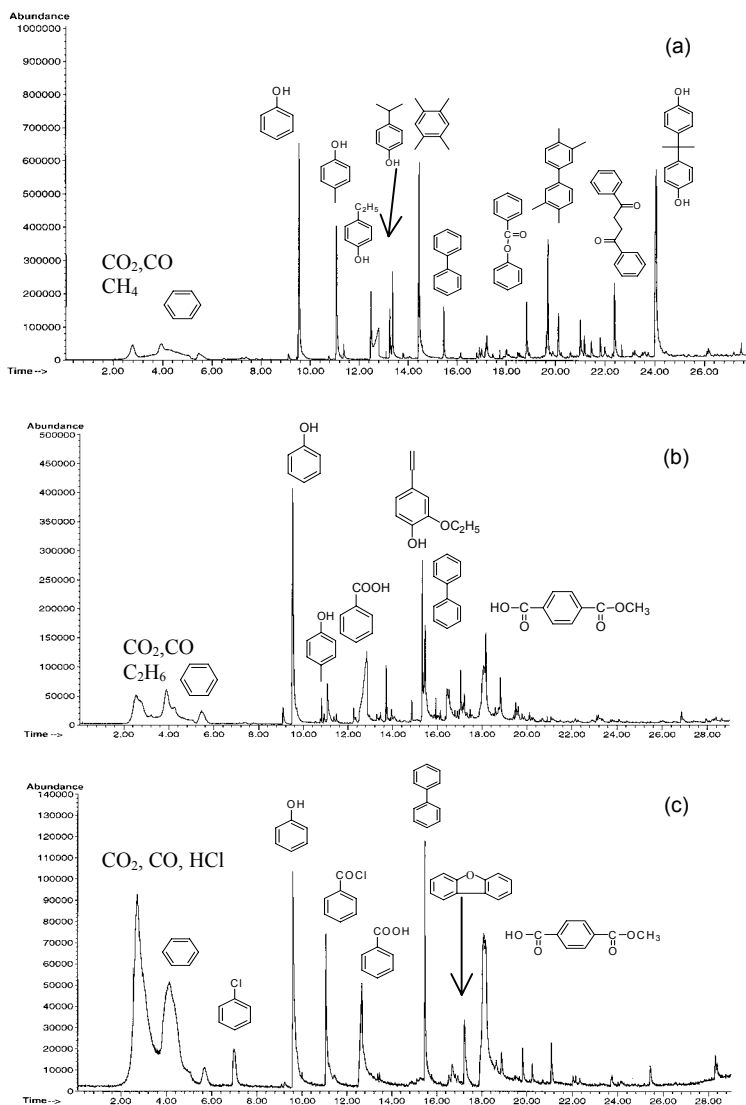


FIGURE 4-4. PYROLYSIS GC/MS TRACES OF BPA-, CHALCON II-, AND BPC II-POLYARYLATES (TEMPERATURE RANGE: 250° ~ 930°C, HEATING RATE: 4.3°C/s)
 (a) BPA-POLYARYLATE, (b) CHALCON II-POLYARYLATE, AND
 (c) BPC II-POLYARYLATE

4.3.3 UV/Visible-Sensitive Chalcon II-Polyarylate.

Chalcon II-polyarylate is a UV/visible-sensitive polymer containing $\text{CH}=\text{CHC}(\text{O})$ groups. The UV spectra of Chalcon II-homopolymer and copolymers are shown in figure 4-5.

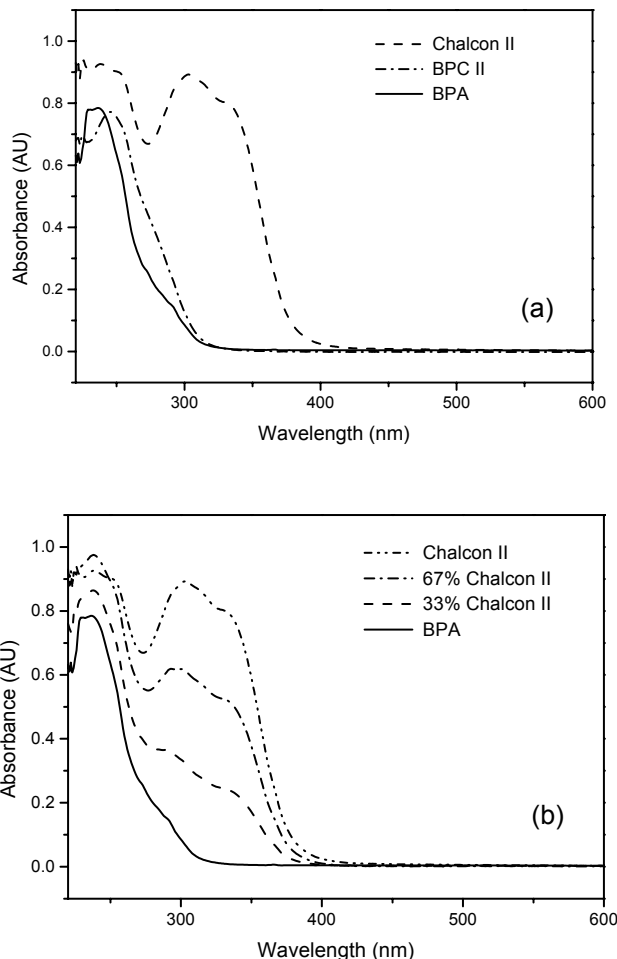


FIGURE 4-5. ULTRAVIOLET SPECTRA OF POLYARYLATES CONTAINING CHALCON II-MONOMER (a) HOMOPOLYMERS AND (b) BPA-CHALCON II COPOLYMERS

According to figure 4-5, besides the peak at 238 nm that can be attributed to the absorption of phenyl ring, there is another broad absorption between 300~400 nm which is due to the $-\text{CH}=\text{CHC}(\text{O})-$ structure. For the copolymers, with the increased content of Chalcon II monomer, the intensity of this absorption increases accordingly.

It had been reported that some UV-sensitive polyarylates with a similar structure can form photo-cross-linking after UV exposure [119]. In these studies, in order to know whether photo-cross-linking has an effect on the thermal decomposition and flammability of these polymers, Chalcon II-polyarylate was exposed to UV or visible light for various amount of time. It was found that Chalcon II polymer is no longer soluble in methylene chloride after exposure, which suggests the formation of photo-cross-links (figure 4-6).

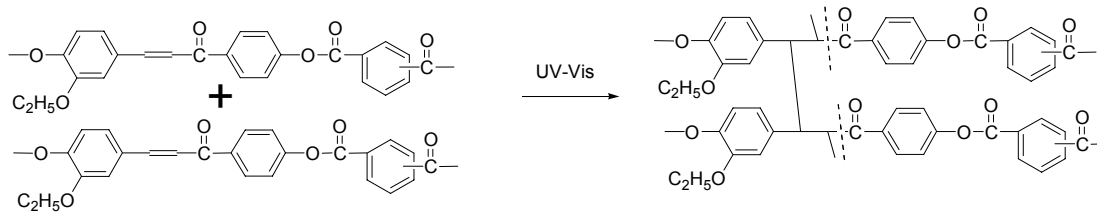


FIGURE 4-6. PHOTO-CROSS-LINKING OF CHALCON II-POLYARYLATE

TGA results show that the thermal stability of the cured polymers has decreased. They start to decompose around 200°~250°C and then merge into the same major decomposition step after about 6% weight loss (figure 4-7). The decrease in thermal stability is apparently due to the disruption of the conjugated system and the formation of weak linkages around cross-linking points (figure 4-6).

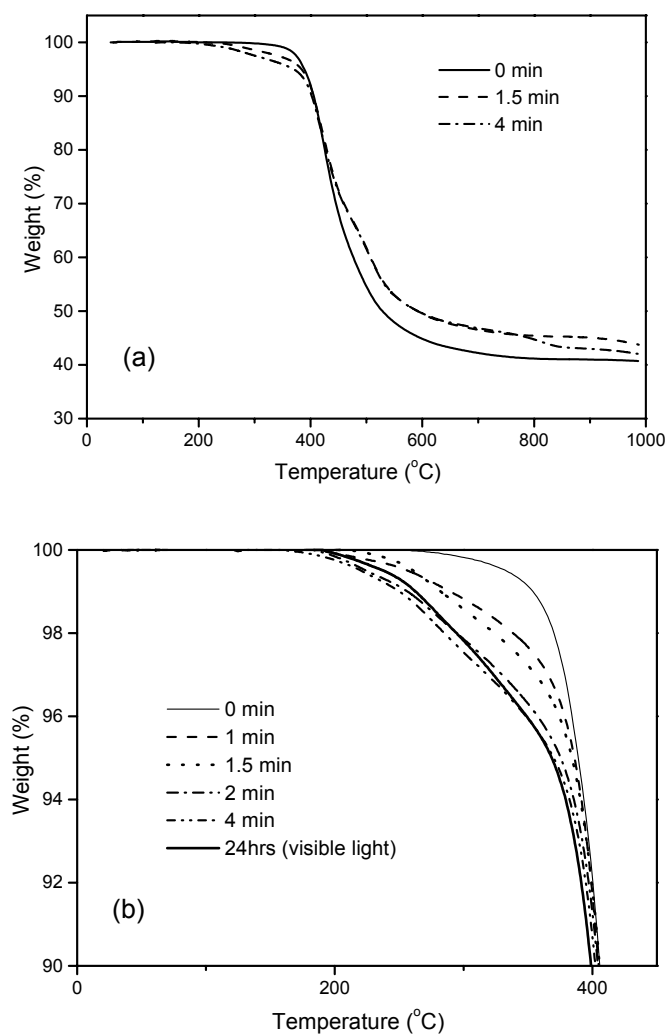


FIGURE 4-7. THERMAL DECOMPOSITION OF CHALCON II-POLYARYLATE AFTER UV/VISIBLE-EXPOSURE (a) FULL TGA CURVES AND (b) INITIAL DECOMPOSITION

It was also found that the TGA curves of polymers cured for more than 4 minutes almost overlap each other, which means the photo-curing process is completed after 4 minutes. This conclusion is confirmed by other studies [111 and 112] that also show that the mechanical properties of the polymers can be greatly improved by curing. However, the flammability measured by the PCFC method shows no difference between cured and noncured samples, except that cured samples have slightly higher char yields.

4.3.4 Thermal Decomposition and Flammability of Copolymers and Terpolymers.

Thermal decomposition and flammability of three series of copolymers (BPA-Chalcon II, BPA-BPC II, and BPC II-Chalcon II) and BPA-Chalcon II-BPC II terpolymers were investigated. The results are shown in figures 4-8 and 4-9 and in table 4-3.

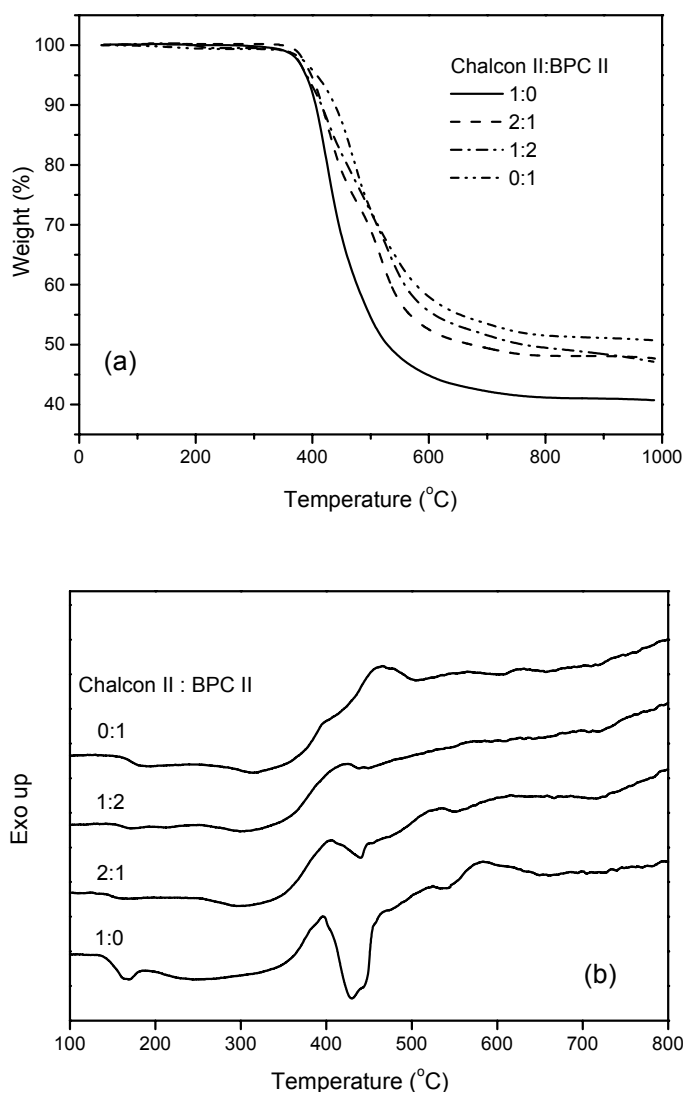


FIGURE 4-8. THERMAL DECOMPOSITION OF CHALCON II-BPC II COPOLYMERS (THE NUMBERS ARE MOLAR RATIOS) (a) TGA AND (b) DSC

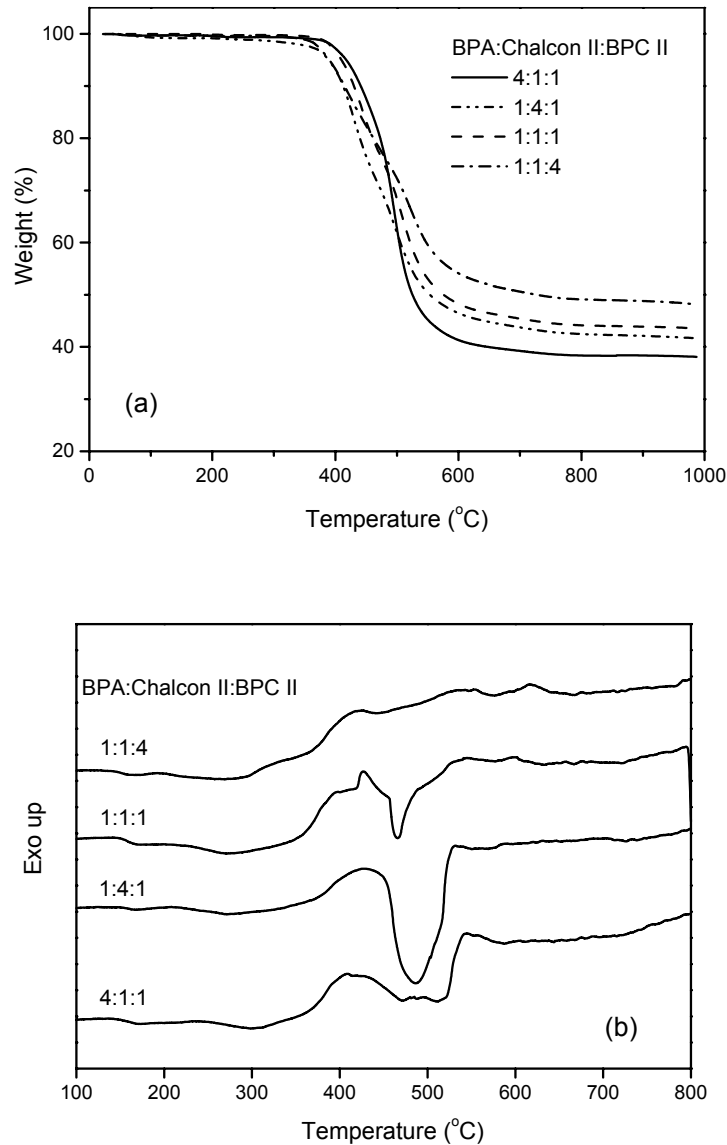


FIGURE 4-9. THERMAL DECOMPOSITION OF BPA-CHALCON II-BPC II TERPOLYMERS (THE NUMBERS ARE MOLAR RATIOS) (a) TGA AND (b) DSC

It can be seen that the thermal decomposition and flammability of copolymers and terpolymers change systematically with composition. With an increased fraction of flame-retardant, high-charring units such as Chalcon II or BPC II, the heat release rate and the total heat released are reduced, and the char yield increases correspondingly (table 4-3).

At a very high concentration of BPC II monomer (67 mol%), the flammability of the copolymers and terpolymers is completely determined by the amount of BPC II units and independent of the structure of the other components (figure 4-10), which indicates that BPC II is an efficient flame-retardant unit. In addition, the heat involved in the decomposition process changes from endothermic to exothermic with the increased molar fraction of BPC II units.

TABLE 4-3. FLAMMABILITY AND THERMAL DECOMPOSITION OF CO- AND TERPOLYMERS

Composition (Molar Ratio)	H.R. Capacity (J/g-K)	Total Heat (kJ/g)	Char (%)	T _{max} (°C)	Max. Mass Loss Rate (x10 ³ /s)	T _{95%} (°C)
BPA : Chalcon II						
2:1	140	16	33	489	1.1	408
1:2	120	14	35	426	0.8	369
BPA : BPC II						
2:1	110	12	40	501	1.2	426
1:2	30	7	50	521	0.5	413
Chalcon II : BPC II						
2:1	76	9	40	425	0.7	398
1:2	30	7	48	428	0.4	390
BPA : Chalcon II : BPC II						
4:1:1	143	14	38	498	1.3	417
1:4:1	83	12	42	431	0.6	389
1:1:1	54	11	46	504	0.7	409
1:1:4	29	8	49	523	0.5	390

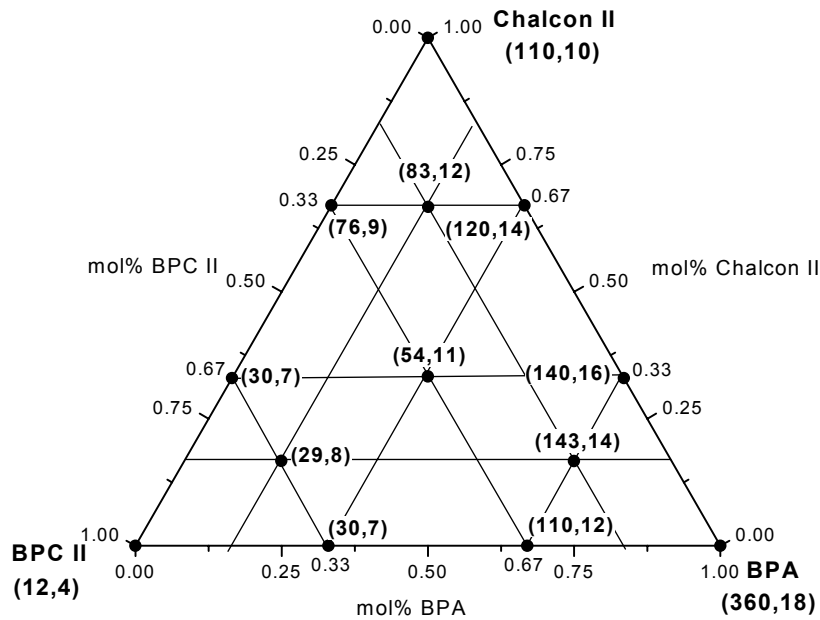


FIGURE 4-10. TERNARY PLOT OF FLAMMABILITY OF COPOLYMERS AND TERPOLYMERS
(The numbers in the parentheses are heat release capacity (J/g-K) and total heat (kJ/g).)

After careful investigation of the relationship between flammability and composition (figure 4-11), the total heat released was found, usually, to change linearly with the composition. However, the change of heat release capacity depends on the chemical structure of the components. For BPA-BPC II and BPA-Chalcon II copolymers, there is an obvious synergistic effect. That means by adding only a very small amount of a low-flammable component, the flammability of polymers can be dramatically reduced. However, the flammability of Chalcon II-BPC II copolymer almost changes linearly with composition.

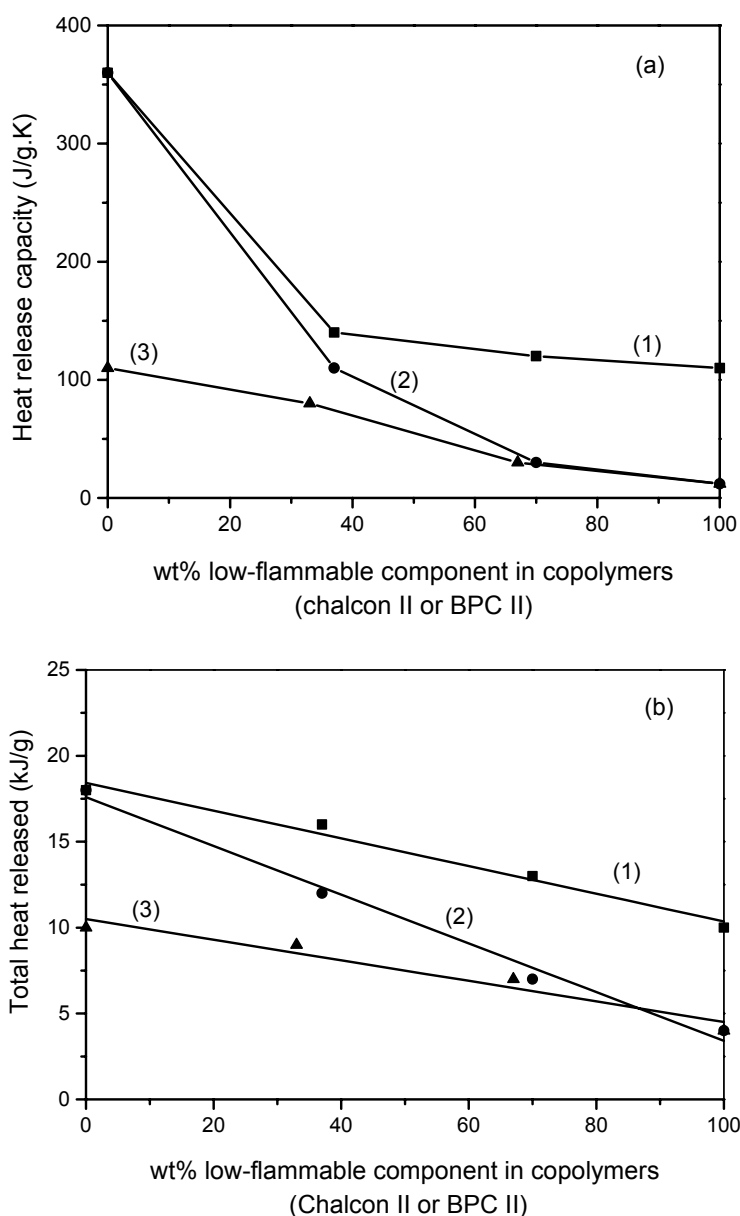


FIGURE 4-11. COMPOSITION AND FLAMMABILITY RELATIONSHIP OF COPOLYMERS (a) HEAT RELEASE CAPACITY, (b) TOTAL HEAT RELEASED, (1) BPA-CHALCON II, (2) BPA-BPC II, AND (3) CHALCON II-BPC II

4.3.5 Thermal Decomposition and Flammability of Blends.

Four kinds of blends were studied, all of which include BPC II-polyarylate as the flame-retardant component. The selection of the other polymer (polysulfone (PSF), BPA-polyarylate, PS, and PEO) is based on the structure of the polymer and whether this polymer is charring on decomposition. Several interesting phenomena were observed regarding thermal stability and flammability. It was found that the thermal stability, decomposition process, and char yield of PSF/BPC II-polyarylate blends change systematically with composition (figure 4-12), and the trend of change is similar to BPA-/BPC II-polyarylate blends [119]. That is, with the increased amount of BPC II-polyarylate, the thermal stability and char yield of the blends gradually shift to the direction of pure BPC II-polyarylate.

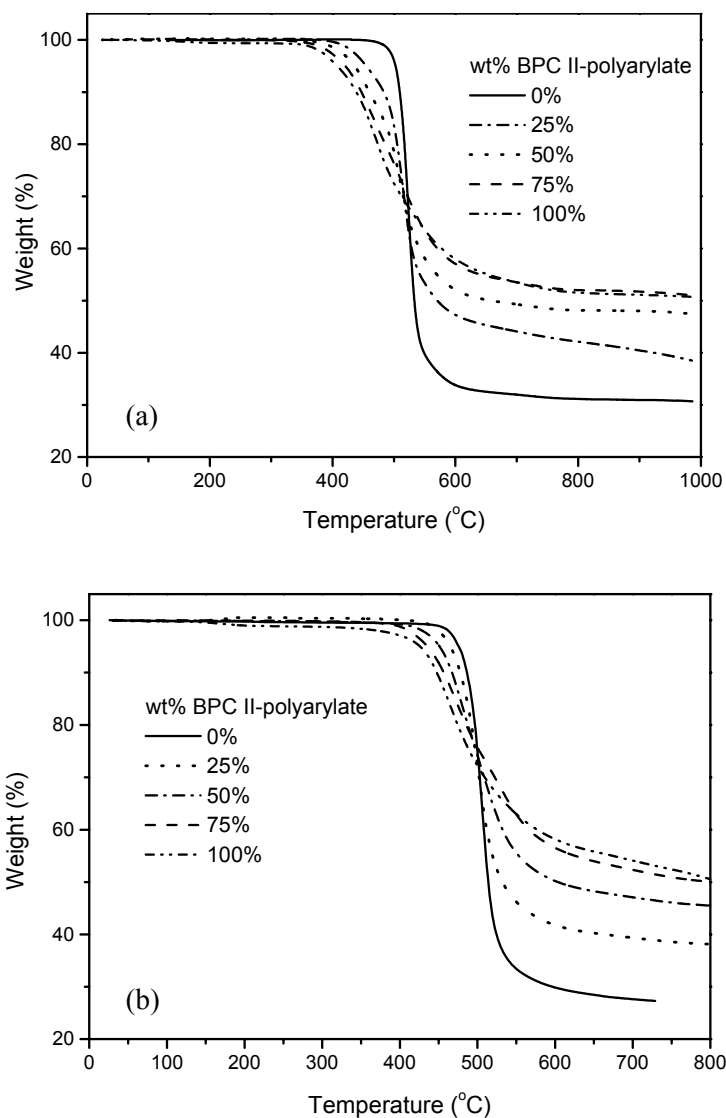


FIGURE 4-12. THE TGA CURVES OF PSF (BPA-)/BPC II-POLYARYLATE BLENDS (a) PSF/BPC II-POLYARYLATE AND (b) BPA-/BPC II-POLYARYLATE [119]

However, blends containing PS or PEO behave completely different during decomposition (figure 4-13). The onset decomposition temperatures of PS/BPC II-polyarylate blends are all the same (approximately 370°C, just between the two homopolymers) regardless of the composition, while all PEO/BPC II-polyarylate blends start to decompose at the same temperature as PEO homopolymer.

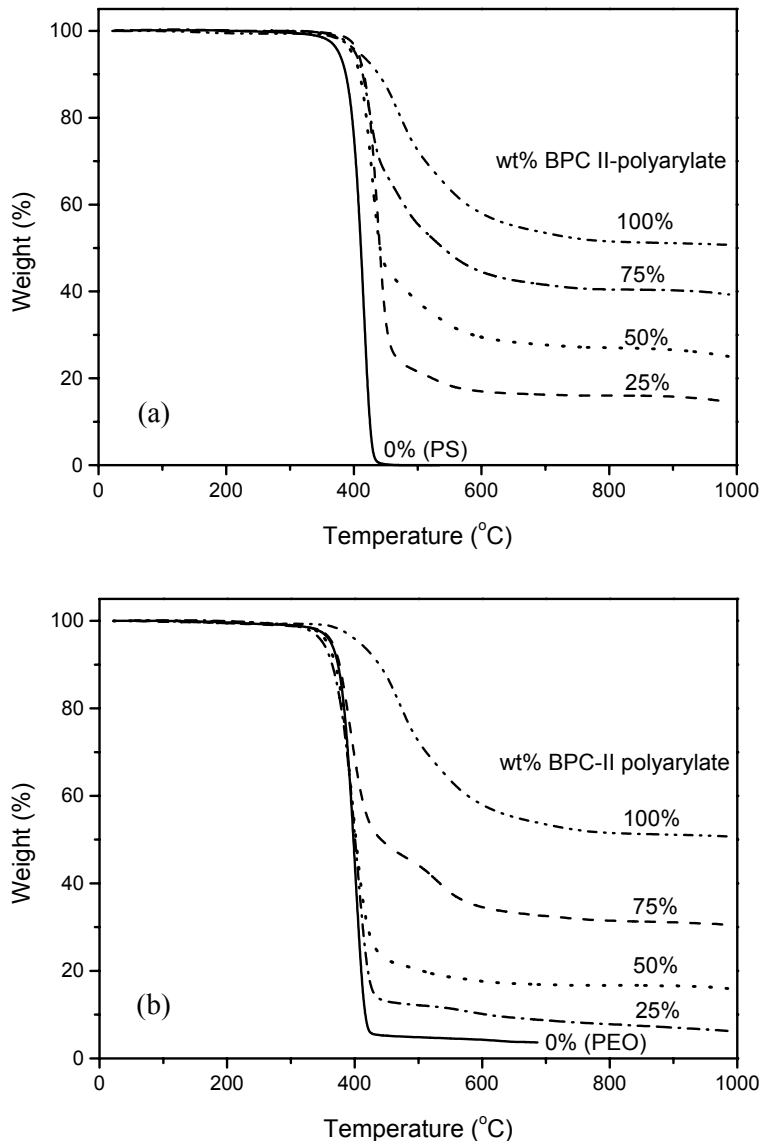


FIGURE 4-13. THE TGA CURVES OF PS (PEO) /BPC II-POLYARYLATE BLENDS
 (a) PS/BPC II-POLYARYLATE AND (b) PEO/BPC II-POLYARYLATE

Similar to copolymers, the total heat of combustion of blends changes linearly with composition, but the change of heat release capacity and char yield is nonlinear with composition (figure 4-14).

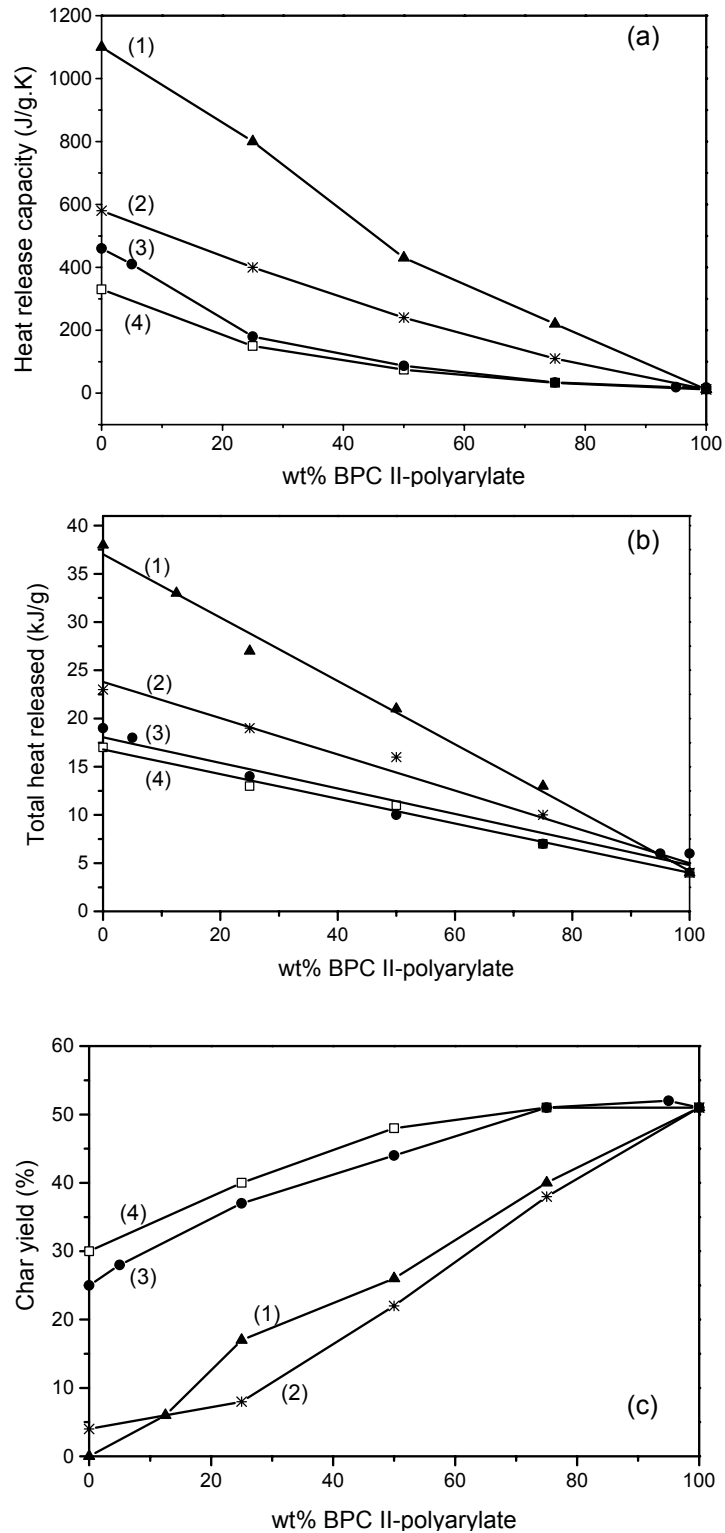


FIGURE 4-14. STRUCTURE-COMPOSITION-FLAMMABILITY OF BLENDS CONTAINING BPC II-POLYARYLATE (a) HEAT RELEASE CAPACITY, (b) TOTAL HEAT RELEASED, (c) CHAR YIELD, (1) PS, (2) PEO, (3) BPA-POLYARYLATE, AND (4) PSF

For the blends containing PSF or BPA-polyarylate, the heat release capacity and char yield change synergistically with composition. However, for PS or PEO, they change almost linearly. This is because PS (or PEO) and BPC II-polyarylate are largely phase separated in the blends due to their distinctive structure differences. Therefore, there is no interaction between these two components during decomposition. However, PSF and BPA-polyarylate have similar aromatic structures to BPC II-polyarylate, and they all can form a certain amount of char on their own. These properties can lead to some kind of intermolecular interaction between two components, which can favor char formation and further slow down the decomposition process. In all, the decrease in the heat release rate of blends is mainly attributed to the wider decomposition temperature range and, therefore, lower mass loss rate.

4.4 DISCUSSION.

BPC II-polyarylate is an extremely heat- and flame-resistant thermoplastic. It can produce about 50% char up to 930°C. Chalcon II-polyarylate also has a very low heat release rate and high char yield. It can be cured under UV/visible light, but the photo-cross-linking formed has no effect on the flammability. The thermal decomposition and flammability of copolymers and terpolymers and blends change systematically with composition. The introduction of a nonflammable, high-charring component (BPC II-arylate units) can conveniently control the flame retardance of these polymers. The total heat of combustion of the copolymers and terpolymers and blends changes linearly with composition. However, the change of peak value of heat release rate and char yield greatly depends on the chemical structures of the components.

5. EFFECTS OF FLAME-RETARDANT ADDITIVES AND CORRELATIONS AMONG PCFC, OSU, AND CONE CALORIMETERS.

5.1 INTRODUCTION.

Flame-retardants have made a great contribution in reducing fire risk to people and property, but there is still plenty of room for improvement. Not only does fire still cause far too much damage, but the continuous development of new products creates a need for new or enhanced flame-retardant additives, especially nonhalogen flame-retardant additives. In addition, how to evaluate the efficiency of different flame retardants, such as the reduction of ease of ignition, burning or flame-spread rate, or smoke emission, and how these flame retardants act in a fire still remain complex topics.

HRR is one of the most important variables that can determine the hazard from a fire [16]. A number of apparatus have been developed over the years for measuring heat release rate such as the OSU calorimeter ASTM E 906 [63], the cone calorimeter ASTM E 1354 [62] and the PCFC [64-66]. Because the heat release rate is not a property of a material and is influenced by numerous external variables, the results from different methods are dependent not only on the physical and chemical characteristics of materials but also on the specific experimental conditions and procedures used.

The OSU test was developed to obtain information on the heat release rate and visible smoke from materials when exposed to different levels of radiant heat [63]. It is the required FAA HRR test for aircraft interior materials with large surface areas such as ceiling panels, wall panels, and stowage bins [18]. In the OSU test, the heat release rate is determined through thermal measurements (by thermopile). However, the thermopile measurement accounts for only the convective heat released by the specimen, thus missing the radiant heat component of the total HRR.

The cone calorimeter is another significant bench-scale instrument in the field of fire tests. It measures the fire response of materials exposed to controlled levels of radiant heat fluxes ranging from 0~100 kW/m² [62]. It can determine the ignitability, heat release rates, total heat released, mass loss rates, effective heat of combustion, visible smoke development, and carbon monoxide and carbon dioxide production of materials and products. The heat release rate is determined by measuring of the oxygen consumption (approximately 13.1 x 10³ kJ of heat are released per 1 kg of oxygen consumed). By using the oxygen consumption principle as the method of measurement, the results are more precise and the apparatus does not need thermal insulation because heat measurements are not required [62].

Generally, it is very difficult to compare the data from different fire test methods due to different experimental conditions and calculation procedures [120-122]. For example, OSU and cone calorimeters all measure the fire response of materials under different external heat fluxes, but specimen melting, sagging, or falling out of the frame could cause problems in the OSU test due to the vertical mounting of specimen. In addition, the impinging pilot flame in the OSU test creates a higher, localized heat flux near the bottom of the specimen, which can cause sooting, deterioration of orifices, and contribute to the heat release rate [63]. Furthermore, the pilot flame can be easily blown out during combustion. An electric spark commonly used in the cone

calorimeter test is free of most of these difficulties. In the PCFC method, the pyrolysis is limited to small samples, and there is no temperature gradient and no mass transfer limitations. Hence, the intrinsic material properties can be evaluated. However, because the pyrolysis and combustion processes are totally separated in PCFC, the effects of some physical processes in a fire that are associated with the sample thickness, physical properties of materials, char buildup, heat and mass transfer, and heat feedback from the flame will not be shown in the results. In all, conflicting results from different methods may be due to different factors such as specimen orientation, specimen size, imposed heat flux, and some other burning characteristics of the specimens including melting and char formation. Despite these difficulties, it is important to understand the relationships among the various test methods and to learn how to interpret the results from these methods.

In this section, the fire behavior of several commercial heat-resistant engineering thermoplastics, including poly(ether ether ketone) (Victrex[®] PEEK[™]), Xydar[®], and polyphthamide (Amodel[®] PPA) as well as their inert fiber-reinforced or flame-retarded composites, were measured by OSU, cone, and PCFC calorimeters. The flammability of PMMA/clay nanocomposites and epoxy/phosphates composites were also studied. The purpose was to gain some fundamental information on the applicability of different test methods and understand the flame-retardant mechanisms of different additives.

5.2 EXPERIMENTAL.

5.2.1 Test Samples.

A list of samples is shown in table 5-1, which includes the details such as the structures, the presence or absence of flame-retardant additives, fillers, and the proportion of major inorganic components. Polysulfones (Udel[®] P-1700, Radel[®] A-300, Radel[®] R-5000), Xydar[®], and polyphthamide (Amodel[®] PPA) resins were supplied by BP Amoco Polymers Inc. (now Solvay Advanced Polymers, L. L. C.). Poly(ether ether ketone) (Victrex[®] PEEK[™]) was obtained from Victrex PEEK Inc. In addition, PMMA/clay nanocomposites [123] were provided by the U.S. Army Reserch Laboratory. Epoxy/phosphates composites were provided by Adam Zerda [124] of the University of Massachusetts, Amherst.

5.2.2 Sample Preparation.

All the sample plaques for cone and OSU calorimeter tests were made by injection molding (BP Amoco Polymers Co.) or hot pressing. After conditioning to moisture equilibrium (constant weight), each specimen was wrapped in aluminum foil so that only the top surface was exposed, while the bottom and sides of the specimen were covered with foil.

5.2.3 Characterization.

The experimental conditions for TGA, STA, pyrolysis GC/MS, and PCFC measurements were the same as those described in section 2.3. The OSU and cone calorimeter tests were performed at the FAA William J. Hughes Technical Center in Atlantic City International Airport, NJ.

TABLE 5-1. SAMPLE COMPOSITIONS

Polymers	Structure and Description
PEEK	
PEEK-GL30	PEEK with 30% glass fiber
PEEK-CA30	PEEK with 30% carbon fiber
Xydar [®]	
Xydar [®] -G930	Xydar [®] with 30% glass fiber
Xydar [®] -M345	Xydar [®] with 45% mineral
PPA A-1000	
A-1133 HS	A-1000 with 33% glass fiber, 0%-10% titanium dioxide and a very small amount heat stabilizer.
A-1145 HS	A-1000 with 45% glass fiber and a very small amount of heat stabilizer.
AF-1133 V-0	A-1000 with 33% glass fiber, 10%-30% polybrominated compound, 3%-7% calcium metasilicate, 0%-5% titanium dioxide, and 0%-5% zinc sulfide.
AF-1145 V-0	A-1000 with 45% glass fiber, 10%-20% polybrominated compound, and 3%-7% calcium.
PPA A-6000	
A-6135 HS	A-6000 with 35% glass fiber and a very small amount of heat stabilizer.
A-6145 HS	A-6000 with 45% glass fiber and a very small amount of heat stabilizer.
A-6133 V-0	A-6000 with 33% glass fiber, 10%-30% brominated compound, 1%-5% antimony compounds, 0%-10% titanium dioxide, and 0%-10% zinc sulfide.
A-6145 V-0	A-6000 with 45% glass fiber, 10%-30% brominated compound, 0%-5% antimony compounds, 0%-5% titanium dioxide, and 0%-5% zinc sulfide.
Udel [®] P-1700	
Radel [®] A-300	
Radel [®] R-5000	

5.2.3.1 Ohio State University Calorimeter Test.

The specimen was 152 mm (6 inches) square and 1.6 mm (1/16 inch) thick (about 70-90 g) and was supported vertically in a metal frame. It was exposed to an external radiant heat flux of 35 kW/m². Ignition of test specimens was achieved by direct flame impingement of a gas pilot. The HRR was measured for 5 minutes after the specimen was injected into the controlled exposure chamber. Three important flammability parameters were reported: the maximum heat release rate during the 5-minute test, the total heat released during the first 2 minutes, and the total heat released for the entire 5 minutes.

The HRR results can be obtained by two kinds of measurements: thermopile and oxygen depletion [125]. The thermopile was used to measure the convective portion of the heat release through the temperature difference between the air entering and leaving the environmental chamber, therefore resulting in lower reported values of heat release than oxygen depletion.

$$\Delta H_{convective} = \frac{(V_m - V_b)}{A} \times K_h \quad (5-1)$$

where V_m is the measured thermopile voltage during the test, V_b is the thermopile baseline voltage averaged over 20 seconds immediately before specimen injection, A is the surface area of specimen (0.02323 m² for 6" by 6" by 1/16" sample), and K_h is the calibration factor. However, besides the convective heat released, the total heat also includes the radiant heat absorbed by the apparatus. This is sometimes quite substantial, especially when the material burns with a high-emissivity flame, i.e., a smoky flame [125].

$$\Delta H_{total} = \Delta H_{convective} + \Delta H_{radiative} \quad (5-2)$$

Oxygen depletion measurements can be used to calculate total heat released. The principle is similar to the cone and PCFC methods.

$$\Delta H_{total} = \frac{(C_m - C_b)}{A} \times K_{oxygen} \quad (5-3)$$

where C_m is the measured concentration of oxygen during the test, C_b is the baseline concentration determined by averaging the 20 data points immediately before specimen injection, and K_{oxygen} is the constant of 13.1 kJ/g-O₂ [125].

5.2.3.2 Cone Calorimeter Test.

The test specimen was 102 mm (4 inch) square and 1.6 mm (1/16 inch) thick (about 15-30 g). The wrapped specimen was placed into the sample container over a ceramic fiber blanket to prevent heat loss through the specimen back face, which can have an influence on the burning rate [62]. Specimens in the test were burned in ambient air conditions. Each material was tested in the horizontal orientation at the external heat flux of 50 kW/m² in the presence of a spark ignition source. Some materials of interest were also tested at external heat fluxes of 75 and 100 kW/m². The error band was ±10% compared to the true value. Two repeats were carried out for

each test. The effective heat of combustion was determined from a measurement of specimen mass loss rate in combination with the heat release rate. Smoke development was measured by obscuration of light by the combustion product stream. Ignition was determined as a measurement of time from initial exposure to time of sustained flaming (existence of flame on or over most of the specimen surface for periods of at least 4 seconds).

5.3 RESULTS.

5.3.1 Poly(Methyl Methacrylate)/Clay Nanocomposites.

Layered silicate minerals, montmorillonite clays, and micas have recently received much attention as possible flame retardants. Most polymer layered silicate (clay) nanocomposites show retardation of heat release rate during burning. The PMMA/clay nanocomposites studied here were made by emulsion polymerization or melt extrusion to achieve molecular-level incorporation of the layered silicate into the polymer [123]. Two kinds of nanomorphology can be induced: exfoliated structure by emulsion polymerization or intercalated structure by melt extrusion. PMMA/MMT (montmorillonite) and PMMA/FH (fluorohectorite) nanocomposites were made by emulsion polymerization, while in PMMA/M18 (C₁₈ modified MMT) and PMMA/F18 (C₁₈ modified FH), PMMA matrix is a commercial PMMA made by melt extrusion. All the composites contain only 5 wt% clay.

The thermal decomposition processes of PMMA/clay nanocomposites are shown in figure 5-1. It can be seen that they all produce about 5% char, which is exactly the amount of clay used. The thermal stability of PMMA/MMT composite is slightly increased, but the other nanocomposites start to decompose at lower temperatures than PMMA. The clay did not change the major decomposition step of PMMA, but it can slightly decrease the decomposition rate (mass loss rate).

The flammability of PMMA/clay nanocomposites is shown in table 5-2. Adding only 5 wt% clay does not change the total heat of combustion, but it can reduce the heat release rate, which is mainly due to the reduction of mass loss rate. It is believed that the layered clay can efficiently slow the release rate of the volatiles due to its physical constriction effects [126]. Therefore, the extruded composites that have layered structures show a 40% decrease in flammability. However, the emulsion composites show less decrease in flammability due to their exfoliated structures. Compared with FH, MMT is more effective in reducing flammability.

Although PMMA-control (a commercial PMMA) and PMMA made by emulsion polymerization are the same kind of polymer, they have very different flammability and thermal stability. It was found that the major differences between these two materials are their molecular weights and molecular weight distributions. PMMA made by emulsion polymerization has a higher molecular weight and broader molecular weight distribution (table 5-3). Therefore, it starts to decompose at lower temperatures due to its low molecular weight fraction. The effects of molecular weight of PMMA on their flammability are explained in detail in section 6.

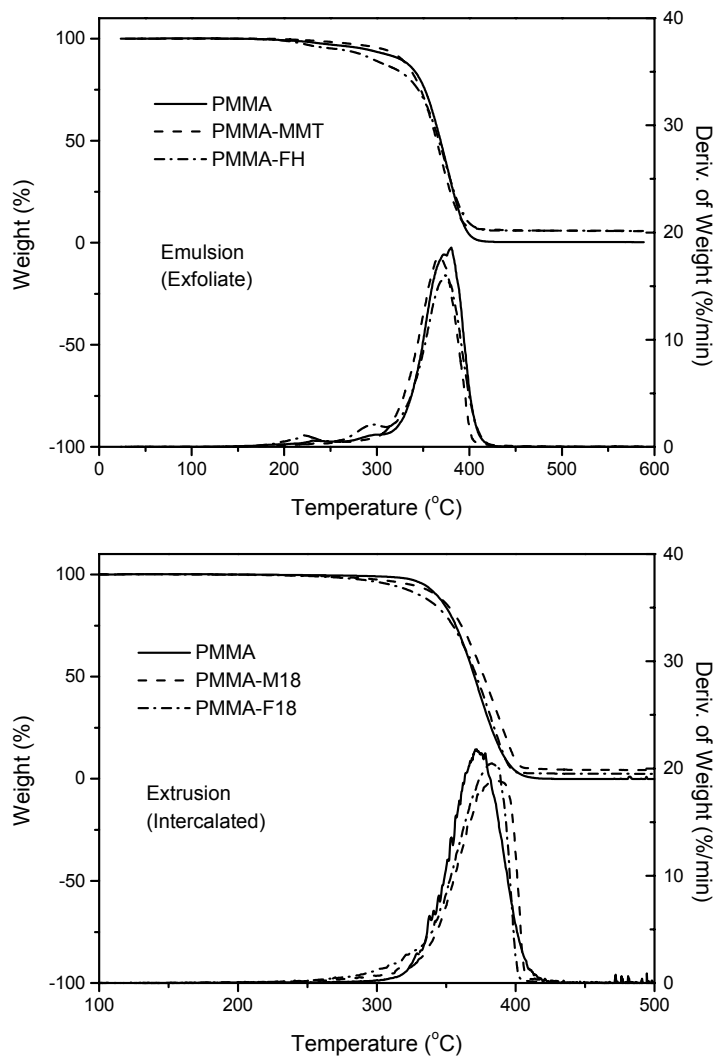


FIGURE 5-1. THERMAL DECOMPOSITION OF PMMA/CLAY NANOCOMPOSITES

TABLE 5-2. FLAMMABILITY AND THERMAL DECOMPOSITION OF PMMA/CLAY NANOCOMPOSITES

Methods	Samples	H.R. Capacity (J/g-K)	Total Heat (kJ/g)	Char Yield (%)	Max. Mass Loss Rate ($\times 10^3/s$)	T _{max} * (°C)	T _{99%} ** (°C)
Extruded	PMMA-control	730	24	0	3.9	378	303
	PMMA-F18	464	24	2.3	3.3	386	259
	PMMA-M18	421	24	4.0	3.1	390	268
Emulsion	PMMA	479	24	0	3.2	379	208
	PMMA-FH	446	23	5.8	2.9	377	200
	PMMA-MMT	331	23	5.6	3.0	371	232

*Temperature at maximum mass loss rate.

**Temperatures at 5% weight loss.

TABLE 5-3. GEL PERMEATION CHROMATOGRAPHY GPC RESULTS OF PMMAS

Polymers	Number Average Molar Mass $\left(\frac{\text{kg}}{\text{Mole}}\right)$	Polydispersity Index
PMMA-control	59	2
PMMA-emulsion	166	4.4

5.3.2 Poly(Ether Ether Ketone) and Composites.

Obviously, inert fillers can reduce fuel content and act as heat sinks. However, many minerals and synthetic inorganic additives do exert further effects [7]. In charring systems, it was observed that fillers can suppress melt viscosity, heat radiation, and modification of the physical structure of the char. For example, glass fiber can prevent melt flow and dripping so that the flame-spread can be reduced in a fire. In this section, the effects of glass and carbon fibers on the thermal decomposition and flammability of PEEK are described.

5.3.2.1 Thermal Decomposition Process.

According to figure 5-2, PEEK and its composites are a group of materials with very high thermal stability. Their onset decomposition temperatures are approximately 575°~580°C. Char yields of these polymers are all above 40%, especially for the composites containing nonflammable glass or carbon fiber. The maximum mass loss rates of the glass or carbon fiber PEEK composites are significantly reduced.

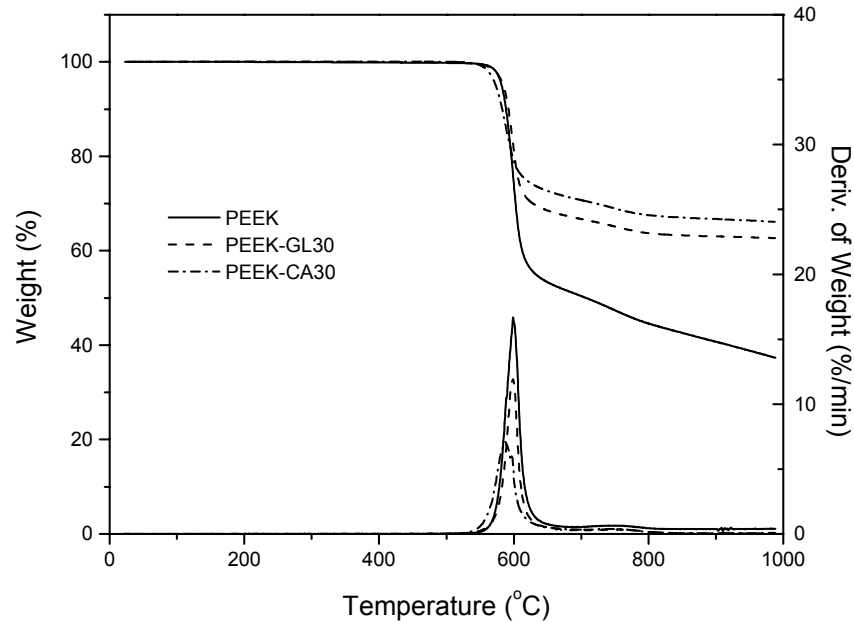


FIGURE 5-2. THERMAL DECOMPOSITION OF PEEK AND ITS COMPOSITES IN N₂

When PEEKs are burned in air, their thermal decomposition behavior is different from that in N₂ (figure 5-3). They all show a two-step decomposition process. The first step is the same as the major decomposition in N₂, and the second step is due to the oxidation of the carbonaceous char formed at the end of the first step. In contrast with the zero char yield of PEEK and carbon fiber-reinforced PEEK, there is still about 30% char left at high temperatures in glass fiber-reinforced PEEK. That indicates that carbonaceous char and carbon fiber can be easily oxidized in air, but glass fiber has a strong resistance to oxidation.

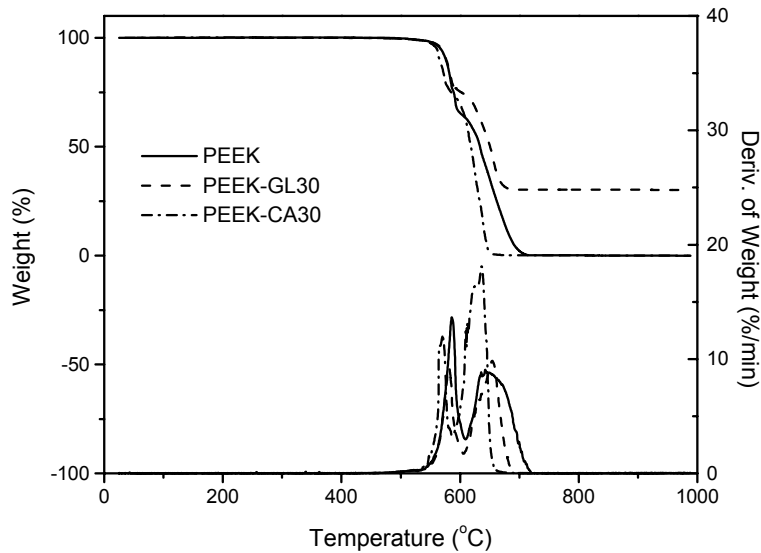


FIGURE 5-3. THERMAL DECOMPOSITION OF PEEK AND ITS COMPOSITES IN AIR

The heat events during the decomposition of these PEEK materials are very complex, which might include a series of endothermic and exothermic reactions (figure 5-4).

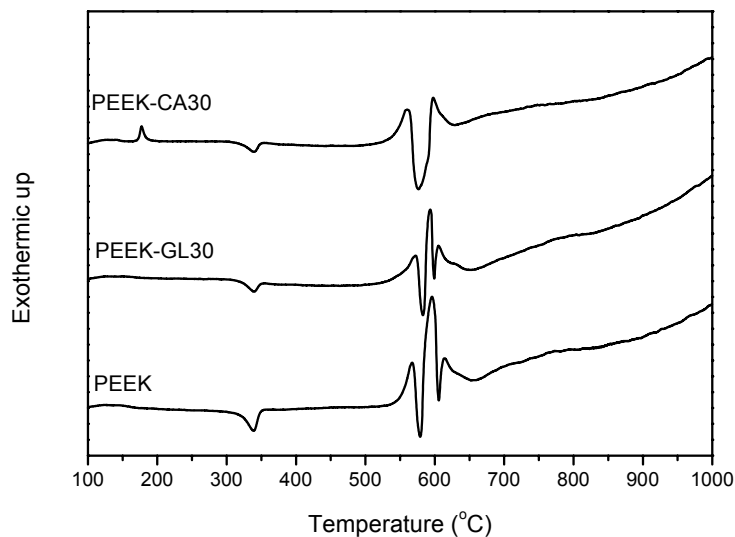


FIGURE 5-4. HIGH-TEMPERATURE DSC CURVES OF PEEKs

The thermal decomposition properties of PEEK and its composites are summarized in table 5-4.

TABLE 5-4. THERMAL DECOMPOSITION PROPERTIES OF PEEKs

Polymer	In N ₂					In Air			
	T _{99%} / T _{95%} ⁽¹⁾ (°C)	T _{max} ⁽²⁾ (°C)	PMLR ⁽³⁾ (x10 ³ /s)	Char (%)	ΔH (J/g)	T _{99%} / T _{95%} ⁽¹⁾ (°C)	T ₂ ⁽⁴⁾ (°C)	T _{max} ⁽²⁾ (°C)	PMLR ⁽³⁾ (x10 ³ /s)
PEEK	565 582	599	2.78	41	-	531 567	618	586	2.28
PEEK- GL30	562 584	599	1.99	63	-	526 568	625	654	1.64
PEEK- CA30	554 573	587	1.19	67	185	531 561	605	636	3.01

- (1) Temperatures at 1% and 5% weight loss.
- (2) Temperature at maximum mass loss rate.
- (3) Maximum mass loss rate.
- (4) Onset of decomposition temperature of the second step.

5.3.2.2 Decomposition Products.

The major decomposition products of PEEK and its composites are the same: CO₂, CO, phenol, and some aromatic ethers. At very high heating rates, the polymer will release more volatiles with low molecular weight, such as benzene and toluene. At the temperature of maximum mass loss rate, the major volatiles are CO₂, CO, and phenol. Figure 5-5 shows the GC/MS traces of PEEK under different pyrolysis conditions.

5.3.2.3 Flammability Measured by the PCFC Test.

According to the PCFC results (table 5-5), the introduction of glass and carbon fibers can further reduce the flammability of PEEK. Especially the 30% carbon fiber, which can bring the heat release capacity down by about 50%. To determine whether the flammability reduction of these composites is purely due to the mass-dilution effect of the inert fillers, the experimental values were compared with the calculated values. The values in the parentheses were calculated by deducting the contribution of the inert fillers on a mass basis. It can be seen that for PEEK-GL30, the measured heat release capacity and total heat released are all very close to the calculated values, indicating the flammability reduction of PEEK-GL30 is purely due to the mass-dilution effect of the glass fiber, but the carbon fiber can further reduce the heat release rate.

5.3.2.4 Flammability Measured by the Cone Calorimeter Test.

The cone calorimeter results of PEEK and its composites are listed in table 5-6 and shown in figure 5-6. The heat release rate (PHRR and HRR_{av}) and total heat released (THR) indicate how fast and how much heat is generated during combustion. The effective heat of combustion of

pyrolysis gases (EHC), smoke extinction area (SEA), and CO/CO₂ ratio indicate the gas-phase combustion efficiency.

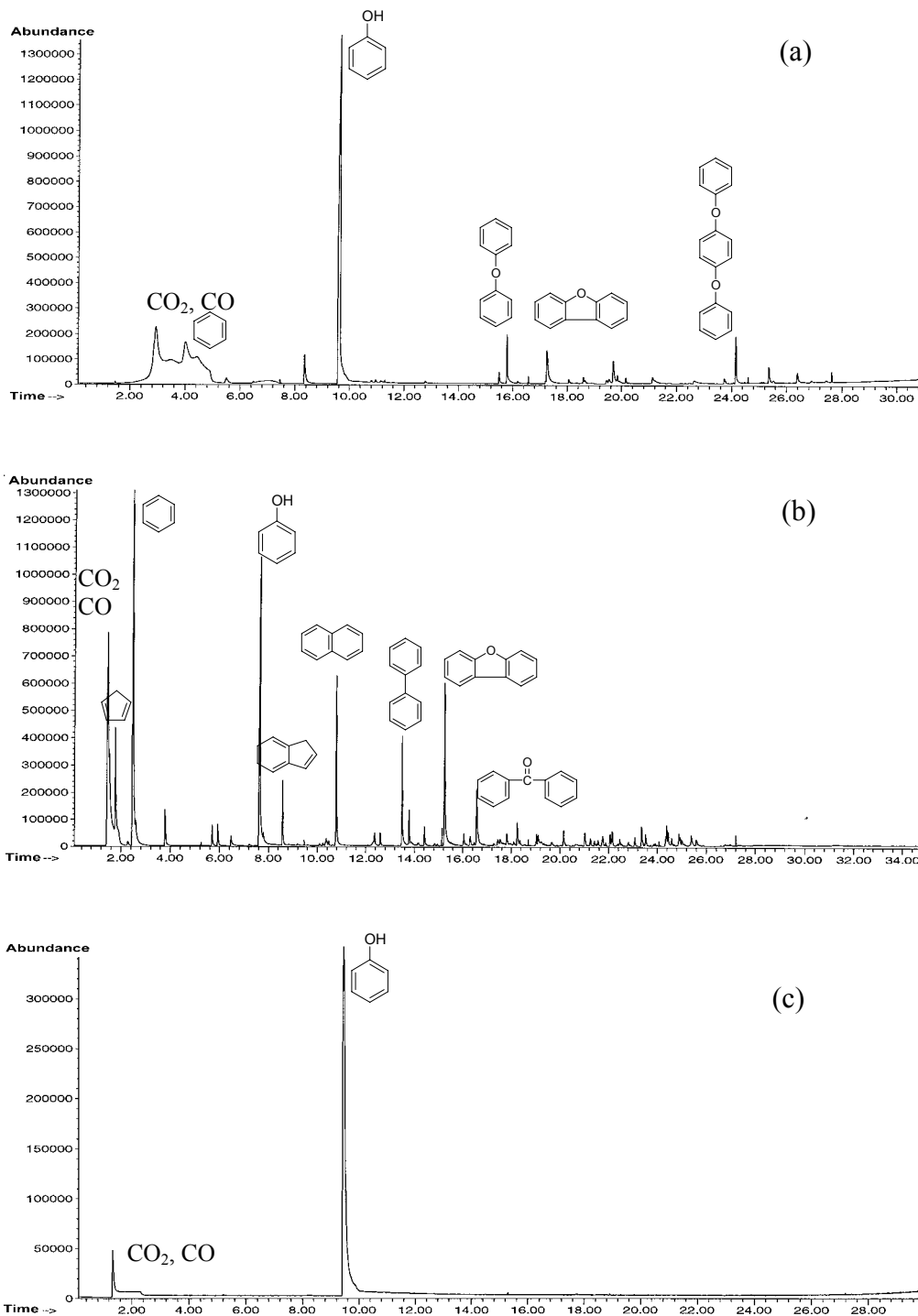


FIGURE 5-5. PYROLYSIS GC/MS TRACES OF PEEK (a) 300°-930°C, 4.3°C/s; (b) 300°-930°C, 10°C/ms; and (c) 585°-590°C, 10°C/min

TABLE 5-5. FLAMMABILITY OF PEEKs MEASURED BY PCFC

Polymers	H. R. Capacity (J/g-K)	Total Heat Released (kJ/g)
PEEK	282	12
PEEK-GL30	188 (197)	9 (8)
PEEK-CA30	110 (197)	8 (8)

Note: The values in the parentheses were calculated by deducting the mass-dilution effect of the inert fillers. For example, the heat release capacity of PEEK-GL30 is equal to the product of the heat release capacity of PEEK (282 J/g-K) and the weight fraction of the polymer matrix (70%).

TABLE 5-6. FLAMMABILITY OF PEEKs MEASURED BY THE CONE CALORIMETER

Polymer	$t_{ig}^{(1)}$ (s)	PHRR ⁽²⁾ (kW/m ²)	HRR _{av} ⁽³⁾ (kW/m ²)	THR ⁽⁴⁾ (MJ/m ²)	MLR ⁽⁵⁾ (g/m ² -s)
PEEK	70	543	103	22.4	4.72
PPEK-GL30	84	133	41	11.2	2.32
PEEK-CA30	67	104	37	9.78	2.39

Polymer	EHC ⁽⁶⁾ (kJ/g)	SEA ⁽⁷⁾ (m ² /kg)	CO/CO ₂
PEEK	20.8	451	0.131
PPEK-GL30	15.6	355	0.117
PEEK-CA30	15.4	189	0.164

- (1) Time to ignition using pilot spark.
- (2) Peak heat release rate.
- (3) Mean values from t_{ig} to 180 sec. after.
- (4) Total heat released.
- (5) Average mass loss rate.
- (6) Effective heat of combustion calculated from total heat release and overall mass loss.
- (7) Smoke-specific extinction area.

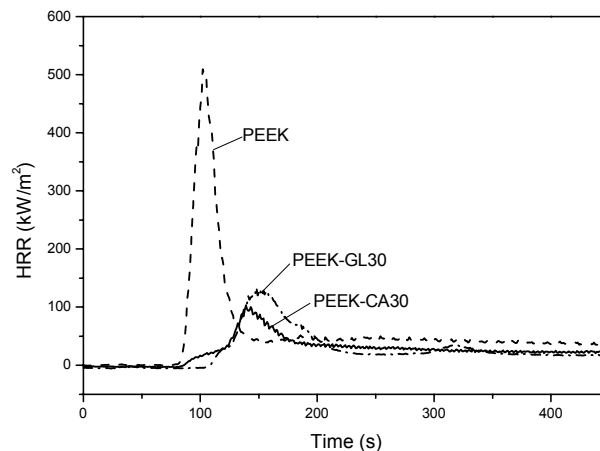


FIGURE 5-6. CONE HRR CURVES OF PEEK AND ITS COMPOSITES

It can be seen that the carbon fiber does not affect ignition time, but the glass fiber can greatly increase the time delay to ignition. However, the heat release rate and total heat released of fiber-reinforced composites are all reduced by more than 50% with only 30% inert fillers. Therefore, the decrease in their flammability in the cone calorimeter test is not only attributed to the mass-dilution effect of the fillers (the reduction of the amount of burning materials available), but it is also due to some other effects. It is known that the char can insulate the polymer substrate from heat and oxygen and reduce the release rate of the volatiles. As a result, the increase of the char formation can greatly improve the fire resistance of materials. In the PCFC test, very small amount of samples are used and the heat generated from combustion cannot transfer back to the sample, so the heat and mass transfer barrier effects of the char cannot be realized in this test. However, in the cone calorimeter test, relatively large amounts of samples are used; therefore, the materials can form a discrete layer of char on the top, which will give good protection to the underlying materials from heat and flame.

In summary, in the PCFC test, the glass and carbon fibers mainly act in the condensed phase by mass-dilution effect. In the cone calorimeter test, the char formed can further slow down polymer decomposition by acting as a heat and mass transfer barrier.

5.3.3 Xydar[®] and Its Composites.

5.3.3.1 Thermal Decomposition Process.

Xydar[®] liquid crystalline polymer has excellent thermal stability and inherent flame retardancy. Xydar[®] and its 30% glass-reinforced and 45% mineral-filled composites all decompose in a single step with a high onset decomposition temperature of 500°C in N₂ (figure 5-7). They all can produce more than 40% char. The inert fillers can further increase the char formation and reduce the mass loss rates, but they did not affect the thermal stability of the materials.

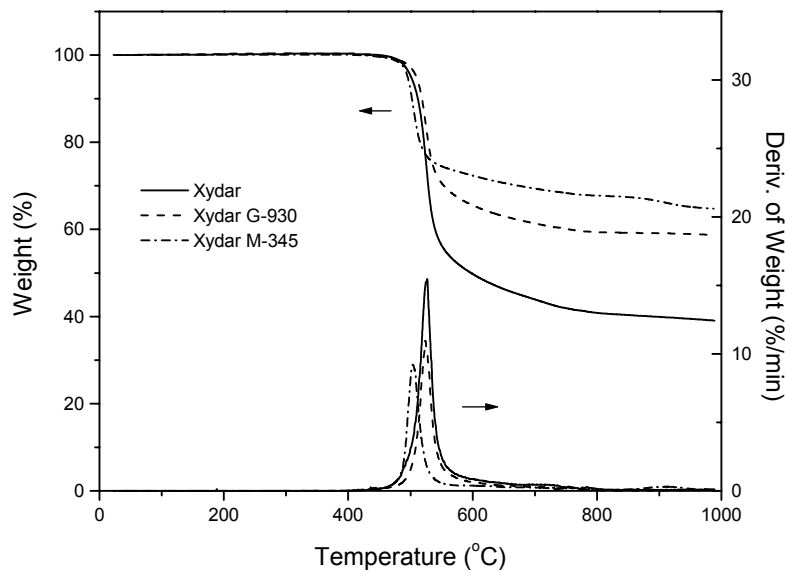


FIGURE 5-7. THERMAL DECOMPOSITION OF XYDAR[®] AND ITS COMPOSITES IN N₂

During decomposition, Xydar[®] and its composites all show two overlapped endothermic peaks (figure 5-8). The introduction of inert glass or mineral fillers can reduce the amount of the heat absorbed during decomposition (table 5-7).

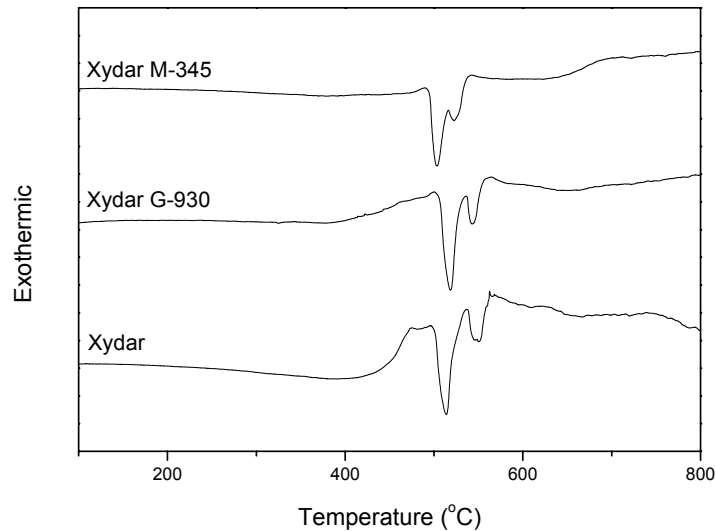


FIGURE 5-8. HIGH-TEMPERATURE DSC CURVES OF XYDAR[®] AND ITS COMPOSITES

TABLE 5-7. THERMAL DECOMPOSITION PROPERTIES OF XYDAR[®] MATERIALS IN N₂

Polymers	T _{99%} (°C)	T _{95%} (°C)	T _{max} (°C)	PMLR (x10 ³ /s)	Char (%)	ΔH (J/g)
Xydar [®]	478	501	525	2.55	40	163
Xydar [®] G-930	477	509	524	1.83	59	135
Xydar [®] M-345	471	495	504	1.54	66	104

Similar to PEEK and its composites, Xydar[®] and its composites all decompose in two steps in air (figure 5-9). The first step is the same as the major decomposition step in N₂. The second step is due to the oxidation of the carbonaceous char formed at the end of the first step. Because the glass fiber and mineral are very difficult to oxidized, both Xydar[®] composites still have a large amount of char left at high temperatures, which is exactly the same as the amount of inert filler incorporated. In air, the glass or mineral-filled composites decompose faster in the second step, which is different from the pure Xydar[®] polymer (table 5-8).

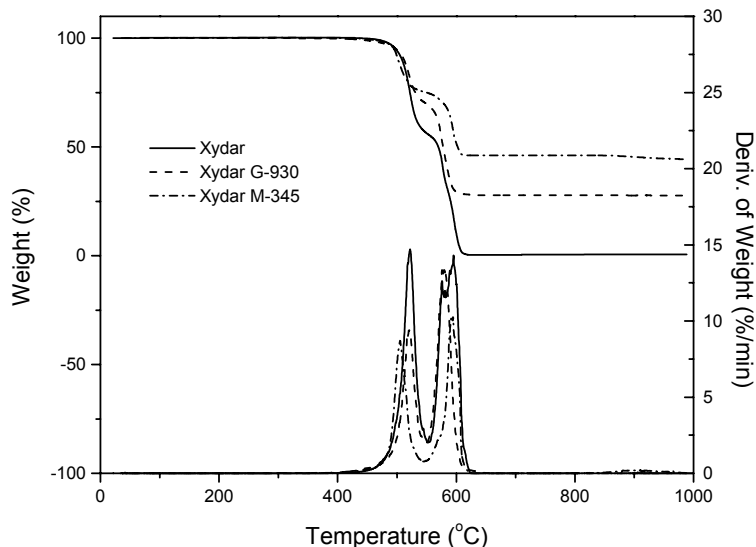


FIGURE 5-9. THERMAL DECOMPOSITION OF XYDAR[®] MATERIALS IN AIR

TABLE 5-8. THERMAL DECOMPOSITION PROPERTIES OF XYDAR[®] MATERIALS IN AIR

Polymers	T _{99%} (°C)	T _{95%} (°C)	T ₂ (°C)	T _{max} (°C)	PMLR (x10 ³ /s)	Char (%)
Xydar [®]	472	498	571	522	2.45	0
Xydar [®] G-930	447	498	566	580	2.23	28
Xydar [®] M-345	465	495	582	593	1.73	45

5.3.3.2 Flammability Measured by the PCFC Test.

Because Xydar[®] G-930 contains more polymer components and has a higher maximum mass loss rate, it is more flammable than Xydar[®] M-345 from PCFC method (table 5-9). According to pyrolysis GC/MS results (figure 5-10), the flammability of Xydar[®] materials mainly comes from the phenol volatile. Similar to PEEK composites, the flammability reduction of the Xydar[®] composites measured by the PCFC test is mainly due to the mass-dilution effect of the nonflammable glass or mineral fillers.

TABLE 5-9. FLAMMABILITY OF XYDAR[®] AND ITS COMPOSITES BY PCFC

Polymers	H. R. Capacity (J/g-K)	Total Heat (kJ/g)
Xydar [®]	215	11
Xydar [®] G-930	137 (151)	8 (8)
Xydar [®] M-345	120 (118)	6 (6)

Note: The values in the parentheses are calculated by deducting the mass-dilution effect of the inert fillers.

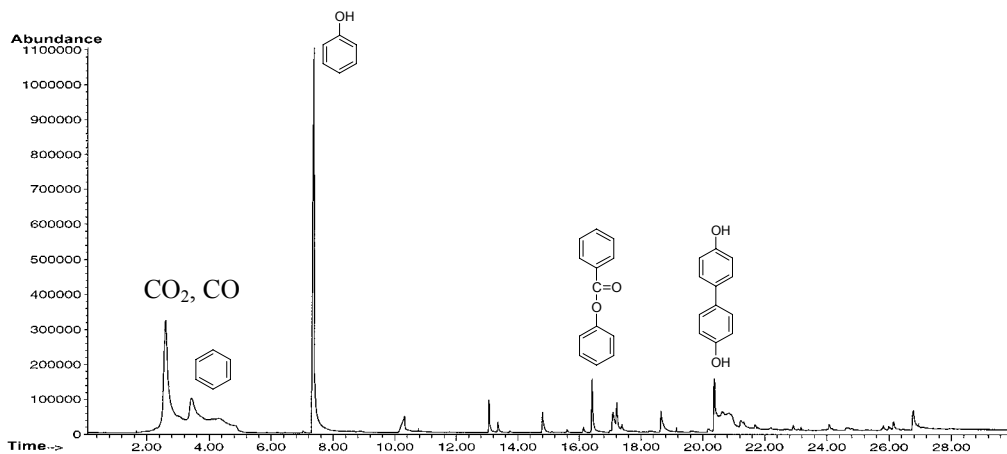


FIGURE 5-10. PYROLYSIS GC/MS TRACES OF XYDAR[®] (4.3°C/s TO 930°C)

5.3.3.3 Flammability Measured by the OSU Calorimeter Test.

In contrast to PCFC results, the OSU calorimeter test shows that Xydar[®] M-345 is more flammable than Xydar[®] G-930. In addition, Xydar[®] G-930 has an extremely low 2-min heat release due to its slow burning rate at the beginning of the 2 minutes (figure 5-11).

It was also found that the 5-minute heat release from Xydar[®] G-930, measured by the OSU calorimeter (table 5-10), is smaller than the total heat released measured by the PCFC test. In the PCFC test, the pyrolysis and combustion temperatures are 930° and 900°C, respectively, so the materials are completely decomposed and the volatiles produced are totally oxidized. As a result, the total heat released measured by PCFC indicates the maximum flammability of materials, based on their chemical structure and composition. However, in the OSU test, the burning process of most high-charring materials is not completed by the end of the 5-minute test. The incomplete burning of Xydar[®] G-930 can also be proven by the high char yield of 69% from the OSU test versus 59% from the PCFC test.

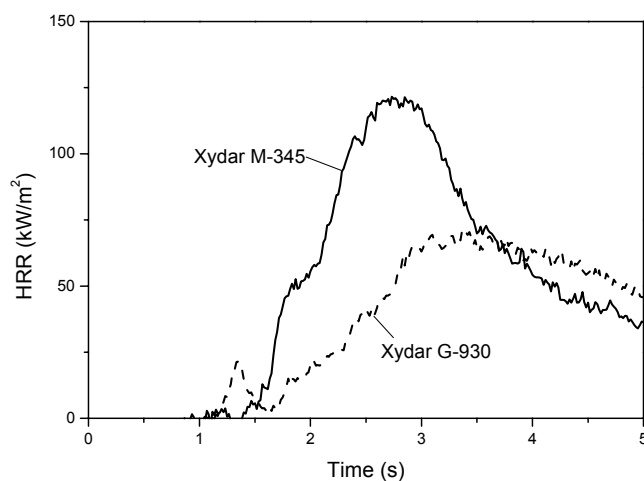


FIGURE 5-11. OHIO STATE UNIVERSITY HRR CURVES OF XYDAR[®] COMPOSITES BY THERMOPILE

TABLE 5-10. OHIO STATE UNIVERSITY RESULTS OF XYDAR[®] COMPOSITES

Method	Parameters	Xydar [®] m-345	Xydar [®] G-930
Thermopile	PHRR (kW/m ²)	123	69
	2-min HR (kW.min/m ²)	13	2
	5-min HR (kW.min/m ²)	234	146
O ₂ consumption	PHRR (kW/m ²)	179	103
	2-min HR (kW.min/m ²)	37	14
	5-min HR (kW.min/m ²)	275	208
Char (%)		69	69

Nonetheless, why does Xydar[®] M-345 have a lower mass loss rate but a higher heat release rate in the OSU test? It is probably because, besides the chemical structure and composition of materials, there are some other factors, such as the physical properties of the materials and mass and heat transfer during burning that also affect the flammability. In the PCFC test, materials are forced to pyrolyze at a fixed heating rate, and the volatiles produced are completely oxidized in the high-temperature furnace. In addition, the pyrolysis and combustion (oxidation) processes are totally separated, thus, the heat generated by the combustion cannot be delivered back to the polymer to further affect polymer decomposition. Therefore, the PCFC results are mainly determined by the chemical structure and composition of materials (mass loss rate, char yield, and heat of combustion of volatiles). As a result, a high mass loss rate usually leads to a high heat release capacity in the PCFC test if the materials have similar structures. However, the OSU test is a real flame-combustion test, and the sample surface is directly exposed to the flame. Therefore, the heat produced in the gas phase can feed back to form a real combustion cycle. Because Xydar[®] M-345 is mineral-filled, it is more likely to absorb the heat from its surroundings to facilitate the decomposition and combustion process thereafter, which might lead to its high flammability.

5.3.3.4 Flammability Measured by the Cone Calorimeter Test.

The cone calorimeter results show that both Xydar[®] M-345 and Xydar[®] G-930 have very good flame resistance, but Xydar[®] M-345 has a relatively higher heat release rate, which is consistent with the OSU results (table 5-11 and figure 5-12). The increase of the heat flux can increase heat release rate, mass loss rate, and total heat released but decrease the CO/CO₂ ratio, which means flammability and efficiency of combustion are both increased.

TABLE 5-11. CONE CALORIMETER RESULTS OF XYDAR[®] COMPOSITES

Polymer	Heat flux (kW/m ²)	t _{ig} (s)	PHRR (kW/m ²)	HRR _{av} (kW/m ²)	THR (MJ/m ²)	MLR (g/m ² -s)
Xydar [®] M-345	50	72	105	44	16.3	4.5
	75	39	235	66	21.4	6.8
	100	26	228	72	20.0	8.1
Xydar [®] G-930	50	50	92	50	19.6	3.8
	75	25	137	74	25.0	6.1
	100	14	141	82	23.5	7.4

Polymer	Heat Flux (kW/m ²)	EHC (kJ/g)	SEA (m ² /kg)	CO/CO ₂
Xydar [®] M-345	50	12.2	318	0.063
	75	14.6	350	0.021
	100	14.1	365	0.015
Xydar [®] G-930	50	15.2	251	0.047
	75	16.0	405	0.011
	100	15.5	429	0.007

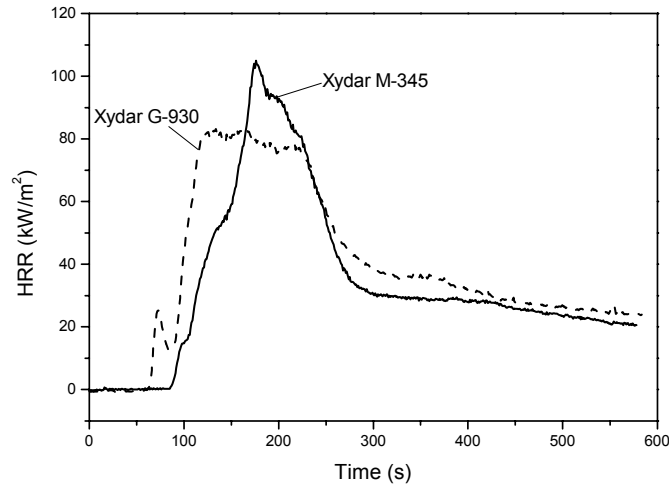


FIGURE 5-12. CONE HRR CURVES OF XYDAR[®] COMPOSITES

5.3.4 Polyphthalamides and Composites.

Recently, halogenated flame retardants have been the subject of environmental concerns, but the effectiveness of these compounds has maintained their position in the market place. In this section, two series of poly(phthalamide) materials (A-1000 and A-6000 series) with brominated flame retardants and/or glass fiber were studied. The composition of the materials was detailed in table 5-1.

5.3.4.1 Thermal Decomposition Process.

The TGA results show that all these materials decompose in a single step under N₂ (figure 5-13). They all have relatively high thermal stability up to 400°C. The heat stabilizer does increase the thermal stability of materials. For example, the temperature at 5% weight loss for A-6135HS is increased from 402°C (A-6000) to 421°C (A-6135HS). Correspondingly, the temperature at maximum mass loss rate is also increased from 453°C (A-6000) to 468°C (A-6135HS). On the contrary, the introduction of brominated flame retardants decreases the thermal stability and increases the mass loss rate if the reduction effect of the glass fiber is excluded. In addition, because A-1000 and A-6000 have zero char yield, the char of all the composites comes mainly from the nonflammable glass fiber.

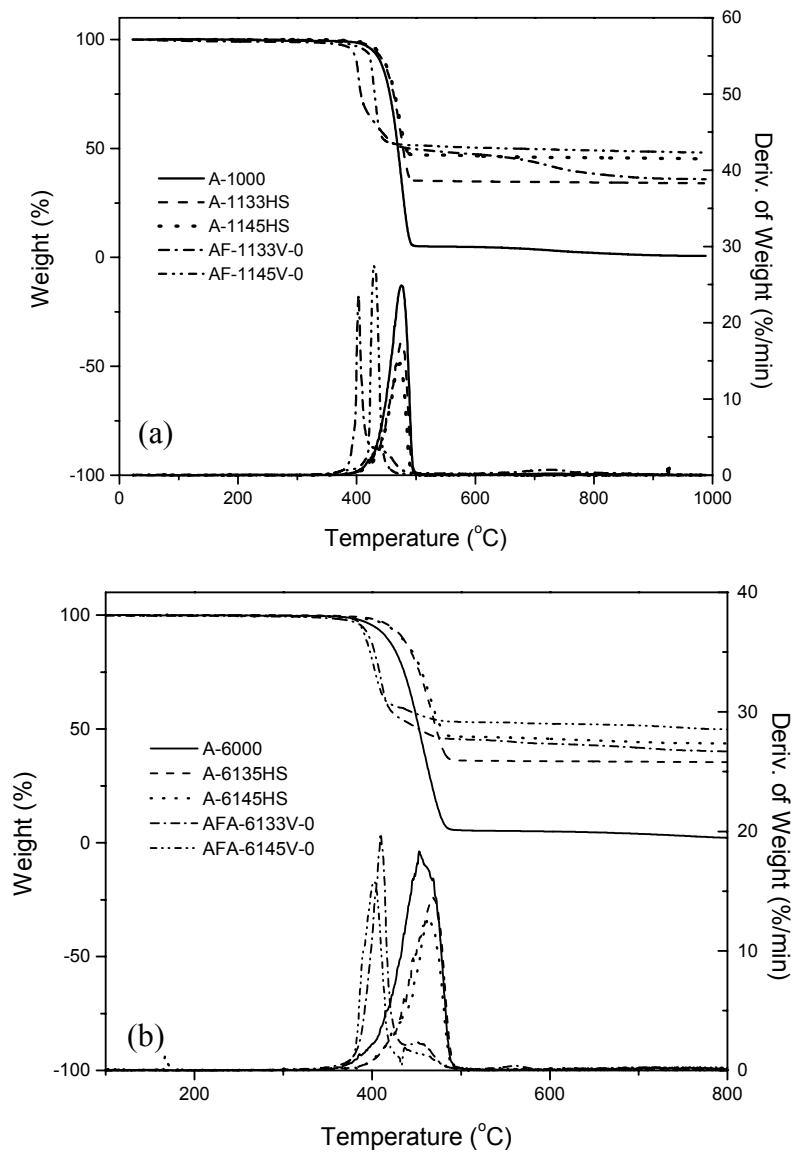


FIGURE 5-13. THERMAL DECOMPOSITION OF PPA MATERIALS (a) A-1000 SERIES AND (b) A-6000 SERIES

High-temperature DSC curves of A-1000, A-6000, and some of their flame-retardant and/or glass-fiber composites are shown in figure 5-14. All the materials exhibit an endothermic decomposition peak. The introduction of glass fiber can reduce the heat of decomposition due to the lower amount of fuel available. The presence of flame retardants can make the decomposition peak sharper. In addition, the melting peaks (around 340°C) in the flame-retardant composites have disappeared.

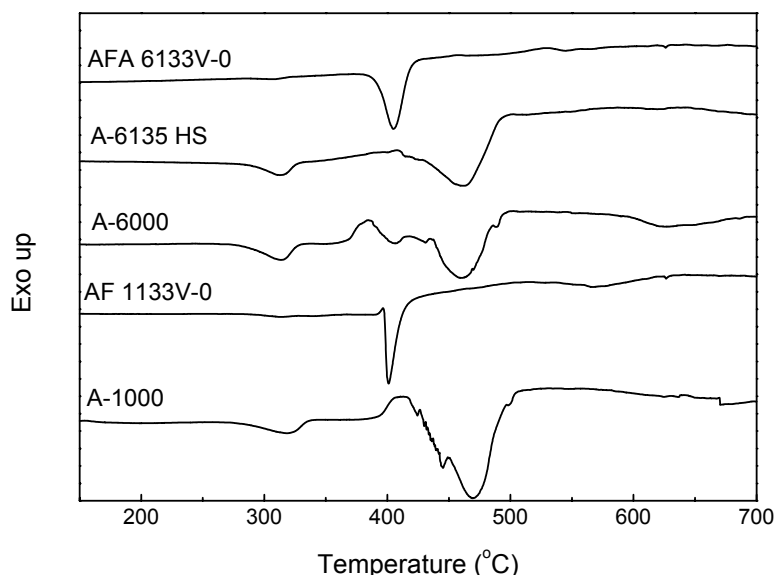


FIGURE 5-14. HIGH-TEMPERATURE DSC CURVES OF PPA MATERIALS

5.3.4.2 Thermal Decomposition Products.

The GC/MS traces of A-1000, A-6000, and their composites under different pyrolysis conditions are shown in figure 5-15. The major decomposition products of A-1000 and A-6000 are similar, including CO₂, CO, some aliphatic olefins, benzonitriles (typical volatiles for amides), and a series of aromatic-aliphatic amides with different lengths of CH₂ units. A-6000 also releases more hexanedinitrile than A-1000. The decomposition products of the glass fiber-reinforced composites are the same as those from virgin polymers. Therefore, the decrease in the heat release capacity and total heat released of these composites is only due to the mass dilution effect of the glass fiber. However, the major decomposition products of the flame-retardant composites are quite different. For AFA-6133 V-0 and AFA-6145V-0, bromostyrenes, dibromobenzonitriles, and tribromobenzonitrile are the predominant volatiles. In contrast, AF-1133 V-0 and AF-1145 V-0 release not only some brominated compounds such as dibromobenzonitriles and tribromobenzonitrile, but also a certain amount of other aromatic compounds. At the temperature of maximum mass loss rate, these flame-retardant materials mainly produce brominated volatiles.

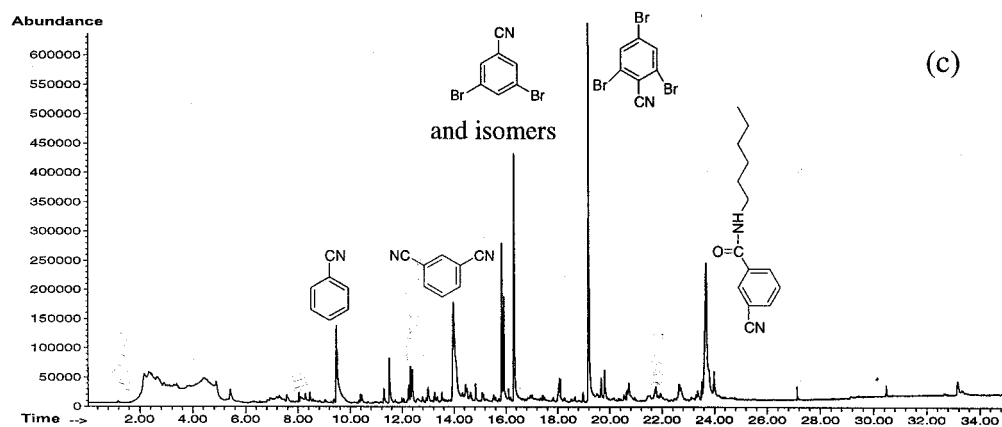
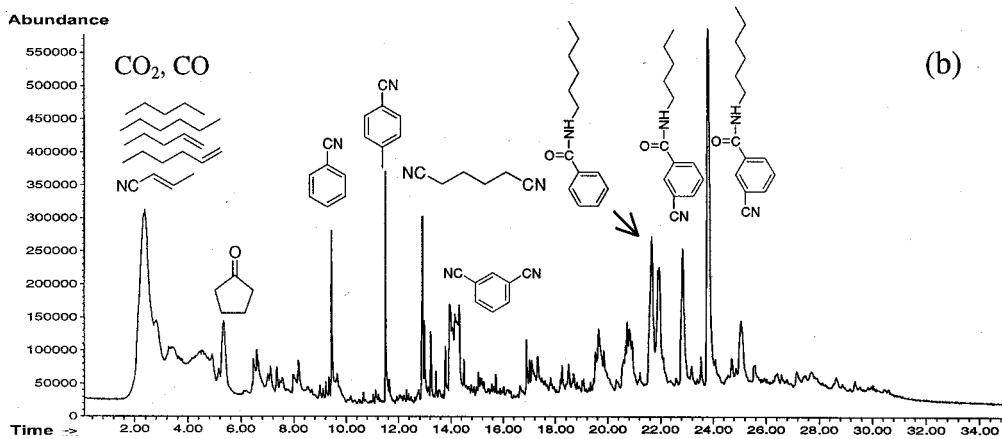
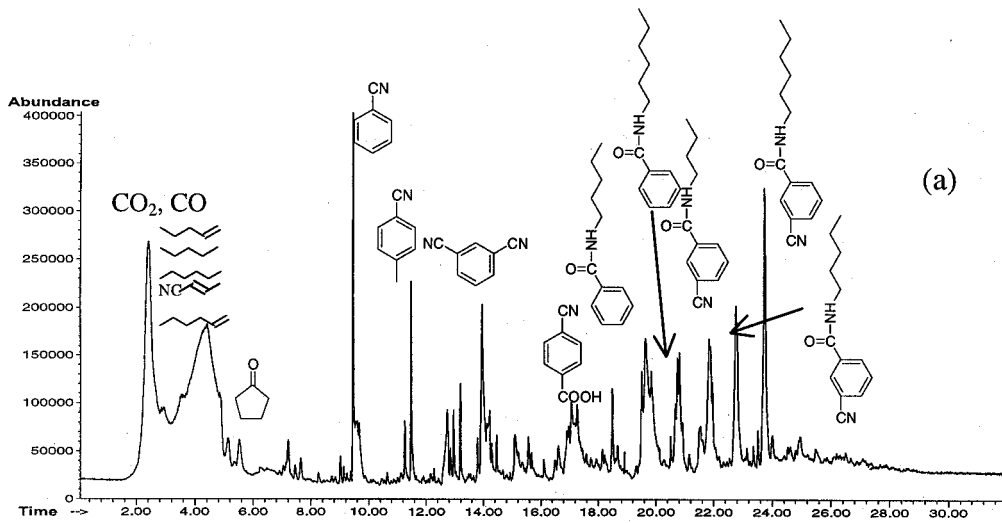


FIGURE 5-15. PYROLYSIS GC/MS TRACES OF PPA MATERIALS (PYROLYSIS CONDITION: $300^{\circ}\sim 930^{\circ}\text{C}$ AT A HEATING RATE OF 4.3°C/s FOR (a) A-1000; (b) A-6000; (c) AF-1133 V-0; (d) AFA-6133 V-0, 10°C/min FOR (e) AF-1133 V-0, $400^{\circ}\sim 405^{\circ}\text{C}$; AND (f) AFA-6133 V-0, $405^{\circ}\sim 410^{\circ}\text{C}$)

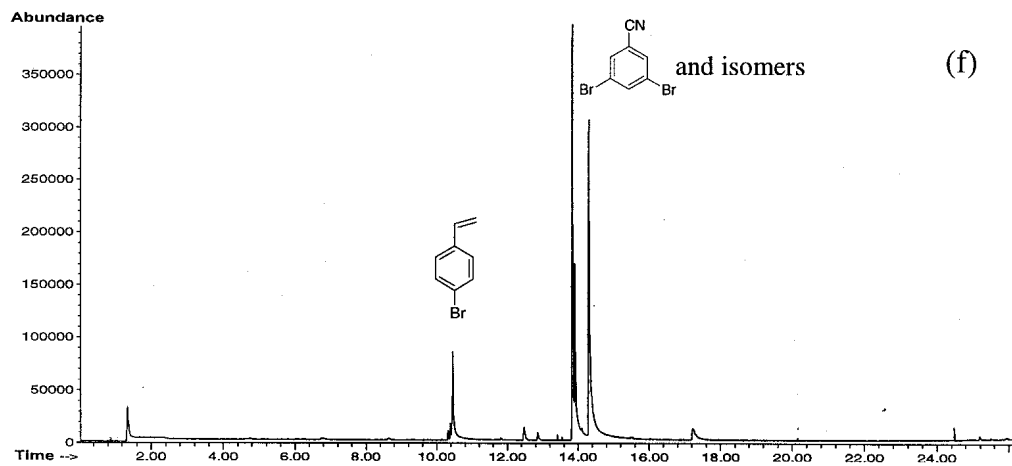
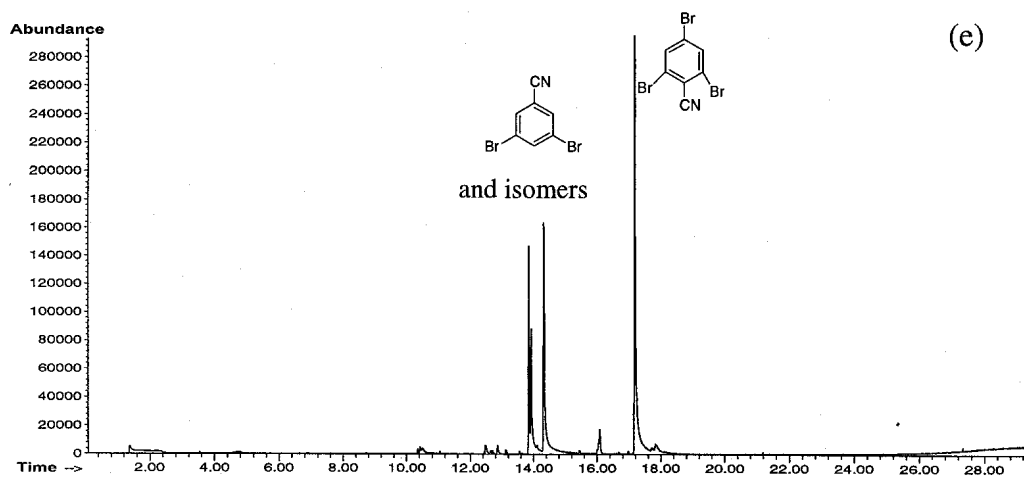
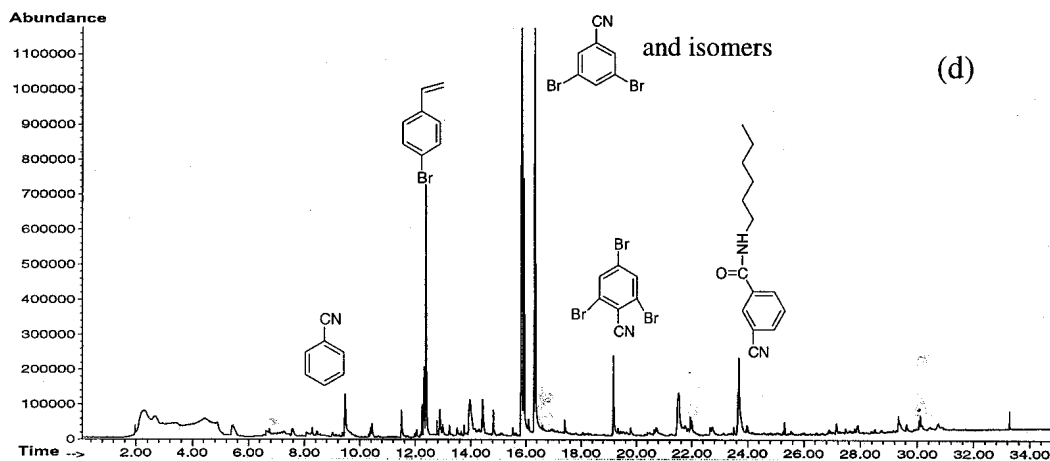


FIGURE 5-15. PYROLYSIS GC/MS TRACES OF PPA MATERIALS
(PYROLYSIS CONDITION: 300°~930°C AT A HEATING RATE OF 4.3°C/s FOR
(a) A-1000; (b) A-6000; (c) AF-1133 V-0; (d) AFA-6133 V-0, 10°C/min FOR
(e) AF-1133 V-0, 400°~405°C; AND (f) AFA-6133 V-0, 405°~410°C) (Continued)

5.3.4.3 Flammability Measured by PCFC Test.

The thermal decomposition and flammability of PPA materials are summarized in table 5-12. It can be seen that the heat release capacity of A-1000 is slightly higher than that of A-6000 because A-1000 contains more aliphatic units. The reduction in the heat release capacity and total heat released of A-6135HS, 6145 HS, 1135HS, and 1145HS is completely due to the mass-dilution effect of glass fiber (the measured values are close to the calculated values in the parentheses).

TABLE 5-12. THERMAL DECOMPOSITION AND FLAMMABILITY OF PPA MATERIALS

Polymers	T _{99%} (°C)	T _{95%} (°C)	T _{max} (°C)	PMLR (x10 ³ /s)	Char (%)	H. R. Capacity (J/g-K)	Total Heat (kJ/g)
A-1000	387	427	476	4.15	0	610	31
A-1133 HS	399	431	476	2.91 (2.78)	34	408 (409)	22 (21)
A-1145 HS	404	435	473	2.45 (2.28)	45	349 (336)	17 (17)
AF-1133 V-0	363	394	403	3.91 (2.78)	36	394 (409)	13 (21)
AF-1145 V-0	368	414	429	4.59 (2.28)	48	444 (336)	11 (17)
A-6000	372	402	453	3.06	0	537	33
A-6135 HS	389	421	468	2.42 (1.99)	35	365 (349)	21 (22)
A-6145 HS	371	419	463	2.14 (1.68)	44	301 (295)	18 (18)
AFA-6133 V-0	334	389	410	3.30 (2.05)	39	265 (359)	13 (22)
AFA-6145 V-0	368	388	401	2.64 (1.68)	49	209 (295)	10 (18)

*Values in the parentheses are the product of the property of the base polymers (A-1000 or A-6000) and the weight fraction of polymer matrix.

The brominated flame retardants can reduce the total heat released, but their effects on the heat release capacity are more complicated. For AFA-6133 V-0 and AFA-6145 V-0, the heat release capacity is further reduced even after excluding the contribution of the glass fiber. However, for AF-1145 V-0, the measured heat release capacity is higher than the calculated value, which indicates that the introduction of polybrominated flame retardant actually increases the flammability after the deduction of mass-dilution effect of the glass fiber. This is because the PCFC measurement is not a real flame-combustion test. All the pyrolysis gases produced can be completely oxidized in the high-temperature furnace. Therefore, the instantaneous gas-phase inhibition of the halogenated flame retardants will not be achieved in the PCFC test. As a result, the sharp and high mass loss rate peaks in these flame-retarded materials might induce high heat release rates. However, because the major decomposition volatiles from these flame-retarded materials are halogenated compounds that have relatively lower flammability than corresponding hydrocarbon volatiles, the total heat released of these materials can still be reduced. It was also found that the combination of brominated compounds with antimony compounds in AFA-6133 V-0 and 6145 V-0 can synergistically reduce flammability, which is also shown in the PCFC results.

5.3.4.4 Flammability Measured by the OSU Calorimeter Test.

A-1000 and A-6000 are very flammable and dripped extensively during the OSU test. Therefore, their flammability measured by the OSU test is underestimated because some melt falls to the bottom of the furnace and are not burned. After adding 33% glass fiber and 30% flame retardant, the dripping problem of AF-1133 V-0 is greatly reduced. Because the brominated volatiles released during decomposition can act in the gas phase and slow down the combustion process in the OSU test, AF-1133 V-0 shows a dramatic decrease in both heat release rate and total heat released (table 5-13). However, a lot of smoke was also produced.

TABLE 5-13. FLAMMABILITY OF A-1000 SERIES MEASURED BY THE OSU CALORIMETER

Method	Parameters	A-1000	AF-1133 V-0
Thermopile	PHRR (kW/m ²)	190	110
	2-min HR (kW.min/m ²)	136	94
	5-min HR (kW.min/m ²)	359	275
O ₂ consumption	PHRR (kW/m ²)	417	262
	2-min HR (kW.min/m ²)	305	228
	5-min HR (kW.min/m ²)	514	494
Char (%)		0	40

It was found that the flame-retarded AF-1133 V-0 had a lower and broader burning peak (figure 5-16). The char of AF-1133 V-0 can hold together, so the shape and size of the burned sample were the same as the original sample. Interestingly, the char had a two-layered structure in which the surface layer is the white char formed by the glass fiber and underneath is the black carbonaceous char formed by the polymer matrix and brominated flame retardant.

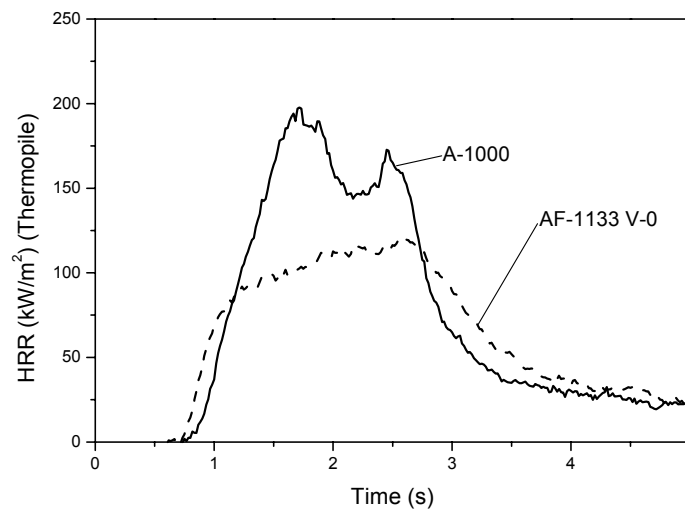


FIGURE 5-16. OHIO STATE UNIVERSITY HRR CURVES OF A-1000 SERIES

According to the OSU results of A-6000 series (table 5-14), A-6135 HS and A-6145 HS have higher flammability than A-6000. This is because the glass fiber can reduce the flammability mainly by its nonflammable property. Generally, it cannot induce char formation in the polymer matrix or act in the gas phase. Therefore, the glass fiber cannot change the thermal decomposition mechanism or gas-phase combustion of the materials. However, the incorporation of glass fiber does change the physical properties of materials. For example, the increase of the thermal conductivity can increase the composite's ability to absorb the heat and spread the heat along the sample. This might increase the decomposition rate of the material and speed up the burning process. On the other hand, the reduction of the dripping will also reserve more burning materials available. As a result, high flammability is observed in OSU results.

TABLE 5-14. FLAMMABILITY OF A-6000 SERIES MEASURED BY THE OSU CALORIMETER

Method	A-6000	A-6135HS	A-6145 HS	AFA-6133 V-0	AFA-6145 V-0
Thermopile					
PHRR (kW/m ²)	198	207	232	90	93
2-min HR (kW.min/m ²)	161	202	220	96	96
5-min HR (kW.min/m ²)	375	480	493	250	247
O ₂ consumption					
PHRR (kW/m ²)	411	420	433	306	289
2-min HR (kW.min/m ²)	293	362	379	312	269
5-min HR (kW.min/m ²)	521	673	606	548	490
Char (%)	0	31	44	39	49

For the flame-retardant composites (AFA-6133 V-0 and AFA-6145 V-0), their flammability is dramatically reduced due to the synergetic effects of brominated compounds and antimony compounds. They all show a low and steady heat release peak during burning (figure 5-17). Their two-layered char is similar to AF-1133 V-0, while only white fragmented char is formed in A-6135 HS and A-6145 HS.

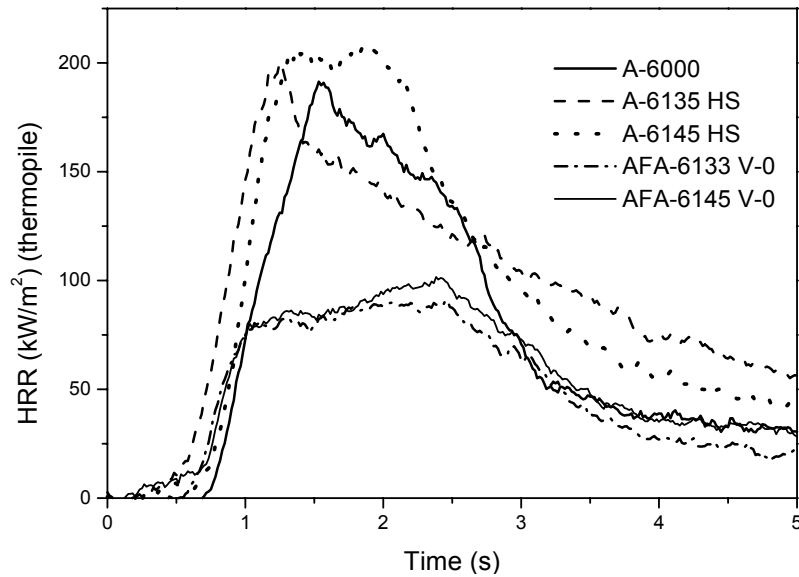


FIGURE 5-17. OHIO STATE UNIVERSITY HRR CURVES OF A-6000 SERIES

5.3.4.5 Flammability Measured by the Cone Calorimeter Test.

The cone HRR curves of the A-1000 series are shown in figure 5-18. It can be seen that all the glass fiber or flame-retarded composites are less ignition resistant than A-1000. A-1000 and the glass fiber-reinforced composites A-1135 HS and A-1145 HS all show a sharp and high heat release peak, but the flame-retarded composites AF-1133 V-0 and AF-1145 V-0 have a very low heat release rate. The burning peak in AF-1133 V-0 is very broad, which suggests some steady-burning process.

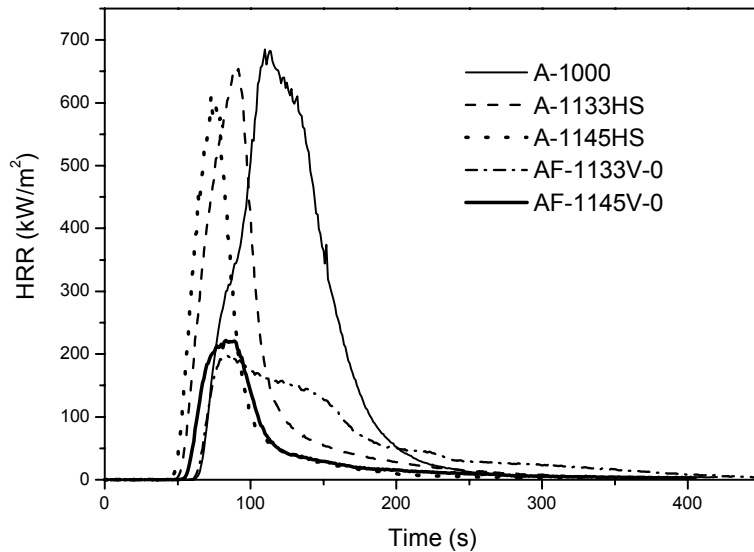


FIGURE 5-18. CONE HRR CURVES OF A-1000 SERIES

The cone HRR curves of the A-6000 series (figure 5-19) are similar to those of the A-1000 series. The glass fiber-reinforced composites A-6135 HS and A-6145 HS have a lower heat release rate than A-6000, and the flame-retarded composites AFA-6133 V-0 and AFA-6145 V-0 show a kind of steady-burning process with very low heat release rates. It seems that the peak heat release rates of these flame-retarded composites are independent of the amount of glass fiber inside.

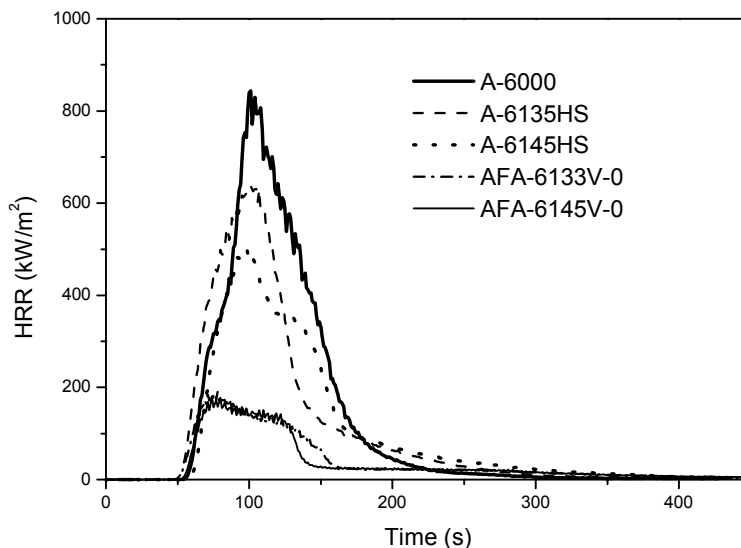


FIGURE 5-19. CONE HRR CURVES OF A-6000 SERIES

The cone calorimeter results of A-1000 and A-6000 and their composites are shown in table 5-15. In the A-1000 series, the ignition time of both glass fiber-reinforced and flame-retarded composites is shorter than A-1000. The addition of glass fiber can reduce the mass loss rate and total heat released due to the mass-dilution effect. However, due to the change of some physical properties of the materials, the peak heat release rates of A-1135HS and A-1145HS are not significantly reduced by the inert glass fiber. In addition, their effective heat of combustion and smoke evolution are the same as A-1000, which indicates that the decomposition volatiles released, as well as the gas-phase combustion chemistry, are not changed. For the flame-retarded composites AF-1133 V-0 and AF-1145 V-0, the flammability is greatly reduced by the polybrominated flame retardant. Their peak heat release rates are about three times lower than A-1000, the total heat released and effective heat of combustion are about 50% lower. In contrast, the smoke production is about two times higher, and the CO/CO₂ ratio is about ten times higher. All these results suggest that the polybrominated flame retardant acts in the gas-phase by the incomplete combustion. In other words, the brominated compounds released during decomposition can reduce the active, flame-carrying H· and OH· radicals from the propagation and chain-branching steps and replace them with less active bromine radicals. As a result, the burning process is slowed in the gas phase.

TABLE 5-15. CONE CALORIMETER RESULTS OF PPA MATERIALS

Polymer	Heat Flux (kW/m ²)	t _{ig} (s)	PHRR (kW/m ²)	HRR _{av} (kW/m ²)	THR (MJ/m ²)
A-1000	50	39	685	262	48.2
A-1135 HS	50	27	657	160	30.1
A-1145 HS	50	23	612	115	20.9
A-1133 V-0	50	37	198	100	21.7
A-1145 V-0	50	31	222	63	12.1
A-6000	50	36	876	240	50.4
	75	22	1231	258	51.1
	100	11	1794	338	60.8
A-6135 HS	50	33	640	235	45.1
	75	16	805	250	45.1
	100	10	953	259	46.6
A-6145 HS	50	34	505	207	41.4
	50	28	191	77	16.9
	75	14	289	109	21.1
A-6133 V-0	75	14	289	109	21.1
	100	11	323	107	20.2
A-6145 V-0	50	31	181	69	15.0

Polymer	Heat Flux (kW/m ²)	MLR (g/m ² -s)	EHC (kJ/g)	SEA (m ² /kg)	CO/CO ₂
A-1000	50	21.2	22.0	593	0.019
A-1135 HS	50	10.3	22.8	535	0.030
A-1145 HS	50	10.0	23.2	507	0.036
A-1133 V-0	50	9.1	11.0	938	0.114
A-1145 V-0	50	8.1	11.0	966	0.127
A-6000	50	15.9	25.0	525	0.016
	75	10.1	25.0	621	0.013
	100	37.6	27.2	535	0.019
A-6135 HS	50	11.9	26.7	505	0.022
	75	17.4	24.4	638	0.023
	100	19.6	25.7	644	0.022
A-6145 HS	50	8.6	22.8	443	0.018
	50	9.0	8.6	1072	0.138
	75	14.0	10.4	1231	0.160
A-6133 V-0	100	16.1	10.4	1237	0.169
	50	7.81	9.0	1109	0.155

In the A-6000 series, there is some decrease in the heat release rates of A-6135 HS and A-6145 HS, and the amount of decrease in total heat released is not proportional to the amount of glass fiber inside. As expected, the flame-retarded composites AFA-6133 V-0 and AFA-6145 V-0 have a dramatic decrease in flammability. Their peak heat release rates were about four times lower than A-6000, the total heat released and effective heat of combustion were about 70% lower, the smoke production is twice as high, and the CO/CO₂ ratio are ten times higher. The combination of the brominated flame retardant with antimony compound in AFA-6133 V-0 and

AFA-6145 V-0 is more effective because the antimony-halogen systems can affect the combustion of polymers both in the gas and condensed phases. It can also be seen that with the increase of the heat flux, the heat release rate, mass loss rate, and total heat released all increase, but the effective of heat of combustion does not change dramatically.

It can be concluded that the heat stabilizer can increase the thermal stability of materials. The addition of glass fiber can reduce the flammability, mainly by mass-dilution effects. However, it can also change some physical properties of the materials such as thermal conductivity, density, and heat capacity. Therefore, the mass-dilution effect of the glass fiber observed in OSU and cone calorimeter tests is not as dramatic as in PCFC tests. Brominated compounds mainly act in the gas phase by reducing the combustion efficiency. The combination of brominated compounds with the antimony compound is more efficient due to their synergistic effect. However, the gas-phase inhibition effects of the brominated flame retardants can only be seen in OSU and cone calorimeter tests, not in PCFC tests.

5.3.5 Epoxy Resins With Phosphate Flame Retardants.

Interest in halogen-free flame retardants help drive the market toward phosphorus-based flame retardants. In this section, the effects of three different phosphates (dimethoxy methyl phosphate (DMMP), trimethyl phosphate (TMP), and triphenyl phosphate (TPP)) on the flammability of an epoxy resin (EPON 825 cured by Jeffamine D230) were studied. In these systems, phosphates also serve as viscosity depressants. The composites were made in three steps: (1) mixing the three components together, (2) heating the mixture at 75°C for about 3 hours, and (3) increasing the temperature to 125°C for another 3 hours [124]. The structure of each component is shown in figure 5-20.

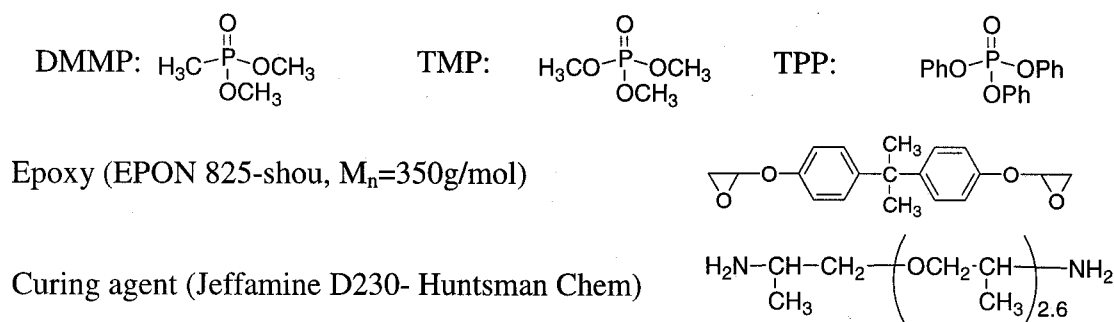


FIGURE 5-20. COMPOSITION OF PHOSPHATE-RETARDED EPOXY RESIN

The thermal decomposition processes of different epoxy/phosphate composites are shown in figure 5-21. It can be seen that with the increased amount of DMMP, TMP, or TPP, the thermal stability and mass loss rates of the composites decrease systematically. The phosphate additives tend to volatilize from the composites below 300°C due to their low boiling points (figure 5-22). The major decomposition step is due to the breakdown of the epoxy network, which releases a series of olefins and phenols. The char yields of epoxy/TMP resins increase with the concentration of TMP, which suggests that TMP can act in the condensed phase to reduce flammability. However, DMMP and TPP cannot significantly increase the char yields of the composites.

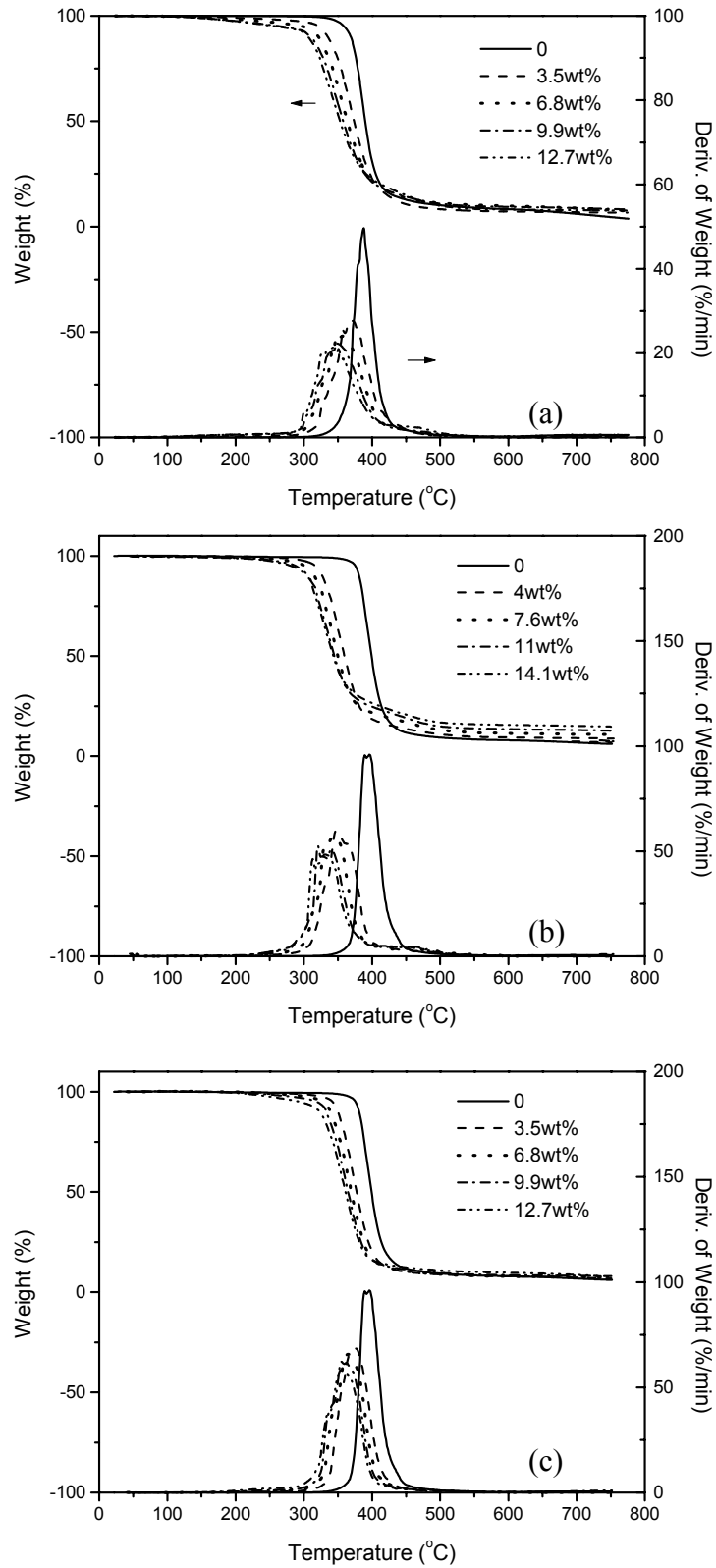


FIGURE 5-21. THERMAL DECOMPOSITION OF EPOXY/PHOSPHATE COMPOSITES [124] (a) DMMP, 20°C/min; (b) TMP, 40°C/min; AND (c) TPP, 40°C/min

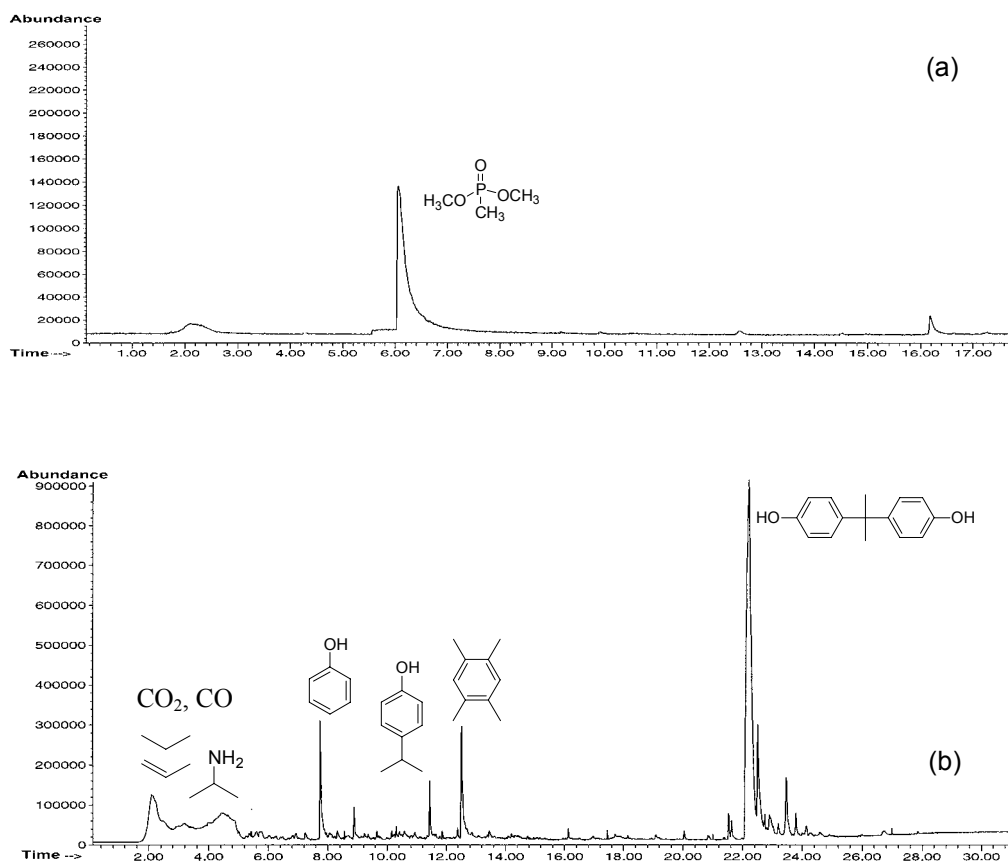


FIGURE 5-22. PYROLYSIS GC/MS TRACES OF EPOXY/DMMP COMPOSITES (HEAT RATE, 4.3°C/s) (a) 150°~300°C AND (b) 300°~930°C

According to table 5-16, the heat release capacity and total heat released are lower for all the composites by adding phosphate additives. The dramatic decrease of heat release capacity is due to the significant reduction of maximum mass loss rate. It was also found that the heat release capacity of epoxy/TMP composites changes linearly with the maximum mass loss rate, which indicates that the flammability reduction is mainly due to the reduction of the decomposition rate in the condensed phase.

The cone calorimeter results of epoxy/TMP are shown in table 5-17 and figure 5-23. It can be seen that adding only 4 wt% of TMP does not have a big effect on the flammability. Only when the amount of TMP is increased to about 8 wt%, are the peak heat release rate and total heat released dramatically reduced. The reduction of the effective heat of combustion and increase of the CO production implies that besides the condensed-phase inhibition, TMP also acts in the gas phase by reducing the combustion efficiency. However, because the chars formed by all the composites are extremely foamy and sometimes swell into the cone heater, the flammability measured might not be accurate.

TABLE 5-16. THERMAL DECOMPOSITION AND FLAMMABILITY OF EPOXY/PHOSPHATE COMPOSITES

Additive	wt%	T _{99%} (°C)	T _{95%} (°C)	T _{max} (°C)	PMLR (x10 ³ /s)	Char (%)	H. R. Capacity (J/g-K)	Total heat (kJ/g)
TMP ^a	0	347	376	396	16	6	1100	27
	4	268	318	348	10	9	710	26
	7.6	242	303	346	9.6	11	680	25
	11	191	282	321	8.8	13	580	24
	14.1	207	289	331	8.1	15	550	23
DMMP ^b	0	334	359	388	8.3	6	1100	27
	3.5	205	322	372	4.6	7	470	25
	6.8	167	298	357	4.0	7	370	24
	9.9	148	266	349	3.7	8	370	24
	12.7	147	260	346	3.5	8	380	24
TPP ^c	0	347	376	396	16	6	1100	27
	3.5	287	342	374	11.4	7	880	26
	6.8	258	329	365	11.0	7	700	25
	9.9	236	318	356	10.3	8	620	26
	12.7	216	295	358	9.7	8	740	25

Heating rate: ^a40°C/min

^b20°C/min

^c40°C/min

TABLE 5-17. CONE CALORIMETER RESULTS OF EXPOXY/TMP COMPOSITES

wt% TMP	t _{ig} (s)	PHRR (kW/m ²)	HRR _{av} (kW/m ²)	THR (MJ/m ²)	EHC (kJ/g)	SEA (m ² /kg)	CO/ CO ₂
0	29	1324	235	42.6	23.7	655	0.030
4	22	1294	217	39.6	21.5	577	0.054
7.6*	21	494	120	22.9	14.7	520	0.119
14.1	22	519	144	28.1	16.1	473	0.099

* Results might not be accurate due to the irregular sample shape.

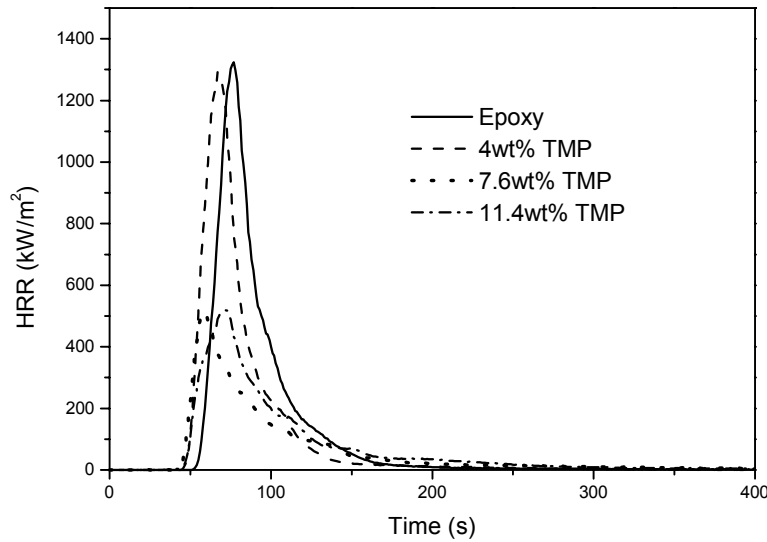


FIGURE 5-23. CONE HRR CURVES OF EXPOXY/TMP COMPOSITES

5.3.6 Ignitability.

Time delay before ignition (t_{ig}) is an important parameter characterizing material flammability. It depends on many factors such as thickness, density, thermal conductivity, and heat flux [19]. In cone calorimeter tests, the change of t_{ig} to a range of external heat flux can produce valuable information for the ignitability of a material such as the critical heat flux, the minimum incident heat flux required for sustained piloted ignition of a material. The critical heat flux can be obtained experimentally by exposing a sample at decreasing incident heat fluxes until a flux is found at which ignition time is infinitely long [19]. Another method is to plot $1/t_{ig}$ (thin materials) or $1/\sqrt{t_{ig}}$ (thick materials) against external heat flux \dot{q}_e'' based on the following equations [19 and 127].

$$t_{ig} = \rho c l \frac{(T_{ig} - T_{\infty})}{(\dot{q}_e'' - \dot{q}_{cr}'')} \quad (\text{thin materials}) \quad (5-4)$$

$$t_{ig} = \frac{\pi k \rho c (T_{ig} - T_{\infty})^2}{4 (\dot{q}_e'' - \dot{q}_{cr}'')^2} \quad (\text{thick materials}) \quad (5-5)$$

where k is the thermal conductivity, ρ is the density, c is the specific heat, l is the thickness, T_{ig} is the ignition temperature, T_{∞} is the ambient temperature, \dot{q}_e'' is the external heat flux, \dot{q}_{cr}'' is the critical heat flux, and $k\rho c$ is the thermal inertia, which determines how fast the material responds to a heat flux.

For the thin samples, if the ignition temperature T_{ig} is assumed to be the temperature at maximum mass loss rate, the thermal inertia and critical heat flux can be calculated from the

slope and interception of plot $1/t_{ig}$ versus \dot{q}_e'' . The results are listed in table 5-18 and shown in figure 5-24.

TABLE 5-18. CRITICAL HEAT FLUX AND THERMAL PROPERTY CALCULATED FROM THE CONE CALORIMETER

Polymers	Critical Heat Flux (kW/m ²)	ρc (kJ/m ³ -K)
A-6133 V-0	15	1552
Xydar [®] M-345	22	2676
PES	25	1720
PSU	26	1792
A-6135 HS	29	1005
Xydar [®] G-930	32	1226
PPhS	35	1271

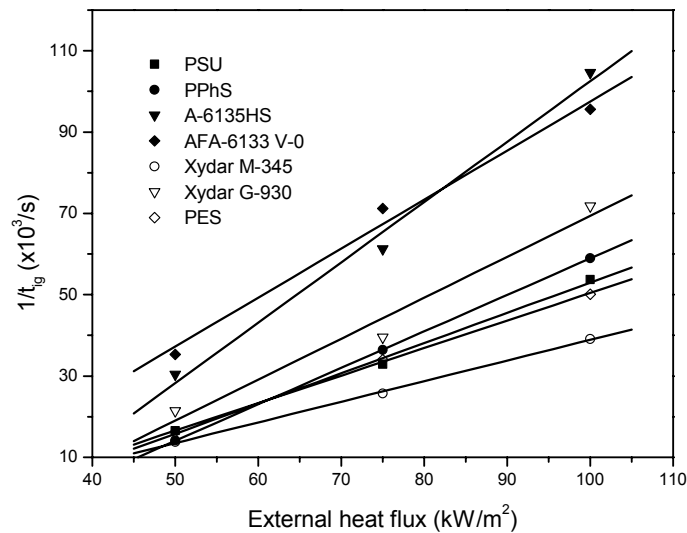


FIGURE 5-24. IGNITION TIME OF POLYMERS UNDER DIFFERENT EXTERNAL HEAT FLUXES

5.3.7 Heat Release Rate.

Cone calorimeter data obtained over a range of external heat fluxes can also be used to obtain some other flammability parameters. Lyon found that the heat produced from combustion of a material in the presence of external flux \dot{q}_{ext} is a function of its chemical structure and combustion efficiency [128]:

$$\dot{q}_c = \chi \frac{h_c^o}{L_g} (\dot{q}_{ext} + \dot{q}_{flame} - \dot{q}_{loss}) = \chi \frac{h_c^o}{L_g} \dot{q}_{net} \quad (5-6)$$

Where \dot{q}_{net} is the net heat flux, \dot{q}_{flame} is heat flux from surface flame, \dot{q}_{loss} is the heat loss due to radiation and convection, and χ is the combustion efficiency. The effect of chemical structure is reflected in terms of the effective heat of combustion h_c^o and its heat of gasification per unit mass of volatiles L_g [128]. The h_c^o represents the total amount of energy released by combustion of unit mass of volatile. The heat of gasification, L_g , is the energy required to volatilize the unit mass of the fuel. The L_g represents the average effects during vaporization of the fuel and does not include transient burning effects [128]. If the heat release rate data are plotted as a function of external heat flux, the heat release parameter, $\chi \frac{h_c^o}{L_g}$, can be obtained from the slope of the curve [129] (figure 5-25).

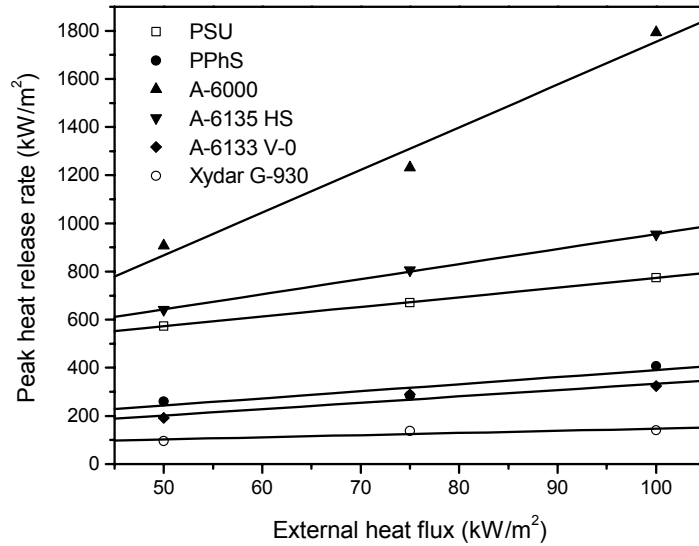


FIGURE 5-25. PEAK HEAT RELEASE RATE OF POLYMERS UNDER DIFFERENT EXTERNAL HEAT FLUXES

Lyon also found that the intercept of the curve, HRR_0 , is another flammability criterion that can be used to predict the tendency to self-extinguish at zero external heat flux [129].

$$\dot{q}_c = \chi \frac{h_c^o}{L_g} (\dot{q}_{ext} + \dot{q}_{flame} - \dot{q}_{loss}) = \chi \frac{h_c^o}{L_g} \dot{q}_{ext} + \underbrace{\chi \frac{h_c^o}{L_g} (\dot{q}_{flame} - \dot{q}_{loss})}_{HRR_0}$$

Lyon found that in the absence of an external heat flux, there is a critical heat release rate at flame extinction, $HRR^* \cong 100 \text{ kW/m}^2$. When $HRR_0 > HRR^*$, a flame will propagate; when $HRR_0 < HRR^*$, a flame will extinguish. By using this approach, UL 94 and LOI test results can be well predicted. When $HRR_0 > 100 \text{ kW/m}^2$, the material will be rated as HB in a UL 94 test;

when $HRR_0 < 100 \text{ kW/m}^2$, the material will be rated as V-0/1/2; when HRR_0 is negative, there is no ignition at all [129].

The heat release parameter ($\chi \frac{h_c^o}{L_g}$) and heat release rate at zero external heat flux (HRR_0) of several materials are listed in table 5-19. It can be seen that the smaller the heat release parameter, the more ignition resistant the material is, as evidenced by UL 94 V-0 rating. Except for A-6000, there is a correlation between HRR_0 and UL 94 rating.

TABLE 5-19. MATERIAL FLAMMABILITY OBTAINED BY CONE CALORIMETER DATA

Materials	$\chi \frac{h_c^o}{L_g}$	HRR_0 (kW/m^2)	UL 94 Rating
Xydar [®] G-930	0.88	58	V-0
A-6133 V-0	2.64	69	V-0
PPhS	2.9	96	V-0
PSU	4.0	371	HB
A-6135 HS	6.3	329	HB
A-6000	17.7	-18	HB

5.3.8 Correlation Between Different Flammability Tests.

The applicability of the PCFC method to different materials is a very important issue. Because complete oxidation is assumed in the high-temperature furnace of PCFC, it has been suspected whether the gas-phase flame-retardant effects of the halogenated additives can be achieved in the PCFC test. This question can be clarified by comparing the PCFC test with some standard real-flame combustion tests, such as the OSU and cone calorimeter tests.

The flammability of more than 20 kinds of materials including pure polymers and their fiber-reinforced or flame-retarded composites is measured by the OSU calorimeter at an external heat flux of 35 kW/m^2 , the cone calorimeter at an external heat flux of 50 kW/m^2 , and the PCFC calorimeter at a heating rate of 4.3°C/s to 930°C . The results from different methods are shown in table 5-20 and figures 5-26 and 5-27, in which the OSU results are based on the oxygen depletion measurements. In figures 5-26 and 5-27, the straight lines are fitted only by the data from pure polymers.

TABLE 5-20. FLAMMABILITY MEASURED BY PCFC, OSU, AND CONE CALORIMETERS

Number	Polymers	Peak Heat Release Rate			Total Heat Released (kJ/g)		
		PCFC (J/g-K)	Cone (kW/m ²)	OSU (kW/m ²)	PCFC	Cone	OSU
1	Radel [®] R-5000	171	260	173	13	11	7
2	Radel [®] A-300	165	357	203	12	11	6
3	PEEK 450G	282	510		12	15	
4	Udel [®] P-1700	336	573	288	17	18	12
5	PPA A-1000	610	685	417	31	21	12
6	PPA A-6000	540	844	411	33	24	14
7	Epoxy	1100	1324		27	23	
8	Xydar [®] G-930	137	84	103	8	7	4
9	Xydar [®] M-345	120	105	179	6	5	5
10	PEEK 450CA30	110	104		8	6	
11	PEEK 450GL30	188	133		8	6	
12	AFA-6145 V-0	210	181	287	10	5	8
13	AFA-6133 V-0	270	191	306	13	6	10
14	AF-1133 V-0	400	198	262	13	7	
15	AF-1145 V-0	440	222		11	5	
16	A-6145 HS	300	505	433	18	14	12
17	Epoxy/7.5% TMP	710	494		25	13	
18	A-1145 HS	350	612		17	12	
19	A-6135 HS	370	640	420	21	18	14
20	A-1133 HS	410	657		21	15	9
21	Epoxy/4% TMP	680	1294		26	21	
22	Epoxy/14.1% TMP	550	519		23	14	

*The OSU results are based on oxygen consumption.

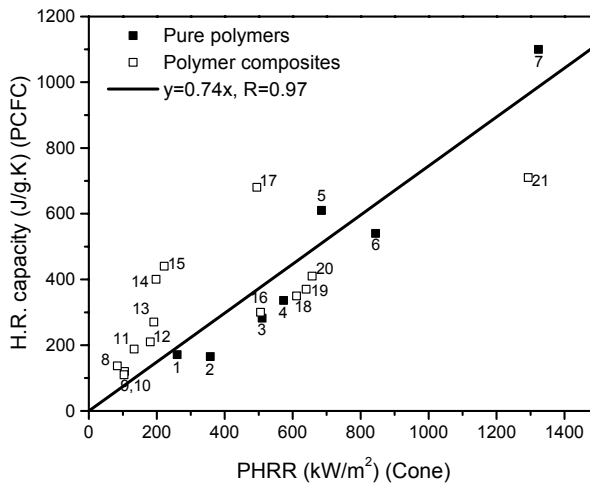
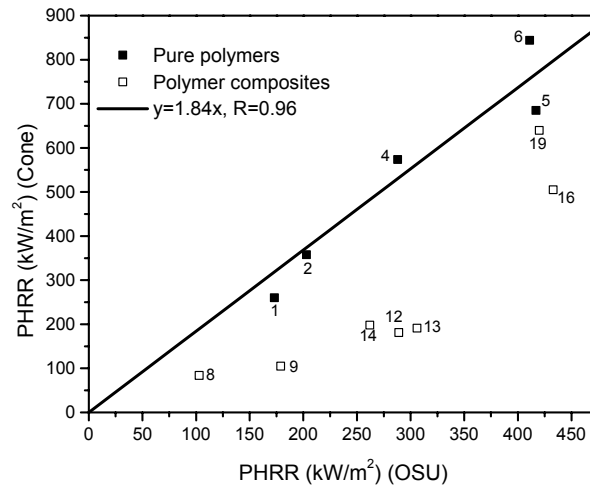
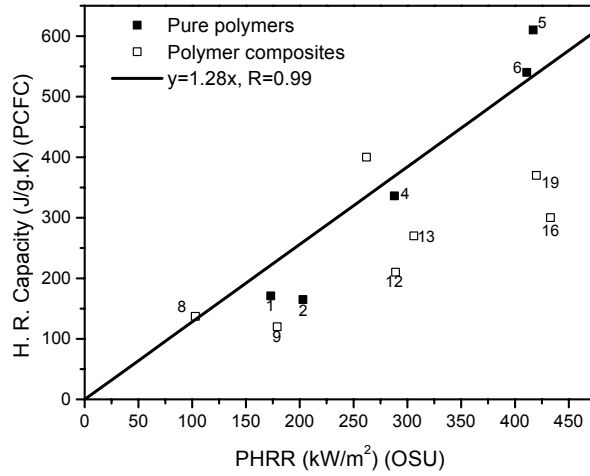


FIGURE 5-26. CORRELATIONS OF PHRR BETWEEN DIFFERENT FLAMMABILITY TESTS

(The OSU results are based on oxygen consumption and the straight lines are fitted only by the data from pure polymers.)

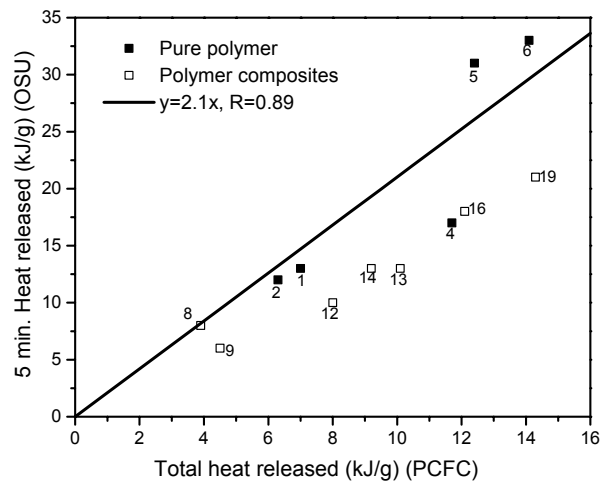
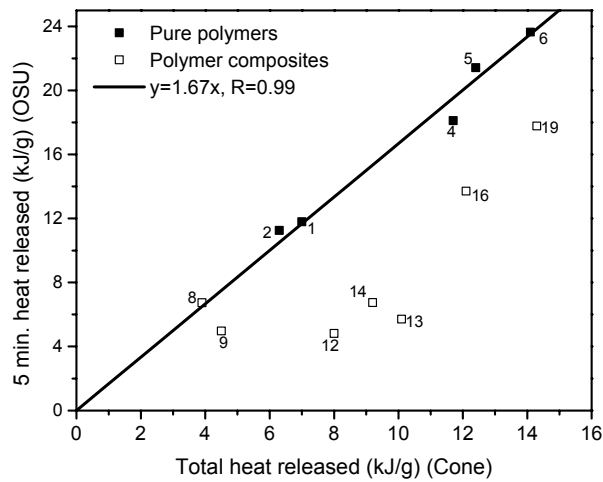
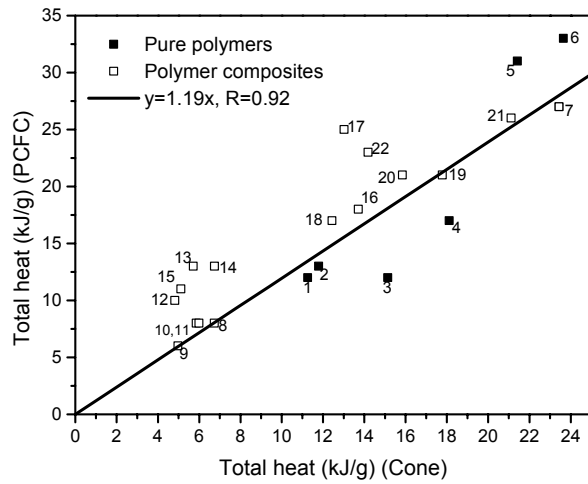


FIGURE 5-27. CORRELATIONS OF TOTAL HEAT RELEASED BETWEEN DIFFERENT FLAMMABILITY TESTS

(The OSU results are based on oxygen consumption and the straight lines are fitted only by the data from pure polymers.)

Previous FAA research shows that there is good correlation between the cone calorimeter and the PCFC methods for pure polymers. According to the results, relatively good correlations between different methods are also observed for pure polymers. However, for the composites with inert fillers or flame-retardant additives, the OSU and cone calorimeter tests are the better evaluation methods. This is because the OSU and cone calorimeter tests are real flame-combustion tests. Therefore, the halogenated additives can achieve the inefficient gas-phase combustion and reduce the heat released. The heat feeding back to the polymer surface will then be reduced, and the decomposition of the polymers will be slowed down thereafter. However, as mentioned before, the PCFC method is not a direct flame-combustion test, the pyrolysis and combustion processes are totally separated, and the combustion in the furnace is complete oxidation. As a result, the effects of the halogenated additives in the gas phase cannot be achieved and the influence of the heat and mass transfer processes in a real fire are not observed. However, the PCFC method stresses flammability more as a material property. The results are greatly dependent on the chemical structure and composition of materials. Therefore, it is still a very convenient screening tool for newly synthesized polymers without any additives.

The materials studied were (1) Poly(phenyl sulfone) (Radel[®] R-5000), (2) Poly(ether sulfone) (Radel[®] A-300), (3) PEEK 450G (Vitrex[®] PEEK[™] 450G), (4) Polysulfone (Udel[®] P-1700), (5) PPA A-1000 (Amodel[®] PPA), (6) PPA A-6000 (Amodel[®] PPA), (7) Epoxy, (8) Xydar[®] G-930, (9) Xydar[®] M-345, (10) PEEK CA-30 (Vitrex[®] PEEK[™] 450CA-30), (11) PEEK GL-30 (Vitrex[®] PEEK[™] 450GL-30), (12) AFA-6145 V-0 (Amodel[®] PPA), (13) AFA-6133 V-0 (Amodel[®] PPA), (14) AF-1133 V-0 (Amodel[®] PPA), (15) AF-1145 V-0 (Amodel[®] PPA), (16) A-6145 HS (Amodel[®] PPA), (17) Epoxy/7.5 wt% TMP (trimethoxy-phosphate), (18) A-1145 HS (Amodel[®] PPA), (19) A-6135 HS (Amodel[®] PPA), (20) A-1133 HS (Amodel[®] PPA), (21) Epoxy/4 wt% TMP, and (22) Epoxy/14.1 wt% TMP. Please refer to table 5-1 and figure 5-20 for detailed information about the structure and composition of each material.

5.4 DISCUSSION.

Flammability is determined by the physical and chemical characteristics of the materials. Inert fillers can reduce the flammability mainly by the mass-dilution effect and promoting the char formation. However, the addition of inert fillers can also change the physical properties of the materials such as thermal conductivity, density, and heat capacity that will affect the ignition and burning characteristics of the exposed surface. Therefore, the flame-retardant effect of the inert fillers in the real flaming-combustion OSU and cone calorimeter tests is usually not as dramatic as in the nonflaming PCFC test. If halogenated flame retardants or antimony compounds are used, the flammability can be greatly reduced due to the inefficient combustion in the gas phase. The only disadvantage is that the thermal stability of the materials will be decreased and a great deal of corrosive smoke will be generated. As to the instrumentation, because different methods have different experimental setups and are operated in different ways, the results from one method cannot be directly related to the other. It was found that only pure polymers have relatively good correlations between different methods. Therefore, different types of materials require different test methods to ensure valid and realistic results. The PCFC method is more sensitive to the chemical structure and composition of the materials; therefore, it is a good

screening tool for the pure polymers without any additives or inert fillers. However, the OSU and cone calorimeter tests are the better flammability tests for composite materials because these two methods also include some physical processes, which are much more representative of the real fire conditions.

6. STRUCTURE-COMPOSITION-FLAMMABILITY RELATIONSHIPS OF POLYMERS.

6.1 INTRODUCTION.

A great deal of research has been done on measuring the flammability of polymers. Systematically relating polymer structure and composition to their flammability is, however, more important for materials design and evaluation.

It was found that the thermal stability depends on the structure of repeating units and, in particular, on the weakest bonds present in this structure [7]. C-C bonds are particularly resistant to homolytic scission relative to other bonds between identical atoms (except H-H bonds) [130]. C-H, C-O, C-F, and C-B bonds are stronger than C-C bonds. Aromaticity strengthens C-C bonds and the presence of electronegative atoms (other than fluorine) weakens them. Thus, when aromatic groups or fluorine atoms are introduced into polymers, their thermal stability will increase [7].

Quantitative structure-property relations are of interest. Some research had been done to estimate the char yield, heat of combustion, or thermal decomposition temperature from the chemical structure by using molar group additivity principles [67 and 73].

In this section, the different factors that affect polymer flammability were studied in detail, such as chemical structures, molecular weight, free radicals in the polymer system, and composition of copolymers and blends. The goal is to establish the structure-composition-flammability relationships of polymers and to help guide the development of new fire-resistant polymers.

6.2 EXPERIMENTAL.

6.2.1 Materials.

The materials evaluated were obtained from different sources. The specific detailed information is provided in each section. All samples were dried at proper temperatures under vacuum for about 24 hours before measurements.

6.2.2 Characterization.

The experimental conditions for TGA, STA, pyrolysis GC/MS, PCFC, OSU calorimeter, and cone calorimeter tests were the same as described in previous sections.

6.3 CHEMICAL STRUCTURE.

6.3.1 Main Chain—Polysulfones.

Aromatic polysulfones possess considerable thermal stability and good chemical resistance [6]. They are among the most fire-resistant, non-halogen-containing thermoplastic polymers. Their other properties such as high-heat deflection temperature, excellent toughness, and dimension stability allow them to be used in the electrical, automotive, and aircraft industries where a special combination of mechanical, thermal, or fire resistance are required [6].

In this section, three kinds of polysulfones supplied by BP Amoco Polymers Inc. (now Solvay Advanced Polymers, L.L.C.) were used to study how the aromaticity of polymer main chain affects its flammability. Their structures are listed in figure 6-1.

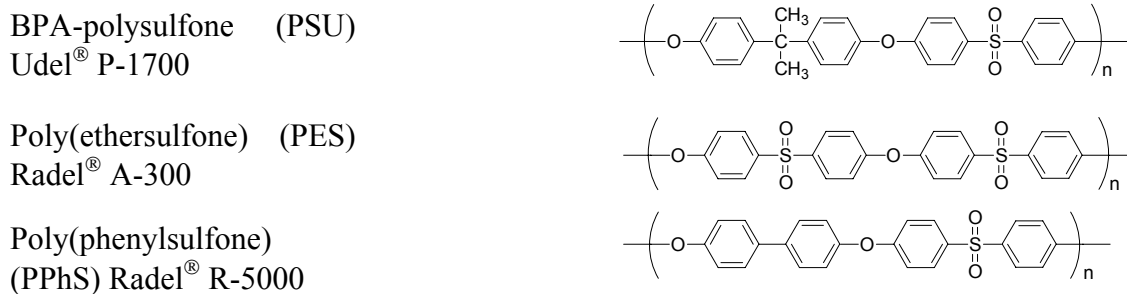


FIGURE 6-1. CHEMICAL STRUCTURES OF POLYSULFONES

6.3.1.1 Thermal Decomposition Processes.

The thermal decomposition processes of three kinds of polysulfones, BPA-polysulfone (PSU), polyethersulfone (PES), and polyphenylsulfone (PPhS), are shown in figure 6-2. It can be seen that all these polysulfones decompose in a single step under N₂. They all have relatively high thermal stability and char yields due to their aromatic structures in the main chain. They start to decompose around 450°C, then after a sharp weight loss, leave more than 30% residue at 1000°C. By replacing the flexible BPA units in PSU with more rigid phenyl or biphenyl units in PES or PPhS, the thermal stability and char yields increase significantly. The reduction in the mass loss rates indicates that the decomposition rates of PES and PPhS are also slowed by the presence of more aromatic rings.

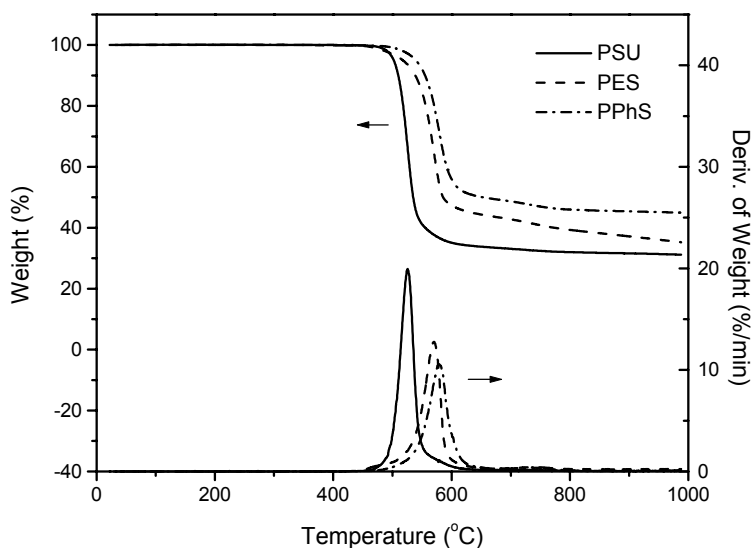


FIGURE 6-2. THERMOGRAVIMETRIC ANALYSIS AND DTG CURVES OF POLYSULFONES IN N₂

However, all these polysulfones decompose in two distinct steps in air (figure 6-3). The first step is the same as in N₂, starting and ending at almost the same temperatures and losing the same amount of weight. The second step leads to the complete burning of the polymers (no residue left). It is believed that the first step is mainly due to the chain scission reactions and the release of volatiles, while the second stage is mainly due to the oxidation of the carbonaceous char formed at the end of the first stage.

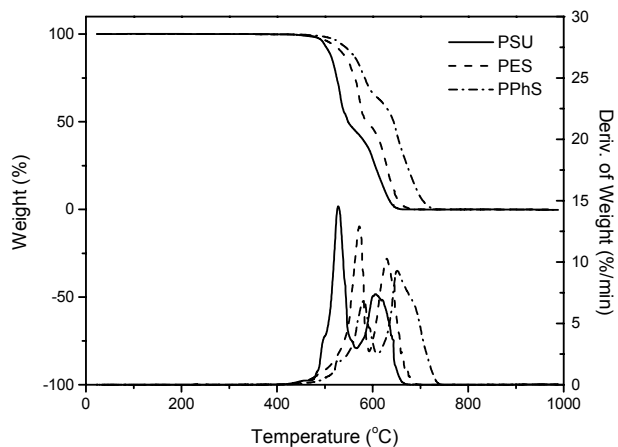


FIGURE 6-3. THE TGA AND DTG CURVES OF POLYSULFONES IN AIR

High-temperature DSC data of polysulfones are shown in figure 6-4 and in table 6-1. It can be seen that during decomposition in N₂, all the polysulfones exhibit two endothermic peaks related to different chemical and physical processes. The first peak corresponds to the major part of the weight loss, which might be due to the combination of bond dissociation, formation, and vaporization of the volatiles. The second peak occurs at high temperatures and corresponds to a narrow temperature range, which might be due to the char-forming process. Compared with PSU, PES and PPhS absorb more heat during decomposition, which might increase the energy needed to sustain the combustion and reduce flammability.

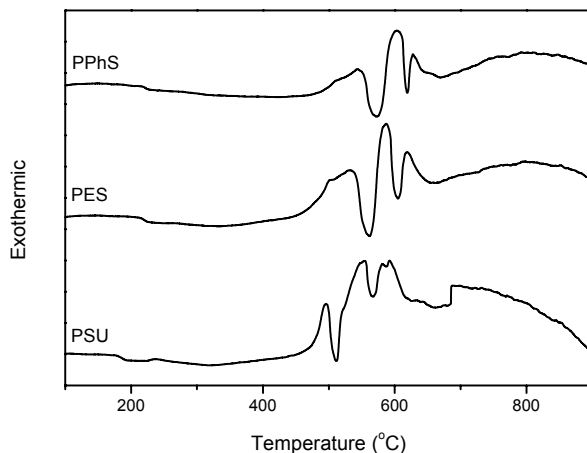


FIGURE 6-4. HIGH-TEMPERATURE DSC CURVES OF POLYSULFONES

TABLE 6-1. THERMAL DECOMPOSITION PROPERTIES OF POLYSULFONES

Polymer	In N ₂					In air			
	T _{99%/T_{95%}} ^a (°C)	T _{max} ^b (°C)	PMLR ^c (x10 ³ /s)	Char ^d (%)	ΔH ^e (J/g)	T _{99%/T_{95%}} ^f (°C)	T ₂ ^g (°C)	T _{max} (°C)	PMLR (x10 ³ /s)
PSU	482	526	3.33	31	61	462	588	528	2.42
	502				28	497			
PES	471	570	2.13	37	120	470	610	572	2.15
	517				38	511			
PPhS	504	579	1.77	45	123	488	638	651	1.55
	540				25	531			

- ^a Temperatures at 1% and 5% weight loss
- ^b Temperatures at maximum mass loss rate
- ^c maximum (peak) mass loss rate
- ^d Residual left at 930°
- ^e Heat of decomposition
- ^f Onset of decomposition temperature of the second stage

TGA measurements of polysulfones were also carried out at different heating rates to determine the global thermal decomposition activation energies. It can be seen that with the increase of heating rates, the onset decomposition temperatures and mass loss rates of the polysulfones increase, but the char yields do not change significantly (figure 6-5). The increase of the onset decomposition temperature does not mean that the thermal stability of the polymers has increased. It is mainly due to a kinetics effect, i.e., the thermal response of the polymers is delayed at fast heating rates.

The relatively simple Kissinger method (equation 6-1) was used to determine the activation energies [131]

$$\ln(\phi / T_m^2) = \ln(nRAW_m^{n-1} / E_a) - E_a / RT_m \quad (6-1)$$

where ϕ is the heating rate in the TGA experiment, T_m is the temperature at the maximum rate of weight loss, R is the gas constant, E_a is the activation energy, A is the pre-exponential factor, W_m is the weight of the sample at the maximum rate of weight loss, and n is the apparent order of the reaction with respect to the sample weight. The value of E_a can be determined from a plot of $\ln(\phi / T_m^2)$ vs $1/T_m$ at various heating rates. The particular advantage of this method is that it requires only the temperature at the maximum rate of weight loss to determine the value of E_a and one need not assume the order of the reaction [132]. The disadvantage of this method is that it is sometimes difficult to determine the maximum rate of weight loss accurately.

A plot of $\ln(\phi / T_m^2)$ vs $1/T_m$ of polysulfones is shown in figure 6-6. It can be seen that three reasonable straight lines were obtained. The activation energies were calculated from the slopes of these straight lines (table 6-2). It was found that PES and PPhS have higher decomposition activation energies than PSU, which agrees with their higher thermal stability.

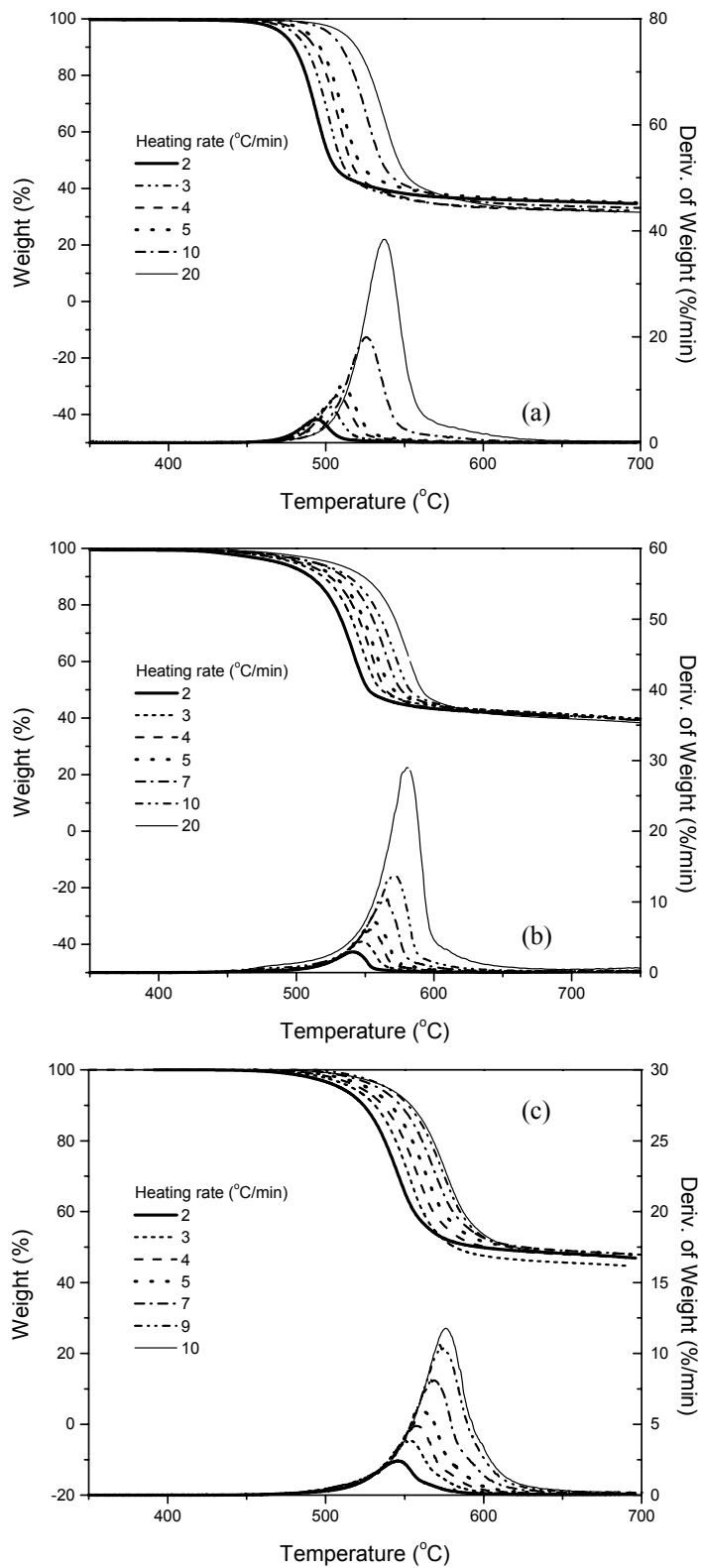


FIGURE 6-5. THE TGA AND DTG CURVES OF POLYSULFONES AT DIFFERENT HEATING RATES (a) PSU, (b) PES, AND (c) PPhS

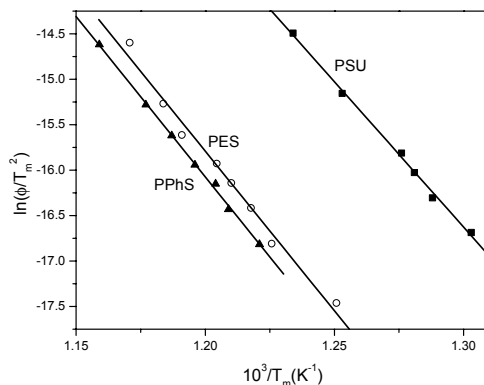


FIGURE 6-6. KISSINGER PLOT OF POLYSULFONES DECOMPOSED IN N₂

TABLE 6-2. BOND DISSOCIATION ENERGIES AND ACTIVATION ENERGIES OF POLYSULFONES

Polymers	Bond Dissociation Energies (kJ/mol) ^a	E _a (kJ/mol) ^b
PSU		268
PES		292
PPhS		293

^a Calculated by B3LYP/6-31G(d) from Gaussian 98 package of programs. The uncertainty is 33 kJ/mol

^b Calculated by Kissinger method based on TGA data

The bond dissociation energies of these polysulfones can be calculated by using B3LYP [74 and 75] density-functional method with a standard polarized split-valence 6-31G(d) [76] basis set from the Gaussian 98 package of programs [77] (table 6-2). It can be seen that the weakest bond in PSU is the C-CH₃ bond in isopropyl groups, while the C-S bond in the sulfone linkage is the weakest in PES and PPhS. In addition, activation energies measured by TGA data seem very close to the calculated weakest bond dissociation energies when calculation errors are considered. This result indicates that the thermal decomposition of these polysulfones is consistent with initiation by the rupture of the weakest bond.

6.3.1.2 Decomposition Volatiles.

It was found that the major decomposition volatiles from these polysulfones are SO₂, CO₂, CO, phenol, and a series of aromatic ethers derived from the polymer main chain (figure 6-7). The volatiles from PPhS contain more biphenyl structures than PES, and the decomposition products

from PSU contain more flammable aliphatic groups due to the isopropyl groups in the polymer, which is also one of the reasons for its high flammability.

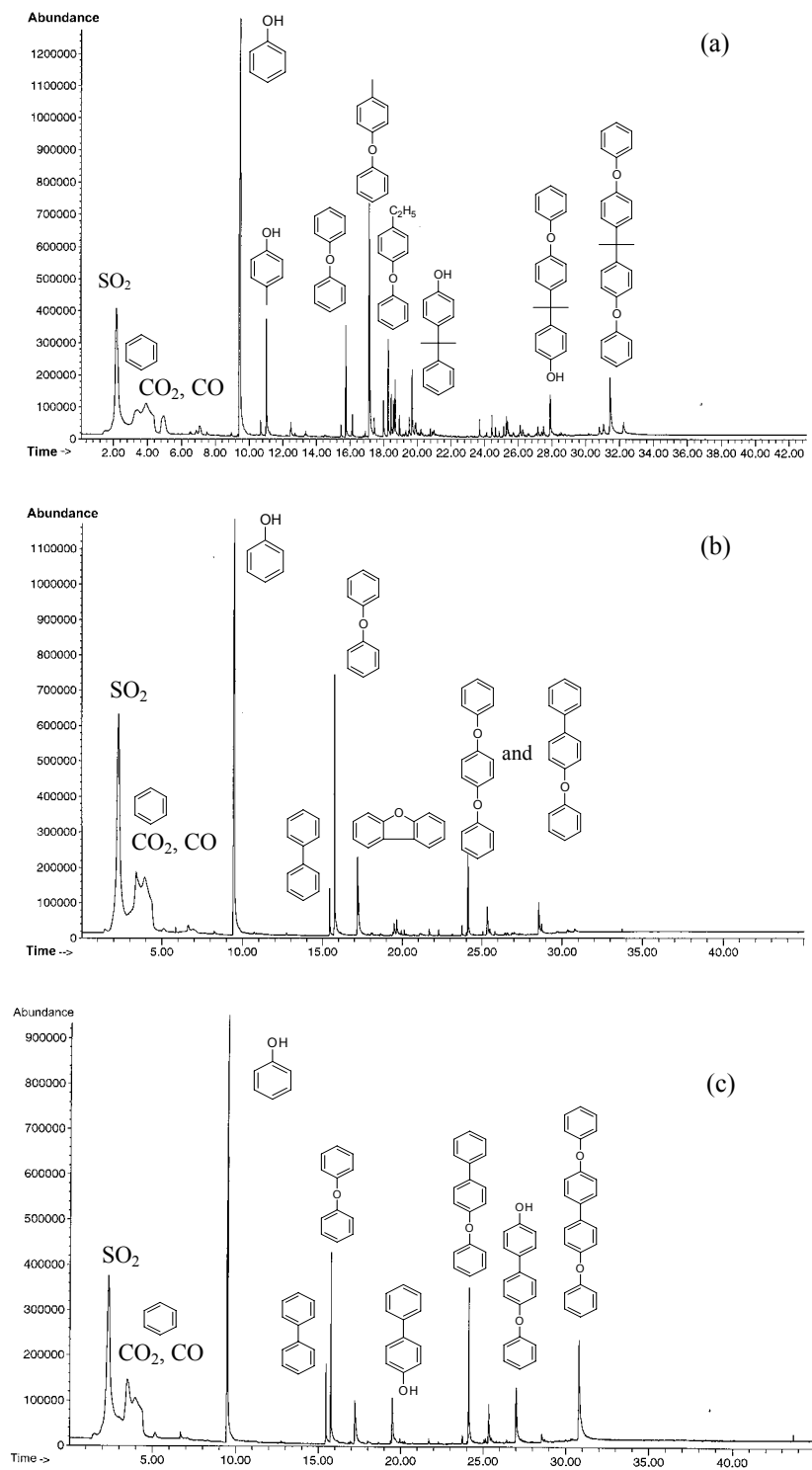


FIGURE 6-7. PYROLYSIS GC/MS TRACES OF POLYSULFONES (a) PSU, (b) PES, AND (c) PPhS

6.3.1.3 Flammability Measured by PCFC.

The PCFC results are shown in table 6-3, from which one can see that the rigid PES and PPhS are more fire-resistant than PSU. The order of the flammability is $PSU > PES \geq PPhS$. The heat release capacities and the total heats of combustion of PES and PPhS are only half of those of PSU. Their low mass loss rate and high char yields are part of the reasons for their low flammability. According to pyrolysis GC/MS results, the major decomposition products of all three polysulfones at the temperatures of maximum mass loss rates are SO_2 and phenol. However, PSU also releases a high molecular weight flammable compound, $C_6H_5C(CH_3)_2C_6H_4OH$. Considering this factor and its high mass loss rate, the high heat release capacity of PSU is easy to understand.

TABLE 6-3. FLAMMABILITY OF POLYSULFONES MEASURED BY PCFC

Polymers	H.R. Capacity (J/g-K)	Total Heat (kJ/g)	Char (%)	Cov (%) ^a
PSU	336	17	31	2.5
PES	171	13	37	7.7
PPhS	165	12	45	4.8

^a Coefficient variation of heat release capacity

6.3.1.4 Flammability Measured by the OSU Calorimeter.

The flammability of these polysulfones, measured by the OSU calorimeter, also decreases in the order of $PSU > PES \geq PPhS$ (table 6-4). Because some of the melt from PSU drips down to the bottom of the furnace during burning, its measured flammability was underestimated.

TABLE 6-4. FLAMMABILITY OF POLYSULFONES MEASURED BY THE OSU CALORIMETER

Method	Parameters	PSU	PES	PPhS
Thermopile	PHRR (kW/m^2)	135	98	86
	2-min HR ($kW \cdot min/m^2$)	73	42	18
	5-min HR ($kW \cdot min/m^2$)	317	199	211
O ₂ consumption	PHRR (kW/m^2)	288	203	173
	2-min HR ($kW \cdot min/m^2$)	169	85	43
	5-min HR ($kW \cdot min/m^2$)	473	288	312
Char (%)		39	52	55

According to the requirements in FAA Amendment 25-61(Code of Federal Regulations Part 25.853 [a-1]), if a material has less than $65kW/m^2$ as the peak of heat release rate and less than $65 kW \cdot min/m^2$ as the 2-minute total heat release for the thermopile measurement, the material is qualified as an aircraft cabin material. According to table 6-4, PPhS is a promising material that

could easily pass the FAA requirements after some composition modification, perhaps with additives. The high thermal stability and low mass loss rate of PPhS play an important role in its low flammability.

The burning processes of three polysulfones are shown in the OSU HRR curves (figure 6-8). It can be seen that the initial burning time of the polymers is primarily determined by their thermal stability. PPhS has a more rigid structure, so it is more thermally stable and has a long time delay before burning. Furthermore, it burns more slowly and produces more char.

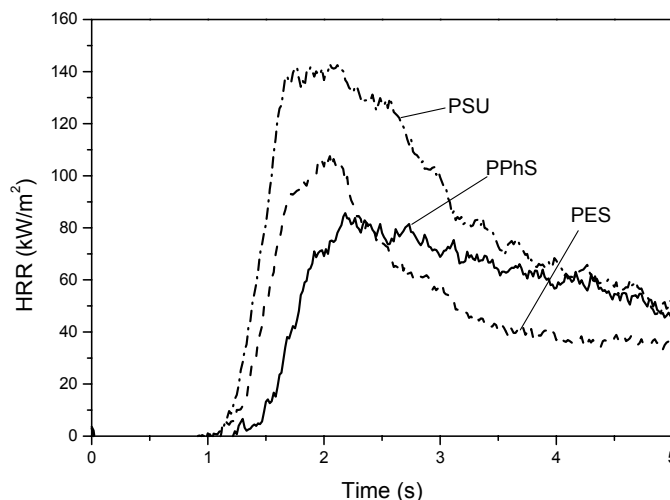


FIGURE 6-8. THE OSU HRR CURVES OF POLYSULFONES MEASURED BY THERMOPILE

It was found that char yield measured at the end of the 5-minute burning in the OSU tests is higher than from the TGA and PCFC results, which indicates that the burning process of these polysulfones was not yet complete at the end of 5 minutes. Therefore, the 5-min HR measured by the OSU test is less than the total heat released measured by PCFC. In addition, the char of PPhS can remain intact after the test, while PSU and PES only form fragmented chars due to dripping or sagging problems during combustion. All the chars formed are porous because a large amount of SO_2 is released during decomposition.

6.3.1.5 Flammability Measured by the Cone Calorimeter.

The cone calorimeter results include ignition time, heat release rate, and smoke evolution at different heat fluxes (table 6-5). As expected, increasing heat flux can lead to a reduction in t_{ig} , an increase in heat release rate with generally shorter times of burning, and an increase in mass loss rate. The decrease of CO/CO_2 ratios indicates that the combustion tends to be complete at high heat flux. However, the total heat released and the effective heat of combustion are not substantially different over the heat flux range tested.

The order of the flammability from the cone calorimeter test is the same as from the OSU results. Compared with PSU, PES and PPhS have a significantly lower PHRR, HRR_{av} , and THR. In addition, the low effective heats of combustion of PES and PPhS suggest the release of low fuel

value volatiles during decomposition. Their increased char yields might also give a good radiation shield protection to the underlying materials.

TABLE 6-5. FLAMMABILITY OF POLYSULFONES MEASURED BY THE CONE CALORIMETER

Polymer	Heat Flux ^a (kW/m ²)	t _{ig} ^b (s)	PHRR ^c (kW/m ²)	HRR _{av} ^d (kW/m ²)	THR ^e (MJ/m ²)	MLR ^f (g/m ² .s)
PSU	50	57	598	183	43.6	8.18
	75	30	671	198	42.1	10.10
	100	19	738	203	40.0	12.01
PES	50	61	381	119	31.7	6.78
	75	29	379	132	29.4	9.92
	100	20	561	153	34.8	10.61
PPhS	50	71	267	108	26.9	5.88
	75	28	284	127	28.6	8.17
	100	17	407	134	29.2	8.39

Polymer	Heat Flux (kW/m ²)	EHC (kJ/g) ^g	SEA (m ² /kg) ^h	CO/CO ₂ ⁱ
PSU	50	19.8	581.3	0.149
	75	19.8	685.9	0.051
	100	19.1	784.0	0.024
PES	50	15.4	419.9	0.144
	75	13.8	551.0	0.041
	100	14.6	523.5	0.018
PPhS	50	15.7	721.0	0.135
	75	16.4	890.1	0.048
	100	15.1	784.8	0.026

^a External heat flux

^b Time to ignition using a pilot spark

^c Peak heat release rate

^d Mean values from t_{ig} to 180s after

^e Total heat released

^f Average mass loss rate

^g Effective heat of combustion calculated from total heat released and overall mass loss

^h Smoke specific extinction area

ⁱ Ratio of production of CO to CO₂ during combustion

The cone heat release rate curves of these polysulfones are shown in figure 6-9. Generally, at the beginning of the test, the samples were increasing in temperature and starting to produce pyrolysis gases. At a certain point, ignition occurred and flaming combustion started. For

thermally thin thermoplastic samples, the heat release rate rose quickly to a peak heat release rate after ignition and then decreased as the fuel in the sample was consumed [133 and 19]. It can be seen that although PSU and PES showed one sharp burning peak, the heat release peak of PPhS is much broader. The fact that heat release rates of all three polysulfones did not return to zero at the end of the tests might be attributed to the smoldering burning under the char.

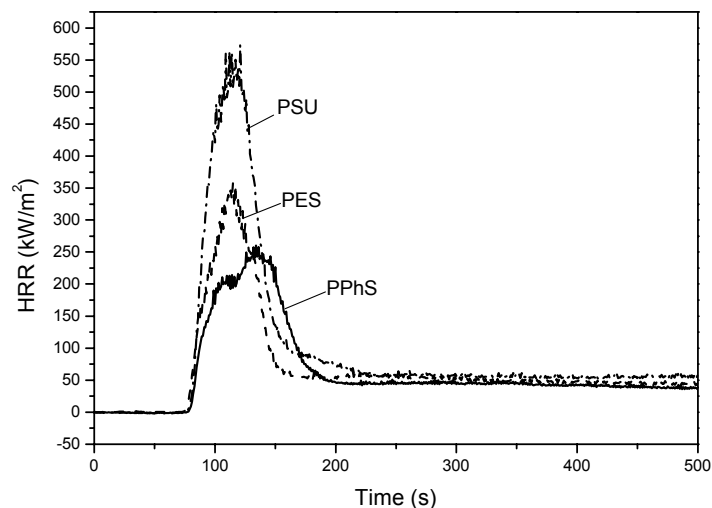


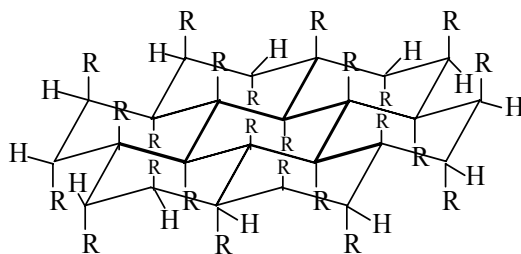
FIGURE 6-9. CONE HRR CURVES OF POLYSULFONES

Based on all the experimental results, it can be seen that the main-chain structure can greatly affect the thermal decomposition and flammability of the polymers. Increasing the chain aromaticity cannot only increase the thermal stability and char yield, but also, it can decrease the flammability by reducing the release rate and amount of flammable pyrolysis gases. By changing the structure of PSU to more rigid PES and PPhS, the polymers become much more fire resistant.

It was also found that the order of the flammability of these polysulfones measured by PCFC, OSU, and cone calorimeters is consistent with each other, even though experimental conditions and calculation procedures in these three tests are very different. This result indicates that for pure polymers, the chemical structure is the predominant factor that can determine the flammability of polymers.

6.3.2 Semiorganic Network Structure—Polycarbynes and Polysilynes.

Semiorganic polymers have inorganic chains (such as silicons) framed by organic substituents or organic backbones surrounded by inorganic substituents. In this part, polycarbynes and polysilynes with random carbon or silicon network structures were studied. These polymers were provided by Prof. Patricia Bianconi [134] at the University of Massachusetts, Amherst. It is believed that the polymers consist of sp^3 -hybridized C or Si atoms bonded via C-C or Si-Si single bonds to three other backbone atoms and one substituent [134]. This unique backbone structure will confer novel properties; for example, pyrolytic conversion to diamond or diamond-like carbon at atmospheric pressures. The schematic structures are shown in figure 6-10.



Polymers	Poly(carboxyl carbyne)	Poly(hydro-carbyne)	Poly(phenyl silyne)	Poly(methyl silyne)
Central atom	C	C	Si	Si
R	COOH	H	C ₆ H ₅	CH ₃

FIGURE 6-10. SCHEMATIC STRUCTURES OF POLYCARBYNES AND POLYSILYNES [134]

6.3.2.1 Thermal Decomposition Processes.

The thermal decomposition processes of two polycarbynes (poly(hydrocarbyne) and poly(carboxyl carbyne)) are shown in figure 6-11.

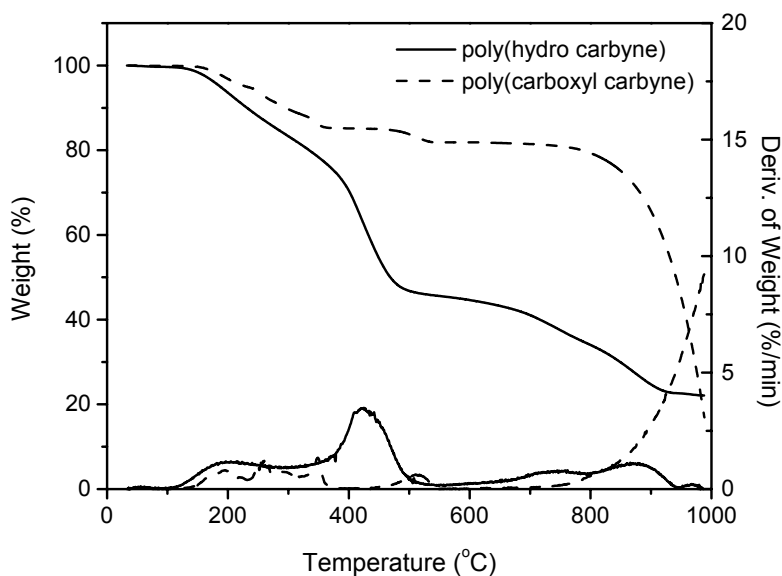


FIGURE 6-11. THE TGA AND DTG CURVES OF POLYCARBYNES

It can be seen that they all have relatively low thermal stability, starting to decompose around 150°C. After 500°C, the thermal decomposition of poly(carboxyl carbyne) reaches a plateau, but then it begins to lose weight dramatically after 800°C, which might be due to the extensive breakdown of the main network structure. However, poly(hydrocarbyne) loses weight continuously until 900°C, leaving about 20% char at 1000°C.

Figure 6-12 shows the thermal decomposition processes of two polysilynes (poly(methyl silyne) and poly(phenyl silyne)). Similar to the polycarbynes, these polysilynes also have very low thermal stability. Above 600°C, the thermal decomposition processes of these polysilynes reach a plateau, leaving more than 60% char. Compared with poly(methyl silyne), poly(phenyl silyne) decomposes at a much slower rate and produces more char.

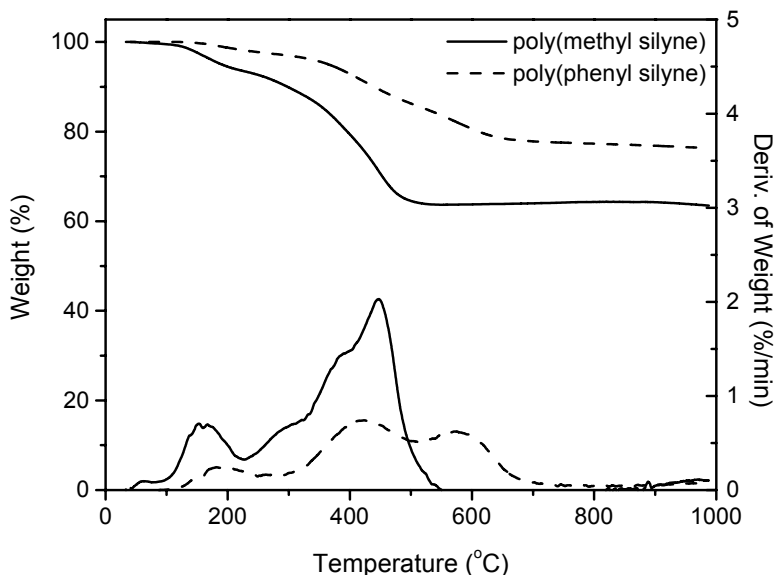


FIGURE 6-12. THE TGA AND DTG CURVES OF POLYSILYNES

6.3.2.2 Thermal Decomposition Products.

The thermal decomposition products of poly(carboxyl carbyne) are small gas molecules with very low flammability, i.e., CO₂, O₂, CO, and H₂O. Poly(methyl silyne) releases a series of siloxanes, which might be due to the oxidation. Poly(phenyl silyne) releases a series of low-flammable, phenyl-substituted silanes. However, poly(hydrocarbyne) releases a series of flammable alkenes and aromatic hydrocarbons and phenolics.

6.3.2.3 Flammability.

The flammability of polycarbynes and polysilynes is shown in table 6-6. It can be seen that all these polymers have very low flammability. Poly(carboxyl carbyne) has the lowest heat release rate and total heat released, which is due to the release of volatiles with low flammability. However, its flammability might dramatically increase above 800°C due to its suddenly increased mass loss rate. The flammability of two polysilynes mainly comes from the methyl or phenyl side groups. The relatively high mass loss rate and flammable hydrocarbon volatiles are the major reasons for the high flammability of poly(hydrocarbyne).

TABLE 6-6. FLAMMABILITY AND THERMAL DECOMPOSITION OF POLYCARBYNES AND POLYSILYNES

Polymers	H.R. Capacity (J/g-K)	Total Heat (kJ/g)	Char Yield (%)	Max. Mass Loss Rate (x10 ³ /s)	T _{max} (°C)	T _{onset*} (°C)
Poly(carboxyl carbyne) (C, -COOH)	11	3	55			144
Poly(phenyl silyne) (Si, -C ₆ H ₅)	32	13	77	0.12	425	140
Poly(methyl silyne) (Si, -CH ₃)	92	15	64	0.34	447	126
Poly(hydrocarbyne) (C, -H)	107	19	23	0.58	423	149

*Onset decomposition temperature

6.3.3 Substituents.

6.3.3.1 Size of Substituents—Polymethacrylates.

Three polymethacrylates (poly(ethyl methacrylate), poly(isobutyl methacrylate) and poly(benzyl methacrylate)) have been used to study the effects of the steric substituents on polymer flammability. The polymers were provided by Javid Rzayev [135] at the University of Massachusetts, Amherst. Their chemical structures are shown in figure 6-13.

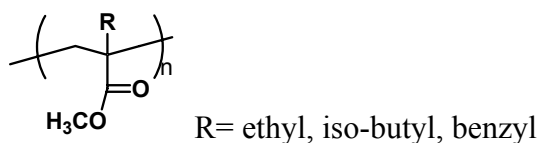


FIGURE 6-13. CHEMICAL STRUCTURES OF POLYMETHACRYLATES

The thermal decomposition processes of these polymethacrylates are shown in figure 6-14. It can be seen that both poly(isobutyl methacrylate) and poly(benzyl methacrylate) have lower thermal stability than poly(ethyl methacrylate). The multistep decomposition in these two polymers is also different from the single step in poly(ethyl methacrylate). The decomposition at low temperatures is mainly caused by the cleavage of the bulky side groups. Their broad decomposition leads to a dramatic decrease in the mass loss rates.

The flammability and thermal decomposition of these polymethacrylates are summarized in table 6-7.

The introduction of bulky and rigid benzyl side groups makes the poly(benzyl methacrylate) chain more rigid, which leads to its high glass transition temperature. Its low heat release rate is mainly due to its broad decomposition range and low maximum mass loss rate. Although the maximum mass loss rate of poly(isobutyl methacrylate) is also significantly lower than poly(ethyl methacrylate), their heat release capacities are almost the same. This is because poly(isobutyl methacrylate) has a relatively higher concentration of carbon and hydrogen (fuel sources), and the volatiles produced have higher heat of combustion. In addition, all three

polymethacrylates produce no char. Therefore, the total heat of combustion will completely depend on the heat of combustion of the volatiles they released. As a result, the total heat released of poly(isobutyl methacrylate) is the highest due to its high fuel value volatiles.

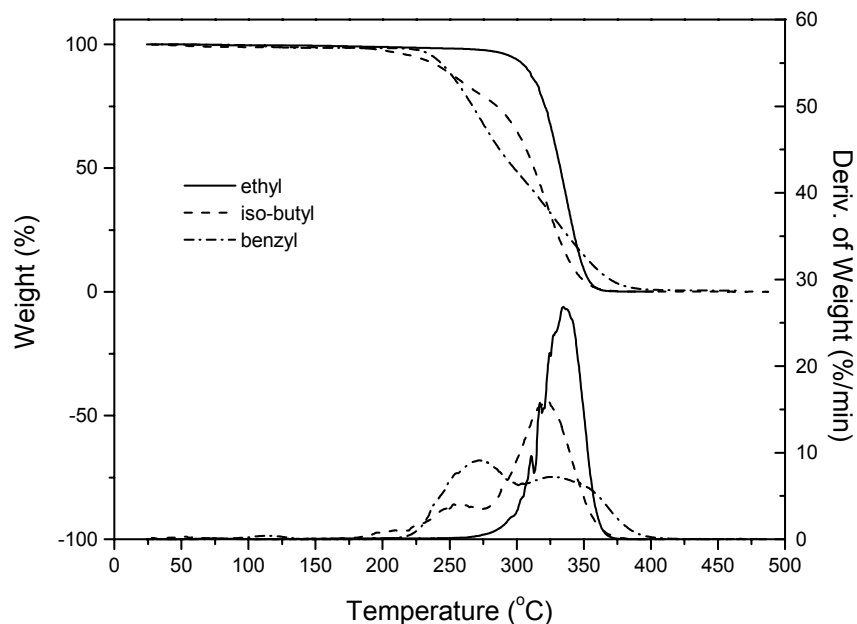


FIGURE 6-14. THE TGA AND DTG CURVES OF POLYMETHACRYLATES

TABLE 6-7. FLAMMABILITY AND THERMAL DECOMPOSITION OF POLYMETHACRYLATES

R	H.R. Capacity (J/g-K)	Total Heat (kJ/g)	Max. Mass Loss Rate ($\times 10^3/s$)	T_{max} (°C)	$T_{95\%}$ (°C)	T_g (°C)
Ethyl	840	26	4.5	335	295	71
Iso-butyl	890	29	2.7	323	224	63
Benzyl	240	28	1.5	273	238	122

From pyrolysis GC/MS results (figure 6-15), it can be seen that the thermal decomposition mechanisms can be changed by the size of the substituents. The major decomposition product of poly(ethyl methacrylate) is the monomer, which indicates an unzipping mechanism. However, although monomer is still one of the major decomposition products for poly(isobutyl methacrylate) and poly(benzyl methacrylate), some other volatiles such as isobutylene, styrene, and fragmented dimers have also been detected. Therefore, the thermal decomposition mechanisms of these two polymers are a combination of unzipping, cleavage of the side groups, and random chain scission.

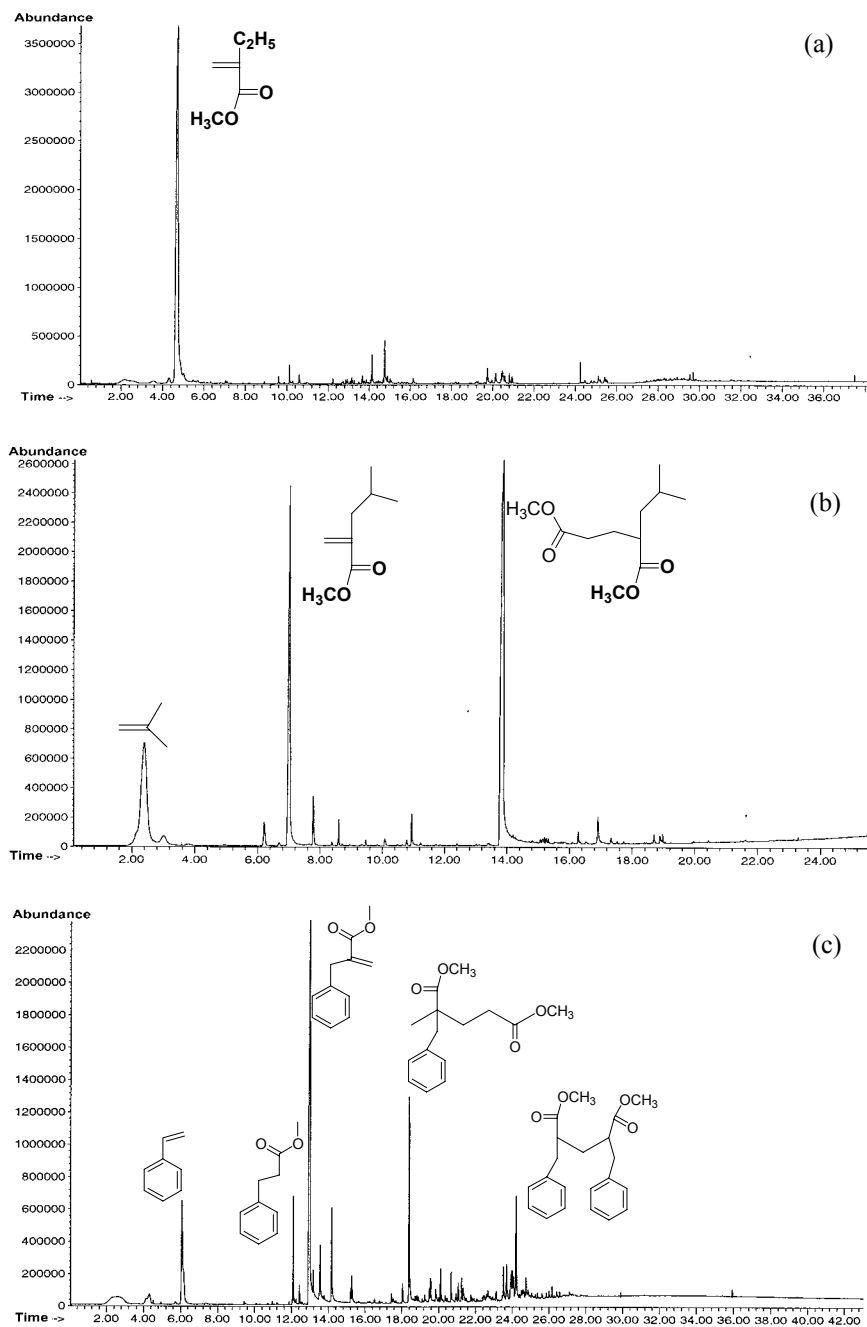


FIGURE 6-15. THERMAL DECOMPOSITION PRODUCTS OF POLYMETHACRYLATES
 (a) ETHYL METHACRYLATE, (b) ISOBUTYL METHACRYLATE,
 AND (c) BENZYL METHACRYLATE

6.3.3.2 Cyano-Substituted Aromatic Polymers.

A dramatic flammability reduction caused by cyano groups has been observed in a series of cyano-substituted aromatic polymers that were synthesized by Terry Hobbs [136] at the University of Massachusetts, Amherst. The chemical structures of these polymers are shown in figure 6-16.

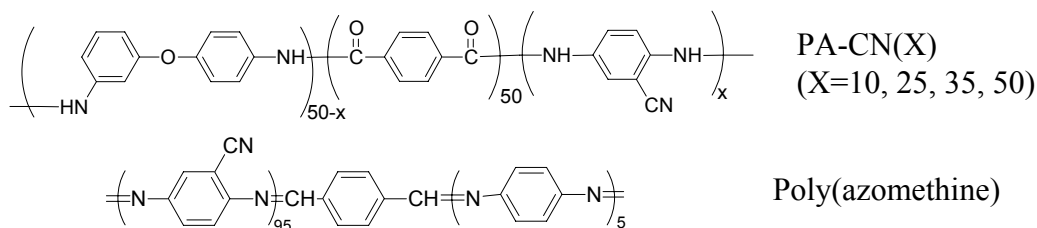


FIGURE 6-16. CHEMICAL STRUCTURES OF CYANO-SUBSTITUTED POLYMERS

The TGA and DTG curves of PA-CN(X) series are shown in figure 6-17. It can be seen that with the increased amount of CN-substituted diamine units, the thermal stability and char yield all increase correspondingly. In addition, the thermal decomposition processes are changed from a sharp single peak with a small shoulder into two peaks, then merging into another single peak, because polymer structures are changed from copolymers to a homopolymer (PA-CN(50)).

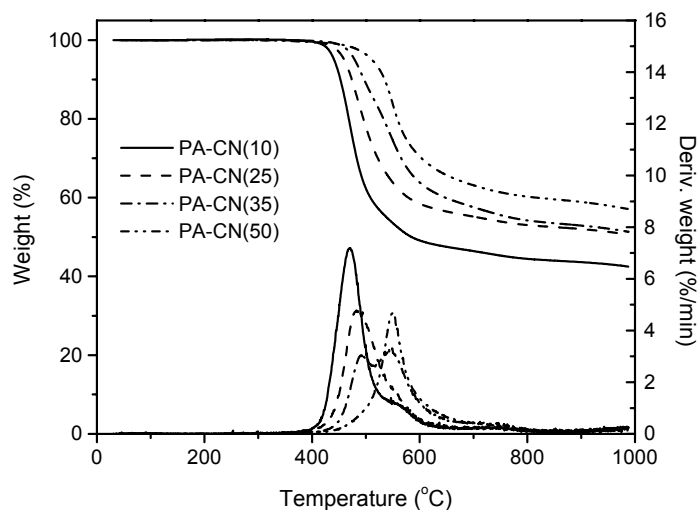


FIGURE 6-17. THE TGA AND DTG CURVES OF CYANO-SUBSTITUTED POLYAMIDES

More interestingly, PA-CN(25) and PA-CN(50) have similar backbone structures to Technora[®] and Kevlar[®], respectively. The only difference between them is that PA-CN(X) polymers contain CN side groups. Comparing their decomposition processes, the introduction of a CN group can greatly increase the char yield and reduce the mass loss rate (figure 6-18). However, the thermal stability is slightly reduced. It was also found that if the C=N bond is incorporated in the polymer main chain to form a highly conjugated system, such as poly(azomethine), the char yield can be dramatically increased and the decomposition rate can be dramatically decreased.

The heat events during decomposition are more complicated (figure 6-19). PA-CN(X) polyamides show an endothermic decomposition peak, but poly(azomethine) shows an obvious exothermic peak, which might be due to the cross-linking reactions during decomposition.

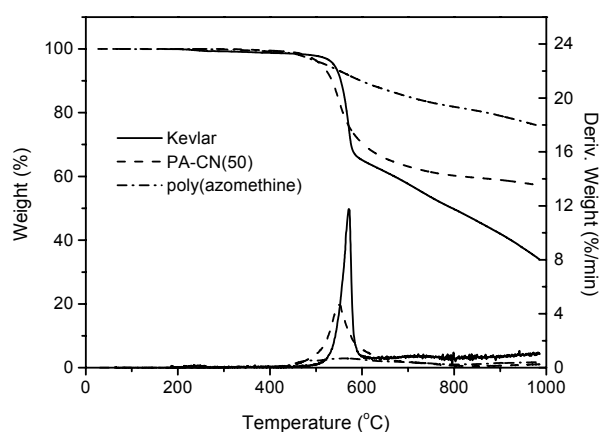
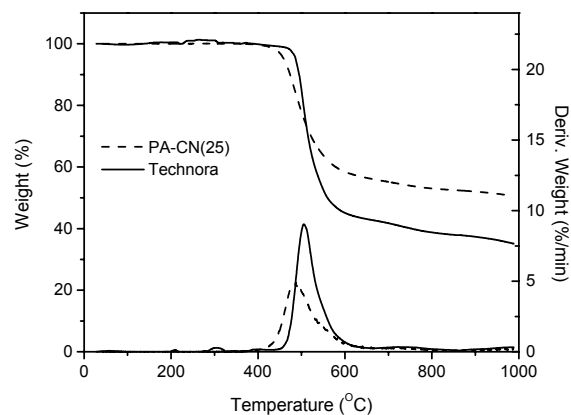


FIGURE 6-18. THE TGA AND DTG CURVES OF PA-CN(X) AND POLY(AZOMETHINE) COMPARED WITH TECHNORA[®] AND KEVLAR[®]

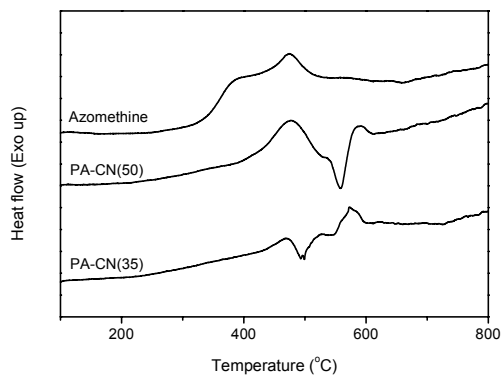


FIGURE 6-19. HIGH-TEMPERATURE DSC CURVES OF CN-SUBSTITUTED POLYMERS

According to pyrolysis GC/MS results (figure 6-20), with the increased amount of CN side groups, lower amounts of benzene and flammable high-molecular-weight volatiles are released. However, more benzonitrile and benzodinitrile are released. The major decomposition products of poly(azomethine) are CO₂, CO, and a series of aromatic compounds with CN groups.

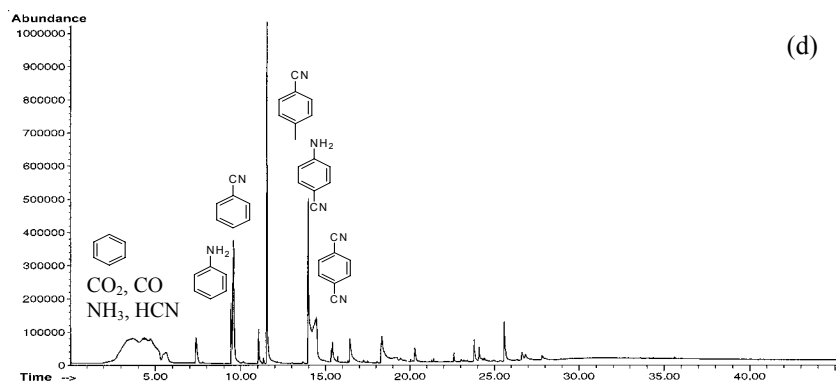
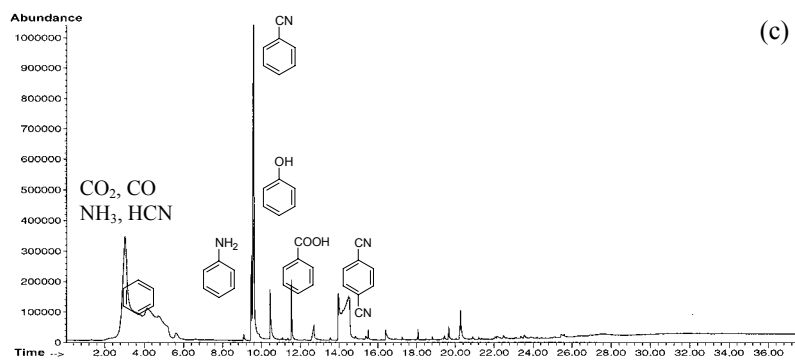
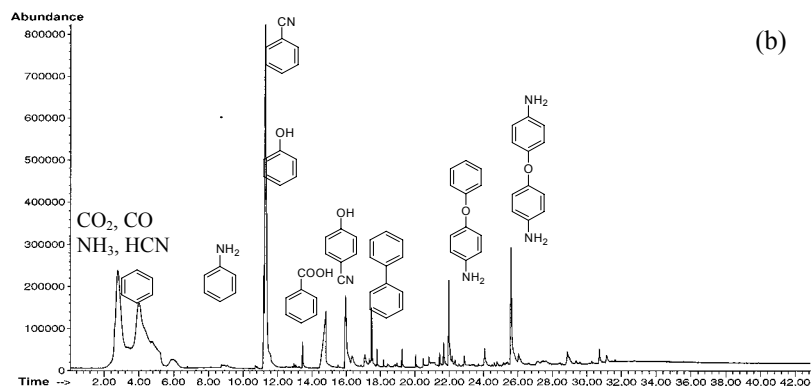
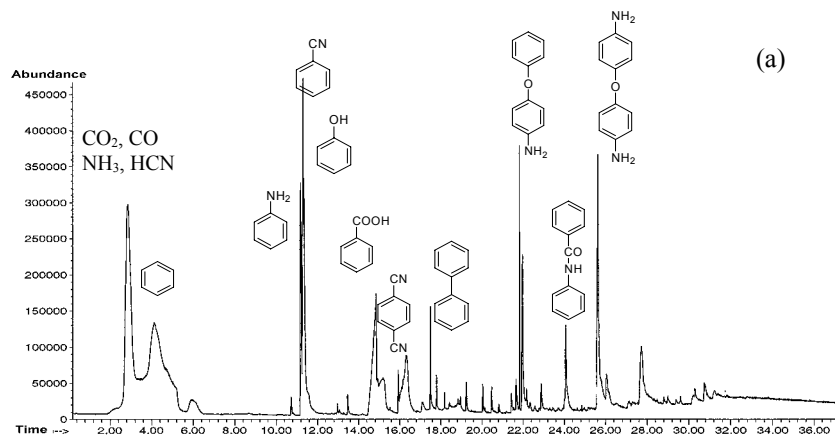


FIGURE 6-20. PYROLYSIS GC/MS TRACES OF PA-CN (X) AND POLY(AZOMETHINE) (a) TECHNORA[®], (b) PA-CN (25), (c) PA-CN (50), AND (d) POLY(AZOMETHINE)

Table 6-8 summarizes the flammability and thermal decomposition of PA-CN(X) and poly(azomethine), which are compared with Technora[®] and Kevlar[®]. It was found that with the introduction of more CN groups, the heat release capacity and total heat released all decrease, which indicates the CN group is an efficient flame-retardant unit. In particular, the introduction of C=N groups in the polymer main chain, such as poly(azomethine), can dramatically reduce the flammability. It was also found that the total heat released changes almost linearly with the molar fraction of CN-substituted diamine, while the heat release capacity is synergistically reduced by only a very small amount of CN groups.

TABLE 6-8. FLAMMABILITY AND THERMAL DECOMPOSITION OF PA-CN(X) POLYAMIDES

X	H.R. Capacity (J/g-K)	Total Heat (kJ/g)	Char Yield (%)	Max. Mass Loss Rate (x10 ³ /s)	T _{max} (°C)	T _{onset} (°C)
10	110	15	43	1.20	469	441
25	87	14	51	0.80	485	460
35	57	11	53	0.54	546	479
50	55	9	58	0.77	549	512
Technora [®]	131	15	42	1.71	502	487
Kevlar [®]	292	15	39	1.96	572	539
Poly(azomethine)	37	9	78	0.11	563	522

6.3.4 Flame-Retardant Comonomers.

6.3.4.1 Silicon-Based Comonomer—Polyethylene/Polyhedral Oligomeric Silsesquioxanes Hybrid.

The effects of a silicon-based comonomer (polyhedral oligomeric silsesquioxanes (POSS) monomer containing seven cyclopentyl and one norbornylene group) on polymer flammability were studied by using polyethylene POSS hybrid copolymers. The copolymers with a wide range of POSS concentrations were synthesized by Lei Zheng [137] at the University of Massachusetts, Amherst. The synthesis is shown in figure 6-21.

The thermal decomposition process of PE/POSS hybrid copolymer with 56 wt% of POSS is shown in figure 6-22. It can be seen that the introduction of POSS can greatly delay the major decomposition step of polyethylene by about 40°C and produce about 4% char. The copolymer starts to lose weight around 300°C, which is similar to the POSS monomer. The maximum mass loss rate of the copolymer is the same as polyethylene, but it shifts to a higher temperature.

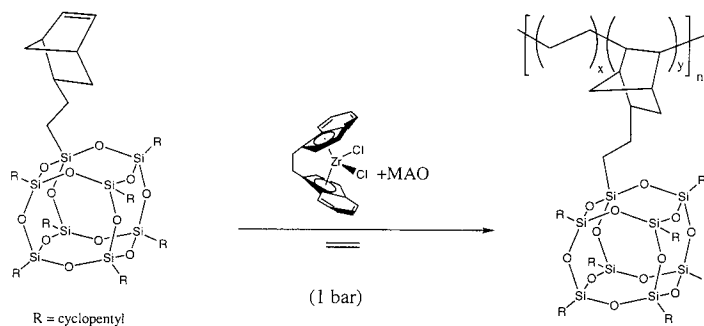


FIGURE 6-21. COPOLYMERIZATION OF POLYETHYLENE WITH POSS-NORBORNENE [137]

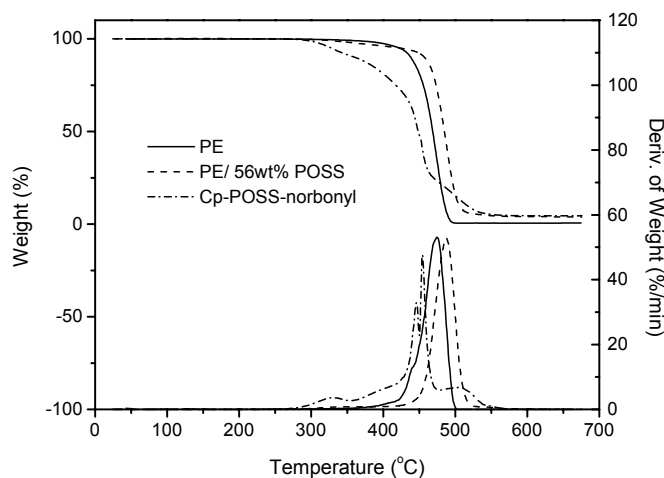


FIGURE 6-22. THE TGA AND DTG CURVES OF THE PE/POSS COPOLYMER

The thermal decomposition products of the POSS monomer, PE/POSS copolymer and PE, are shown in table 6-9. Referring to the TGA results, the small weight loss of a copolymer between 300°~450°C is due to the cleavage of the cyclopentyl side groups in the POSS monomer. At high temperatures, the C-C backbone will randomly cleave into small aliphatic fragments, which is similar to the random chain scission of PE. The high-molecular-weight silicon cage in the POSS monomer is not detected by pyrolysis GC/MS, which might be trapped in the GC column.

TABLE 6-9. THERMAL DECOMPOSITION PRODUCTS OF PE/POSS COPOLYMERS

Cp-POSS	1.3-cyclopentadiene, CO, CO ₂
PE/POSS 300°~450°C	1.3-cyclopentadiene, CO ₂
450°~930°C	A series of alkanes, alkenes, and dienes
PE	A series of alkanes, alkenes, and dienes

The flammability of PE/POSS copolymers with different amounts of POSS is shown in table 6-10. It can be seen that the introduction of the POSS monomer can systematically reduce flammability. Because the mass loss rate and char yield do not change significantly with the composition, the flammability reduction with increased POSS monomer is mainly due to the release of more POSS volatiles with low flammability. It was also found that both the heat release capacity and total heat released of copolymers change linearly with the amounts of POSS monomer (figure 6-23).

TABLE 6-10. FLAMMABILITY AND THERMAL DECOMPOSITION OF PE/POSS COPOLYMERS

POSS (wt %)	H.R. Capacity (J/g-K)	Total Heat (kJ/g)	Char Yield (%)	Max. Mass Loss Rate ($\times 10^3/s$)	T _{max} (°C)	T _{99%} (°C)
0	2007	41	0	8.83	474	363
19	1457	37	1.5	9.92	477	357
27	1330	35	1.8	11.68	486	336
37	1161	33	1.8	9.91	487	336
56	1034	32	3.9	8.83	487	328
100	314	19	4.6	7.86	455	293

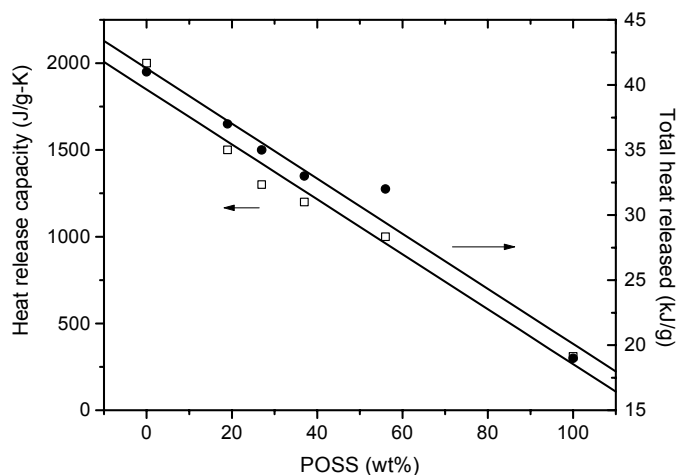


FIGURE 6-23. FLAMMABILITY-COMPOSITION RELATIONSHIP OF PE/POSS COPOLYMERS

6.3.4.2 Halogenated Comonomers—BPC-Epoxy Vinyl Ester Resins.

A group of cross-linked epoxy vinyl ester resins based on chlorobisphenol I and II (BPC I and II) were studied. The polymers were provided by Prof. Zbigniew Brzozowski at the Warsaw Institute of Technology. The syntheses are shown in figure 6-24. The composition of these polymers is summarized in table 6-11.

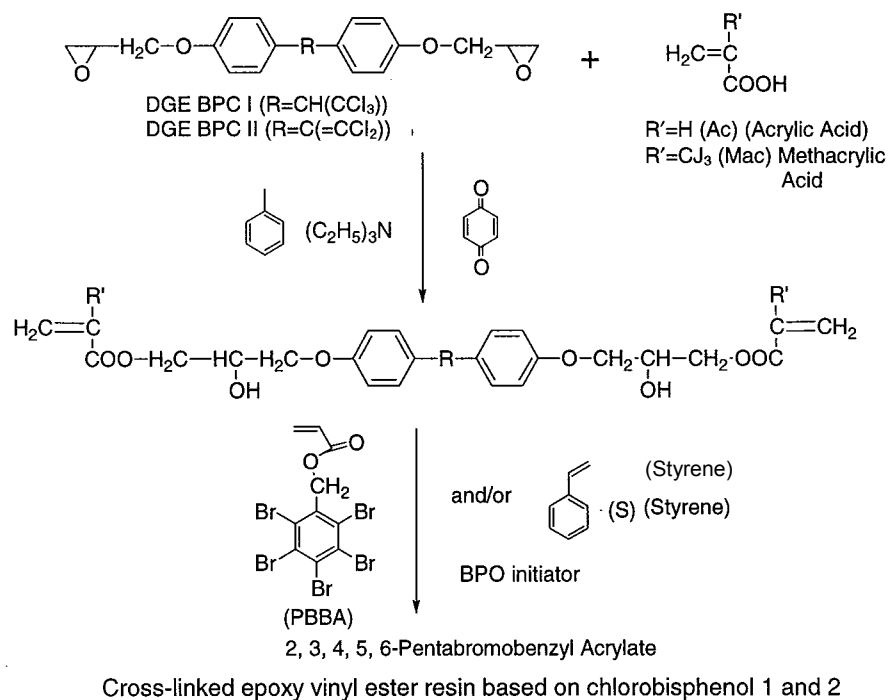


FIGURE 6-24. SYNTHESIS OF CROSS-LINKED EPOXY VINYL ESTER RESINS BASED ON BPC I AND II

TABLE 6-11. COMPOSITION OF BPC-BASED EPOXY VINYL ESTER RESINS (wt%)

Polymers	DGE BPC I	DGE BPC II	Ac	MAc	S	S+PBBA
A1	57%		19%		23%	
A2	57%		19%			23%
A3	56%			20%	23%	
A4	56%			20%		23%
B1		55%	21%		23%	
B1		55%	21%			23%
B3		52%		24%	23%	
B4		52%		24%		23%

Note: They all contain 1% benzoyl peroxide (BPO) and 0.1% *N,N*-dimethylamine.

The thermal decomposition processes of epoxy vinyl ester resins based on BPC I (A series) and BPC II (B series) are very similar. The TGA and high-temperature DSC curves of BPC II-based epoxy vinyl ester resins (B series) are shown in figure 6-25. According to the TGA curves, they all show a two-step decomposition, in which the minor first step starts at approximately 180°~220°C. The major second step starts at approximately 340°C. The introduction of brominated monomer PBBA will reduce the thermal stability, but slightly increase the char yield.

All the polymers can produce about 20% char up to 1000°C. They all show an obvious exothermic decomposition peak (about 140~180 J/g). For the polymers without PBBA, the exothermic peak is followed by an endothermic tail. For the polymers with PBBA, this tail totally disappeared.

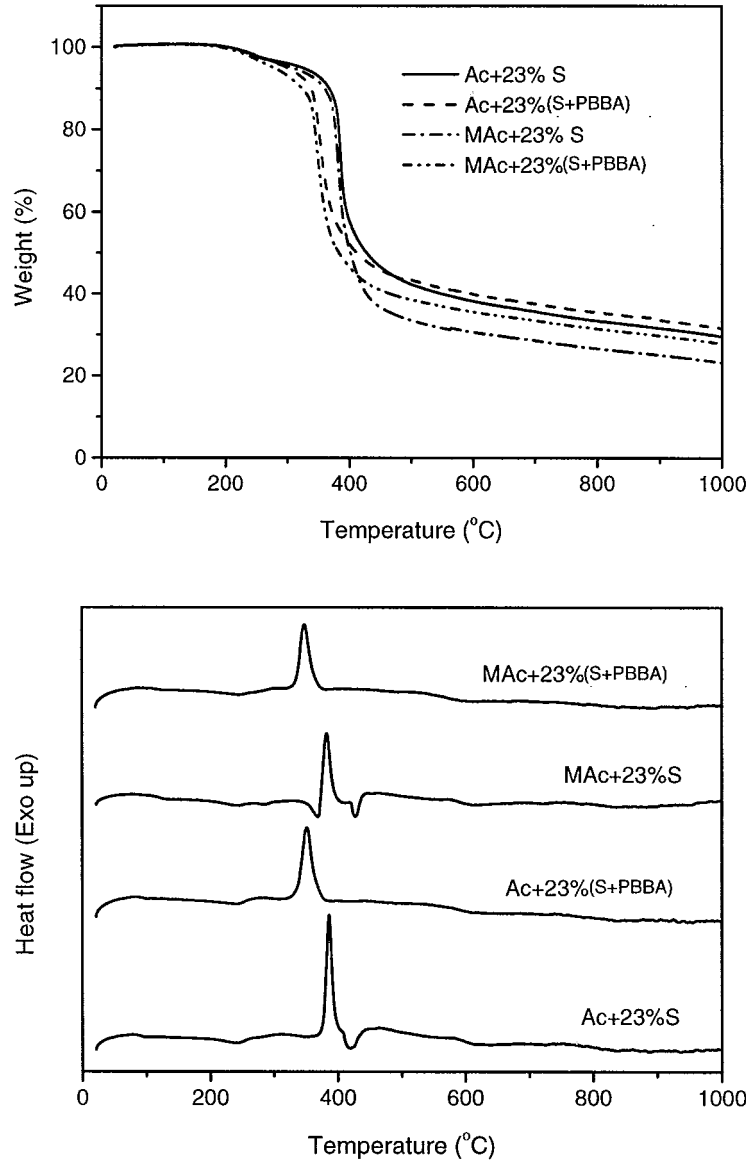


FIGURE 6-25. THE TGA AND DSC CURVES OF BPC II-BASED EPOXY VINYL ESTER RESINS (B SERIES) (a) TGA AND (b) DSC

According to table 6-12, the flammability of these polymers is close to BPA-PC or Kevlar, which is significantly lower than BPA-based epoxy vinyl ester resin. The introduction of brominated monomer PBBA cannot reduce the heat release capacity, but it can reduce the total heat released. The polymers containing methacrylic acid have slightly higher total heat of combustion than those with acrylic acid.

TABLE 6-12. THERMAL DECOMPOSITION AND FLAMMABILITY OF BPC-BASED EPOXY VINYL ESTER RESINS

Polymers	H.R. Capacity (J/g-K)	Total Heat (kJ/g)	Char Yield (%)	Max. Mass Loss Rate ($\times 10^3/s$)	T _{max} (°C)	T _{99%} (°C)	ΔH (J/g)
A1	197	18	28	1.31	345	187	178
A2	200	13	31	1.61	330	177	187
A3	229	20	28	1.44	344	168	136
A4	230	18	27	1.34	344	162	145
B1	373	17	32	4.60	387	164	194
B1	285	16	34	2.34	348	204	178
B3	325	21	24	3.37	384	190	176
B4	310	17	30	2.15	351	161	147

The thermal decomposition products are shown in figure 6-26. It can be seen that the weight loss in the first step is due to the release of additives or solvents such as ethyl chloride, toluene, and dibutyl phthalate. The major decomposition products of all the polymers are styrene and dibutyl phthalate. The polymers containing PBBA also release some brominated compounds.

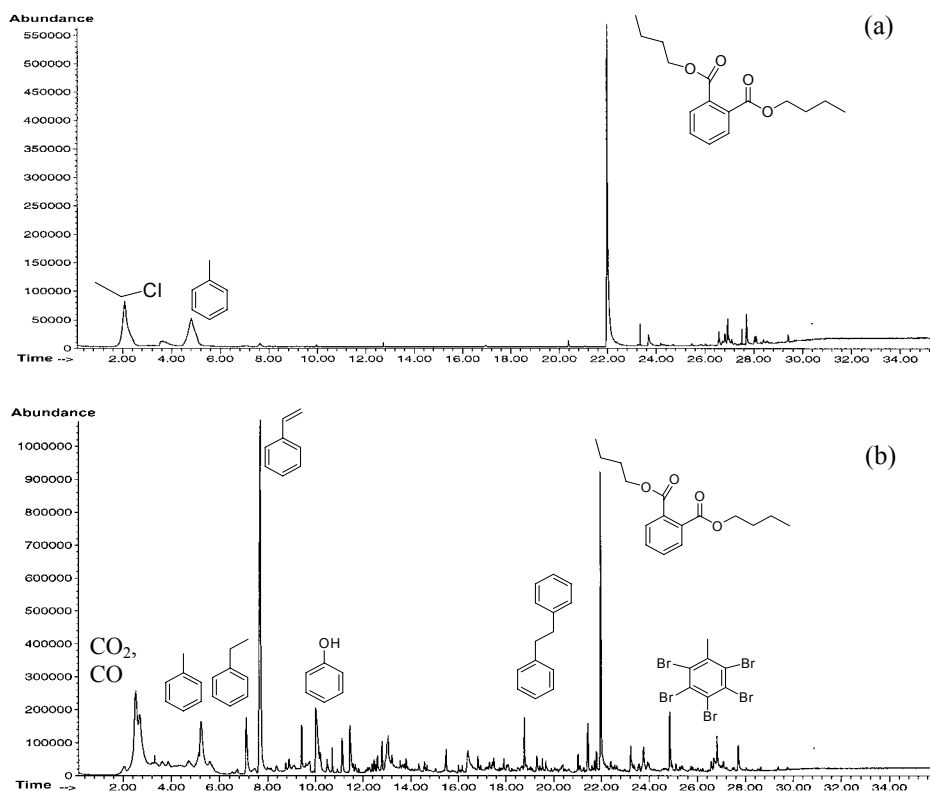


FIGURE 6-26. PYROLYSIS GC/MS TRACES OF BPC I-BASED EPOXY VINYL ESTER RESIN A1 (a) 170°~330°C AND (b) 170°~930°C

6.4 COMPOSITION—COPOLYMERS AND BLENDS.

6.4.1 Poly(Methyl Methacrylate)/Polystyrene Random Copolymers.

A series of PMMA/PS random copolymers with 30, 40, 50, 60, and 70 mol% of PS was studied. They were obtained from Prof. Thomas Russell's group at the University of Massachusetts, Amherst. All the polymers were synthesized by Craig Hawker at the IBM Almaden Research Center through radical polymerization [138]. The number average molecular weight of these copolymers is 125 ~ 178 k and PDI is 1.4 ~ 1.8. Figure 6-27 shows the thermal decomposition processes of these polymers. It was found that the thermal stability, decomposition rate, and the temperature at maximum mass loss rate all change systematically with the composition. With the increased amount of PS, the thermal stability increases, the decomposition rate increases, and the decomposition peak is shifted to higher temperatures.

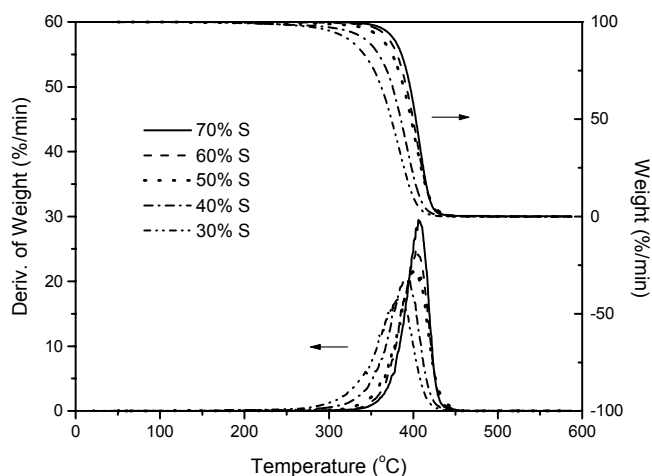


FIGURE 6-27. THE TGA CURVES OF PMMA/PS COPOLYMERS BY RADICAL POLYMERIZATION

Table 6-13 summarizes the flammability and thermal decomposition properties of these copolymers. Corresponding to the systematic change in thermal decomposition, the heat release capacity and total heat released also change systematically. With the increased amount of PS, the flammability of the copolymers increases. According to figure 6-28, the total heat of combustion changes linearly with the composition. However, the heat release capacity does not show a significant increase until the copolymer contains more than 50 mol% PS.

6.4.2 Poly(Methyl Methacrylate)/Polystyrene Blends.

A series of PMMA/PS blends with 0, 20, 40, 60, 80, and 100 mol% of PS were prepared by mixing PMMA and PS (both from Aldrich) in Tetrahydrofuran (THF), then solution casting into films. Figure 6-29 shows the thermal decomposition processes of these blends. Similar to the copolymers, the thermal stability, decomposition rate, and the temperature at maximum mass loss rate all change systematically with the composition. With the increased amount of PS, the thermal decomposition processes are shifted to PS.

TABLE 6-13. FLAMMABILITY AND THERMAL DECOMPOSITION OF PMMA/PS COPOLYMERS

PS (mol%)	H.R. Capacity (J/g-K)	Total Heat (kJ/g)	Max. Mass Loss Rate ($\times 10^3/s$)	T _{max} (°C)	T _{95%} (°C)
30	580	27	2.9	383	306
40	640	28	3.4	393	325
50	640	30	3.6	400	352
60	810	32	4.2	403	363
70	1000	33	4.9	406	369

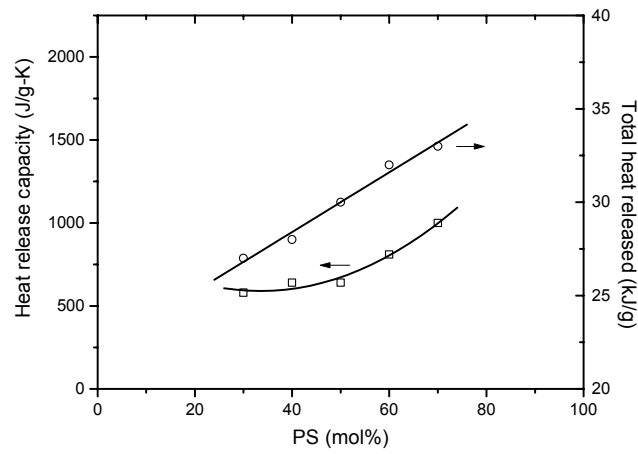


FIGURE 6-28. FLAMMABILITY-COMPOSITION RELATIONSHIP OF PMMA/PS RANDOM COPOLYMERS

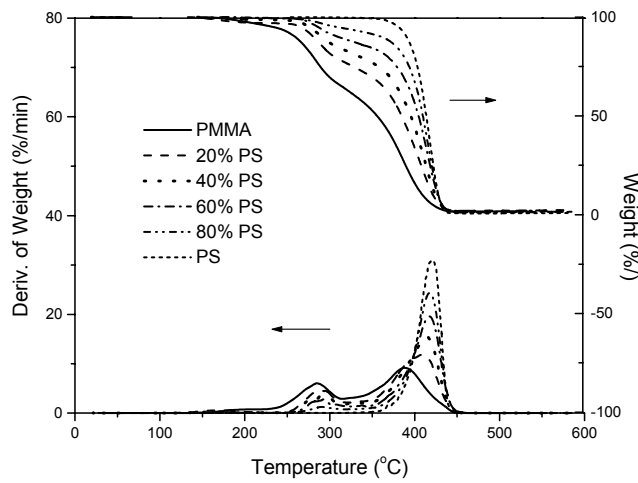


FIGURE 6-29. THERMAL DECOMPOSITION PROCESSES OF PMMA/PS BLENDS

Similarly to the random copolymers, the flammability increases systematically with the amount of PS (table 6-14). The total heat of combustion changes linearly with the composition of blends, but the heat release capacity will not increase dramatically until the amount of PS is above 50 mol% (figure 6-30).

TABLE 6-14. FLAMMABILITY AND THERMAL DECOMPOSITION OF PMMA/PS BLENDS

PS (mol %)	H.R. Capacity (J/g-K)	Total Heat (kJ/g)	Max. Mass Loss Rate ($\times 10^3/s$)	T _{max} (°C)	T _{95%} (°C)
0	340	24	1.6	389	180
20	250	27	2.0	411	169
40	380	29	2.6	415	194
60	570	32	3.3	418	259
80	760	34	4.1	420	246
100	1200	37	5.2	421	356

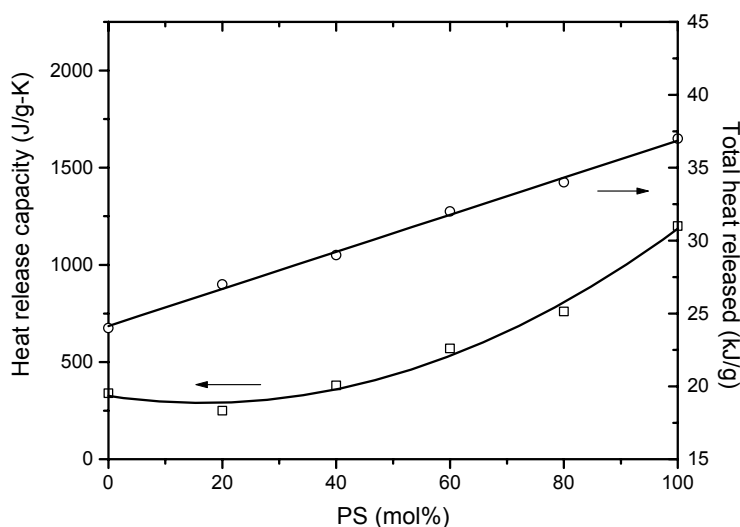


FIGURE 6-30. FLAMMABILITY-COMPOSITION RELATIONSHIP OF PMMA/PS BLENDS

6.5 MOLECULAR WEIGHT.

PMMA, PS, and PEO were chosen to study the effects of the molecular weight on polymer flammability because they decompose by different mechanisms.

6.5.1 Poly(Methyl Methacrylate).

All the PMMAs were obtained from Polymer Laboratories. They were synthesized by anionic polymerization using high-vacuum techniques. The polymerization was initiated with 2,2-

diphenyl hexyl lithium using a coordinating ligand salt and was terminated with alcohol by hydrogen abstraction. The peak molecular weights (M_p) of the samples measured by gel permeation chromatography were 30, 49, 64, 75, 88, and 480 kg/mole with a narrow molecular weight distribution of 1.04 ~1.09.

As shown in figure 6-31, the thermal decomposition processes of PMMAs with different molecular weights are very different. PMMAs with lower molecular weights such as 30 and 49 k clearly show a two-step decomposition, but PMMAs with high molecular weights decompose in a single step and have relatively higher thermal stability. Correspondingly, the maximum mass loss rate occurs at high temperatures for the PMMAs with high molecular weight.

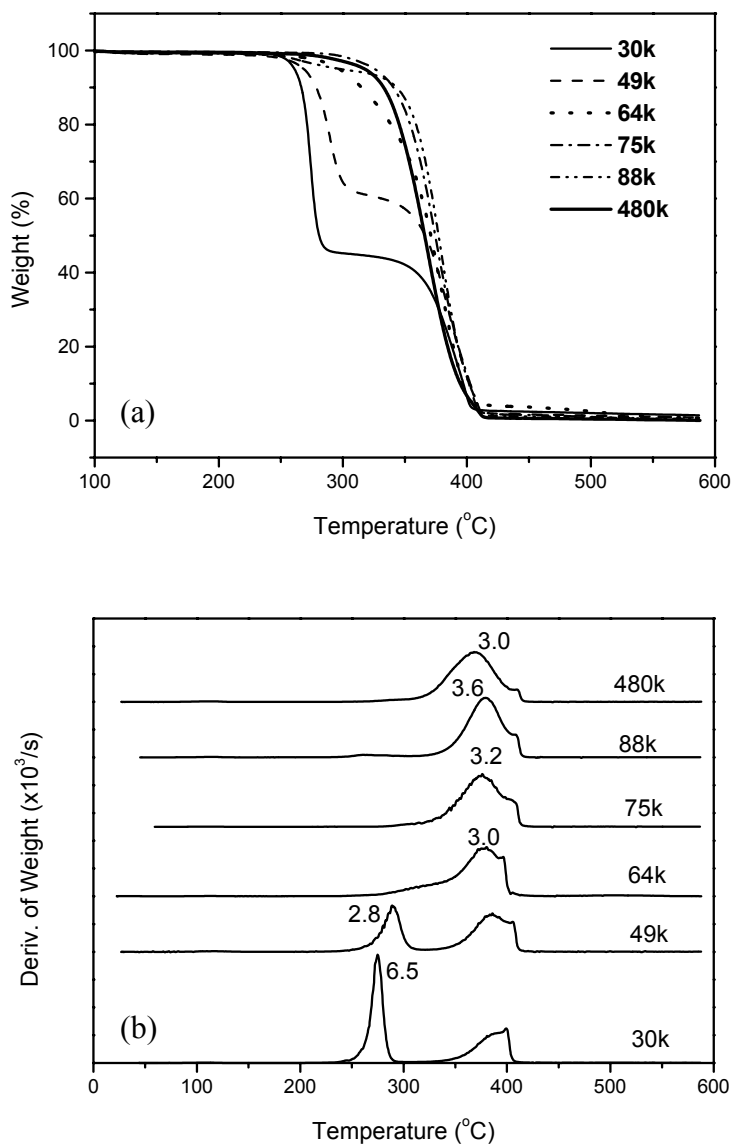


FIGURE 6-31. THE TGA AND DTG CURVES OF PMMAs WITH DIFFERENT MOLECULAR WEIGHTS (a) TGA AND (b) DTG

Corresponding to the DTG curves, the PCFC heat release rate curves of PMMAs shown in figure 6-32 change from double peaks into a single peak. According to table 6-15, although the total heat of combustion of all the PMMAs is the same, their heat release capacity is mainly determined by the mass loss rates. Therefore, PMMAs with different molecular weight have different flammability.

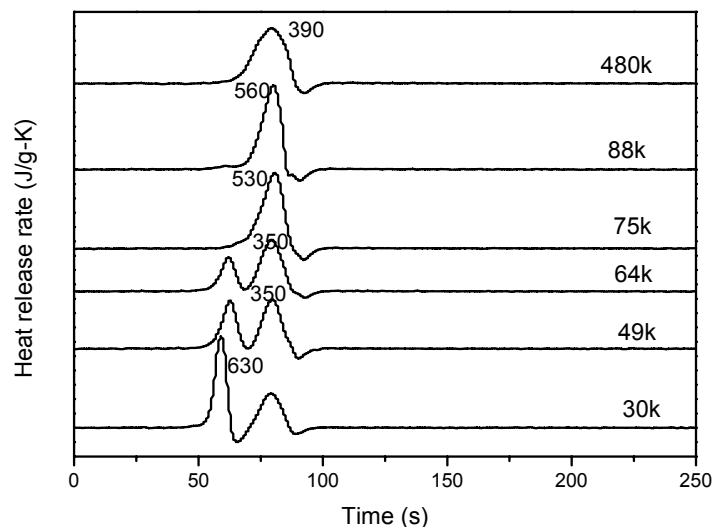


FIGURE 6-32. THE PCFC CURVES OF PMMAs WITH DIFFERENT MOLECULAR WEIGHTS

TABLE 6-15. FLAMMABILITY AND THERMAL DECOMPOSITION OF PMMAs

M_p (kg/mole)	H.R. Capacity (J/g-K)	Total Heat (kJ/g)	Max. Mass Loss Rate ($\times 10^3/s$)	T_{max} ($^{\circ}C$)	$T_{95\%}$ ($^{\circ}C$)
30	630 (d1)	25	6.5	275	261
49	350 (d2)	25	2.8	289	268
64	350 (d2)	24	3.0	380	298
75	530 (s)	24	3.2	376	325
88	560 (s)	24	3.6	379	321
480	390 (s)	25	3.0	370	308

*d: double peaks; 1 or 2: first or second peak; s: single peak

6.5.2 Polystyrene.

All the polystyrenes were also obtained from Polymer Laboratories. They were synthesized by anionic polymerization using inert gas blanket or high-vacuum techniques. The polymerization was initiated with n-butyl lithium and terminated with alcohol by hydrogen abstraction. The molecular weights (M_p 's) of the samples were 30, 50, 66, 96, 127, 220, 460, 553, 760, 1030, 1130, 2880 kg/mole. The molecular weight distribution was polydispersity index (PDI) = 1.03~1.07.

According to figure 6-33, the thermal decomposition processes of these polystyrenes with different molecular weights are almost the same. As to the flammability (table 6-16), the heat release capacity slowly increases with the molecular weight, but the change is not as evident as in PMMA.

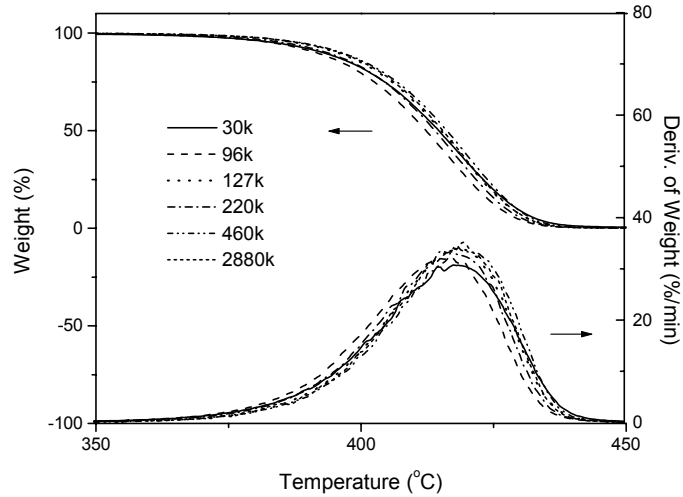


FIGURE 6-33. THERMAL DECOMPOSITION OF PS WITH DIFFERENT MOLECULAR WEIGHTS

TABLE 6-16. FLAMMABILITY AND THERMAL DECOMPOSITION OF PS

M_p (kg/mole)	H.R. Capacity (J/g-K)	Total Heat (kJ/g)	Max. Mass Loss Rate ($\times 10^3/s$)	T_{max} (°C)	$T_{95\%}$ (°C)
30	930	39	5.1	418	394
50	960	38	5.2	417	391
66	890	39	4.9	413	390
96	930	40	5.3	416	393
127	1000	40	5.5	418	395
220	1100	38	5.4	420	396
460	1100	39	5.6	418	396
553	1100	38	5.7	419	397
760	1100	38	5.5	420	398
1030	1100	40	5.6	418	391
1130	1200	39	5.7	419	398
2880	1300	40	5.8	420	398

6.5.3 Poly(Ethylene Oxide).

PEO samples were from Aldrich, which were inhibited with butylated hydroxy toluene. The molecular weights based on inherent viscosity were 8, 100, 300, 600, and 4000 kg/mole. According to figure 6-34, their decomposition processes are not changed with the molecular weight at all, nor is their flammability (table 6-17).

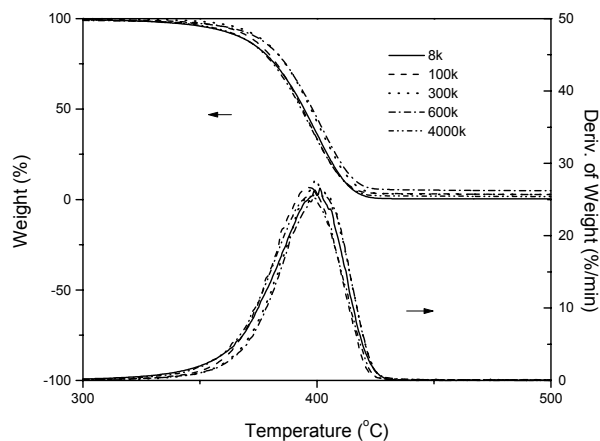


FIGURE 6-34. THERMAL DECOMPOSITION OF PEO WITH DIFFERENT MOLECULAR WEIGHT

TABLE 6-17. FLAMMABILITY AND THERMAL DECOMPOSITION OF PEOs

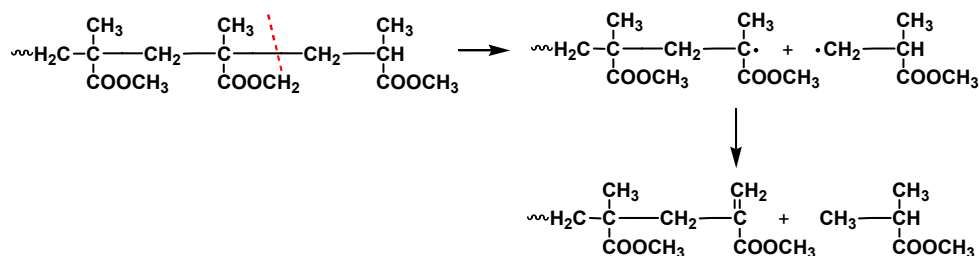
M_p (kg/Mole)	H.R. Capacity (J/g-K)	Total Heat (kJ/g)	Max. Mass Loss Rate ($\times 10^3/s$)	T_{max} (°C)	$T_{95\%}$ (°C)
8	600	23	4.4	402	372
100	600	23	4.5	397	368
300	530	24	4.4	399	368
600	580	23	4.4	400	371
4000	680	24	4.3	398	366

6.5.4 Mechanisms of the Effects of the Molecular Weight.

Kashiwagi found that a number of properties affect the thermal and oxidative decomposition of thermoplastics, such as molecular weight, prior thermal damage, weak linkage, and primary radicals [132, 58, 139, 140]. Kashiwagi also found that there are two or three decomposition stages in PMMA polymerized by free-radical initiation [140]. Generally, the first stage might be initiated by scission around the defects in the polymer chain such as head-to-head linkages. The next stage was proposed to be chain-end initiation due to the double bond-terminated polymer chain. The last one is initiation by random chain scission. Kashiwagi believed because anionically polymerized PMMA did not have many unsaturated double bonds at the ends, it decomposed by random scission.

However, according to the present results, anionically polymerized PMMAs with low molecular weights show a two-stage decomposition, which corresponds to the initiation of both end-chain and random-chain scission. It is believed that at low temperatures, the thermal decomposition starts mainly from the chain end by stripping the monomers. At high temperatures, the polymer will randomly break along the chain and release monomers by unzipping (figure 6-35). For the PMMAs with high molecular weights, the number of chain ends is very limited. Therefore, the thermal decomposition is mainly initiated by the random chain scissions. As a result, PMMAs with high molecular weights decompose in a single step.

(1) First stage—End-chain initiation (low temperatures)



(2) Second stage—Random-chain initiation (high temperatures)

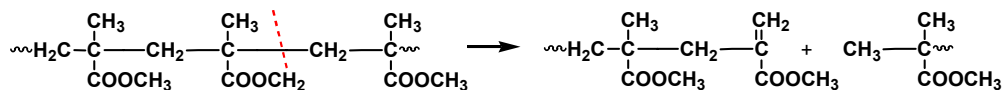


FIGURE 6-35. THERMAL DECOMPOSITION OF PMMAs WITH LOW MOLECULAR WEIGHT

To summarize the experimental results, the effects of the molecular weight on polymer flammability are greatly determined by their thermal decomposition mechanisms. For the polymers that decompose by an unzipping mechanism such as PMMA and poly(α -methyl styrene), the molecular weight will have a big effect on thermal decomposition and flammability due to different chain-scission initiations. For the polymers that decompose by random chain scission, such as PEO, poly(ethylene), and most polycondensation polymers, the molecular weight does not have a dramatic effect on the flammability. For the polymers that decompose by a combination of unzipping and random scission mechanisms, such as polystyrene, molecular weight will have some effect on the flammability.

6.6 FREE-RADICAL SCAVENGER—TEMPO.

Earlier it was found that the action of halogen flame-retardant systems could be enhanced substantially by the addition of peroxide in polystyrenics and polyolefins [7]. It has also been proposed that the free-radical inhibitor might retard the condensed-phase pyrolysis or surface oxidation of the burning process. In this study, blends of PS or PMMA with TEMPO and PS/PMMA random copolymers initiated by TEMPO were used to investigate how the free-radical scavenger TEMPO affects the flammability of polymers.

6.6.1 Polystyrene or PMMA/TEMPO Blends.

PS/TEMPO blends with 2 wt% or 6 wt% of TEMPO were studied. PS and TEMPO were obtained from Aldrich. According to figure 6-36, TEMPO is released around 150°C, which is well below the thermal decomposition temperature of PS. Therefore, it does not effect the decomposition rate and flammability of the blends (table 6-18).

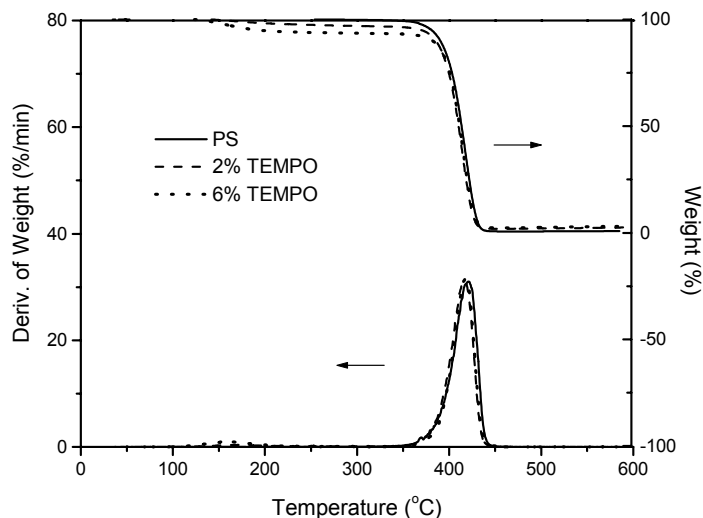


FIGURE 6-36. THE TGA AND DTG CURVES OF PS/TEMPO BLENDS

TABLE 6-18. FLAMMABILITY OF PS/TEMPO BLENDS

TEMPO (wt %)	H.R. Capacity (J/g-K)	Total Heat (kJ/g)
0	1200	37
2	1100	37
6	1100	36

In PMMA/TEMPO blends, TEMPO can delay the second step of decomposition to higher temperatures (figure 6-37). However, it also increases the maximum mass loss rate. As a result, the heat release capacity is slightly increased (table 6-19).

6.6.2 The PMMA/PS Random Copolymers Initiated by TEMPO.

A series of PMMA/PS random copolymers initiated by TEMPO were studied. All the polymers were obtained from Prof. Thomas Russell at the University of Massachusetts, Amhurst and were synthesized by Craig Hawker at the IBM Almaden Research Center [138]. The number average molecular weights of these polymers were around 10 k. The structure of the copolymer is shown in figure 6-38.

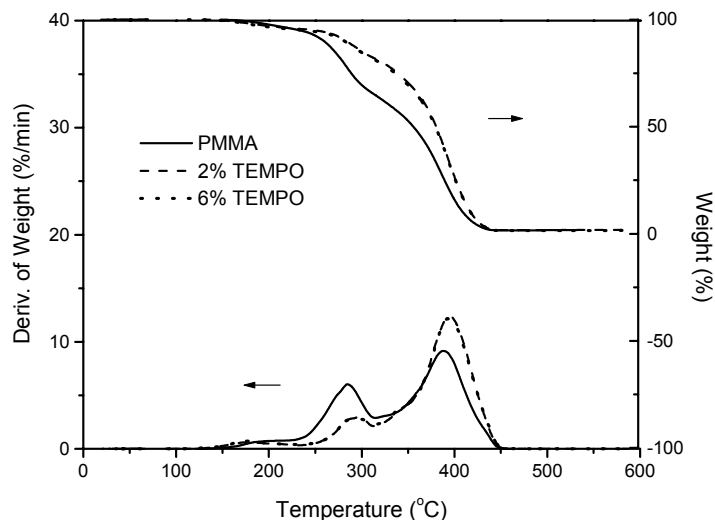


FIGURE 6-37. TGA AND DTG CURVES OF PMMA/TEMPO BLENDS

TABLE 6-19. FLAMMABILITY OF PMMA/TEMPO BLENDS

TEMPO (wt %)	H.R. Capacity (J/g-K)	Total Heat (kJ/g)
0	335	24
2	359	23
6	372	23

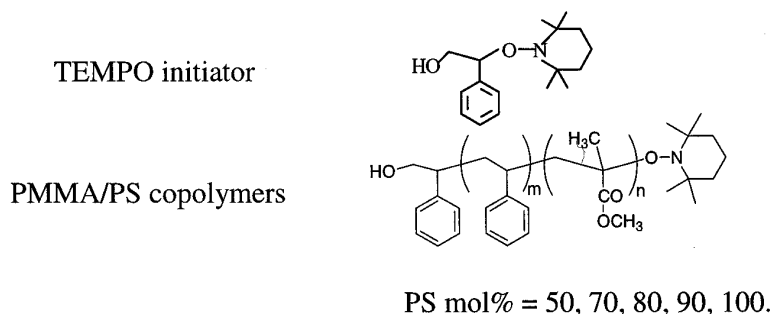


FIGURE 6-38. TEMPO-INITIATED PMMA/PS COPOLYMERS

The TGA and DTG curves are shown in figure 6-39. It can be seen that with the increased amount of PS, the thermal stability of copolymers increases, but the peak of mass loss rate becomes sharper and is shifted to the direction of PS, indicating the thermal decomposition becomes faster and is dominated by PS.

According to table 6-20, both heat release capacity and total heat of combustion change systematically with the composition, that is, the flammability increases with more PS. However, neither of them changes linearly with the composition (figure 6-40).

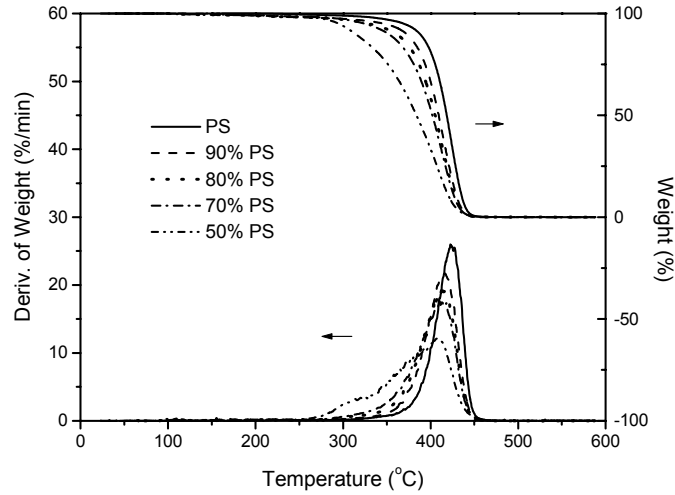


FIGURE 6-39. THE TGA AND DTG CURVES OF TEMPO-INITIATED PMMA/PS COPOLYMERS

TABLE 6-20. FLAMMABILITY AND THERMAL DECOMPOSITION OF PMMA/PS COPOLYMERS INITIATED BY TEMPO

PS (mol %)	H.R. Capacity (J/g-K)	Total Heat (kJ/g)	Max. Mass Loss Rate ($\times 10^3/s$)	T_{max} ($^{\circ}C$)	$T_{95\%}$ ($^{\circ}C$)
50	270	29	2.0	409	297
70	400	33	2.9	410	324
80	510	34	3.3	413	330
90	800	35	3.6	416	345
100	930	35	4.3	422	371

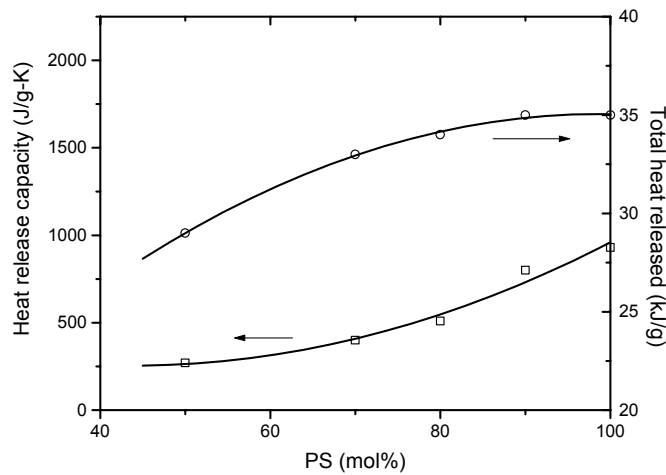


FIGURE 6-40. FLAMMABILITY-COMPOSITION RELATIONSHIP OF PMMA/PS COPOLYMERS INITIATED BY TEMPO

If these TEMPO-initiated PMMA/PS copolymers are compared with standard PMMA/PS random copolymers (figure 6-27), it can be seen that the thermal decomposition of the TEMPO-initiated copolymers spans a broader temperature range, and the mass loss rate is relatively lower. As a result, the flammability is lower. Some volatiles with TEMPO units are detected in the gas phase (figure 6-41). It is speculated that TEMPO can reduce the decomposition rate by recombining with the free radicals produced during decomposition, then releasing them through an equilibrium reaction (figure 6-42).

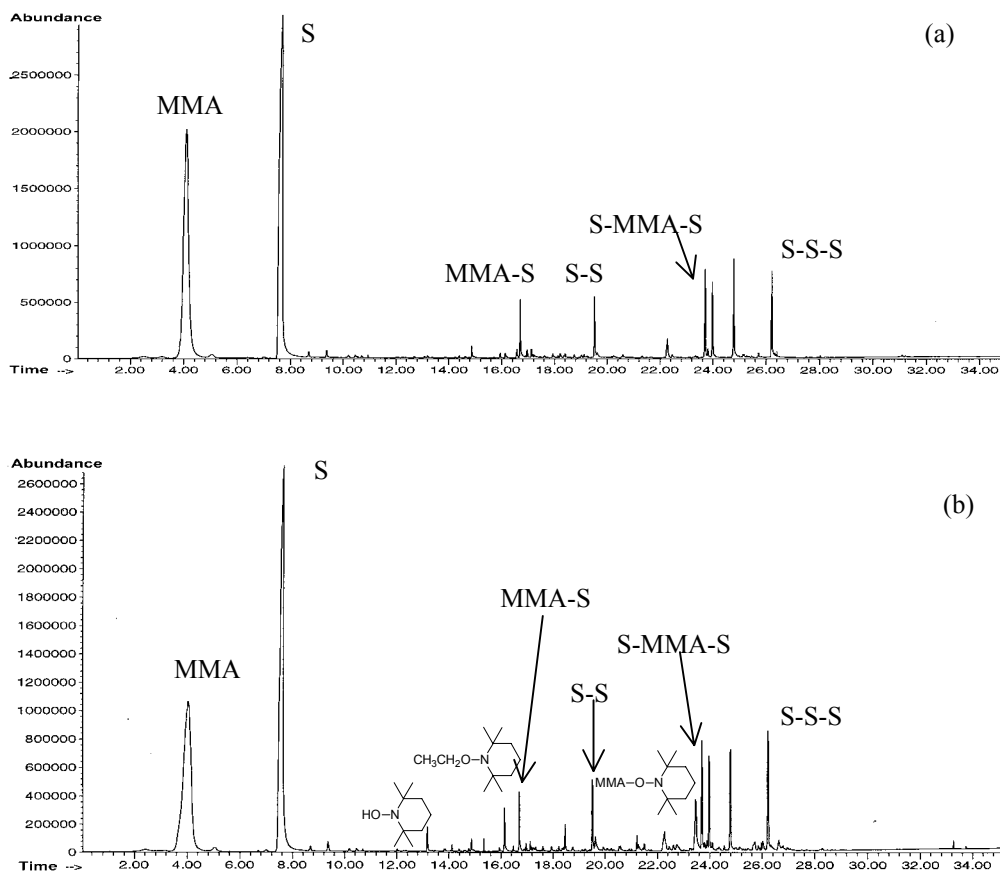


FIGURE 6-41. PYROLYSIS GC/MS TRACES OF PMMA/PS COPOLYMERS (a) RANDOM COPOLYMER AND (b) TEMPO INITIATED

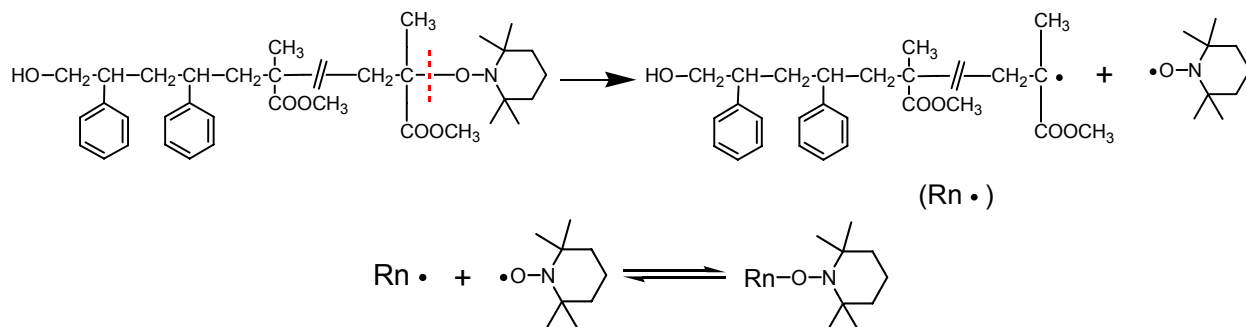


FIGURE 6-42. EFFECTS OF TEMPO ON POLYMER DECOMPOSITION

6.7 DISCUSSION.

There are many factors that can affect polymer flammability. However, the most important one is the chemical structure of the polymers. Introducing aromatic or heteroaromatic rings and heteroatoms into a polymer main chain can efficiently reduce polymer flammability. The bulky side groups in polymethacrylates can be easily cleaved off and released as fuels. However, they can also expand the decomposition temperature range by multiple decomposition stages. As a result, the mass loss rates are reduced. The CN substituent is a very efficient flame-retardant unit to be incorporated into a polymer structure to increase char formation and reduce heat released. The silicon-based or halogen-based comonomers that have low heats of combustion themselves can be used as reactive flame-retardant additives to adjust polymer flammability systematically. The silicon-based inorganic network structure can greatly promote the char formation. It was also found that the effects of molecular weight on polymer flammability are dependent on the thermal decomposition mechanisms of polymers. The introduction of TEMPO can slightly delay the thermal decomposition of polymers if TEMPO does not volatilize before the decomposition of polymers. For the copolymers and blends of PMMA/PS, the total heat of combustion generally changes linearly with composition, but the heat release capacity shows some synergetic, i.e., adding a small amount of low flammable component (PMMA) can dramatically reduce the flammability.

7. MOLECULAR MODELING OF THERMAL CYCLIZATION OF POLY(HYDROXYAMIDE).

7.1 INTRODUCTION.

It is very difficult to predict everything that will happen in a fire. However, theoretical modeling provides an important tool to investigate and understand the fire properties of various materials and the reactions involved in the thermal decomposition and combustion process.

There are two kinds of modeling. One is an empirical mathematical model based on mass and energy conservation to estimate the macroscopic fire behavior. For example, Lyon has developed a mechanistic mass loss model for char-forming polymers, from which the nonisothermal mass loss during constant heating rate can be effectively predicted [141]. The other is molecular modeling based on quantum and statistical mechanics to simulate the chemical structure and reactions numerically. Molecular modeling is a complementary method that can be used as an adjunct to the experimental measurements and macroscopic modeling to provide new insights into the polymer flammability and fire resistance [142]. Therefore, it can help design new fire-retardant additives and fire-resistant materials on a molecular level.

Dr. Marc Nyden of the NIST has successfully used the molecular modeling technique to identify factors that affect the condensed-phase thermal decomposition chemistry of polymers [143 and 144]. A novel computer program called MD-REACT has been developed. It is based on molecular dynamics and can account for the chemical reactions in the thermal degradation process of polymers. This code has been improved and extended [145].

Previous experimental results show that the thermal decomposition and flammability of PHA, its methoxy, phosphinate, and phosphate derivatives are quite different from each other though they have the same backbone structure (section 3). In order to have a better understanding of the thermal decomposition mechanism of these polymers, electronic structure methods Gaussian 98 [77] were used to study the thermal decomposition process of PHA. The computations were carried out on systems in the gas phase. Considering the trade-off between computational cost and accuracy of result, the B3LYP [74 and 75] method with a 6-31G(d,P) [76] basis set was selected for the whole calculation. The thermal cyclization of PHA to PBO had been studied preliminarily by Rotem [146]. However, the model compounds Rotem used were very small in size and the method chosen was low-level Hartree-Fock (HF). In this research, to more precisely represent the structure of PHA and get high-quality quantitative prediction, a bigger model compound, a high-level density-functional theory (B3LYP) (the least expensive ab initio method, which includes the effects of electron correlation that are neglected in the HF method), and a 6-31G(d,p) basis set were used. This part of the work was in collaboration with Stanislav Stoliarov [147].

7.2 PREVIOUS EXPERIMENTAL RESULTS.

It was found that PHA, its methoxy, phosphinate, and phosphate derivatives decompose very differently in the first step (figure 7-1). However, they all show a new decomposition step around 600°C, which is believed due to the decomposition of some similar structure that might contain some PBO rings.

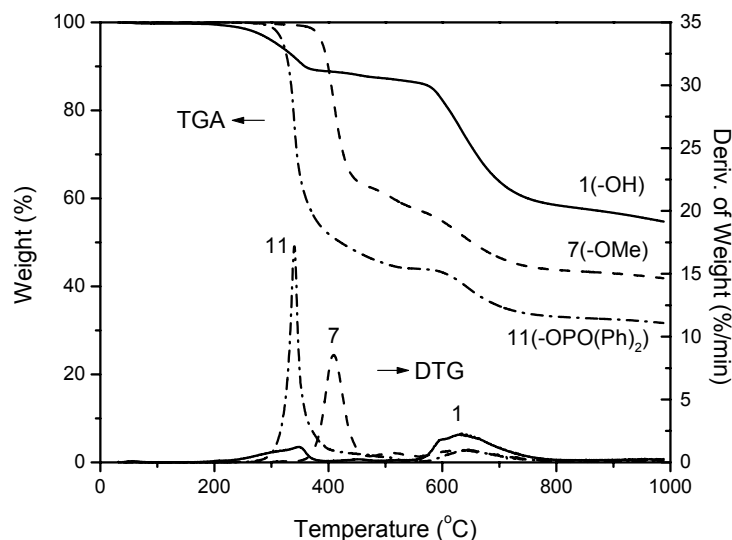


FIGURE 7-1. THERMAL DECOMPOSITION PROCESSES OF PHA AND ITS DERIVATIVES

According to pyrolysis GC/MS, FTIR, and elemental analysis, PHA will cyclize into PBO by releasing water during the first decomposition step (figure 7-2). However, if the hydroxyl groups are totally replaced by methoxy, phosphinate, or phosphate groups, these PHA derivatives cannot achieve the same cyclization as PHA without main-chain scission or cleavage of side groups. To understand how this small structural difference affects the cyclization reaction, the detailed cyclization pathway of PHA needs to be clarified.

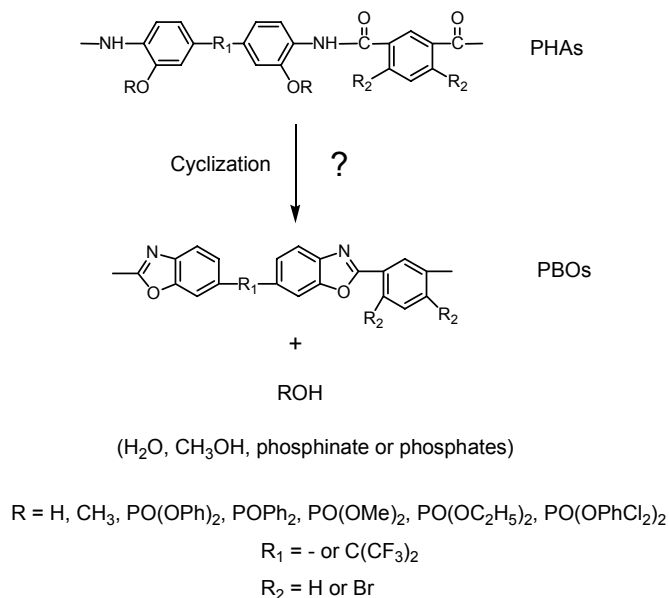


FIGURE 7-2. POSSIBLE THERMAL CYCLIZATION MECHANISM OF PHA AND ITS DERIVATIVES

7.3 RESULTS.

To know where the thermal decomposition is initiated, the weakest linkage along the polymer chain needs to be identified. The bond dissociation energies of PHA and its methoxy and phosphate derivatives are shown in figure 7-3. It can be seen that the weakest bond in these PHAs is the bond between oxygen and hydrogen (PHA) or methyl (methoxy PHA) or phosphate groups (phosphate PHA). Especially, O-Me and O-P bonds in methoxy or phosphate PHAs are much weaker than the O-H bond in PHA, which suggests that methyl and phosphate groups are more easily cleaved off during decomposition. The amide linkage in the polymer main chain is the second weakest bond, which can cause the breakdown of polymer backbones as shown in methoxy PHA.

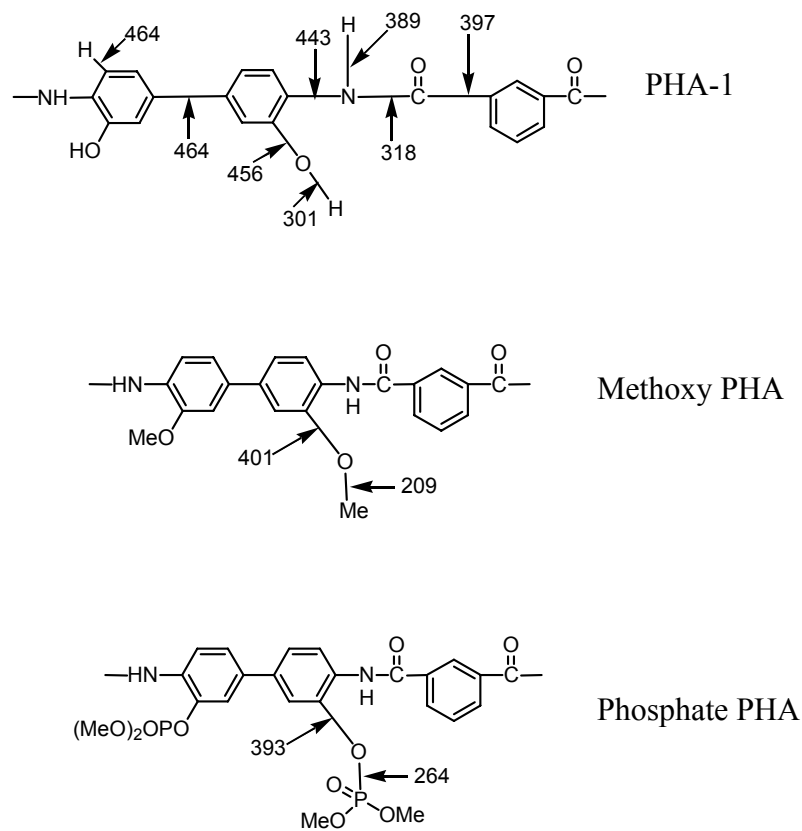


FIGURE 7-3. BOND DISSOCIATION ENERGIES OF PHA, ITS METHOXY AND PHOSPHATE DERIVATIVES (UNIT IN kJ/mol)

The model compound selected is the smallest structure unit in PHA, which is involved in cyclization. The optimized structure of this model compound is shown in figure 7-4. It has two stable structures (PHA-1 and PHA-2) whose energy difference is only about 26 kJ/mol. The transition between PHA-1 and PHA-2 can be easily achieved by rotation around the N-C bond in the amide linkage. The activation energy for this transition is only 63 kJ/mol in the model compound.

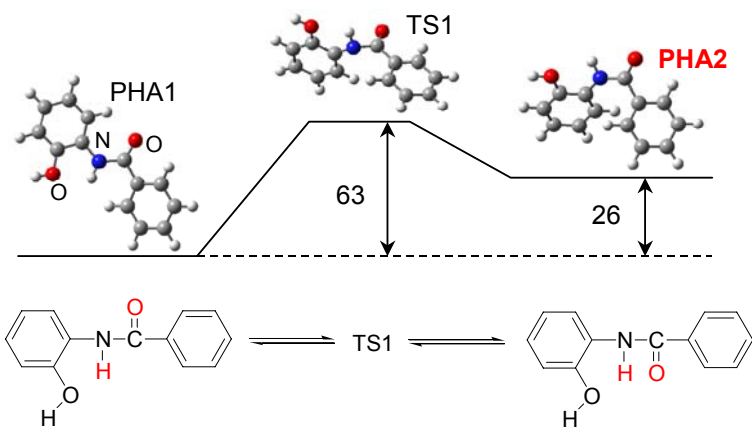


FIGURE 7-4. MOLECULAR STRUCTURES OF THE MODEL COMPOUND

The thermal cyclization of PHA into PBO was proposed to proceed by the overall steps of keto-enol rearrangement followed by water release to form the PBO structure (figure 7-5). The enthalpy changes in these two steps are 49 kJ/mol and -42 kJ/mol, respectively. The key step is the formation of the enol intermediate.

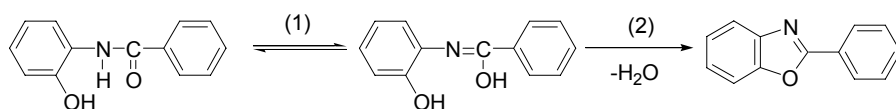


FIGURE 7-5. PROPOSED CYCLIZATION MECHANISM OF PHA

There are several pathways for the keto-enol transition. One is through a direct hydrogen shift, as shown in figure 7-6. The starting structure is PHA-2 with H and O atoms on the same side of the N-C bond. Then through a four-member ring transition state, the H atom is shifted to the carbonyl group and the C=N bond is formed. However, the energy barrier of this pathway is 154 kJ/mol, which is too high compared with the activation energy (40 kJ/mol) observed in the TGA data.

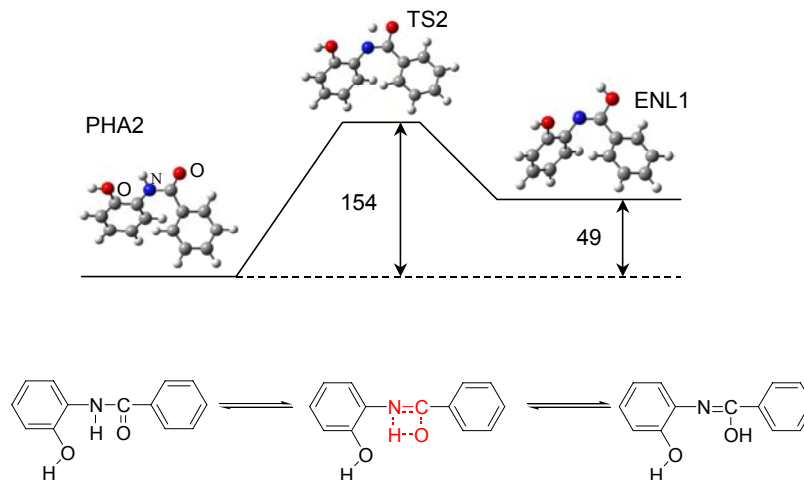


FIGURE 7-6. KETO-ENOL REARRANGEMENT BY A DIRECT HYDROGEN SHIFT

The second pathway for this keto-enol rearrangement is to form a six-member ring transition state, as shown in figure 7-7. At first, the amide linkage in the main chain and the hydroxy groups, which might come from the other PHA molecules or water, forms a six-member ring structure through intermolecular hydrogen bonding. Then by a concerted pericyclic reaction, the enol-intermediate ENL1 is formed. In this pathway, the energy barrier from the ordered complex to the six-member ring transition state is only 57 kJ/mol, which corresponds to the activation energy calculated by the TGA data. It can also be seen that the formation of hydrogen bonds is a very important step to form the enol intermediate. Methoxy and phosphate PHAs do not have hydroxyl side groups; therefore, they cannot form the hydrogen bonds that can lead to the formation of a six-member ring transition state. As a result, when they are heated up, they will not have the same cyclization reactions as PHA with hydroxyl groups but rather will cleave off the methyl or phosphate groups or have some main-chain scissions.

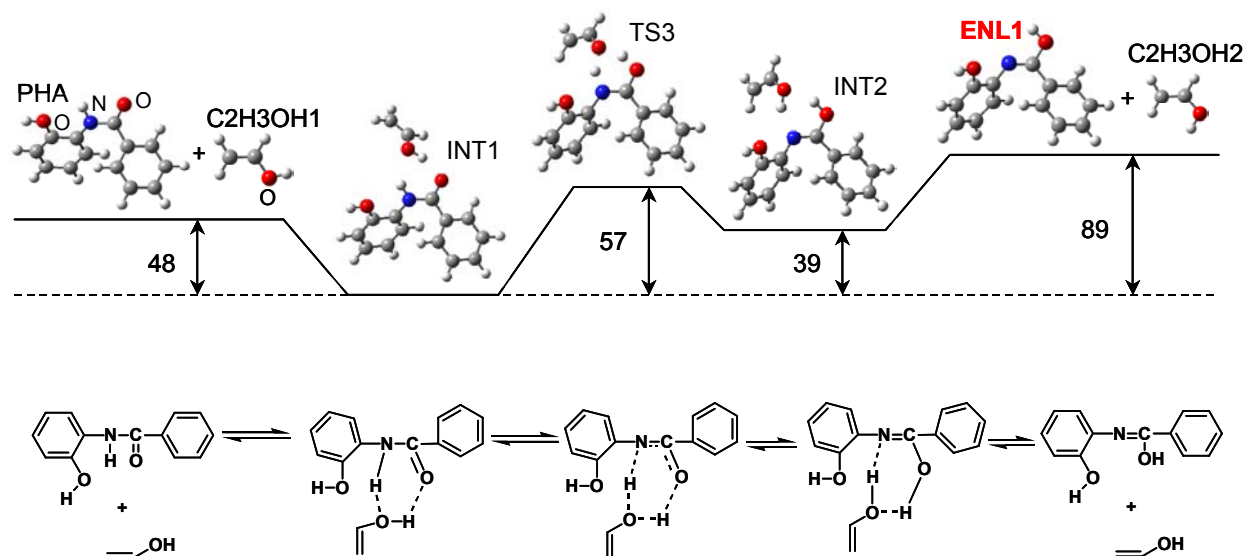


FIGURE 7-7. KETO-ENOL REARRANGEMENT BY A SIX-MEMBER RING TRANSITION STATE

After enol-intermediate ENL1 is formed, it can be transformed into another enol structure (ENL2), which has a more favorable configuration for the final cyclization reaction. The ENL2 can be further transformed into ENL4, which might also be a structure leading to cyclization. All these transitions can be done by several rotations and bending motions. The activation energies of these transitions are about 50 kJ/mol (figure 7-8), which can be easily achieved at low temperatures.

Starting with two different enol structures, ENL2 or ENL4, there are two mechanisms for cyclization. For the ENL2, the aromatic C-OH bond and O-H bond in the enol structure will break first, then a water molecule is formed in transition state TS7. With the release of water, the rest of the structure collapsed into a ring. Therefore, the water released during cyclization is formed by the phenolic hydroxyl side group and the hydrogen in the enol structure (figure 7-9). However, the activation energy of this reaction is about 267 kJ/mol. It is too high to be achieved at approximately 250°C.

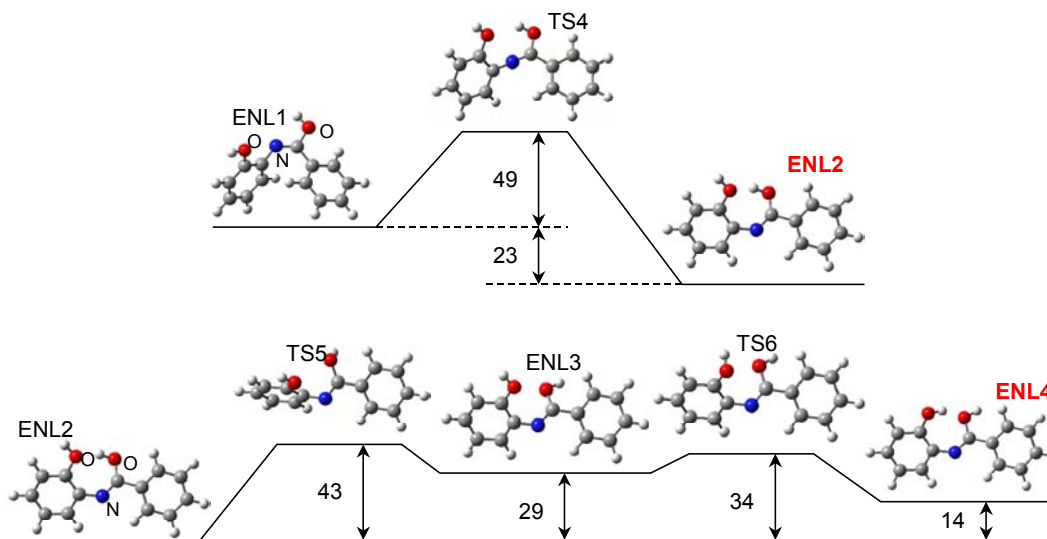


FIGURE 7-8. ENOL-STRUCTURE TRANSFORMATIONS BY ROTATION AND BENDING

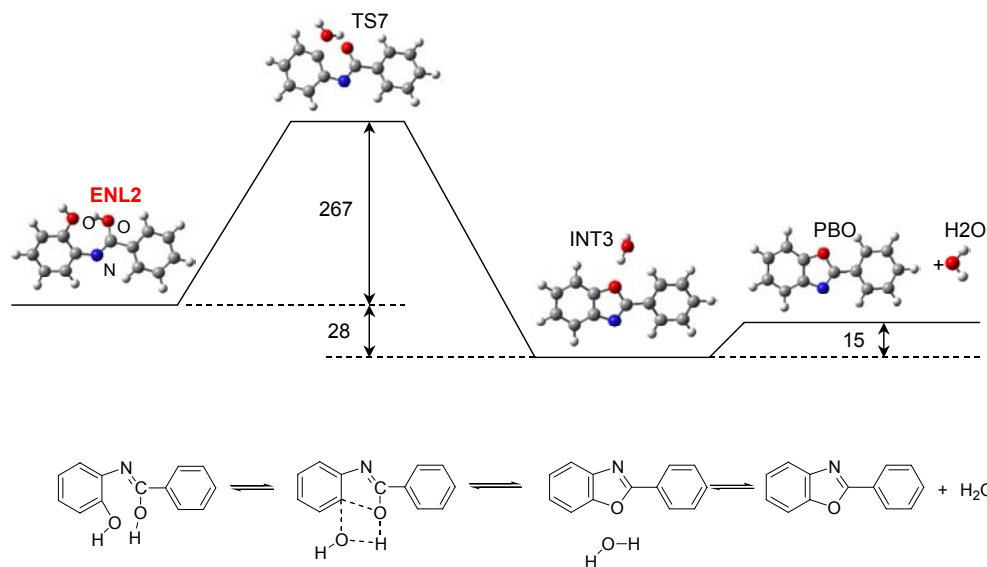


FIGURE 7-9. CYCLIZATION INTO PBO THROUGH ENL2 INTERMEDIATE

Another possible mechanism is through the ENL4 intermediate, as shown in figure 7-10. In this mechanism, the C-OH bond in an enol structure and O-H bond in a phenol group will break to form a water molecule and a biradical structure. After the water molecule is moved further away from the biradical structure, the benzoxazole ring will form. In addition, it seems that the water is not formed immediately after the bond breakage and needs a four-member ring transition state. The activation energy of this key reaction is only 126 kJ/mol, which can be easily achieved at 250°C. Therefore, it is believed that the cyclization proceeds by this mechanism through the ENL4 intermediate.

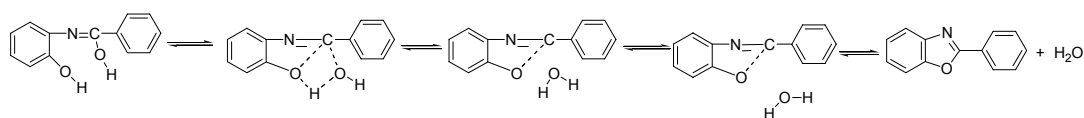
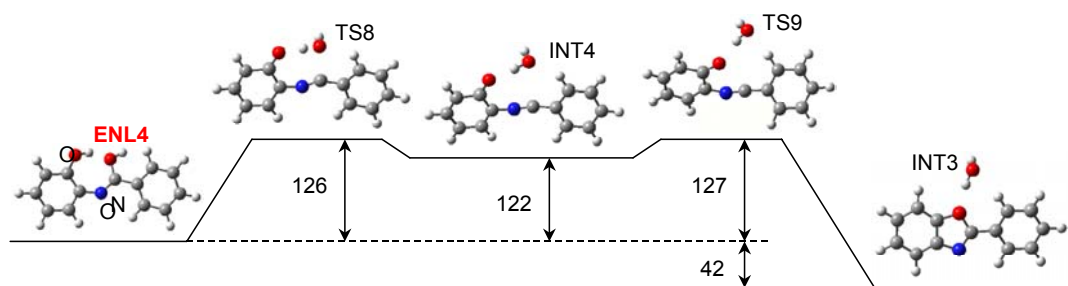


FIGURE 7-10. CYCLIZATION INTO PBO THROUGH ENL4 INTERMEDIATE

7.4 DISCUSSION.

The formation of the enol intermediate is the determining step in the thermal cyclization reaction of PHA. The hydroxyl side groups in PHA play a very important role in forming a six-member ring transition state that can lead to the formation of enol structure later. Because methoxy and phosphate PHAs cannot form this transition state through hydrogen bonds, they cannot cyclize in the same way as PHA. The water released during cyclization comes from the hydroxyl group in the enol structure and the hydrogen in the phenol groups.

8. CONCLUSIONS AND RECOMMENDATIONS.

8.1 CONCLUSIONS.

Fire is a potential hazard for human life, especially in an enclosed and inescapable area, such as high-rise buildings, submarines, ships, and aircraft cabins. Lightweight, high-performance polymeric materials offer many advantages in these applications, but their inherent flammability greatly increases the fire risk. By exploring the intrinsic relationships between polymer structure, composition, and their fire behavior and understanding the thermal decomposition and fire-resistant mechanisms of polymers, the goal of this research is to help identify and design new fire-safe polymeric materials.

8.1.1 Characterization of Thermal Decomposition and Flammability of Polymers.

Three significant milligram-scale experimental techniques, including pyrolysis GC/MS, simultaneous thermal analysis (STA) and pyrolysis-combustion flow calorimeter (PCFC), have been combined to fully characterize the thermal decomposition and flammability of different polymers and polymer composites. Each method stresses one specific aspect of the burning process of materials; therefore, they are complementary to each other. So far, the PCFC is the only accepted milligram-scale flammability test in the field of fire testing. It overcomes the deficiencies of existing bench-scale heat release tests, which require relatively large amount of samples. In the PCFC test, heat release capacity obtained by the oxygen consumption principle is found to be a real material property. As a result, beyond rank ordering and simple product comparison, PCFC can provide significant additional insights for new product development. The combination of these three small-scale tests is efficient for screening newly synthesized fire-safe materials. However, the fire behavior of materials is a very complicated issue. It is associated with not only many chemical reactions but also a series of physical processes. Therefore, the combination of PCFC method with some other large-scale flammability tests is especially important for a comprehensive evaluation.

The general thermal decomposition and flammability of different polymers ranging from highly flammable to highly fire resistant were studied. Generally, several important parameters can determine the ease of polymer combustion, including thermal stability, mass loss rate, the nature and properties of the decomposition products, and the char yield. The thermal stability of most polymers ranges from 200°C poly(methyl methacrylate (PMMA) to 600°C polybenzthiazole (PBZT), which greatly depends on the chemical structures of the polymers. Most aliphatic polymers with hydrocarbon backbones, especially the ones with bulky side groups, are less stable than wholly aromatic polymers. Most homopolymers decompose in a single step, but some polymers such as PMMA and poly(vinyl chloride) decompose by multiple steps. The heat of decomposition is another important parameter that is usually neglected due to the difficulty in measurements, especially for the aromatic high-charring polymers. Most polymers show an endothermic peak of 100 to 900 J/g. Very few polymers, such as charring halogenated polymers and polymers that can cyclize during decomposition, show exothermic peaks.

By analyzing the decomposition products at different pyrolysis conditions, the thermal decomposition mechanisms can be identified. Some addition polymers with 1,1-substitution (PMMA) and some polyaldehydes poly(oxymethylene) (POM) usually decompose by an

unzipping mechanism. Most addition polymers and condensation polymers decompose by random scission mechanism.

Flammability was found to be the integrated effect of the thermal decomposition process and the properties of decomposition products. Generally, nonburning heteroatoms such as halogens, O, N, S and P, aromatic rings, heteroaromatic rings, and any units that can lead to the formation of cross-linking or fused-aromatic rings, are the fundamental structural units for the fire-resistant polymers. All these structures can enhance char formation, reduce mass loss rate, reduce the amount of burning materials available, and produce volatiles with relatively low flammability.

In addition, the quantum computation results show that there is no simple correlation between bond dissociation energy and activation energy calculated by thermogravimetric analysis (TGA) data. The relatively low thermal stability of aliphatic polymers measured by TGA sometimes is not because they have weaker bonds than aromatic polymers, but due to the easy release of low-molecular-weight volatiles.

On the other hand, the total heat of combustion and heat release capacity of polymers can also be estimated either by combining the results from pyrolysis GC/MS and STA or the chemical structures and TGA. The calculated values agree well with the results directly measured from PCFC.

8.1.2 Inherently Fire-Resistant Polymers.

The most efficient way to prevent polymer combustion is to design inherently fire-resistant polymers that have high thermal stability, resistance to the spread of flame, and low burning rate, even under high heat flux.

8.1.2.1 Poly(hydroxyamide) and Its Derivatives.

Poly(hydroxyamide) (PHA) and some of its derivatives are potential candidates as solvent-processable, fire-resistant polymers. PHA and its halogen derivatives have extremely low flammability. They can totally cyclize into a poly(benzoxazole) (PBO) structure when heated to 250°C. Methoxy PHA is more thermally stable, but it exhibits higher flammability due to the main-chain scission at approximately 360°~400°C. Phosphinate or phosphate PHAs (PHA-10 and -11) are very flammable due to the extensive cleavage of fuel-forming phosphinate and phosphate groups. However, the flammability of copolymers formed by the combination of different side groups is greatly reduced.

Roughly, the thermal decomposition process of all the PHAs can be divided into two stages. In the first stage (below 500°C), small molecules such as water, methanol, phosphinates, or phosphates, as well as their ester fragments, are released to form some quasi-PBO structures. In the second stage (above 500°C), the random scission of the polymer backbone with some benzoxazole rings will occur. Most PHAs show an endothermic peak at low temperatures, but due to different mechanisms such as cyclization (PHA), melting (methoxy PHA), and decomposition (phosphate PHAs). Halogenated PHA-3 and -5 show a distinct exothermic decomposition peak at high temperatures due to the formation of HBr and some cross-linking

reactions. However, PHA-1 shows a mixed endo- and exothermic behavior during high-temperature decomposition. Infrared spectroscopy, elemental analysis, and pyrolysis GC/MS all prove that the first decomposition stage of PHA-1 corresponds to cyclization to PBO. It was also found that the major decomposition products of most PHAs (except for phosphinate or phosphate PHAs) are CO, CO₂, H₂O, HCN, and a small amount of aromatic compounds.

The low-flammable volatiles, low mass loss rates and high char yields are the major reasons for the low flammability of most PHAs. In addition, the endothermic cyclization of PHA and release of water might also increase the energy needed to sustain the whole combustion process. Differently from the complete cyclization of PHA and halogenated PHA, methoxy-, phosphinate- or phosphate-substituted PHAs can only partially cyclize into PBO structures.

8.1.2.2 Aromatic Polyarylates, Copolymers, and Blends.

Aromatic polyarylates make up another group of polymers with enhanced fire resistance. The three polyarylates based on bisphenol A (BPA), 1,1-dichloro-2,2-bis(4-hydroxy-phenyl)ethylene (BPC II), and 4, 4'-dihydroxy-3-ethoxy-benzylidenoacetophenone (Chalcon II) are very thermally stable up to at approximately 370°C. However, the introduction of bulky side groups or halogens in Chalcon II or BPC II can greatly reduce their thermal stability. It was found that BPC II-polyarylate is an extremely fire-resistant thermoplastic with a char yield of more than 50% and dramatically low heat release rate and total heat released. Chalcon II-polyarylate is an ultraviolet (UV)/visible-sensitive polymer. It also had a relatively low heat release rate and high char yield. However, the photo-cross-linking formed after UV/visible exposure had no effect on its flammability.

The low flammability of Chalcon II-polyarylate was mainly due to its high char yield and low mass loss rate. However, the halogenated volatiles released by BPC II-polyarylate also contribute to its exceptional fire resistance. It is believed that the C=C bonds in both polymers can facilitate the char formation. The BPC-II unit is an especially valuable source for generating of char and HCl.

Copolymerization or blending of two polymers with different thermal decomposition behavior can efficiently adjust the flammability of the polymers. The total heat of combustion of polyarylate copolymers or blends was found to change linearly with the composition, but the change of peak heat release rate and char yield also greatly depends on the chemical structure of the components. Some synergetic effect was observed in some copolymers or blends, such as the blends of BPA-/BPC II-polyarylates or polysulfone (PSF)/BPC II-polyarylate. The results indicate that by adding only a very small amount of a low-flammable component such as BPC-II polyarylate, the heat release rate can be dramatically reduced. It was also found that at high content of BPC II-arylate units (>67 mol%), the flammability of the copolymers remains low and independent of the structure of the other component. Therefore, the BPC II unit is really an efficient flame-retardant agent for copolymers and blends.

In all, the ideal fire-resistant polymers have the following characteristics: high decomposition temperature, low amount and release rate of volatile fuels, low heat of combustion of volatiles, high char yield, endothermic phase transition or decomposition, and release of chemical flame-retardant molecules (halogen, water, etc.).

8.1.3 Effects of Flame-Retardant Additives and Correlations Among Different Flammability Tests.

Flame retardants are widely used in the industry to reduce polymer flammability. Recently, due to some environmental concerns, searching for nonhalogenated flame retardants has become a major interest. In addition, evaluation of the efficiency of different flame retardants and how these flame retardants act in a fire still remain complex topics.

It was found that inert fillers can reduce the flammability, mainly by its nonburning property (mass-dilution effect) and promoting char formation. However, the addition of inert fillers can also change the physical properties of the materials such as thermal conductivity, density, and heat capacity that will affect the ignition and burning characteristics of the exposed surface. Therefore, the flame-retardant effect of the inert fillers in the Ohio State University (OSU) and cone calorimeter tests sometimes was not seen as dramatically as in PCFC tests.

Halogenated flame retardants with or without antimony compound can reduce the flammability by the inefficient combustion in the gas phase. The only disadvantages were that the thermal stability of the materials was decreased and considerable corrosive smoke was generated. However, the flame-retardant effects of the halogenated additives were not significant in the PCFC test.

Polymer-clay nanocomposites are a new group of flame-retardant materials. However, the clay can only slow the heat release rate without changing the total heat released. The mechanism is purely based on the condensed-phase inhibition.

The phosphorus-based additive is another group of promising flame retardants. They can form an excellent foamy char barrier and, at the same time, reduce the gas-phase combustion efficiency.

Depending on the composition, shape, form, and application of materials, different test methods are required to ensure valid and accurate results. However, the results from one method generally cannot be directly related to the other due to different operating principles and experimental conditions. It was found that only for pure polymers, a relatively good correlation among PCFC, OSU, and cone calorimeter tests can be achieved. Polymer composites that contain flame retardants or inert fillers showed different flammability results in different tests. There are several possible reasons. First, PCFC is not a direct flame-combustion test. In this test, the materials are first pyrolyzed at a controlled heating rate, and then the pyrolysis gases produced are totally oxidized in a separate high-temperature furnace. Therefore, the heat generated during combustion cannot be reflected back to the burning surface and cannot affect the further decomposition of the materials, which is different from the situation in a real fire. Secondly, due to the complete oxidation in PCFC, the effects of the additives, such as halogenated additives that mainly act in the gas phase, cannot be achieved. As a result, the flame-retardant effects of these additives will be underestimated. However, OSU and cone calorimeter tests are real flame-combustion tests, and an interactive combustion cycle can be formed during burning. Therefore, any changes in condensed phase, gas phase or heat feedback will all be coordinately reflected in the overall flammability results.

Nonetheless, because the PCFC method is more sensitive to the chemical structures of the materials, it is still a good screening tool for the pure polymers without additives or inert fillers. However, OSU and cone calorimeter tests are the better flammability tests for composite materials.

8.1.4 Structure, Composition, and Flammability Relationships.

There are many factors that can affect polymer flammability, such as the chemical and physical characteristics of the polymers and specific burning conditions. However, the most important factor is the chemical structure of the polymers.

It was found that introducing aromatic or heteroaromatic rings and heteroatoms into the polymer main chain can efficiently reduce polymer flammability. The silicon- or halogen-based comonomers that have relatively low heat of combustion on their own can be used as reactive flame-retardant additives to adjust polymer flammability systematically. The silicon-based inorganic network structure can greatly promote the char formation.

Different side groups also play a very important role in polymer thermal stability, decomposition process, and flammability. For example, the bulky hydrocarbon side groups in polymethacrylates can be easily cleaved off and released as fuels at low temperatures. However, due to the multiple decomposition stages, the decomposition temperature range of these polymers is extended. As a result, the decomposition rate and heat release rate sometimes can be reduced. On the other hand, the CN substituent was found to be a very efficient flame-retardant unit to be incorporated into a polymer structure to increase char formation and reduce flammability. Generally, the bulky flammable hydrocarbon side groups should be avoided in order to get good flame resistance.

It was also found that some other factors, such as molecular weight, free radicals, and composition, can affect polymer flammability. However, the effect of molecular weight is dependent on the thermal decomposition mechanisms of polymers. For the polymers that decompose by an unzipping mechanism, such as PMMA, the molecular weight does have a big effect on their thermal decomposition and flammability due to different chain-scission initiation mechanisms. However, for the polymers that decompose by random chain-scission mechanism, the molecular weight does not have a big effect on their thermal decomposition and flammability. The introduction of TEMPO can slightly delay the thermal decomposition of polymers if TEMPO can remain in solid phase without volatilization. For the copolymers and blends of PMMA/ polystyrene(PS), the total heat of combustion generally changes linearly with composition, but the heat release capacity changes sluggishly until the copolymers or blends contain more than 50% of PS.

In all, the ideal fire-resistant polymers have the following characteristics: high decomposition temperature, low amount and release rate of volatile fuels, low heat of combustion of volatiles, high char yield, endothermic phase transition or decomposition, and release of flame-retardant molecules such as water or halogenated molecules.

8.1.5 Thermal Cyclization Mechanism of PHA.

Previous experimental results show that PHA can completely cyclize into PBO around 250°~400°C, but its methoxy and phosphate derivatives exhibit different behaviors upon heating. To understand how the cyclization of PHA occurs, an ab initio B3LYP method and 6-31G (d,p) basis set were used to investigate the thermal cyclization pathway of PHA. It was found that the formation of the enol intermediate is the rate-determining step during cyclization. The hydroxyl side groups in PHA play a very important role in forming a six-member ring transition state that can lead to the formation of an enol structure. Because methoxy and phosphate PHAs cannot form this transition state through hydrogen bonds, they cannot cyclize in the same way as PHA. The water released during cyclization comes from the hydroxyl group in the enol structure and the hydrogen in the phenol groups.

8.2 RECOMMENDATIONS.

How to reduce the fire risks in human life is a very old research topic. In this dissertation, a detailed study on the thermal decomposition and flammability of polymers was performed by using different methods. Some fundamental understanding of the thermal decomposition and fire-resistant mechanisms was also proposed. However, considering the complex issues involved in a fire, there are still many aspects to be explored in the future.

Establishing the PCFC method was a big advance in measuring heat release rate appropriate for normal laboratory use. It provides quantitative information useful for polymer development. Therefore, it has potential uses for screening, quality control, and production monitoring. However, despite the large amount of research done so far, more research on instrument development and utilization should be done in the years to come. One important aspect that should be focused on is applying the PCFC method to composite materials. Currently, only for pure polymer systems without flame retardants or inert fillers, it correlates well with the other two bench-scale flammability tests—OSU and cone calorimeter tests. This application limitation is mainly due to the separation of pyrolysis and combustion processes and the nonflame but complete oxidation process. Therefore, the experimental conditions used in the PCFC method do not exactly reflect realistic fire conditions. To improve this method, the instrument needs to be further modified, such as introducing a real flame in a microfurnace where both pyrolysis and combustion can be performed simultaneously. In addition, several important aspects should also be addressed. For example, standard operational procedures need to be clarified to improve validity of the measurements and rank different products according to their performance. Micro-scale, bench-scale, and full-scale correlations should be investigated, especially for polymer composites. Real-time analysis of gas species during combustion can be used to verify the effect of halogenated additives. For the purpose of valid rank ordering, a fire characteristic index that integrates several fire-performance parameters (such as the ratio of peak heat release rate divided by the time to ignition) should be identified to collectively address the flammability of materials.

During the last 30 years, many inherently fire-resistant polymers with different structures have been developed, but only a few have been commercialized due to their high cost and difficulty in processing. Because many fire-resistant structures such as different heteroaromatic rings have been explored, designing some exotic expensive structures would not be realistic. The imminent project is how to reduce cost and balance different properties such as flammability,

processability, and mechanical properties so that all the fire-resistant polymers that have been successfully developed in the laboratory can be used in real life. Copolymerization and blending of different polymers with different thermal decomposition and flammability could be an ideal solution for this problem. It was found that by introducing only a small amount of fire-resistant components, the heat release rate can be dramatically reduced. On the other hand, properly selecting the other component can tailor some other properties to meet special requirements. For example, PHA was found to be a good fire-resistant polymer, but it is very expensive and can only be processed in solution. If some chain-distorting groups such as bisphenol A, sulphone, and iso-aramide units are incorporated, the copolymers formed might be able to be melt-processed at a proper composition. In addition, introducing chlorobisphenol C units into different aromatic polymers and polymer blends would also be an efficient way to reduce both polymer flammability and the amount of halogens inside polymers. These systems would also be useful to study whether there is one clear relationship between composition and flammability for all the copolymers and blends. In all, identifying the fire-resistant units and properly combining them with other units to get the desired properties should be the most efficient way to design new fire-safe polymers.

Current environmental pressures require the development of new environmental-friendly flame retardants to replace the halogenated additives, which are the most efficient and used in the largest volume so far. Although some new phosphorus- or silicon-based additives have been developed as the substituents, they are not as efficient as the halogenated additives. Therefore, searching for both environment-friendly and efficient flame retardants is still a very promising research direction, especially in the industry. However, if only a single element is considered, the choices are pretty much limited. To achieve the maximum efficiency and reduce the amount of addition, the combination of different additives need to be considered. Because different additives act in different mechanisms and have different effects on different polymer systems, some fundamental understanding of the flame-retardant mechanisms of these additives need to be applied when designing new systems. For example, the combination of gas-phase and condensed-phase inhibitions of halogen-P systems should be very efficient. In addition, how to induce polymer cross-linking and char formation by special chemical reactions is another possible way to reduce polymer flammability.

Although some factors that can affect polymer flammability have been preliminarily studied, more research needs to be conducted to further confirm the final conclusions. For example, the effect of TEMPO radical on the flammability of PS is not significant due to the volatilization of TEMPO at low temperatures. To avoid this problem, larger stable radicals can be used. In addition, it has been proposed that the molecular weight of polymers, which decompose by an unzipping mechanism, will affect their thermal decomposition and flammability. However, only PMMA was studied in this research. More polymers such as POM and poly(α -methyl styrene) with the same decomposition mechanism need to be studied to prove the validity of this conclusion. Furthermore, the threshold molecular weight of PMMA also needs to be identified. It was also found that Nomex[®] has exceptional flame resistance compared to Kevlar[®], although they have the same composition and are both aramides. The only difference between them is the para or iso linkage in amide groups. This observation raises one important question: Does the iso-type polymers always have lower flammability than para-type polymers? The investigation of some other type of polymers with para and iso structures will help clarify this question. In

addition, the structural integrity of materials during burning is another important issue. Therefore, studies of the residual mechanical properties of materials during decomposition are also of great significance.

Using molecular modeling to further understand the thermal decomposition and fire-resistance mechanisms still needs to be strengthened. Several fundamental aspects need to be studied. For example, it was found that there is no simple correlation between the bond dissociation energy calculated by molecular modeling and the activation energy calculated by TGA data. This result seems contradictory to the belief that the activation energy should be directly related to the bond dissociation energy of the weakest bond because the thermal decomposition is supposed to be initiated by the breaking of the weakest bond. However, it also raises a question of what the activation energy calculated by TGA represents. Generally, the TGA experiments measure the weight loss, which does not directly correspond to a single bond scission, especially for the polymers that decompose by random-chain scission mechanism. In these polymers, the TGA will not show a significant weight loss until small volatiles are formed by multiple bond scissions. Therefore, the activation energy obtained is the consequence of the behavior of many bonds. In addition, for some high-charring aromatic polymers, the assumption of first-order decomposition for activation energy calculation does not hold. As a result, searching for a better model to calculate the activation energy should be done first. On the other hand, due to the limitation of computational methods, the experimental and calculation results need to be combined to get a valid explanation. Some calculations on high-temperature decomposition to predict various decomposition products would be valuable for future research.

9. REFERENCES.

1. Troitzsch, J., *International Plastics Flammability Handbook*, Hanser, New York, 1983.
2. Brossas, J., *Polym. Degrad. and Stability* **1989**, 23, pp. 313-325.
3. Gann, R.G., Dipert, R.A., and Drews, M.J., *Encyclopedia of Polymer Science and Engineering*, 2nd ed., John Wiley & Sons, New York, 1987, Vol. 7.
4. Sarkos, C.P., In *ANTEC Technical Conference Proceedings*, 1996, 54 (3), p 3068.
5. Lyon, R.E., In *International SAMPE Symposium and Exhibition (Proceedings)*, 1996, 41(I), p. 344.
6. Landrock, A.H., *Handbook of Plastics Flammability and Combustion Toxicology*, Noyes publication, Park Ridge, New Jersey, 1983.
7. Cullis, C.F. and Hirschler, M., *The Combustion of Organic Polymers*, Clarendon Press, Oxford, 1981.
8. Lyon, R.E., In *International SAMPE Symposium and Exhibition (Proceedings)*, 1997, 42(II), pp. 1325-1334.
9. Glassman, I., *Combustion*, 3rd ed., Academic Press, New York, 1996.
10. Nelson, G.L., In *Fire and Polymers II: Materials and Tests for Hazard Prevention*, Nelson, G.L., ed., American Chemical Society, Washington, D.C., 1995, Vol. 599, pp. 1-26.
11. Hartzell, G.E., In *Fire Protection Handbook*, 18th ed., Cote, A.E., ed., National Fire Protection Association, Quincy, MA, 1997, Vol. Chapter 2.
12. UL 94, Underwriters Laboratories, Northbrook, IL, 1991.
13. ASTM E 84, *Standard Test Method for Surface Burning Characteristics of Building Materials*, American Society for Testing and Materials, Philadelphia.
14. ASTM E 662, *Standard Test Method for Optical Density of Smoke Generated by Solid Materials*, American Society for Testing and Materials, Philadelphia.
15. ASTM D 2863, *Standard Test Method for Measuring the Minimum Oxygen Concentration to Support Candle-Like Combustion of Plastics (Oxygen Index)*, American Society for the Testing of Materials, Philadelphia, 2000.
16. Babrauskas, V. and Peacock, R.D., *Fire Safety J.*, **1992**, 18, pp. 255-272.
17. Babrauskas, V., In *SFPE Handbook of Fire Protection Engineering*, 2nd ed., Dinunno, P.J., ed., National Fire Protection Association, Quincy, MA, 1995; p. 3.

18. "FAA Fire Test Handbook," FAA report, DOT/FAA/CT-89/15, Washington, DC, September 1990.
19. Scudamore, M.J., Briggs, P.J., and Prager, F.H., *Fire Mater.*, **1991**, *15*, pp. 65-84.
20. Frazer, A.H., *High Temperature Resistant Polymers*, John Wiley & Sons, New York, 1968.
21. Lin, S.-H., Li, F., Cheng, S.Z.D., and Harris, F.W., *Macromolecules*, **1998**, *31*, pp. 2080-2086.
22. Mallakpour, S.E., Hajipour, A.R., Mahdavian, A.R., and Khoei, S., *J. Appli. Polym. Sci.*, **2000**, *76*, pp. 240-248.
23. Chang, J.-H., Chen, M.J., and Farris, R.J., *Polymer*, **1998**, *39*, p. 5649.
24. Sirkecioglu, O., Tunca, A.A., Talinli, N., and Akar, A., *Angew. Makrom. Chem.*, **1999**, *271*, p. 8-1.
25. Gajiwala, H.M. and Zand, R., *Polymer*, **2000**, *41*, pp. 2009-2015.
26. Barbosa, V.F.F., MacKenzie, K.J.D., and Thaumaturgo, C., *Int. J. of Inorg. Mater*, **2000**, *2*, pp. 309-317.
27. Kumar, D., Gupta, A.D., and Khullar, M., *J. Polym. Sci. Part A: Polym. Chem.*, **1993**, *31*, pp. 2739-2745.
28. Lyons, J.W., *The Chemistry and Uses of Flame Retardants*, John Wiley & Sons, New York, 1970.
29. Dubois, A.B., *Fire and Smoke: Understanding the Hazards*, National Academy Press, Washington, D.C., 1986.
30. Bolger, R., *Ind. Minerals*, **1996**, *340*, p. 29.
31. Hirschler, M.M., In *Flame Retardants '96*, Grayson, S.J., ed., Interscience Communications, London, 1996, p. 199.
32. Hornsby, P.R., *Fire Mater*, **1994**, *18*, p. 269.
33. Hornsby, P.R., *Macrol. Symp.*, **1996**, *108*, p. 203.
34. O'Driscoll, M., *Ind. Minerals*, **1994**, *318*, p. 23.
35. Hilado, C.J., *Flammability Handbook for Plastics*, 3rd ed., Technomic Publication, Westport, CT, 1982.
36. Green, J., In *Fire Retardancy of Polymeric Materials*, Wilkie, C.A., ed., Marcel Dekker Inc., New York, 2000, p. 147.

37. Lee, F.T., Green, J., and Gibilisco, R.D., *J. Fire Retard. Chem.*, **1982**, 9, p. 232.
38. Allen, C.W., *J. Fire Sci.*, **1993**, 11, p. 320.
39. Green, J.J., *Fire Sci.*, **1994**, 12, p. 257.
40. Inoue, K., Nakamura, H., Ariyoshi, S., Takagi, M., and Tanigaki, T., *Macromolecules*, **1989**, 22, p. 4466.
41. Montaudo, G., Scamporrino, E., and Vitalini, D., *J. Polym. Sci. Part A: Polym. Chem.*, **1983**, 21, p. 3321.
42. Horacek, H. and Grabner, R., *Polym. Degrad. and Stability*, **1996**, 54, p. 205.
43. Horacek, H. and Grabner, W., *Makromol. Chem., Macromol. Symp.*, **1993**, 74, p. 271.
44. Iji, M. and Serizawa, S., *Polym. Adv. Technol.*, **1998**, 9, p. 593.
45. Kambour, R.P., Klopper, H.J., and Smith, S.A., *J. Appli. Polym. Sci.*, **1981**, 26, p. 847.
46. Zaikov, G.E. and Lomakin, S.M., *Polym. Degrad. Stabil.*, **1996**, 54, p. 223.
47. Allen, N.S., Edge, M., and Corrales, T., *Polym. Degrad. Stabil.* **1997**, 56, p. 125.
48. Chao, T.C., Sarmah, S.K., Boisvert, R.P., Burns, G.T., Katsoulis, D.E., and Page, W.C., In *Proceedings of 43rd International SAMPE Symposium*, Anaheim, 1998, pp. 1029-1041.
49. Bolf, A.G. and Lichtenhan, J.D., *Am. Chem. Soc. Polym. Prepr*, **1994**, 35, pp. 527-528.
50. Gilman, J.W., Jackson, C.L., and Morgan, A.B., *Chem. Mater*, **2000**, 12, pp. 1866-1873.
51. Giannelis, E.P., *Adv. Mater.*, **1996**, 8, p. 29.
52. Allen, C.W., *Trends in Polymer Science*, **1994**, 2, p. 342.
53. Mark, J.E., Allcock, H.R., and West, R., *Inorganic Polymers*, Prentice Hall, New Jersey, 1992.
54. Zingde, G., In *ANTEC Technical Conference Proceedings*, 1996, 54 (3), p. 3004.
55. Van Krevelen, D.W., *Polymer*, **1975**, 16, p. 615.
56. Levchik, S. and Wilkie, C.A., In *Fire Retardancy of Polymeric Materials*, Wilkie, C.A., ed., Marcel Dekker Inc., New York, 2000.
57. Kelen, T., *Polymer Degradation*, Van Nostrand Reinhold, New York, 1983.
58. Kashiwagi, T. and Inabi, A., *Ploym. Degrad. Stabil.*, **1989**, 26, pp. 161-184.

59. Haken, J.K., *J. of Chromatography A*, **1998**, 825, pp. 171-187.
60. Chiu, J., In *Applied Polymer Analysis and Characterization: Recent Development in Techniques, Instrumentation, Problem Solving*, Mitchell, J.J., ed., Hanser, New York, 1987; pp. 175-212.
61. Factor, A., In *Fire and Polymers: Hazards Identification and Prevention*, Nelson, G.L., ed., American Chemical Society, Washington, DC, 1990, pp. 274-287.
62. ASTM E 1354, *Standard Test Method for Heat and Visible Smoke Release Rates for Materials and Products Using an Oxygen Consumption Calorimeter*, American Society for the Testing of Materials, Philadelphia, 1999.
63. ASTM E 906, *Standard Test Method for Heat and Visible Smoke Release Rates for Materials and Products*, American Society for the Testing of Materials, Philadelphia, 1999.
64. Lyon, R.E. and Walters, R.N., In *International SAMPE Symposium and Exhibition (Proceedings) 45th*, 2000, 45(2), pp. 1721-1729.
65. Walters, R.N. and Lyon, R.E., In *International SAMPE Symposium and Exhibition (Proceedings) 42nd*, 1997, 42(2), pp. 1335-1344.
66. Lyon, R.E., Walters, R.N., and Gandhi, S., In *9th Annual BCC Conference on Flame Retardancy*, Stamford, CT, 1998.
67. Walters, R.N. and Lyon, R.E., *J. Appli. Polym. Sci.*, **2003**, 87, pp. 548-563.
68. Beran, J.A. and Kevan, L., *J. Chem. Phys.* **1969**, 73, p. 3866.
69. Alberti, R., Genoni, M.M., and Pascual, C.J., *Int. J. Mass. Spectrom. Ion Phys.* **1974**, 14, p. 89.
70. Fitch, W.L. and Sauter, A.D., *Anal. Chem.* **1983**, 55, pp. 832-835.
71. Benson, S.W., *Thermochemical Kinetics*, John Wiley & Sons, New York, 1968.
72. Lyon, R.E., *Polym. Degrad. Stabil.*, **1998**, 61, p. 201.
73. Van Krevelen, D.W., *Properties of Polymers*, 3rd ed., Elsevier, Amsterdam, 1990.
74. Kohn, W. and Sham, L.J., *Physical Review*, **1965**, 140, p. 1133.
75. Becke, A.D., *J. Chem. Phys.*, **1993**, 98, p. 5648.
76. Hehre, W.J, Ditchfield, R., and Pople, J.A., *J. Chem. Phys.*, **1972**, 56, p. 2257.
77. Foresman, J.B. and Frisch, E., *Exploring Chemistry With Electronic Structure Methods*, 2nd ed., Gaussian Inc., Pittsburgh, PA, 1996.

78. *CRC Handbook of Chemistry and Physics*, 79th ed., CRC Press, Cleveland, OH, 1998-1999.
79. Yang, H.H., *Aromatic High-Strength Fibers*, John Wiley & Sons, New York, 1989.
80. Wolfe, J.F. and Arnold, F.E., *Macromolecules*, **1981**, *14*, p. 909.
81. Hunsaker, M.E., Price, G.E., and Bai, S.J., *Polymer* **1992**, *33*, p. 2128.
82. Brinker, K.C., Cameron, D.D., and Robinson, I.M., U.S. Patent 2,904,537, 1959.
83. Moyer, W.W., Cole, C., and Anyos, T. *J. Polym. Sci, Part A: Polym. Chem.* **1965**, *3*, p. 2107.
84. Kubota, T. and Nakanishi, T., *J. Polym. Sci, Part B: Polym. Phys.* **1964**, *2*, p. 655.
85. Maruyama, Y., Oishi, Y., Kakimoto, M., and Iami, Y., *Macromolecules*, **1988**, *21*, p. 2305.
86. Joseph, W.D., Mercier, R., Prasad, A., Marand, H., and McGrath, J.E., *Polymer* **1993**, *34*, p. 866.
87. Hsiao, S.H. and Dai, L.R., *J. Polym. Sci, Part A: Polym. Chem.* **1999**, *37*, p. 2129.
88. Chaudhuri, A., Min, B.Y., and Pearce, E.M., *J. Polym. Sci, Part A: Polym. Chem.*, **1980**, *18*, p. 2949.
89. Khanna, Y.P., Pearce, E.M., Forman, B.D., and Bini, D.A., *J. Polym. Sci, Part A: Polym. Chem.*, **1981**, *19*, p. 2799.
90. Whang, W.T. and Pearce, E.M., *J. Polym. Sci, Part A: Polym. Chem.*, **1987**, *25*, p. 171.
91. Kapuscinski, M. and Pearce, E.M., *J. Polym. Sci, Part A: Polym. Chem.*, **1984**, *22*, p. 3999.
92. Pearce, E.M., Weil, E., and Barinov, V.Y., In *Fire and Polymers: Materials and Solutions for Hazard Prevention*, ACS Symposium Series 797, Wilkie, C.A., ed, Am. Chem. Soc., Washington, D.C., 2001, pp. 37-48.
93. Khanna, Y.P. and Pearce, E.M., *J. Appli. Polym. Sci.*, **1982**, *27*, p. 2053.
94. Khanna, Y.P. and Pearce, E.M., *J. Polym. Sci, Polym. Chem. Ed.*, **1981**, *19*, pp. 2817-2834.
95. Karydas, A.C., Kapuscinski, M., and Pearce, E.M., *European Polymer J.*, **1983**, *19*, p. 935.
96. Karydas, A.C., Whang, W.T., and Pearce, E.M., *J. Polym. Sci, Part A: Polym. Chem.* **1984**, *22*, p. 847.

97. Kim, S.S. and Pearce, E.M., *Makromol. Chem. Suppl.*, **1989**, *15*, p. 187.
98. Kim, S.S., Pearce, E.M., and Kwei, T.K., *Polym. Adv. Technol.*, **1990**, *1*, pp. 49-73.
99. Gao, C. and Kantor, S.W., In *ANTEC Technical Conference Proceedings*, 1996, 54(3), p. 3072.
100. Zhang, H., Westmoreland, P.R., and Farris, R.J., In *Proceedings of the American Chemical Society Division of Polymeric Materials: Science and Engineering, Fall Meeting*, Chicago, IL, 2001, 85(2), pp. 463-464.
101. Musto, P., Karasz, F.E., and Macknight, W.J., *Polymer*, **1993**, *34*, p. 2934.
102. Rusanov, A.L., *Prog. Polym. Sci.*, **1994**, *19*, pp. 589-662.
103. Brzozowski, Z.K., Porejko, S., Kiekiewicz, J., and Kaczorowski, J., Pol. Patent 76,755, 1974.
104. Brzozowski, Z.K., *Vistnik Lviv Polytechnic University (Ukraine)(English)*, **2000**, *388*, pp. 92-104.
105. Brzozowski, Z.K., *Polimery (English)*, **1984**, *29*, pp. 415-421.
106. Porejko, S., Brzozowski, Z.K., and Maczynski, C., Polish Patent 48, 893, 1964.
107. Porejko, S. and Wielgosz, Z., *Polimery (English)*, **1968**, *13*, p. 55.
108. Brzozowski, Z.K., Petrus, J., and Dudczynski, J., *Macromol. Sci. Chem.*, **1979**, *A13*, 875-886, pp. 887-897.
109. Brzozowski, Z.K. and Jozawik, B., *J. Photochem.* **1986**, *35*, pp. 341-352.
110. Brzozowski, Z.K., Zadrozna, I., and Lato, E., *Polymers and Polymer Composites*, **1994**, *2*, pp. 253-258.
111. Brzozowski, Z.K. and Karwowski, P., *Macromol. Reports*, **1995**, *A32*, pp. 1263-1270.
112. Zadrozna, I., Brzozowski, Z.K., Noniewicz, K., and Dyrda, M., *Polymers and Polymer Composites*, **1997**, *5*, pp. 57-62.
113. Brzozowski, Z.K., and Pijewski, M. *Polimery (English)* **1998**, *43*, pp. 720-727.
114. Factor, A. and Orlando, C.M., *J. Polym. Sci., Chem. Ed.*, **1980**, *18*, pp. 579-592.
115. Zhang, H., Coughlin, E.B., Westmoreland, P.R., Farris, R.J., Plichta, A., and Brzozowski, Z.K., *Polymer Preprints* **2002**, *43(1)*, pp. 340-341.
116. Ramirez, M.L., M.S. thesis, University of Puerto Rico, 2000.

117. Stoliarov, S.I. and Westmoreland, P.R., *Mechanism of the Thermal Decomposition of Bisphenol C Polycarbonate: Nature of Its Fire Resistance*, Manuscript, 2002.
118. Lyon, R.E., In *Proceeding of the Third Triennial International Aircraft Fire and Cabin Safety Research Conference*, Atlantic City, NJ, 2001.
119. Stewart, J., *Synthesis and Characterization of Inherently Fire-Safe Polymers: Chlorinated Bisphenol Based Polymers and Polycarbodiimides*, Ph.D. dissertation, University of Massachusetts, Amherst, 1999.
120. Babrauskas, V., *J. of Fire Science*, **1986**, 4, pp. 148-159.
121. Tsuchiya, Y. and Mathieu, J.F., *Fire Safety J.* **1991**, 17, pp. 291-299.
122. Babrauskas, V., In *Heat Release in Fires*, Grayson, S.J., ed., Elsevier Applied Science, New York, 1992, pp. 583-590.
123. Bandyopadhyay, S., Giannelis, E.P., and Hsieh, A.J., In *ABSTR PAP AM CHEM S 219: 75-PMSE Part 2*, March 26, 2000.
124. Zerda, A., *Molecular and Nanoscale Reinforcement of Polymers*, Ph.D., University of Massachusetts, Amherst, 2002.
125. Filipczak, R.A. and Lyon, R.E., The Correlation of Heat Release Calorimetry Measurements, FAA report DOT/FAA/AR-TN02/104, November 2002.
126. Gilman, J.W., Jackson, C.L., Morgan, A.B., Harris, R., Manias, E., Giannelis, E.P., Wuthenow, M., Hilton, D., and Phillips, S.H., *Chem. Mater.*, **2000**, 12, pp. 1866-1873.
127. Mikkola, E. and Wichmann, I.S., *Fire and Materials* **1989**, 14, pp. 87-96.
128. Lyon, R.E., *Fire and Materials*, **2000**, 24, pp. 179-186.
129. Lyon, R.E., In *CUMIRP, Fall 2002*, University of Massachusetts, Amherst, 2002.
130. McMillen, D.F. and Golden, D.M. *Ann. Rev. Phys. Chem.* **1982**, 33, pp. 493-532.
131. Kissinger, H.E., *Anal. Chem.*, **1957**, 29, p. 1702.
132. Hirata, T., Kashiwagi, T., and Brown, J.E., *Macromolecules*, **1985**, 18, pp. 1410-1418.
133. Whiteley, R.H., Elliot, P.J., and Staggs, J.E., In *Proceedings of the Seventh International Flame Retardant 1996*, InterScience Communication Limited, England, 1996, pp. 71-78.
134. Best, S.A., Bianconi, P.A., and Merz, K.M.J., *J. Am. Chem. Soc.*, **1995**, 117, pp. 9251-9258.
135. Rzaev, J. and Penelle, J., *J. Polym. Sci. Part A: Polym. Chem.*, **2002**, 40, p. 836.

136. Hobbs, T., *New Routes to High Performance Fibers and Films*, Ph.D. dissertation, University of Massachusetts, Amherst, 2000.
137. Zheng, L., Farris, R.J., and Coughlin, E.B., *Macromolecules*, **2001**, *34*, pp. 8034-8039.
138. Mansky, P., Liu, Y., Huang, E., Russell, T.P., and Hawker, C.J., *Science*, **1997**, *275*, p. 1458.
139. Kashiwagi, T., Hirata, T., and Brown, J.E., *Macromolecules*, **1985**, *18*, pp. 131-138.
140. Kashiwagi, T., Inabi, A., and Brown, J.E., *Macromolecules*, **1986**, *19*, pp. 2160-2168.
141. Lyon, R.E., In *International SAMPE Symposium and Exhibition (Proceedings)*, 1997, v42(II), pp. 1325-1334.
142. Nyden, M.R., In *Fire Retardancy of Polymeric Materials*, Grand, A.F. and Wilkie, C.A., eds., Marcel Dekker Inc., New York, 2000, p. 501.
143. Berry, R.J., Ehlers, C.J., Burgess, D.R., Zachariah, M.R., Nyden, M.R., and Schwartz, M., *Theochem.-J. Mol. Struc.*, **1998**, *422*, pp. 89-98.
144. Nyden, M.R. and Gilman, J.W., *Comput. Theor. Polym. Sci.*, **1997**, *7*, pp. 191-198.
145. Stoliarov, S.I., Westmoreland, P.R., Nyden, M.R., and Forney, G.P., *Polymer* **2003**, *44*, p. 883-894.
146. Rotem, K., *Computational Quantum Chemistry Applied to NO_x Chemistry and New Fire-Resistant Polymers*, Ph.D. dissertation, University of Massachusetts, Amherst, 1999.
147. Stoliarov, S.I., Rotem, K., Zhang, H., and Westmoreland, P.R., In *CUMIRP Cluster F Meeting, Fall 2002*, University of Massachusetts, Amherst, 2002.

10. BIBLIOGRAPHY.

Gilman, J.W.; Ritchie, S.J., Kashiwagi, T., *Fire Mater.* **1997**, *21*, p. 23.

Hirschler, M.M., In *Fire and Polymers: Hazards Identification and Prevention*, Nelson, G. L., ed., American Chemical Society, Washington, DC, 1990, p. 462.

Horrocks, A.R., Tunc, M., Price, D., *Textile Prog.* **1989**, *18*, p. 1.

Kubisa, P., Corley, L. S., and Vogl, O., *J. Macromol. Sci. Chem.*, **1980**, *14*, pp. 1145-1169.

Kubisa, P., Teshirogi, T., Hatada, K., Corley, L.S., O., V. *Makromol. Chem.*, **1980**, *181*, p. 2267.

Lyon, R.E., "Solid-State Thermochemistry of Flaming Combustion," FAA report DOT/FAA/AR-99/56, p. 12, July 1999.

Nyden, M.R. and Noid, D.W., *Phys. Chem.*, **1991**, *95*, pp. 940-945.

Ostman, A.L. and Svensson, I.G., *Fire and Materials*, **1985**, *9*, pp. 176-184.

Rusanov, A.L., Tugushi, D.S., and Korshak, V.V., *Advances in Polyheteroarylenes Chemistry*, TGU Press, Tiflis, 1988.

Schwartz, L.D., Whiteley, R.H., Elliot, P.J., and Grand, A.F., In *International Aircraft Fire and Cabin Safety Research Conference*, Atlantic City, NJ, 1998.

Smith, E.E. *Fire Technology*, **1996**, *32*, pp. 333-347.

Vogl, O. and Hatada, K.J., *J. Polym. Sci., Polymer Lett. ed.*, **1975**, *B13*, p. 609.

Vogl, O., Miller, H.C., and Sharkey, W. H., *Macromolecules*, **1972**, *5*, p. 656.

Zhang, H., Coughlin, E.B., Westmoreland, P.R., Farris, R.J., Plichta, A., and Brzozowski, Z.K., *Polymer*, **2002**, *43(20)*, pp. 5463-5472.

APPENDIX A—SUPPLEMENTARY DATA

TABLE A-1. GROSS HEAT OF COMPLETE COMBUSTION OF SMALL ORGANIC COMPOUNDS

Formula	Name	Reference ^a (kJ/mol)	Calculated (1) ^b (kJ/mol)	Calculated (2) ^c (kJ/mol)
Inorganic substances				
C	Carbon (graphite)	393.5		
H ₂	Hydrogen (g)	285.8		
CO	Carbon monoxide (g)	283	209.5	393.5
H ₃ N	Ammonia (g)	382.8	380.2	428.7
H ₄ N ₂	Hydrazine (g)	667.1	507.0	571.6
Hydrocarbons				
CH ₄	Methane (g)	890.8	926.0	965.1
C ₂ H ₂	Acetylene (g)	1301.1	1091.5	1072.8
C ₂ H ₄	Ethylene (g)	1411.2	1345.0	1358.6
C ₂ H ₆	Ethane (g)	1560.7	1598.4	1644.4
C ₃ H ₆	Propylene (g)	2058	2017.4	2037.9
C ₃ H ₆	Cyclopropane (g)	2091.3	2017.4	2037.9
C ₃ H ₈	Propane (g)	2219.2	2270.9	2323.7
C ₄ H ₆	1,3-Butadiene (g)	2541.5	2436.4	2431.4
C ₄ H ₁₀	Butane (g)	2877.6	2943.4	3003
C ₅ H ₁₂	Pentane (l)	3509	3615.9	3682.3
C ₆ H ₆	Benzene (l)	3267.6	3274.4	3218.4
C ₆ H ₁₂	Cyclohexane (l)	3919.6	4034.9	4075.8
C ₆ H ₁₄	Hexane (l)	4163.2	4288.4	4361.6
C ₇ H ₈	Toluene (l)	3910.3	3946.9	3897.7
C ₇ H ₁₆	Heptane (l)	4817	4960.8	5040.9
C ₁₀ H ₈	Naphthalene (s)	5156.3	5203.9	5078.2
Alcohols and ethers				
CH ₄ O	Methanol (l)	726.1	716.5	679.3
C ₂ H ₆ O	Ethanol (l)	1366.8	1388.9	1358.6
C ₂ H ₆ O	Dimethyl ether (g)	1460.4	1388.9	1358.6
C ₂ H ₆ O ₂	Ethylene glycol (l)	1189.2	1179.4	1072.8
C ₃ H ₈ O	1-Propanol (l)	2021.3	2061.4	2037.9
C ₃ H ₈ O ₃	Glycerol (l)	1655.4	1642.4	1466.3
C ₄ H ₁₀ O	Diethyl ether (l)	2723.9	2733.9	2717.2
C ₅ H ₁₂ O	1-Pentanol (l)	3330.9	3406.4	3396.5
C ₆ H ₆ O	Phenol (s)	3053.5	3064.9	2932.6

TABLE A-1. GROSS HEAT OF COMPLETE COMBUSTION OF SMALL ORGANIC COMPOUNDS (Continued)

Formula	Name	Reference ^a (kJ/mol)	Calculated (1) ^b (kJ/mol)	Calculated (2) ^c (kJ/mol)
Carbonyl compounds				
CH ₂ O	Formaldehyde (g)	570.7	463.0	393.5
C ₂ H ₂ O	Ketene (g)	1025.4	882.0	787
C ₂ H ₄ O	Acetaldehyde (l)	1166.9	1135.5	1180.5
C ₃ H ₆ O	Acetone (l)	1789.9	1807.9	1967.5
C ₃ H ₆ O	Propanal (l)	1822.7	1807.9	1967.5
C ₄ H ₈ O	2-Butanone (l)	2444.1	2480.4	2754.5
Acids and esters				
CH ₂ O ₂	Formic acid (l)	254.6	253.5	285.8
C ₂ H ₄ O ₂	Acetic acid (l)	874.2	926.0	787
C ₂ H ₄ O ₃	Methyl formate (l)	972.6	716.5	679.3
C ₃ H ₆ O ₂	Methyl acetate (l)	1592.2	1598.4	1644.4
C ₄ H ₈ O ₂	Ethyl acetate (l)	2238.1	2270.9	2323.7
C ₇ H ₆ O ₂	Benzoic acid (s)	3226.9	3274.4	3218.4
Nitrogen compounds				
CHN	Hydrogen cyanide (g)	671.5	545.7	536.4
CH ₃ NO ₂	Nitromethane (l)	709.2	380.2	428.7
CH ₅ N	Methylamine (g)	1085.6	1052.7	1108
C ₂ H ₃ N	Acetonitrile (l)	1247.2	1218.2	1215.7
C ₂ H ₅ NO	Acetamide (s)	1184.6	1262.2	1215.7
C ₃ H ₉ N	Trimethylamine (g)	2443.1	2397.7	2466.6
C ₅ H ₅ N	Pyridine (l)	2782.3	2728.7	2682
C ₆ H ₇ N	Aniline (l)	3392.8	3401.2	3361.3

^a Reference values from CRC Handbook of Physics and Chemistry

^b Calculated values based on oxygen consumption principle

^c Calculated values based on atom additivity principle

TABLE A-2. NET HEAT OF COMPLETE COMBUSTION AND HEAT RELEASE CAPACITY OF POLYMERS

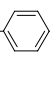
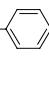
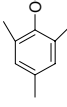
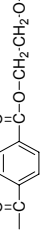
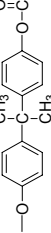
Polymers	Structure	Repeating Unit Composition	Mn (g/mol)	Char ^a (%)	Max. Mass Loss Rate ^a (%/s)	Net Heat of Combustion (kJ/g)			Heat Release Capacity (J/g-K)		
						PCFC ^b	Calc. (1) ^c	Calc. (2) ^d	PCFC ^b	Calc. (1) ^c	Calc. (2) ^d
HDPE	$-\text{CH}_2-\text{CH}_2-$	C_2H_4	28	0	6.4	42 ^e	44.89	45.38	1676 ^e	1724	1906
PP	$-\text{CH}_2-\text{CH}-$ CH_3	C_3H_6	42	0	5.23	41	44.89	45.38	1584	1409	1424
PS	$-\text{CH}_2-\text{CH}-$ 	C_8H_8	104	0	5.29	37	40.29	39.57	1199	1279	1256
POM	$-\text{CH}_2\text{O}-$	CH_2O	30	0	4.56	14	13.97	13.12	261	382	359
P(α -methyl styrene)	$-\text{CH}_2-\text{C}-$ CH_3 	C_9H_{10}	118	0	2.52	42	40.83	40.26	730	617	609
Nylon66	$-\text{C}(=\text{O})-(\text{CH}_2)_4-\text{C}(=\text{O})-\text{NH}-(\text{CH}_2)_6-\text{NH}-$	$\text{C}_{12}\text{H}_{22}\text{O}_2\text{N}_2$	198	0	3.45	28	34.92	34.84	648	723	721
PEO	$-\text{CH}_2-\text{CH}_2\text{O}-$	$\text{C}_2\text{H}_4\text{O}$	44	4	4.4	23	22.85	22.45	580	603	592
PPO		$\text{C}_8\text{H}_8\text{O}$	120	23	2.48	22	25.54	24.85	409 ^e	380	370
PET		$\text{C}_{10}\text{H}_8\text{O}_4$	192	8	3.7	17	20.08	18.86	393	446	419
PC		$\text{C}_{16}\text{H}_{14}\text{O}_3$	254	17	3.8	19	24.74	23.82	382	564	543

TABLE A-2. NET HEAT OF COMPLETE COMBUSTION AND HEAT RELEASE CAPACITY OF POLYMERS
(Continued)

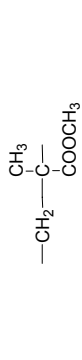
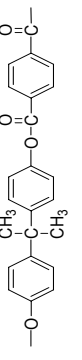
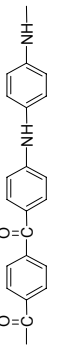
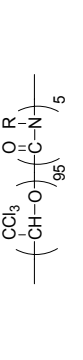
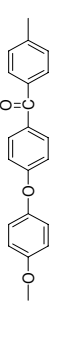
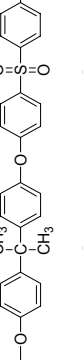
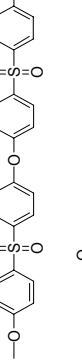
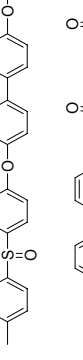
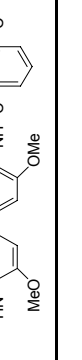
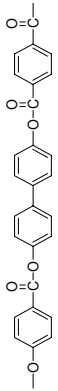
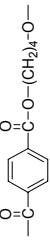
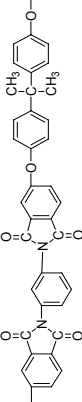
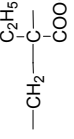
Polymers	Structure	Repeating Unit Composition	Mn (g/mol)	Char (%)	Max. Mass Loss Rate (%/s)	Net Heat of Combustion (kJ/g)		Heat Release Capacity (J/g-K)			
						PCFC	Calc. (1)	Calc. (2)	PCFC	Calc. (1)	Calc. (2)
PMMA		C ₅ H ₈ O ₂	100	0	2.06	23	25.14	24.51	376	311	303
BPA-polyarylate		C ₂₃ H ₁₈ O ₄	358	27	2.2	18	21.79	20.92	360	288	276
Kevlar®		C ₁₄ H ₁₀ O ₂ N ₂	238	32	1.96	15	18.62	17.88	292	219	210
PTFE	-CF ₂ CF ₂ -	C ₂ F ₄	100	0	2.9	6	8.38	7.87	58	146	137
Poly(chloral)		C ₂ HOC _l ₃	147.5	0	1.22	5	4.97	6.46	33	36	47
PEEK		C ₁₉ H ₁₂ O ₃	288	46	2.2	13	16.09	15.37	163	212	203
BPA-polysulfone		C ₂₇ H ₂₂ O ₄ S	442	31	3.3	17.0	19.95	19.23	336	395	381
Poly(ether sulfone)		C ₁₈ H ₁₂ O ₄ S	324	36	2.13	12	15.73	14.95	165	201	191
Poly(phenyl sulfone)		C ₂₄ H ₁₆ O ₄ S	400	45	1.71	13	14.98	14.32	156	154	147
PHA-OMe		C ₂₂ H ₁₈ O ₄ N ₂	374	43	1.4	18	15.65	15.04	130	131	126

TABLE A-2. NET HEAT OF COMPLETE COMBUSTION AND HEAT RELEASE CAPACITY OF POLYMERS
(Continued)

Polymers	Structure	Repeating Unit Composition	Mn (g/mol)	Char (%)	Max. Mass Loss Rate (%/s)	Net Heat of Combustion (kJ/g)			Heat Release Capacity (J/g-K)		
						PCFC	Calc. (1)	Calc. (2)	PCFC	Calc. (1)	Calc. (2)
Poly(amide-imide)		$C_{28}H_{17}O_5N_3$	475	38	0.7	12	16.40	15.61	60	69	66
Cyano-Kevlar		$C_{15}H_9O_2N_3$	263	58	0.77	9.1	10.80	10.32	55	50	48
PHA		$C_{20}H_{14}O_4N_2$	346	56	0.4	10	11.43	10.91	42	27	26
PI		$C_{16}H_6O_4N_2$	290	50	0.5	8.5	11.18	10.73	29	34	32
BPC-PC		$C_{15}H_8O_3Cl_2$	307	53	1.3	5.7	9.94	9.41	29	78	73
PBZT		$C_{14}H_6N_2S_2$	266	58	0.38	5.0	10.30	9.89	24	23	23
Chalcon II-polyarylate		$C_{25}H_{18}O_6$	414	41	0.9	10	15.82	15.05	110	85	81
Technora®		$C_{34}H_{24}N_4O_5$	568	42	1.71	15.3	16.11	15.45	131	165	159
BPC-polyarylate		$C_{22}H_{12}O_4Cl_2$	411	51	0.6	4.0	11.49	10.90	12	41	38

TABLE A-2. NET HEAT OF COMPLETE COMBUSTION AND HEAT RELEASE CAPACITY OF POLYMERS
(Continued)

Polymers	Structure	Repeating Unit Composition	Mn (g/mol)	Char (%)	Max. Mass Loss Rate (%/s)	Net Heat of Combustion (kJ/g)		Heat Release Capacity (J/g-K)			
						PCFC	Calc. (1)	Calc. (2)	PCFC	Calc. (1)	Calc. (2)
XYDAR®		C ₂₇ H ₁₆ O ₆	436	40	2.55	11	16.14	15.41	215	247	236
PBT		C ₁₂ H ₁₂ O ₄	220	0	4.18	22	24.76	23.66	474	621	593
ULTEM®		C ₃₇ H ₂₄ O ₆ N ₂	592	49		12	14.44	13.79			
Poly(ethyl methacrylate)		C ₆ H ₁₀ O ₂	114	0	4.5	26	27.57	27.07	840	744	731

^a TGA results. Heating at 10°C/min to 930°C in N₂

^b PCFC results. Heating at 4.3°C/s to 930°C in N₂

^c Calculated by oxygen consumption principle

^d Calculated by atom additivity principle

^e FAA data

TABLE A-3. CORRELATION BETWEEN MOLAR FRACTION OF EFFECTIVE CHAR-FORMING ATOMS AND CHAR YIELDS OF POLYMERS

Polymers	Composition	Number of Effective Atoms	Effective Atoms (mol%)	Char (%)
PE	CH ₂	0	0	0
PP	C ₃ H ₆	0	0	0
PS	C ₈ H ₈	0	0	0
Poly(a-methyl styrene)	C ₉ H ₁₀	0	0	0
Nylon 66	C ₁₂ H ₂₂ O ₂ N ₂	0	0	0
PMMA	C ₅ H ₈ O ₂	0	0	0
POM	CH ₂ O	0	0	0
PEO	C ₂ H ₄ O	0	0	4
PTFE	C ₂ F ₄	0	0	0
Poly(chloral)	C ₂ HOCl ₃	0	0	0
PET	C ₁₀ H ₈ O ₄	0	0	8
PBT	C ₁₂ H ₁₂ O ₄	0	0	0
PC	C ₁₆ H ₁₄ O ₃	6	18	17
Poly(phenylene oxide)	C ₈ H ₈ O	6	35	23
BPA-polyarylate	C ₂₃ H ₁₈ O ₄	12	27	27
BPA-polysulfone	C ₂₇ H ₂₂ O ₄ S	12	22	31
Kevlar [®]	C ₁₄ H ₁₀ O ₂ N ₂	12	43	32
BPC-PC	C ₁₅ H ₈ O ₃ Cl ₂	14	50	53
Cyano-Kevlar	C ₁₅ H ₉ O ₂ N ₃	16	55	58
Poly(ether sulfone)	C ₁₈ H ₁₂ O ₄ S	18	51	36
Poly(methoxyamide)	C ₂₂ H ₁₈ O ₄ N ₂	18	39	43
PEEK	C ₁₉ H ₁₂ O ₃	18	53	46
PI	C ₁₆ H ₆ O ₄ N ₂	18	64	50
PBZT	C ₁₄ H ₆ N ₂ S ₂	18	75	58
Chalcon II-polyarylate	C ₂₅ H ₁₈ O ₆	20	41	41
BPC-polyarylate	C ₂₂ H ₁₂ O ₄ Cl ₂	20	50	51
XYDAR [®]	C ₂₇ H ₁₆ O ₆	24	49	40
Poly(phenyl sulfone)	C ₂₄ H ₁₆ O ₄ S	24	53	45
Poly(hydroxyamide)	C ₂₀ H ₁₄ O ₄ N ₂	24	60	56
Poly(amide-imide)	C ₂₈ H ₁₇ O ₅ N ₃	27	51	38
Technora [®]	C ₃₄ H ₂₄ N ₄ O ₅	30	45	42
ULTEM [®]	C ₃₇ H ₂₄ O ₆ N ₂	30	43	49